Harnessing Big Data for Characterizing Driving Volatility in Instantaneous Driving Decisions – Implications for Intelligent Transportation Systems

A Dissertation Presented for the

Doctor of Philosophy

Degree

The University of Tennessee, Knoxville

Behram Wali

August 2018

Copyright © 2018 by Behram Wali
All rights reserved.

To my parents;

To my grandparents;

To my siblings and beloved family.

ACKNOWLEDGEMENTS

First and foremost, I am thankful to Almighty Allah for bestowing me with the strength, ability, and opportunity to accomplish this research study. Without His guidance, satisfactorily completing my dissertation would have been impossible. Had it not been His blessings, my dream of achieving this degree would have remained mere dream.

In my drive towards this degree, I have found a life-changing mentor, counsellor, and a pedestal of strong support in my Guide, Dr. Asad J. Khattak. He has been there providing his timely and powerful mentorship during all these three years and served as an inspiration in my quest for knowledge. It was undoubtedly his leadership and the substance of a genius that I was able to undertake and contribute to an ambitious research program here at UT. He has given me all the freedom to pursue my diverse research interests through several of his competitive nationally and state-funded research projects, while non-obtrusively ensuring that I do not deviate from the core of my research goals and program. It has been my greatest honor working with a mentor like you and I shall always be proud of my association with you.

I have great pleasure in sincerely acknowledging my gratitude to my committee members: Dr. Hamparsum Bozdogan (who also served as my M.S. statistics degree advisor), Dr. Candace Brakewood, and Dr. David B. Clarke. I am honored to have their tremendous guidance, support, and help. Special thanks to Dr. Bozdogan for also supervising my M.S. statistics degree and for overseeing my methodological and data analytic activities. I would also like to wholeheartedly acknowledge the support of Dr. David L. Greene, who along with Dr. Asad J. Khattak guided and supervised several elements of my research program here at UT. My appreciation is also extended to Drs. Lee Han, Christopher Cherry, Airton Kohls, Christian Vossler, and Luiz Lima for their guidance and valuable classes at UT.

Science is a cooperative enterprise. My research (including this dissertation) does not only reflect my own ideas but is also a result of exchange with several of my colleagues/mentors. Several existing and past members of Dr. Khattak's research group at UT (Dr. Jun Liu, Dr. Jackeline Rios-Torres, Xioabing Li, Mohsen Kamrani, Meng Zhang, Ramin Arvin, Jingjing Xu, Abdul Rashid Mussah, Numan Ahmad, and others) participated during sessions aimed at conceptual and scientific issues that emerged during the progression of my research, for which I am very thankful to all of them. I also want to thank all the other transportation students at TESP, UT who have shared in my memorable experiences and never let things get dull or boring. I enjoyed the initiative of celebrating birthdays of ITE members and faculty initiated by

(to the best of my knowledge) Ali Boggs and Mojdeh AzadDisfany. I wish all my colleagues the best in their academic and research endeavors.

In addition, a sincere thank you to my great mentor, Dr. Anwaar Ahmed, who introduced me to serious transportation research back in my M.S. degree back home. He has been a critical commentator on my research work and a genuine guide throughout my post-graduate academic life. Also, I thank the many anonymous reviewers who provided constructive comments on the research articles included in this dissertation. There are my very dear friends who extended their counselling and sympathetic ear to me for ensuring that good times keep flowing. It would be inappropriate to omit my gratitude to Numan Ahmad who is always a frank and credible guide at times when I feel confused and stuck in the puzzle of life.

My acknowledgement would be incomplete without thanking my biggest pillar of unconditional support and guidance, my parents and family. Throughout my educational career till date, their involvement, concern, forbearing, and understanding has been the prime support for me. They all have undoubtedly made a mammoth contribution in helping me reach this stage in my life. Finally, I wish to strongly acknowledge the patience of my mother who sent me far away to pursue my studies and tolerated the temporary separation for three years. This one is for my role models, my parents!

ABSTRACT

This dissertation focuses on combining connected vehicles data, naturalistic driving sensor and telematics data, and traditional transportation data to prospect opportunities for engineering smart and proactive transportation systems.

The key idea behind the *dissertation* is to understand (and where possible reduce) "driving volatility" in instantaneous driving decisions and increase driving and locational stability. As a new measure of micro driving behaviors, the concept of "driving volatility" captures the extent of variations in driving, especially hard accelerations/braking, jerky maneuvers, and frequent switching between different driving regimes. The key motivation behind analyzing driving volatility is to help predict what drivers will do in the short term. Consequently, this dissertation develops a "volatility matrix" which takes a systems approach to operationalizing driving volatility at different levels, trip-based volatility, location-based volatility, event-based volatility, and driver-based volatility. *At the trip-level*, the dynamics of driving regimes extracted from Basic Safety Messages transmitted between connected vehicles are analyzed at a microscopic level, and where the interactions between microscopic driving decisions and ecosystem of mapped local traffic states in close proximity surrounding the host vehicle are characterized. Another new idea relates to extending driving volatility to specific network locations, termed as *"location-based volatility"*. A new methodology is proposed for combining emerging connected vehicles data with traditional transportation data (crash, traffic, road geometrics data, etc.) to identify roadway locations where traffic crashes are waiting to happen. The idea of *event-based and driver-based volatility* introduces the notion that volatility in longitudinal and lateral

directions prior to involvement in safety critical events (crashes/near-crashes) can be a leading indicator of proactive safety.

Overall, by studying driving volatility from different lenses, the dissertation contributes to the scientific analysis of real-world connected vehicles data, and to generate actionable knowledge relevant to the design of smart and intelligent transportation systems. The concept of driving volatility matrix provides a systems framework for characterizing the health of three fundamental elements of a transportation system: health of driver, environment, and the vehicle. The implications of the findings and potential applications to proactive network level screening, customized driver assist and control systems, driving performance monitoring are discussed in detail.

TABLE OF CONTENTS

LIST OF TABLES

LIST OF FIGURES

CHAPTER 1 INTRODUCTION

Among other factors, driving behavior is a critical and most unpredictable component of the surface transportation system, where it significantly contributes to as much as 90 percent of traffic crashes, significant energy use, and emissions. Understanding driver decisions is the key to implementing transportation improvement strategies. Also, the potential to improving safety and energy use through automation and connectivity of the transportation system is enormous. Rapid technological developments, ranging from vehicle-to-vehicle and vehicle-to-infrastructure communications, WI-FI, to continuous video and radar surveillance, have enabled collection of countless terabytes of spatiotemporal data about vehicle and human movement. Driven by big data for science and engineering (S&E), we are at a cusp on a major transformation in transportation, where the future at the human-technology frontier needs to be researched.

As such, this dissertation addresses the grand challenge of harnessing big data generated by automated and connected vehicles using new statistical techniques. In particular, the focus is to assemble and utilize a new comprehensive multidimensional transportation database by combining connected and automated vehicles data, naturalistic driving sensor and telematics data, and traditional transportation data to prospect opportunities for engineering intelligent, well informed, and proactive transportation systems.

The key idea behind the dissertation is be to understand (and where possible reduce) “driving volatility” in instantaneous driving decisions and increase driving and locational stability. As a rigorous measure of micro driving behaviors, the concept of “driving volatility” captures the extent of variations in driving, especially hard accelerations/braking and jerky maneuvers, and

frequent switching between different driving regimes. The key motivation behind analyzing driving volatility is to help predict what drivers will do in the short term. Consequently, we develop a new concept of "driving volatility matrix" which takes a systems approach to operationalizing driving volatility at different levels. In particular, through an integrated research program, the focus is to conceptualize and model the extent of variations in driving at several hierarchies of the real-world traffic ecosystem, i.e., 1) trip-based volatility, 2) event-based volatility, 3) location-based volatility, and 4) driver-based volatility, thus termed as driving volatility matrix (Figure 1.1).

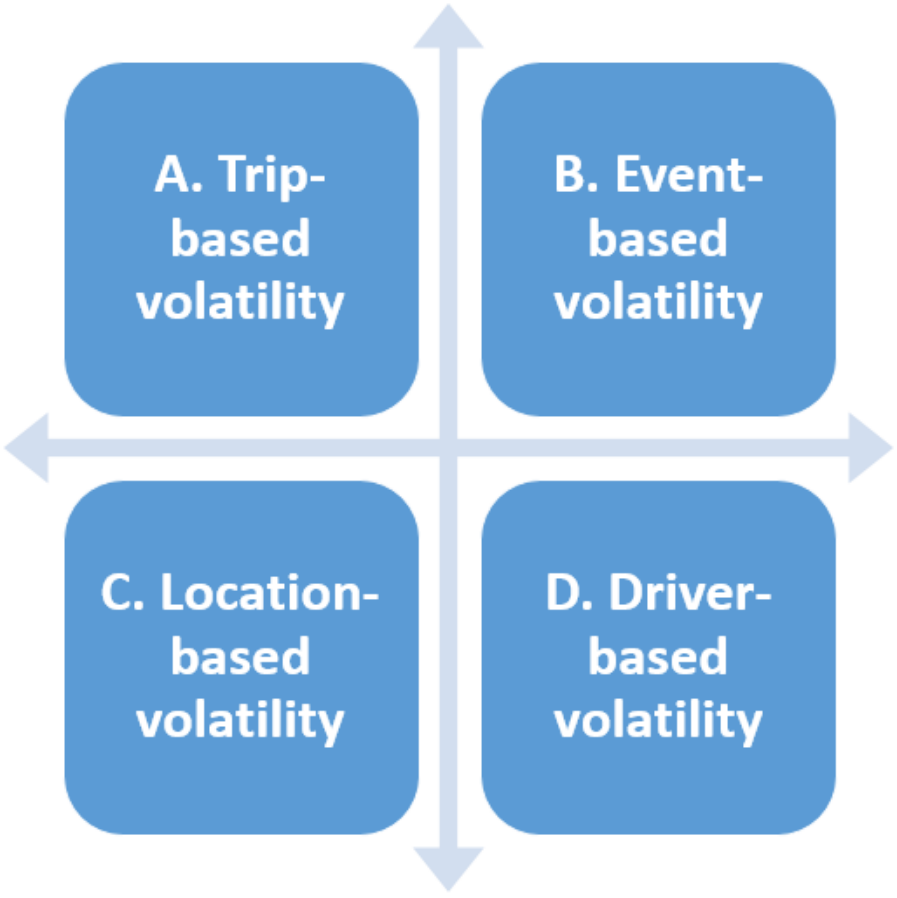

Figure 1.1 New concept of Driving Volatility matrix

At the trip-level, the dynamics of driving regimes extracted from emerging Basic Safety Messages (BSMs) transmitted between connected vehicles are analyzed at a microscopic level. By capturing the interactions between microscopic driving decisions and ecosystem of mapped local traffic states in close proximity surrounding the host vehicle, the dissertation characterizes and quantifies driving regimes, predicting short term associated volatility of each regime, and how long each regime lasts, potentially improving safety, energy use, and emissions. The different elements of volatility matrix are illustrated at a very basic level in Figure 1.2 in space-time dimension. The x-axis is space dimension (e.g., a road facility containing road segments and intersections) and y-axis is time dimension. Trip-based volatility relates to the extent of variations in microscopic driving decisions at an individual trip level. Referring to the first block in Figure 1.2 (indicated by "A"), assume two persons initiate a trip from reference point (home) in Figure 1.2 to a grocery store. The hypothetical speed profiles (in space-time dimension) are shown in Figure 1.2. If we have microscopic driving behavior and telematics data (high-resolution speed, acceleration/deceleration, etc.) at our disposal for these two trips, then we can develop and apply rigorous data analytic methodologies to quantify the extent of variations in microscopic driving decisions, and eventually develop volatility indices for each of the two trips (Figure 1.2). At a very basic level, this is referred to as "trip-based volatility" where the volatility indices will quantify variations in driving decisions at individual trip level.

At the next level, the idea of "event-based volatility" introduces the notion that volatility in longitudinal and lateral directions prior to involvement in safety critical events (crashes/near-crashes) can be a leading and proactive indicator of safety. For example, referring to the second block in Figure 1.2 (indicated by "B"), the two persons now leave the grocery store(s), and start

moving to restaurant(s). On their way, one of the persons (indicated by the red trajectory) gets into a crash, while the other person (indicated by the green trajectory) gets into a near-crash event (Figure 1.2). Assuming that we have observed the two safety-critical events, we can now analyze the driving trajectories for the two trips to understand how volatility in microscopic driving decisions relate to the safety-critical events (in this case a crash and near-crash), and whether such information can be used to predict occurrence of a crash and/or near-crash event (Figure 1.2). Note that the concept of "event-based volatility" relates to both crash propensity (risk of crash against a normal driving event) and injury outcomes, given a crash. By analyzing a plethora of kinematic sensors, video, and radar spatiotemporal naturalistic driving data in this regard, the dissertation seeks the relationship between sequence of instantaneous driving decisions (and the volatility therein) and drivers' propensity to get involved in risky outcomes. Likewise, with an explicit focus on intentional vs. unintentional volatility, we propose a big data analytic and empirical methodology to understand how driving volatility in time to collision may influence crash propensity and the injury outcomes, given a crash.

Continuing analysis of high resolution connected vehicles data, another new idea relates to extending driving volatility to specific network locations, termed as *"location-based volatility"* (see the third block in Figure 1.2). A new methodology is proposed for combining emerging connected vehicles data with traditional transportation data (crash, traffic, road geometrics data, etc.) to identify roadway locations where traffic crashes have not yet happened but perhaps are waiting to happen. This is an encouraging advance as safety managers can identify locations where behaviors of drivers may be more volatile, and can consider proactive countermeasures at such locations, e.g., providing alerts and warnings to drivers through connected vehicles roadside

equipment (RSE). For illustration, continuing in the space-time dimension, the two persons now decide to individually leave the restaurant and go to some other place (see the third block in Figure 1.2 indicated by "C"). As they move from the restaurant, they happen to pass through an intersection (see Figure 1.2). In this case, assuming that we have microscopic driving trajectories, we can quantify volatility in instantaneous driving decisions for each of the two trips (or vehicle passings) and average the volatility indices for the two trips to generate "location-specific" volatility indices, where the location in this case is an intersection. Thus, the idea of "location-based volatility" introduces the notion that high volatility and variability in microscopic driving decisions at a specific location can be related to the safety performance of that location, such as historical crashes. Also, high variability in microscopic driving decisions may indicate an issue with the design of an intersection (or roadway segment), and thus can help in devising proactive road safety management strategies. There are two important dimensions over here. First, as explained above, we can consider the two individual passings at a trip level (i.e., first block in Figure 1.2), analyze the microscopic trajectories of the two passings, and link it to a specific roadway element (which in this case is an intersection). This way, given the availability of connected vehicles data, we can quantify the location-based volatility of each individual intersection and/or road segment in a network. Note, however, that the individual vehicles passing through the intersections (and trajectories of which are used in calculating volatility indices) may not necessarily be involved in historical crashes at that particular location. Having said this, the second element of volatility matrix (i.e., event-based volatility) is highly relevant and can also be linked with location-based volatility a step further (Figure 1.1 and Figure 1.2), as it helps us understand volatility in instantaneous driving decisions in time to safety-critical events, such as crashes/near-crashes. For instance, considering the second block in

Figure 1.2, we have the microscopic vehicle trajectories for the two events (crash and near-crash). We can analyze these trajectories at individual levels and link the volatilities with a specific roadway element over which these two events happened, which in this case is a road segment (see Figure 1.2). This way, the location-based volatility will not be representing the driver performance of general population (which may contain crash and non-crash involved drivers) but microscopic driving performance of drivers who got involved in safety-critical events (such as crashes/near-crashes).

Finally, the last element of volatility matrix is "driver-based volatility" (indicated by "D" in Figure 1.2). As the name implies, driver-based volatility is person/driver specific and incorporates the volatility in driving decisions associated with each individual person. In this regard, the event-based volatility can also be deemed of as driver-based because we have person-specific individual vehicle passing trajectories before involvement into a safety-critical event. However, another equally important element of "driver-based volatility" can be the utilization of information on driver's biometrics and health data. For instance, how the heart rate, head movement, blood pressure, and pulse rate of a driver fluctuates as s(he) undertakes a specific trip (in a trip-based volatility domain), passing through a particular location or getting into a safety-critical event.

As is evident, the concept of driving volatility matrix helps us understand the extent of variations in microscopic driving decisions at several hierarchies of the traffic ecosystem. Overall, by studying driving volatility from different lenses, the dissertation attempts to contribute to the scientific analysis of real-world connected vehicles data, and to generate actionable knowledge

relevant to the design of smart and intelligent transportation systems. Gaining a better understanding of microscopic driving decisions and the variations therein in real-world environments is fundamental to the design of personalized and intelligent driver feedback systems. The concept of driving volatility matrix provides a systems framework for characterizing the health of three fundamental elements of a transportation system: health of driver, environment, and the vehicle. By altering volatility in real-world microscopic driving decisions, vehicle kinematics, and roadway environment, the outcomes help improve transportation safety by proactively predicting crash occurrence and its severity given a crash.

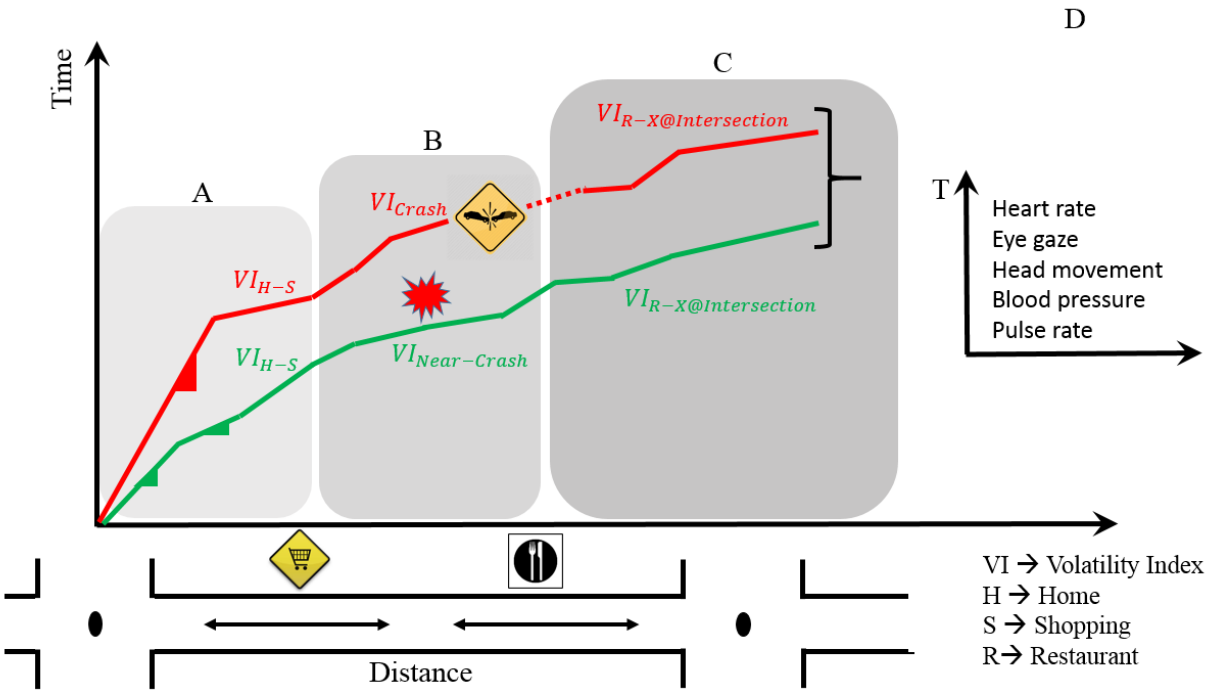

Figure 1.2 Conceptualization of Driving Volatility Matrix in space-time dimension
Note: (A → trip-based volatility, B→ event-based volatility, C→ location-based volatility, D→ driver-based volatility)

The key analyses under this dissertation has led to the following articles:

1. Khattak, A.J. and B. Wali, *Analysis of volatility in driving regimes extracted from basic safety messages transmitted between connected vehicles.*
    - *Peer-review conference paper:* Presented at the 96th Transportation Research Board Annual Meeting 2017, Washington D.C.
    - *Journal article:* Published in Transportation Research Part C: Emerging Technologies, 2017. 84: p. 48-73.
2. Kamrani, M., Wali, B., & Khattak, A. J. (2017). *Can data generated by connected vehicles enhance safety? Proactive approach to intersection safety management.*
    - *Peer-review conference paper:* Presented at the 96th Transportation Research Board Annual Meeting 2017, Washington D.C.
    - *Journal article:* Published in Transportation Research Record: Journal of the Transportation Research Board, (2659), 80-90.
3. Wali, B., A.J. Khattak, and H. Bozdogan, *How Is Driving Volatility Related to Intersection Safety in a Connected Vehicles Environment?*
    - *Peer-review conference paper:* Presented at the 97th Transportation Research Board Annual Meeting 2018, Washington D.C.
    - *Journal article:* Accepted for Publication in Transportation Research Part C: Emerging Technologies.
4. Wali, B., A.J. Khattak, and T. Karnowski, *How Driving Volatility in Time to Collision Relates to Crash Severity in a Naturalistic Driving Environment?*
    - *Peer-review conference paper:* Presented at the 97th Transportation Research Board Annual Meeting 2018, Washington D.C.

- *Journal article:* Under-review in Analytic Methods in Accident Research.

5. Wali. B., Khattak, A.J., Karnowski, T. *Exploring Microscopic Driving Volatility in Naturalistic Driving Environment Prior to Involvement in Safety Critical Events.*
    - *Journal article:* Under second-stage review in Accident Analysis and Prevention.

The dissertation is organized in a journal article format since each chapter is a modified version of an article or combinations of multiple articles which are either published (or accepted) by an academic journal, under-review and/or presented at peer-reviewed international transportation conference. Following this chapter, the second chapter answers important research questions on categorizing the volatility in typical driving profiles in a connected (instrumented) vehicles environment and the average duration of each regime, and identifying the correlates that can be associated with drivers' tendency to stay in a specific regime and/or to switch between different regimes in a real-world connected vehicles environment. The third chapter focuses on developing an analytic methodology to examine instantaneous driving behaviors by instrumented vehicles at specific locations, and its variability. In particular, a new concept of "location-based volatility" is developed and questions related to the mapping of driving volatility to historical safety outcomes such as crashes at specific locations, are addressed. In a bid to facilitate proactive roadway safety management, the fourth chapter extends the big data analytic methodology for characterizing location-based volatility and developing a full Bayesian probabilistic modeling scheme to relate intersection-specific volatility to historical crash outcomes. Altogether, Chapter 3 and 4 highlights the role of emerging large-scale microscopic connected vehicles data to establish proactive roadway safety frameworks. Owing to the need of understanding microscopic driving behavior

immediately prior to involvement in safety-critical events, the fifth chapter focuses on characterizing volatility in instantaneous driving decisions in normal driving events, crash events, and near-crash events. An understanding related to the connections between driving volatility and crash propensity after controlling for other factors, unobserved heterogeneity, and omitted variable bias is developed. Finally, the sixth chapter proposes a big data analytic and empirical methodology to examine how driving volatility in time to collision relates to crash-injury severity (given a crash) in real-world naturalistic driving environment.

In terms of impact, the proposed activities are significant because they enable new and innovative behaviorally-based preemptive early warnings and control assists to drivers based on anticipated maneuvers that are potentially unsafe or can lead to traffic flow disturbances or greater energy use. It leverages a tremendous opportunity to utilize information becoming available from the multifaceted nascent driving monitoring and cyber-physical systems in the vehicle-roadway operation realm. The development of intelligent driver feedback and control assist systems to improve safety is at the core of the dissertation. The proposed activities are transformative because safety gains can be obtained by altering driving volatility matrix in a complex driver, vehicle, and/or roadway space.

From a big data science perspective, the novelty and significance of the proposed research rests in the assembling and utilization of a new comprehensive multidimensional transportation database, containing detailed information on driving behavior in naturalistic and connected vehicles environments, vehicle performance, crash and safety event data, road inventory, and the built-environment factors. *From a methodological perspective,* the work rests on development of

"big data" driven new and innovative simulation-assisted heterogeneity-based statistical methods to extract new knowledge buried in emerging transportation databases. To harness the richness provided by big data and engineering intuition/expertise, both frequentist and Bayesian modeling paradigms are employed. In particular, emerging time-series and cross-sectional econometric methods are employed in this dissertation. To reflect the reality and complexity of real-world transportation systems, traditional frequentist approaches, simulation-assisted frequentist methods, as well as full Bayesian probabilistic modeling schemes are employed. The empirical methods revolve around addressing key methodological issues (mainly heterogeneity in the effects of covariates) usually encountered in transportation data analysis, and ignoring which can have serious implications on the final inferences being made. We present a conceptual framework to understand heterogeneity in transportation data modeling, and important the different components of heterogeneous effects.

Figure 1.3 shows the overall outline of the dissertation and highlights in each chapter.

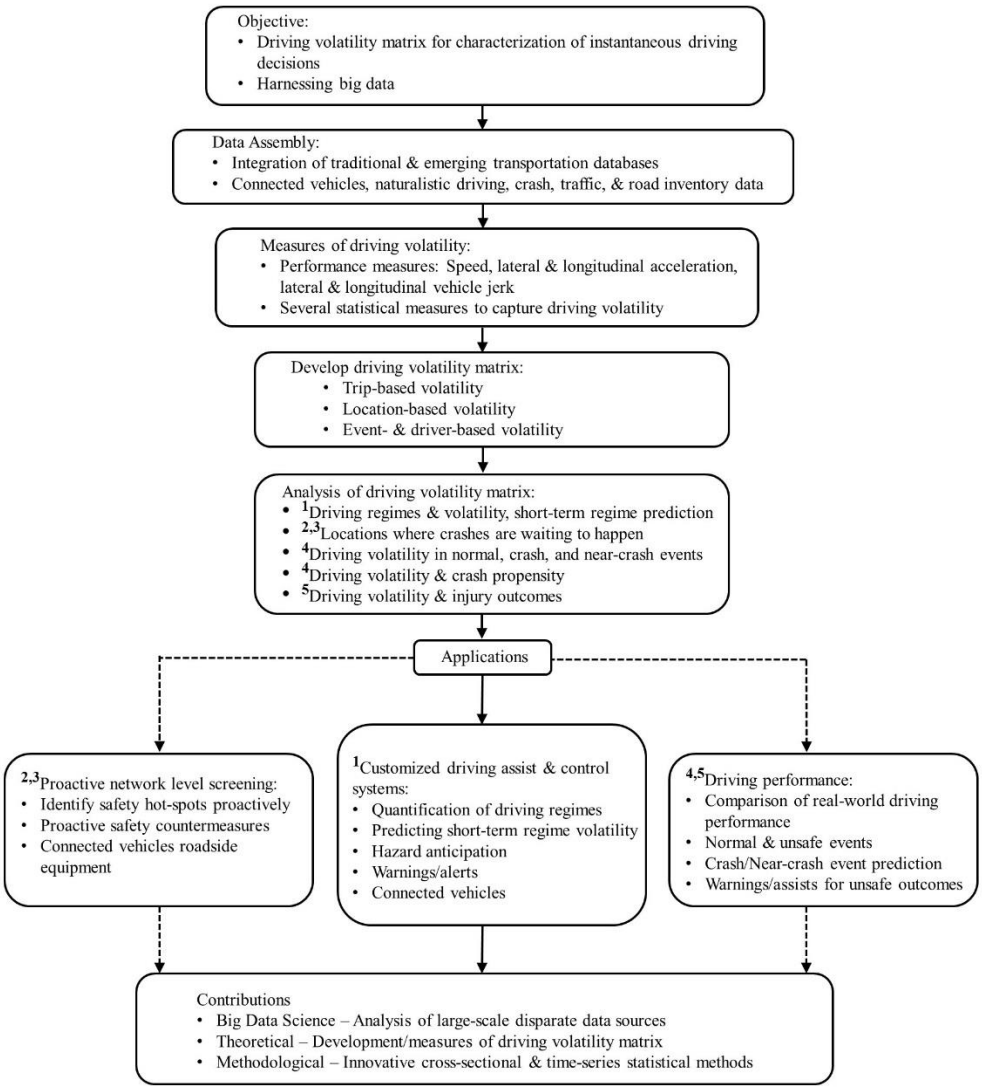

Notes:

[1] Relevant paper published in Transportation Research Part C (TR-C): Emerging Technology

[2] Relevant paper published in Transportation Research Record: Journal of Transportation Research Board.

[3] Relevant paper presented in TRB Annual Meeting & published in TR-C.

[4] Relevant paper under second-stage review in Accident Analysis and Prevention.

[5] Relevant paper presented in TRB Annual Meeting & under-review in Analytic Methods in Accident Research.

Figure 1.3 Dissertation outline

CHAPTER 2 ANALYSIS OF VOLATILITY IN DRIVING REGIMES EXTRACTED FROM BASIC SAFETY MESSAGES TRANSMITTED BETWEEN CONNECTED VEHICLES

This chapter presents a modified version of two research articles by Behram Wali and Asad J. Khattak. *Analysis of volatility in driving regimes extracted from basic safety messages transmitted between connected vehicles.* Peer-review conference paper: Presented at the 96th Transportation Research Board Annual Meeting 2017, Washington D.C. Journal article: Published in Transportation Research Part C: Emerging Technologies, 2017. 84: p. 48-73.

ABSTRACT

Driving volatility captures the extent of speed variations when a vehicle is being driven. Extreme longitudinal variations signify hard acceleration or braking. Warnings and alerts given to drivers can reduce such volatility potentially improving safety, energy use, and emissions. This study develops a fundamental understanding of instantaneous driving decisions, needed for hazard anticipation and notification systems, and distinguishes normal from anomalous driving. In this study, driving task is divided into distinct yet unobserved regimes. The research issue is to characterize and quantify these regimes in typical driving cycles and the associated volatility of each regime, explore when the regimes change and the key correlates associated with each regime. Using Basic Safety Message (BSM) data from the Safety Pilot Model Deployment in Ann Arbor, Michigan, two- and three-regime Dynamic Markov switching models are estimated for several trips undertaken on various roadway types. While thousands of instrumented vehicles with vehicle to vehicle (V2V) and vehicle to infrastructure (V2I) communication systems are being tested, nearly 1.4 million records of BSMs, from 184 trips undertaken by 71 instrumented vehicles are analyzed in this study. Then even more detailed analysis of 43 randomly chosen trips (N = 714,340 BSM records) that were undertaken on various roadway types is conducted. The results indicate that acceleration and deceleration are two distinct regimes, and as compared

to acceleration, drivers decelerate at higher rates, and braking is significantly more volatile than acceleration. Different correlations of the two regimes with instantaneous driving contexts are explored. With a more generic three-regime model specification, the results reveal high-rate acceleration, high-rate deceleration, and cruise/constant as the three distinct regimes that characterize a typical driving cycle. Moreover, given in a high-rate regime, drivers' on-average tend to decelerate at a higher rate than their rate of acceleration. Importantly, compared to cruise/constant regime, drivers' instantaneous driving decisions are more volatile both in "high-rate" acceleration as well as "high-rate" deceleration regime. The study contributes to analyzing volatility in short-term driving decisions, and how changes in driving regimes can be mapped to a combination of local traffic states surrounding the vehicle.

2.1 INTRODUCTION

As a crucial part of technology driven progressive life, automobiles and transportation systems have continued to advance since its inception decades ago. The advent of rapid technological advancements in recent decades have established the elemental foundation for Cooperative Intelligent Transportation Systems (C-ITS), a.k.a. connected and automated vehicles. This said, equipping motor vehicles and transportation systems with wireless communication technologies in a bid to establish cooperative, well informed, and proactive transportation systems is expected to be the next frontier of transportation revolution (Lu et al., 2014, Fagnant and Kockelman, 2015). Specifically, connected and automated vehicle technologies refer to integrated systems that establish bidirectional wireless connectivity among vehicles itself (vehicle-to-vehicle V2V)

and the infrastructure (vehicle-to-infrastructure V2I) to capture vehicle position, motion, vehicle maneuvering and instantaneous driving contexts[1] (Kamrani et al., 2017, US-DOT, 2016).

The generated large-scale integrated empirical data from connected and automated vehicles has significant potential in facilitating deeper understanding of instantaneous driving decisions[2]. Variations in driving with respect to the ecosystem of mapped local traffic states in close proximity surrounding the host vehicle can be explored. Important in this respect is the concept of "driving volatility" that captures the extent of variations in driving, especially hard accelerations/braking and jerky maneuvers, and frequent switching between different driving regimes[3] (Khattak et al., 2015, Wali et al., 2018e, Wali et al., 2018d, Kamrani et al., 2018, Kamrani et al., 2017). However, a fundamental understanding of instantaneous driving decisions is needed for hazard anticipation and notification systems, and for distinguishing normal from anomalous driving. The research issue is to explore different regimes of typical driving behavior and how long they last and the key correlates associated with each regime.

As a part of U.S. Department of Transportation's (USDOT) Real-Time Data Capture and Management Program, Safety Pilot Model Deployment (SPMD) in Ann Arbor, Michigan

[1] In this study, instantaneous driving contexts refer to the surroundings of host vehicle equipped with V2V and V2I technologies. An example can be how much a driver constrained is in terms of different objects surrounding the vehicle and the distance of the host vehicle to the surrounding objects.

[2] By instantaneous driving decisions, we mean the instantaneous decisions that driver may undertake to navigate the vehicle from one point to another. Such decisions may include decisions in longitudinal direction such as speeding, braking, high-rate acceleration, and/or high-rate deceleration, or in lateral direction such as lane change maneuvers. However, throughout the paper, we use the term "instantaneous driving decisions" to refer to driving decisions in longitudinal direction.

[3] In Economics literature, the key variable(s) that characterizes time-series system(s) occasionally exhibit dramatic breaks or abrupt changes in its behavior. The portions of data profile before and after the abrupt change are typically referred to "regimes" (Hamilton, 2010). In this paper, we refer to the abrupt changes that may be expected in a typical driving cycle as "driving regimes".

features real-world demonstration of connected vehicle safety applications, technologies, and systems by hosting approximately 3,000 vehicles instrumented with V2V and V2I communication systems (Henclewood, 2014). Altogether, 75 miles of roadway in Ann Arbor, Michigan are instrumented with roadside equipment (RSE) that are capable of communicating with appropriately instrumented vehicles, and devices via advanced communication and sensor technologies such as dedicated short-range communications (DSRC) (Henclewood, 2014). Furthermore, data acquisition systems (DAS) are installed in vehicles to facilitate V2V and V2I infrastructure communications. The core output from DAS are Basic Safety Messages (BSM) that describe (frequency of 10 Hz) vehicle's instantaneous position (latitude, longitude, and elevation), motion (vehicle speed, longitudinal and lateral acceleration), vehicle maneuvering (acceleration pedal, brake pedal and cruise control) and instantaneous driving contexts (number of objects around host vehicle, distance to the closest object, and relative speed of the closest object) (Henclewood, 2014, Khattak and Wali, 2017). The availability of such large-scale high resolution data is successfully used for developing a basis for improved real-time alerts, warnings, and control assistance applications (Liu and Khattak, 2016b, Kamrani et al., 2017).

By using real-world large-scale data transmitted between connected vehicles and infrastructure, the present study creates new knowledge for connected vehicle technologies by explicitly investigating time-series instantaneous driving decisions (and the embedded regimes) of connected vehicle drivers at a detailed microscopic level, and mapping such decisions to instantaneous driving contexts. This analysis is important in sense that driving decisions (e.g., acceleration or deceleration decisions) primarily depend on surrounding traffic states (Åberg et al., 1997, Haglund and Åberg, 2000, Choudhury, 2007, Choudhury et al., 2010), and a detailed

understanding of driving decisions can significantly help us with better anticipating hazardous situations and providing warnings and alerts to drivers.

2.2 LITERATURE REVIEW

A careful review of literature reflects the prompt response by government agencies, automotive industry and academia to such disruptive yet beneficial connected and autonomous vehicles innovation. Recently, the proceedings of 9th University Transportation Centers (UTC) Spotlight Conference by the Transportation Research Board (TRB) on connected and automated vehicles reflected the perspectives of several stakeholders in order to assemble a goal oriented road map to achieve maximum benefits from connected and automated vehicle technologies (Turnbull, 2016). Specifically, efficient and reliable transportation connectivity solutions are being explored for its applicability to address real world safety challenges (Fagnant and Kockelman, 2015, Kamrani et al., 2018, Kamrani et al., 2017, Hu et al., 2015, Kim et al., 2007, Liu and Khattak, 2016b, US-DOT, 2016), mobility problems (Zhu et al., 2009, Hu et al., 2015, Zhu and Ukkusuri, 2015, Weber, 2015, Koulakezian and Leon-Garcia, 2011, Zeng et al., 2012, Kianfar and Edara, 2013, Moylan and Skabardonis, 2015, Genders and Razavi, 2015), and environmental challenges (Wang et al., 2015, Liu et al., 2015b, Fagnant and Kockelman, 2015, Shin et al., 2015, GM, 2015, Weber, 2015, Zeng et al., 2012, Liu et al., 2016, Kamalanathsharma and Rakha, 2016). Such emerging applications together with connected vehicle infrastructure deployment strategies can address potential challenges related to operations and safety which can in turn benefit state and local transportation agencies (Hill and Garrett, 2011).

Connected and automated vehicle solutions can potentially help in addressing transportation

challenges by primarily targeting the human factor involved in surface transportation. In special relevance to transportation safety solutions, several studies have focused on monitoring driving behavior to develop cooperative collision warning systems (Abe and Richardson, 2006, Chrysler et al., 2015, Doecke et al., 2015, Goodall et al., 2014, Lee et al., 2004, Naseri et al., 2015, Osman et al., 2015, Sengupta et al., 2007, Yang et al., 2000). By carefully characterizing driving behavior, the afore-mentioned studies contributed by developing effective collision warning systems and documented the potential of connected vehicle technologies in addressing major transportation safety challenges (Chrysler et al., 2015, Goodall et al., 2014, Osman et al., 2015, Doecke et al., 2015). However, the previous studies either utilized driving simulator/algorithm developments or localized closed course experiments, which may not cover different driving contexts/conditions. Moreover, the key to success of connected vehicle technologies rely on how well and effective connectivity of vehicles and/or infrastructure can perform in real life situations. Important in this regard are the recent innovations that enable realization of V2V and V2I technologies such as DSRC, Wi-Fi, Bluetooth, and cellular networks (Cheng et al., 2007, Chou et al., 2009, Sugiura and Dermawan, 2005).

Towards this end, recent studies utilized large scale behavioral data integrated with sensor technologies to introduce the concept of "driving volatility", which can be regarded as a measure of driving practice for characterizing instantaneous driving decisions and more specifically extreme driving behaviors (Wang et al., 2015, Liu et al., 2015b). The studies by (Wang et al., 2015) and (Liu et al., 2015b) investigated relationships between driving volatility (for each trip) and factors such as driver demographics, trip related factors (purpose, duration) and detailed vehicle characteristics such as body type, fuel type, transmission and power train (Wang et al.,

2015, Liu et al., 2015b). Collectively, the potential of individual level driving volatility in developing advanced traveler information systems, driving feedback devices, and alternative fuel vehicle purchase frameworks for consumers was documented (Wang et al., 2015, Liu et al., 2015b). Likewise, (Noble et al., 2014) utilized naturalistic driving data collected through the Strategic Highway Research Program 2 for developing a vehicle to infrastructure (V2I) warning algorithm. Specifically, in realistic driving behavior context, (Choudhury, 2007) and (Choudhury et al., 2010) focused on developing framework for "more realistic" driving lane changing and freeway merging behavior models that accounted for "unobserved driving plans" behind the observed driving decisions (Choudhury, 2007, Choudhury et al., 2010). Among other innovative techniques, Hidden Markov Models were introduced to account for "regime-dependence" in driving decisions in congested and freeway merging scenarios, where the current driving plan depended on all previous actions (Choudhury, 2007, Choudhury et al., 2010). In addition to simulation validations, empirical vehicle trajectory data was used to justify the use of regime-dependent plans in microscopic traffic simulator environment (Choudhury, 2007). While afore-mentioned studies provided valuable information about driving actions (Noble et al., 2014) and extreme driving events (Wang et al., 2015, Liu et al., 2015b), such extreme events could not be mapped to local traffic conditions due to unavailability of data. Similarly, the study by (Choudhury, 2007) focused on lane changing and freeway merging driving decisions, and not micro-level instantaneous driving decisions and the impact of local traffic conditions on instantaneous driving decisions.

SPMD provides an exciting opportunity by using state-of-the-art technologies to generate Basic Safety Messages (BSMs) that describe vehicle's instantaneous position, vehicle maneuvering,

and instantaneous driving contexts (Henclewood, 2014). In special relevance to current study, study by (Liu and Khattak, 2016b) extracted critical information from raw BSMs that captured trip level extreme driving events. An understanding of occurrence of extreme driving events was sought by identifying its correlates such as trip attributes, vehicle maneuvering and driving context for successful generation of real-time improved alerts, warnings, and control assistance systems (Liu and Khattak, 2016b). While the study by (Liu and Khattak, 2016b) utilized large-scale BSM data sent and received by vehicles and roadside equipment, the study primarily focused on conceptualizing trip-level extreme driving events (based on specific thresholds) and did not explore the instantaneous driving actions (within the trip) and its associations with instantaneous driving contexts that are taken along a specific trip.

2.2.1 Research Objective

Given the prevalent gap in connected vehicle literature, the present study builds upon the existing body of connected vehicle knowledge by focusing on, 1) categorizing time-series based driving tasks[4] into different regimes using information contained in BSMs; 2) categorizing the volatility in each regime and the average duration of each regime, and 3) Identifying the correlates that can be associated with drivers' tendency to stay in a specific regime and/or to switch between different regimes. By doing so, a fundamental understanding of instantaneous short-term driving decisions is sought (with respect to different roadway types) and how can we map time-series instantaneous driving behavior to a combination of local traffic states such as instantaneous driving contexts. Given the temporal dependency in instantaneous driving

[4] In this paper, the term "driving task" refers to the combination of instantaneous driving decisions that driver may take in the longitudinal direction along an entire trip. Depending on the context, we use the term driving task interchangeably with the term "driving cycle".

decisions, the current study methodologically contributes by introducing rigorous dynamic Markov switching models for conceptualizing micro-level driving behavior into different regimes, while mapping correlates to each regime. To the best of our knowledge, for a deeper understanding of instantaneous driving decisions, such time-series models together with utilization of large-scale real-world connected vehicle data have not been used.

2.3 METHODOLOGY

2.3.1 Conceptual Framework

A key objective of this study is to explore volatility in driving behavior by applying appropriate analytic tools to identify the correlates of instantaneous driving decisions. At a basic level, instantaneous driving decisions can be categorized into at least two regimes, and drivers can switch between these regimes over time. The two regimes/states are unobserved yet distinct, in the sense that in the different regimes, instantaneous driving decision data are generated by separate continuous processes (Hamilton, 1989). By separate continuous processes we mean that data generation in two regimes along a trip can be developed by different effects of instantaneous driving contexts and assuming a time-constant association/effect across a trip irrespective of different regimes may overlay the true data generation process[5].

Therefore, for simplicity and illustration, we first categorize instantaneous short-term driving performance into two regimes. While incorporation of additional regimes is conceptually valid

[5] There can be several reasons to anticipate existence of two regimes. Depending on several factors, instantaneous driving decisions (magnitude and directions of longitudinal accelerations) can vary significantly across the entire trip. Thus, under potentially different conditions (i.e. different instantaneous driving contexts), drivers may respond differently to staying in the same regime or switching to a different regime.

and theoretically possible, doing so significantly complicates the modeling framework due to computational tractability and regime identification issues (discussed later in detail). This is evident from the literature where models with more than two regimes are not common and different time-dependent regime varying processes (such as traffic crashes, economic, or financial data) are usually modelled as a two-regime processes, e.g. (Malyshkina and Mannering, 2009, Hamilton, 1989, Hamilton, 1994, Hansen, 1992, Kim and Nelson, 1999, Malyshkina et al., 2009) and the references therein. Nonetheless, not in transportation field though, very few studies have also considered three-regime models for modeling different financial and economic time-series datasets (Hardy, 2001, Kim et al., 2008).

On the other hand, real-world driving is a complex task and we can anticipate existence of more than two regimes, say three regimes in a typical driving cycle. Thus, as pointed out by the reviewers too, it is plausible to start with a more generic model specification that may capture common driving regimes, and thus can help in extracting important information related to instantaneous driving decisions embedded in real-world connected vehicle data[6]. Having said this, we thoroughly investigate real-world instantaneous driving decisions in connected vehicle environment based on two and three regime dynamic Markov switching models.

Next, we investigate associations of instantaneous driving decisions with critical correlates (available in the data) related to instantaneous driving context such as the number of objects around the host vehicle and distance to the closest object. By doing so, a fundamental

[6] We sincerely thank the two reviewers for suggesting investigation of more than two-regimes in a typical driving cycle. Doing so came at a cost of losing some data (discussed later in detail), nonetheless, exploration of three regime instantaneous driving behavior models helped us in extracting meaningful information from the data which was otherwise not possible from the two-regime specification.

understanding of instantaneous short-term driving decisions is sought (with respect to different roadway types) and how can we map time-series instantaneous driving behavior, especially driving volatility to a combination of local traffic states such as instantaneous driving contexts. This is important in the sense that instantaneous driving contexts, at least at a basic level, can be represented by surrounding vehicles around the host vehicle which may constrain movement and/or motivate driver to get out of congested situation. Assuming (for now) that the driver's tendency is to get out of congested situations, how the driver actually maneuvers the car is an important question which is likely to have important safety (among others) implications (Liu and Khattak, 2016b). Is there frequent switching from acceleration to braking and vice versa? These behaviors are perhaps more dangerous, compared with other behaviors such as constant speed (Liu and Khattak, 2016b).

As instantaneous driving behavior (across an entire trip) is a time-varying process, we use a Markov regime switching dynamic regression framework that assumes Markov switching (over time) between two and three (unobserved) regimes in a typical driving cycle. Note that the regime switching can be based on change in measures of central tendency (averages) and/or dispersion (variance). Having said this, conceptualizing the driving task into two (or three) different regimes can potentially account for existence of several unobserved factors that may be associated with driving performance envelope (Hamilton, 1989). Markov switching models thus can treat driving behaviors in an intuitive manner. As a matter of fact, two-regime Markov switching models are used successfully in solving problems related to traffic safety, for exhaustive applications of Markov switching regressions in safety area, interested readers are referred to (Malyshkina and Mannering, 2009, Malyshkina et al., 2009, Xiong et al., 2014a).

Figure 2.1 presents the hypothesized behavior during a general trip where "1" refers to regime 1; "2" refers to regime 2 and P(1-1) indicates the probability that a driver in regime 1 at current time will continue in regime 1 during the next time period. Figure 1 also illustrates the time-series framework as a Markov regime switching dynamic regression. Assume that a driver is currently (at time instant t = -1 seconds) in regime 1; the driver at next instant of time (t = 0 second) can either decide to remain in regime 1 or to switch to regime 2, given the effects of correlates, i.e. instantaneous driving contexts. If the driver is in regime 2 (or vice versa) at t = 0 second, the challenge is to predict driver action at next instant of time (indicated by t = 1 second) given the effects of associated covariates.

Following similar concept, Figure 2.2 presents a three-regime typical driving cycle based on Markov Switching dynamic regression framework where "1" refers to regime 1; "2" refers to regime 2; and "3" refers to regime 3. If a driver is currently (at time instant t = -1 seconds) in regime 1; the driver at next instant of time (t = 0 second) can either decide to remain in regime 1 or to switch to regime 2 or regime 3, given the effects of correlates, i.e. instantaneous driving contexts. If the driver is in regime 2 (or vice versa) at t = 0 second, the challenge is to predict driver action (to stay in regime 2, or to switch to regime 1 or 3) at next instant of time (indicated by t = 1 second) given the effects of associated covariates.

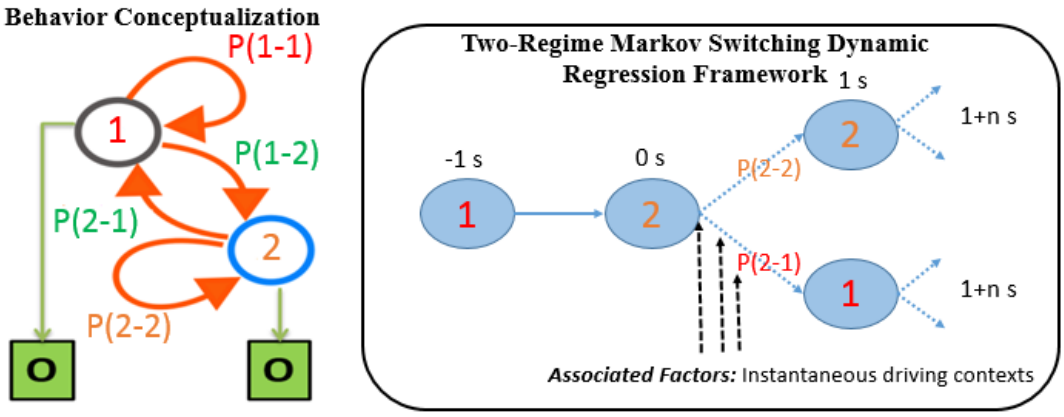

Figure 2.1 Behavior conceptualization of instantaneous driving decisions in a "two-regime" Markov switching dynamic regression framework (Note: O= Any other unobserved regime).

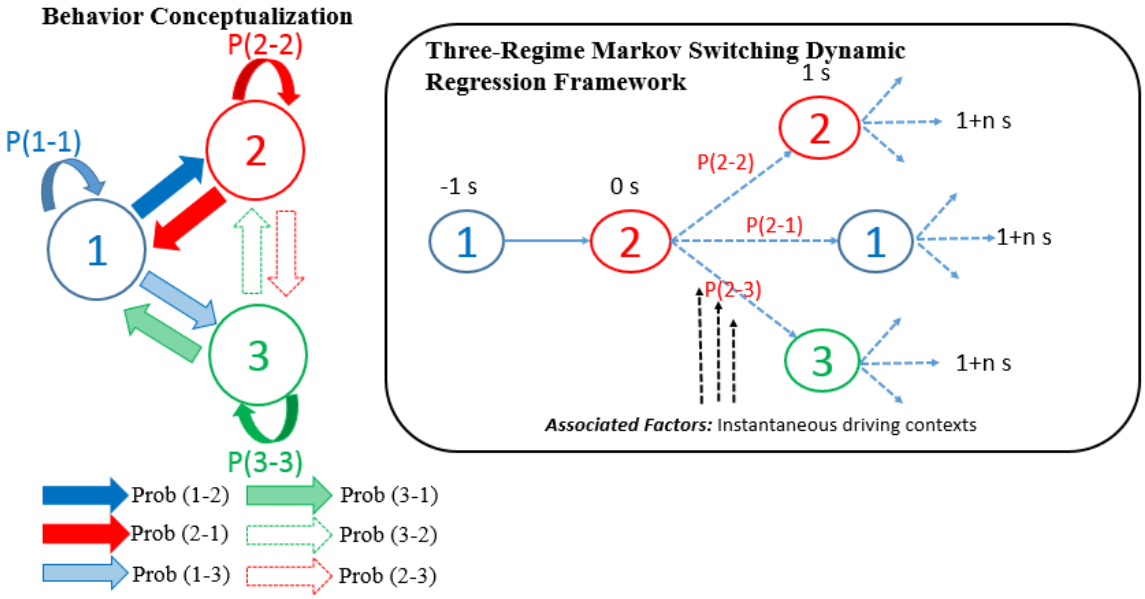

Figure 2.2 Behavior conceptualization of instantaneous driving decisions in a "three-regime" Markov switching dynamic regression framework.

With the empirical framework of two and three regimes Markov Switching dynamic regression models, the research questions are:

- What are these regimes in typical driving cycle?
- How much is the volatility each regime?
- When do the regimes change or how long they last?
- Are driver decisions consistent across different trips undertaken by different drivers?

Precisely, while allowing for differential effects of key correlates across two and three regimes, are the correlations constant across the regimes?

Finally, the proposed methodology has the potential to probabilistically predict a driving regime at a specific instant of time while allowing for the effects of instantaneous driving contexts. This is important in the sense that a change from one regime to another is not perfectly deterministic due to several unobserved factors. Thus, a time-series model should account for the probabilistic nature of the process. The proposed conceptual framework is focused on answering the afore-mentioned critical questions. A detailed description of formulating the given problem in a mathematical framework is presented in later section.

2.3.2 Markov-switching dynamic (abrupt-change) regression models

2.3.2.1 Two-Regime Dynamic Markov-switching regression models

Markov switching models were recently introduced in traffic crash modeling for addressing different important issues related to traffic safety, for exhaustive applications of two-regime Markov switching regressions in safety area, interested readers are referred to (Malyshkina and Mannering, 2009, Malyshkina et al., 2009, Xiong et al., 2014a). As instantaneous driving

behavior (across an entire trip) is a time-varying process, we use a Markov regime switching dynamic regression (MSDR) framework that assumes Markov switching (over time) between two (unobserved) regimes[7], in this case regime 1 and regime 2 for two-regime model. Consider the evolution of driving behavior "y_t", where t = 1, 2, …..,T (i.e. the entire duration of the trip) that is particularly characterized by two regimes/states:

Regime 1: $y_t = \mu_1 + \emptyset y_{t-1} + \varepsilon_t$ Equation 2.1
Regime 2: $y_t = \mu_2 + \emptyset y_{t-1} + \varepsilon_t$ Equation 2.2

Where: μ_1 and μ_2 are the intercept terms in regime 1 and regime 2 respectively; $\emptyset$ is the Autoregressive parameter; and ε_t is the white noise with variance σ^2. The two regime model abrupt shifts in the intercept term (Hamilton, 1994). At times, if the timing of the switching is known to the analyst, the above models (Equation 2.1 and 2.2) can be expressed as:

$$y_t = s_t\mu_1 + (1 - s_t)\mu_2 + \emptyset y_{t-1} + \varepsilon_t \quad \text{Equation 2.3}$$

Where: s_t is 1 if the process (driving behavior cycle) is in regime 1 and 2 if in regime 2. Empirically, the model in Equation 2.3 can be conceptualized as regression with dummy variables and can be estimated with ordinary least squares regression (Hamilton, 1994). However, in the case under consideration, we never know in which regime the process is at current time, or indirectly s_t is unobserved[8]. This said, Markov-switching regression framework specifies that the unobserved s_t follows a Markov chain.

[7] The three-regime MSDR framework is explained later in this section.
[8] It is important to note that the dependent variable (instantaneous driving decisions in longitudinal direction) is observed, but the regimes (s_t) are not observed. That is, we as analysts do not know a-priori what specifically the two-regimes are that characterize a typical driving cycle. We explain this in detail in the results section.

Note that the transition of driving cycle between two regimes can either be abrupt-change (dynamic Markov switching specification) or gradual adjustment (Autoregressive Markov Switching specification) after the process changes regime. However, in our case, due to the high resolution (frequency of 10 Hz) of instantaneous driving behavior data (dependent variable), we allow the driving cycle for a specific trip to switch between two regimes abruptly and not with gradual adjustment, thus called Markov Switching Dynamic Regression (MSDR) (Hamilton, 1994). This alternatively suggests the autoregressive term "$\emptyset$" in equation 2.1 and 2.2 equals zero. Thus, in the simplest case, we can express the framework as regime-dependent abrupt-change intercept term for k regimes (in our case k = 2) as:

$$y_t = \mu_{s_t} + \varepsilon_t \qquad \text{Equation 2.4}$$

Where: $\mu_{s_t} = \mu_1$ when s_t =1 (i.e. regime 1) and $\mu_{s_t} = \mu_2$ when s_t =2 (i.e. regime 2) and ε_t is the white noise with variance σ^2. In the simplest case, with switching in variance term[9] "σ^2" and no explanatory variables, six parameters $\mu_1, \mu_2, {\sigma_1}^2, {\sigma_2}^2, p_{1\to2}, p_{2\to1}$ are estimated. Furthermore, the conditional density of driving cycle y_t is characterized by a first order two- state Markov process as:

$$f(y_t|s_t = i, y_{t-1}; \boldsymbol{\theta}) \qquad \text{Equation 2.5}$$

Where $\boldsymbol{\theta}$ is a vector of parameters i.e. in simplest case with only intercept terms and regime-specific variances, $\boldsymbol{\theta} = [\mu_1, \mu_2, {\sigma_1}^2, {\sigma_2}^2, p_{1\to2}, p_{2\to1}]$. For two regimes, there are two

[9] In addition to switching of intercept term, variances can be regime-dependent (separate variance for two regimes) or regime independent (single variance for the entire process). The decision to allow switching in variance terms can be based on empirical and/or theoretical evidence. In addition to empirical justification from data, we posit that the two unobserved regimes are two distinct components of driving behavior and the variance in the evolution of the two regimes can be significantly different from each other. Thus, constraining the variance term to be regime-independent can potentially hide (as we will show) the true information embedded in data generation process.

conditional densities, and thus estimation of parameter vector $\boldsymbol{\theta}$ is performed by updating the conditional likelihood using nonlinear filter (Hamilton, 1994), as opposed to linear updates by (Harvey, 1990). With a vector of set of explanatory variables "B" along with switching intercepts, the general specification of MSDR can be written as (Hamilton, 1989):

$$y_t = \mu_{s_t} + X_t \propto + Z_t \beta_{s_t} + \varepsilon_t \qquad \text{Equation 2.6}$$

Where: y_t is the dependent variable, μ_{s_t} is the regime-dependent intercept term, X_t is a vector of exogenous variables with regime-independent coefficients $\propto$, Z_t is a vector of exogenous variables with regime-dependent coefficients β_{s_t}, and ε_t is independent and identically distributed (i.i.d.) normal error with mean 0 and regime-dependent variance ${\sigma_{St}}^2$. In Equation 2.6, as the two regime variables s_t are unobservable, the vector of estimable parameters for Equation 2.6 shall include $\boldsymbol{\theta} = [\mu_1, \mu_2, {\sigma_1}^2, {\sigma_2}^2, p_{1\to2}, p_{2\to1}]$ in addition to parameter estimates for regime-dependent and regime-independent explanatory variables[10].

2.3.2.2 Three-Regime Dynamic Markov-switching regression models:

The modeling framework can now be extended to a three-regime specification. Consider the evolution of driving behavior "y_t", where t = 1, 2, …..,T (i.e. the entire duration of the trip) that is particularly characterized by three unobserved regimes/states:

$$y_t = \tau_{s_t} + \varepsilon_t \qquad \text{Equation 2.7}$$

Where:

[10] In our case, we posit that the effects of explanatory variables (i.e. number of objects around host vehicle and distance to closest object) can be different with respect to two regimes. Thus, X_t (vector of regime independent exogeneous variables) is zero. As a result, the vector of estimable parameters for Equation 2.6 is $\boldsymbol{\theta} = [\mu_1, \mu_2, {\sigma_1}^2, {\sigma_2}^2, p_{1\to2}, p_{2\to1}, \beta_{s_t=1}, \beta_{s_t=2}]$, where $\beta_{s_t=1}, \beta_{s_t=2}$ are regime dependent vectors of estimable parameters for exogenous variables.

$$\tau_{s_t} = \begin{cases} \tau_1 \; if \; s_t \; = 1 \text{ (regime 1)} \\ \tau_2 \; if \; s_t \; = 2 \text{ (regime 2)} \\ \tau_3 \; if \; s_t \; = 3 \text{ (regime 3)} \end{cases}$$ Equation 2.8

And, ε_t is the normally distributed white noise with mean 0 and variance $\sigma_{s_t}^2$, s_t = (Åberg et al., 1997) is an unobservable state variable governed by a first-order Markov chain. In the simplest case, with switching in variance term "σ^2" and no explanatory variables, the parameter vector $\boldsymbol{\theta} = [\mu_1, \mu_2, \mu_3, {\sigma_1}^2, \; {\sigma_2}^2, {\sigma_3}^2, p_{1\to1}, p_{1\to2}, p_{2\to1}, p_{2\to2}, p_{3\to1}, p_{3\to2}]$, i.e. twelve parameters are estimated. Similar to the two-regime models, the three conditional densities (for three regimes) associated with estimation of parameter vector $\boldsymbol{\theta}$ is performed by updating the conditional likelihood using nonlinear filter (Hamilton, 1994).

With a vector of set of exogenous explanatory variables "**W**" along with regime-dependent intercepts and variances, the general specification of a three-regime MSDR can be written as (Hamilton, 1989):

$$y_t = \tau_{s_t} + X_t\delta + Z_t\gamma_{s_t} + \varepsilon_t$$ Equation 2.9

Where: y_t is the dependent variable, τ_{s_t} is the regime-dependent intercept term, X_t is a vector of exogenous variables with regime-independent coefficients δ, Z_t is a vector of exogenous variables with regime-dependent coefficients γ_{s_t}, and ε_t is independent and identically distributed (i.i.d.) normal error with mean 0 and regime-dependent variance ${\sigma_{St}}^2$. Given the

inclusion of regime-dependent exogeneous explanatory variables, the estimable parameter vector $\boldsymbol{\theta}$ is now expanded in Equation 2.9[11].

2.3.3. Markov chains

A discrete time Markov chain (DTMC) is assumed during switching mechanism of driving cycle between two regimes i.e. the probability distribution of s_{t+1} depends only on current regime s_t and not on the previous evolution of driving behavior[12] i.e. $s_{t-1}, s_{t-2}, \ldots\ldots$ (Tauchen, 1986). This is commonly referred to a two-state Markov chain and is fairly a standard in applications of Markov Switching models (Xiong et al., 2014a, Hamilton, 2010) (Malyshkina and Mannering, 2009, Hamilton, 1994). Higher order Markov chains where the realization of the future state may depend on current state and previous history brings in high complications to the model estimation process (Kim et al., 2008), and are thus not common in Markov switching applications[13]. Also, the first-order Markov chain seems a natural and intuitive starting point and, as mentioned in (Hamilton, 2010), is clearly preferable to acting as if the shift from regime 1 to 2

[11] The parameter vector $\boldsymbol{\theta}$ for the three-regime MSDR framework has at least 15 parameters to be estimated, i.e. $\boldsymbol{\theta} = [\mu_1, \mu_2, \mu_3, \gamma_{s_t=1}, \gamma_{s_t=2}, \gamma_{s_t=3}, {\sigma_1}^2, {\sigma_2}^2, {\sigma_3}^2, p_{1\to1}, p_{1\to2}, p_{2\to1}, p_{2\to2}, p_{3\to1}, p_{3\to2}]$, where $\gamma_{s_t=1}, \gamma_{s_t=2}, \gamma_{s_t=3}$are regime dependent vectors of estimable parameters for exogenous variables in the three-regime MSDR model.

[12] Another option can be to specify the models in continuous time. However, the advantage of DTMCs is that they have a mathematically easy formal description. A concern, however, can be that modeling continuous process is hard using a time-discrete paradigm. In other words, a uniform step must be artificially introduced, which will always result in errors and abstraction. However, in our case, we are not artificially introducing a time-step. Despite that driving cycle is a continuous process, we observe the driving decisions at discrete time intervals (t = 1, 2, 3, and so on.). Due to the very high data resolution of SPMD connected vehicle data, it is unlikely that drivers will make instantaneous driving decisions and perform frequent regime switching within one second. Also, the basic formulation of Markov property shows that observing a continuous-time Markov chain at regular time intervals gives a discrete-time Markov chain.

[13] An alternative and indirect way of extending the first-order Markov chain property can be to formulate a model specification where the evolution of response outcome may depend on the value of switching mean at its current state and lagged value, and this in turn will lead to four conditional densities where the new state variable is a four-state Markov chain. This specification is mathematically equivalent to Markov Switching Autoregressive framework as shown in Equations 2.1 and 2.2 and is typically used to model low frequency data (Hamilton, 1994, Kim, 1994). Keeping in view the extant literature, Markov switching dynamic regressions are used in the current study given the high resolution of instantaneous driving data (Stata, 2016, Hamilton, 2010).

(or vice versa) was a perfectly deterministic event. Permanence, if any, of the shift between the regimes would be represented by $p_{2\to2}$ (in two regime case) equal 1, and any intra-regime probability of less than one (as we will see later) would indicate lack of permanence which the Markov formulation accommodates. Furthermore, if the regime change in instantaneous driving decisions reflects a change in instantaneous driving contexts, the prudent hypothesis would seem to be to allow the possibility for the regime to change back again when instantaneous driving context changes, and this suggests that $p_{2\to2} < 1$ is a more natural formulation for thinking about the regime changes than the deterministic $p_{2\to2} = 0$ (Hamilton, 2010, Kim et al., 2008). Having said this, assuming s_t to be an irreducible and aperiodic Markov chain originating from its ergodic distribution $\pi = (\pi_1, \ldots\ldots, \pi_k)$, the probability that s_t belongs to, $j \in (1,2)$ (where 1, 2 refers to regime 1 and 2) for two regime model and $j \in (1,2,3)$ (where 1, 2, and 3 refers to regime 1, 2, and 3) in three regime model depends on the most recent realization of driving behavior, s_{t-1}, and thus can be formulated as (Hamilton, 1994):

$$\Pr(s_t = j | s_{t-1} = i) = p_{ij} \qquad \text{Equation 2.10}$$

Thus, all possible transitions from one regime to another, in a two-regime model, can be collected in 2×2 transition matrix while governing the evolution of Markov chain as:

$$\boldsymbol{P} = \begin{bmatrix} p_{1\to1} & p_{1\to2} \\ p_{2\to1} & p_{2\to2} \end{bmatrix} \qquad \text{Equation 2.11}$$

While, the transition probabilities of switching from one regime to another in a three-regime model can be collected in a 3×3 transition probability matrix as:

$$\boldsymbol{P} = \begin{bmatrix} p_{1\to1} & p_{1\to2} & p_{1\to3} \\ p_{2\to1} & p_{2\to2} & p_{2\to3} \\ p_{3\to1} & p_{3\to2} & p_{3\to3} \end{bmatrix} \qquad \text{Equation 2.12}$$

2.3.4 Likelihood function with latent states/regimes

Using the Markov chain property, the conditional density of y_t can be formulated using Equation 2.5 for two or three regime models. However, in order to obtain marginal density of y_t, we weigh the conditional densities (one for each regime) by their respective probabilities, as explained in (Hamilton, 1994, Goldfeld and Quandt, 1973, Frühwirth-Schnatter, 2006):

$$f(y_t|\boldsymbol{\theta}) = \sum_{i=1}^{k} f(y_t|\, s_t = i, y_{t-1}; \boldsymbol{\theta}) \Pr(s_t = i, \boldsymbol{\theta}) \qquad \text{Equation 2.13}$$

Over here, let us introduce a $k \times 1$ vector of conditional densities as:

$$\forall_t = \begin{bmatrix} f(y_t|s_t = 1; y_{t-1}; \boldsymbol{\theta} \\ f(y_t|s_t = 2; y_{t-1}; \boldsymbol{\theta} \\ \vdots \\ f(y_t|s_t = k; y_{t-1}; \boldsymbol{\theta} \end{bmatrix} \qquad \text{Equation 2.14}$$

Where: k is number of regimes respectively. To construct the final likelihood function, the probability that s_t takes on specific value (either 1 or 2 for a two-regime model or 1, 2, or 3 for a three-regime model) using the data through time "t" and model parameters $\boldsymbol{\theta}$ should be estimated. While utilizing the data until time "t", let $\Pr(s_t = i; y_t; \boldsymbol{\theta})$ denote the conditional probability of observing $s_t = 1$, then the resulting likelihood is:

$$\Pr(s_t = i; y_t; \boldsymbol{\theta}) = \frac{f(y_t|s_t = i, y_{t-1}; \boldsymbol{\theta}) Pr(s_t = i; y_{t-1}; \boldsymbol{\theta})}{f(y_t|\, y_{t-1}; \boldsymbol{\theta})} \qquad \text{Equation 2.15}$$

The likelihood can then be estimated through iterating Equation 2.16 and 2.17 as[14]:

$$\aleph_{t|t} = \frac{\aleph_{t|t} * \forall_t}{1'(\aleph_{t|t-1} * \forall_t)} \qquad \text{Equation 2.16}$$

$$\aleph_{t+1|t} = P\aleph_{t|t} \qquad \text{Equation 2.17}$$

[14] To achieve final likelihood function, we transform conditional probabilities for two regimes i.e. $\Pr(s_t = i; y_t; \boldsymbol{\theta})$ and $\Pr(s_{t-1} = i; y_t; \boldsymbol{\theta})$ to $k \times 1$ vector as $\aleph_{t|t}$ and $\aleph_{t|t-1}$ respectively.

Where 1 is $k \times 1$ vector of constants i.e. 1s. The reduced likelihood representation is thus obtained as[15]:

$$\mathrm{L}(\theta) = \sum_{t=1}^{T} log f(y_t|y_{t-1};\theta) \qquad \text{Equation 2.18}$$

Where:
$f(y_t|y_{t-1};\theta) = 1'(\aleph_{t|t-1} * \forall_t)$

2.3.5 Predictions/regime prediction

To be able to predict the unconditional probability of a driving cycle in a specific regime at time "t", we use conditional transition probabilities and the Markov structure of the model. Specifically, the log-likelihood function has a recursive structure (Frühwirth-Schnatter, 2006) that initiates from the unconditional state probabilities $\aleph_{1|0}$. Thus, the unconditional probabilities are estimated as:

$$\pi = (\boldsymbol{A}'\boldsymbol{A})^{-1}\boldsymbol{A}'e_{k+1} \qquad \text{Equation 2.19}$$

Where A is $(k+1) \times k$ matrix formulated as:

$$A = \begin{bmatrix} \boldsymbol{I_k} - P \\ 1' \end{bmatrix} \qquad \text{Equation 2.20}$$

And I_k denotes $k \times k$ identity matrix, and e_k denotes kth column of $\boldsymbol{I_k}$ respectively.

[15] Characterization of maximum likelihood estimates has been performed through implementation of Expectation Maximization (EM) algorithm (Dempster et al., 1977). Due to the nonlinear equation structure for estimating parameter vector $\boldsymbol{\theta}$, it is practically not possible to solve them analytically, and as such, iterative algorithm is used to finding the maximum likelihood estimates. Each iteration of this algorithm consists of two simple steps: An E-step, in which a conditional expectation is calculated over a pre-defined density surface, and an M-step, where the conditional expectation is maximized. For a detailed discussion about EM algorithm in context of aperiodic ergodic Markov chains, interested readers are referred to (Hamilton, 1994).

2.4 DATA DESCRIPTION – DATA ACQUISITION SYSTEMS

The data were extracted from the Data Acquisition System (DAS), which was part of Safety Pilot Model Deployment (SPMD) in Ann Arbor, Michigan. The key objectives of SPMD include evaluation of how drivers adapted to the utilization of connected vehicle technology, providing opportunity to explore real-world effectiveness of connected vehicle safety applications in multi-modal driving conditions (Henclewood, 2014). This study focuses on using the SPMD large-scale connected vehicle sanitized mobility data to understand instantaneous driver decisions in a broader ecosystem of instrumented vehicles and infrastructure on different roadway functional classifications.

As part of DAS, BSMs contain instantaneous (frequency of 10 Hz) information packets describing host vehicle's motion and location information, including vehicle performance (speed and acceleration), vehicle operation (brake and accelerator pedal application), and instantaneous driving contexts (number of objects around host vehicle and distance to the closest object) respectively (Henclewood, 2014). This information is stored in BSMs that are instantaneously sent and received by instrumented vehicles and roadside equipment (Henclewood, 2014). Table 2.1 summarizes the detailed description of key data variables whereas detailed description of all other data sources is available in SPMD Data Handbook (Henclewood, 2014). One-day sample data (04/11/2013) has been used for this study which contains approximately 1.4 million records (1,399,084) of basic safety messages, from 184 trips undertaken by 71 instrumented vehicles. Specifically, the sum of all trip durations is approximately 38.8 hours, whereas the average duration per trip is 12 minutes respectively. From roadway type stand-point, the overall trips are undertaken on combination of freeways, state routes, and local routes respectively.

For this study, a probability based random-sampling procedure is conducted to randomly select 43 trips (out of 184 trips) for further analyses[16]. In the probability based simple random-sampling, random number generator (RNG) was used to generate unique indexes (ranging between 0 and 1) for each of the 184 trips and equal probability was assigned to each of the trip (i.e. probability of selecting each trip was same across the data matrix). Next, a sample of 43 trips is randomly extracted from the original data matrix (containing 184 trips) without replacement.

Table 2.1 Variable Descriptions from DAS SPMD, Ann Arbor, Michigan

Variable		Description
Position	Altitude	A GPS-based estimate of height above sea level (height above the reference ellipsoid that approximates mean sea level)
	Latitude	Current degree of latitude at which the vehicle is located
	Longitude	Current degree of longitude at which the vehicle is located
Motion	Speed (host vehicle)	Current vehicle speed, as determined from the vehicle's transmission
	Longitudinal Acceleration	Longitudinal acceleration measured by an Inertial Measurement Unit (IMU)
	Lateral Acceleration	Lateral acceleration measured by an IMU
Vehicle Maneuvering	Accelerator Pedal	Reflects the amount the accelerator pedal is displaced with respect to its neutral position
	Brake Pedal	Indicates whether the brake light is on or off
	Cruise Control	Indicates whether cruise control is active/engaged
	Turn Signal	Provides information regarding the state of the vehicle turn signals
Driving Context	Number of objects	Number of identified objects, as determined by the Mobileye sensor
	Distance to the closest object	Position of the closest object, relative to a reference point on the host vehicle, according to the Mobileye sensor

Source: SPMD Data Handbook (Henclewood, 2014).

[16] A total of 43 randomly selected trips were categorized and modeled at the microscopic level in this study. Analyzing the entire database of 184 trips was not done since it would be very labor intensive (in terms of categorizing) and computationally burdensome (in terms of modeling). Also, it is important to note that the 43 randomly chosen trips account for 52% of the total one-day BSM sample (714,340 BSM packets out of 1,399,084 packets).

To facilitate more meaningful analysis, the entire vehicle trajectories for 43 randomly selected trips were visualized in Google Earth to identify the roadway functional classification on which the trips were undertaken. As such, significant efforts went into classifying the trips with respect to roadway type. For the sampled 43 trips, four trips are undertaken on freeway and state routes, 2 trips on US state routes, 14 trips on freeways, 18 trips on local roads, and 5 trips on state and local routes. Altogether, the 43 trips are undertaken by 34 vehicles whereas few vehicles undertook two or more than two trips.

The connected vehicle data used in this study are reliable and was error-checked. We linked the microscopic trip data (collected at a frequency of 10 Hz) with a trip-summary file that contains trip-level information, from each instrumented vehicle, and for each trip taken during the study period. The columns in the two files matched well in terms of trip start and end times, vehicle ID and trip ID, distance traveled, average speed, and trip duration. Such concordance increases our confidence in the data.

As stated earlier, the current study focuses on exploring the relationship between driving regimes and most critical correlates i.e. instantaneous driving contexts. This said, descriptive statistics are presented in Table 2 only for instantaneous driving decisions (response variable) and instantaneous driving contexts (explanatory variables) respectively. In Table 2.2, the explanatory variables are as follow:

- Objects indicator: 1 if number of objects around host vehicle ≥ 3, 0 otherwise. While we tried different possible categorizations and also used this variable as discrete in the model specifications, the cutoff point of 3 targets provided the most comparable and empirically

better (based on AIC) results (Wali et al., 2017a). This categorization also helps in comparing the effects of nearby targets on driving regimes across different trips undertaken on different roadway types.

- Range: indicates the distance of closest object to host vehicle in feet.

2.4.1 Data Aggregation

The SPMD connected vehicle data is collected at a frequency of 10 Hz i.e. 10 BSM packets per second are transmitted between connected vehicles and the infrastructure. This provides the opportunity to conduct microscopic empirical assessment of real-world driving data and vehicular movements that vary substantially over time (Liu and Khattak, 2016b). However, as the present study focuses on instantaneous driving decisions, it may be difficult to understand the transition between different regimes, especially within the time frame of one-tenth of a second[17]. Thus, we aggregate the data at relatively lower frequency before conducting detailed econometric analysis of instantaneous driving decisions. However, if the data are aggregated at very lower frequency, it may result in losing short-term extreme or volatile driving decisions (Liu et al., 2015a), which is also a fundamental focus of the present study. According to the study by (Liu et al., 2015a), the feasibility of detecting micro-driving decisions for 1 Hz sampling data (one BSM per second) is 98.54% where 1.46% of the information about micro-decisions can be lost (Liu et al., 2015a). Likewise, if the sampling rate is reduced to 0.5 Hz (one BSM per two seconds), 0.2 Hz (one BSM per five seconds), and 0.1 Hz (one BSM per ten seconds), the information loss can be 4.835%, 17.87%, and 35.86% respectively (Liu et al., 2015a). Given these results and the scope of the present study, we have aggregated the data at 1

[17] We thank the anonymous reviewer for bringing up this conceptual concern to our attention.

Hz (one BSM per second) where averages of the values for each specific variable (identified in Table 2.1) within one-second are taken[18]. This resulted in a total of 71,434 seconds (i.e. 714,340 BSM packets divided by 10) of real-world connected vehicle driving data.

2.5 RESULTS

2.5.1 Descriptive Statistics

The descriptive statistics presented in Table 2.2 summarizes each sampled trip by providing mean, standard deviation, minimum and maximum. The distributions of different driving states for each trip e.g. acceleration/deceleration seem reasonable. As compared to mean acceleration/deceleration values, the standard deviation is relatively large for almost all the trips, indicating larger variation in acceleration/deceleration cycles for a given trip. Trips undertaken on freeways (N=12) are relatively longer with a mean and maximum trip duration of 48.6 and 218.4 minutes respectively (Table 2). The trips undertaken on freeways are also observed to be high-speed trips (as compared to those on freeways and state routes) with mean speed of 78.8 mph and maximum mean speed of 81.19 mph respectively.

[18] Note that we also conducted the entire analyses using original data resolution of 10 Hz. However, doing so did not change our overall inferences regarding the presence and identification of regimes, and its correlations with explanatory variables in typical driving cycle. Results of the analyses conducted at 10 Hz data are available from authors upon request.

Table 2.2 Descriptive Statistics of Selected BSM Variables

	Trip No.	Acc-Dec (Mean/SD/Min/Max)	Number of Targets (Mean/SD/Min/Max)	Range (Mean/SD/Min/Max)	Average Speed	Duration
Freeways & State Routes	1	(-0.0043/0.3623/-3.758/2.241)	0.21/0.40/0/1	0.970/0.540/0.093/1.5	89.79	17.476
	2	(0.008/0.286/-1.5907/2.5759)	0.56/0.49/0/1	0.66/0.47/0.03/1.78	68.25	26.214
	3	(-0.0112/0.5322/-3.2444/2.3138)	0.34/0.47/0/1	0.29/0.28/0.02/1.5	72.48	32.768
	4	(0.0031/0.2269/-1.5928/1.3693)	0.46/0.49/0/1	0.99/0.51/0.04/2.24	74.82	34.953
US State Routes	1	(-0.0383/0.3348/-1.6694/2.3972)	0.09/0.28/0/1	0.73/0.40/0.03/1.77	53.84	4.369
	2	(0.0054/0.6422/-3.60/2.4138)	0.27/0.44/0/1	0.26/0.32/0.02/1.5	49.06	26.214
Freeways	1	(-0.0065/0.4368/-2.921/2.057)	0.72/0.44/0/1	0.35/0.21/0.04/1.59	80.48	19.661
	2	(-0.0008/0.6055/-2.6779/2.9166)	0.26/0.44/0/1	0.60/0.51/0.02/1.54	54.61	52.429
	3	(-0.0202/0.6539/-4.37/2.9)	0.46/0.49/0/1	0.40/0.45/0.01/1.77	72.02	17.476
	4	(-0.0214/0.5873/-1.9694/2.4472)	0.36/0.48/0/1	0.19/0.15/0.02/1.5	48.65	13.107
	5	(0.0102/0.3439/-1.9032/1.7773)	0.37/0.48/0/1	0.99/0.53/0.03/2.17	68.06	26.214
	6	(0.0090/0.4562/-1.8164/2.074)	0.47/0.49/0/1	0.80/0.44/0.025/1.78	66.88	19.661
	7	(0.0018/0.2914/-2.3003/1.8706)	0.30/0.46/0/1	1.05/0.46/0.11/2.16	81.19	21.845
	8	(0.0166/0.5987/-2.1916/2.6777)	0.44/0.49/0/1	0.23/0.22/0.02/1.5	49.2	23.815
	9	(-0.0004/0.1863/-1.6645/1.1566)	0.18/0.39/0/1	0.97/0.52/0.02/2.48	82.1	218.453
	10	(-0.0002/0.1861/-1.8511/1.6970)	0.18/0.39/0/1	1.01/0.47/0.03/2.51	76.2	196.608
	11	(0.0022/0.4081/-1.9227/2.1484)	0.47/0.49/0/1	0.65/0.47/0.03/1.76	72.3	26.214
	12	(0.0017/0.3481/-2.2309/1.7925)	0.30/0.46/0/1	0.91/0.53/0.06/	72.9	21.845

Notes: Acceleration/Deceleration are recorded in units of $^{m}/_{s^2}$; range in hundreds of feet; average speed in $^{miles}/_{hr}$; and duration in minutes.

Table 2.2 Descriptive Statistics of Selected BSM Variables (Continued)

	Trip No.	Acc-Dec (Mean/SD/Min/Max)	Number of Targets (Mean/SD/Min/Max)	Range (Mean/SD/Min/Max)	Average Speed	Duration
Local Routes	1	(0.0064/0.5953/-2.1722/2.0777)	0.16/0.37/0/1	0.71/0.58/0.03/1.68	32.23	13.107
	2	(0.0014/0.900/-3.233/2.4674)	0.01/0.11/0/1	0.28/0.39/0.01/1.5	49.69	6.554
	3	(-0.0028/0.6322/-2.8555/2.8277)	0.18/0.38/0/1	0.43/0.34/0.02/1.5	28.19	19.661
	4	(0.0023/0.6046/-2.100/3.2305)	0.12/0.33/0/1	0.88/0.55/0.02/1.50	33.04	8.738
	5	(0.0241/0.6756/-2.6432/2.0203)	0.18/0.39/0/1	0.27/0.33/0.02/1.5	23.73	10.923
	6	(0.0075/0.4854/-1.911/2.7583)	0.09/0.29/0/1	0.80/0.52/0.04/1.77	48.41	13.107
	7	(-0.0003/0.612/-2.411/2.7886)	0.17/0.38/0/1	0.44/0.45/0.02/1.5	39.66	15.292
	8	(-0.0252/0.5989/-2.3958/1.6883)	0.24/0.42/0/1	0.50/0.53/0.03/1.5	33.88	4.369
	9	(0.0067/0.7795/-3.905/3.480)	0.05/0.27/0/1	0.86/0.57/0.02/1.5	40.51	34.953
	10	(-0.0061/0.5762/-3.1/2.491)	0.007/0.083/0/1	0.93/0.55/0.02/1.5	46	10.923
	11	(0.0105/0.4905/-2.0377/2.0833)	0.06/0.0818/0/1	0.66/0.46/0.03/1.77	57.8	15.292
	12	(0.0173/0.5790/-1.7230/2.6367)	0.40/0.49/0/1	0.53/0.46/0.02/1.5	17.5	6.554
	13	(-0.0062/0.7026/-2.7647/2.5694)	0.25/0.43/0/1	0.51/0.50/0.02/1.52	33.1	17.476
	14	(0.0231/0.485/-1.8722/1.3777)	0.08/0.27/0/1	0.26/0.13/0.04/1.51	67.4	10.923
	15	(0.001/0.6294/-2.4522/2.4110)	0.04/0.19/0/1	0.62/0.51/0.03/2.07	18.7	13.107
State & local Routes	1	(0.0012/0.6672/-2.7908/5.4036)	0.36/0.48/0/1	0.23/0.36/0.01/1.5	31.14	43.691
	2	(0.0128/0.5850/-2.6302/3.3680)	0.24/0.42/0/1	0.46/0.45/0.008/1.63	39.85	24.030
	3	(-0.0067/0.5509/-2.5195/2.4934)	0.32/0.47/0/1	0.48/0.41/0.01/1.62	43.97	21.845
	4	(-0.0045/0.5982/-3.0861/3.1)	0.02/0.16/0/1	1.25/0.43/0.03/1.78	76.74	32.768
	5	(0.0070/0.2776/-1.3715/1.7664)	0.07/0.0266/0/1	1.32/0.35/0.14/1.53	73	24.030

Notes:

1. Sample size = 713, 896 BSM records (N = 38 trips)
2. Descriptive statistics for 38 trips are presented as 5 trips were excluded from the analysis due to relatively shorter duration (i.e. less than 2 minutes) and no objects around the host vehicle were recorded by Mobile Eye sensor for such trips.
3. Acceleration/Deceleration are recorded in units of $^{m}/_{s^2}$; range in hundreds of feet; average speed in $^{m}/_{hr}$; and duration in minutes.

Next, the average trip duration for trips on freeway and state routes (N=4) is 27.8 minutes with maximum trip duration of 34.9 minutes (Table 2.2). Intuitively, trips on freeways and state routes are also high-speed trips with mean speed of 76.33 mph and maximum mean speed of 89.79 mph respectively (Table 2.2). In terms of duration and speed, trips on local roads (N=15) are observed to be both shorter and slower with average trip duration of 13.39 minutes and average speed of 37.98 mph respectively (Table 2.2). The trips on state and local routes follow similar distribution with mean duration of 29.27 minutes and average speed of 52.94 mph (as compared to average speed of 37.98 mph on local routes) (Table 2.2). Note that the detailed trip information and the geo-coded trajectories provided in SPMD (Henclewood, 2014) are not always from start to end of a trip, owing to issues related to privately identifiable data.

To see if the data is characterized by noise, appropriate visualizations are developed. To clarify the relationship between speeds and acceleration, distributions of acceleration are visualized against speed in the top panel of Figure 2.3. High speeds (>50-55 mph) are associated with smaller acceleration magnitudes as well as smaller dispersion (or volatility) in acceleration/deceleration values. The top right panel in Figure 2.3 shows the density scatter plot where the bandwidth of acceleration/deceleration values at high speeds is tighter than the bandwidth of acceleration/deceleration values at low speeds. This seems reasonable as vehicle engines should do more work to maintain the same acceleration at higher speeds to overcome increasing air resistance. Therefore, the ability to accelerate a vehicle decreases naturally at higher speeds (Liu and Khattak, 2016b, Wang et al., 2015).

To gain further insights regarding data quality, we analyze the distribution of longitudinal vs. lateral accelerations, and the relationship resembles a lozenge shaped distribution which implies that lateral and longitudinal accelerations (or decelerations) do not have large magnitudes simultaneously. Also, the instantaneous driving decisions in longitudinal and lateral directions seem to be inversely correlated with a Pearson correlation coefficient of -0.22, which is in agreement with previous literature (Wang et al., 2015). Such concordance again increases our confidence in the data.

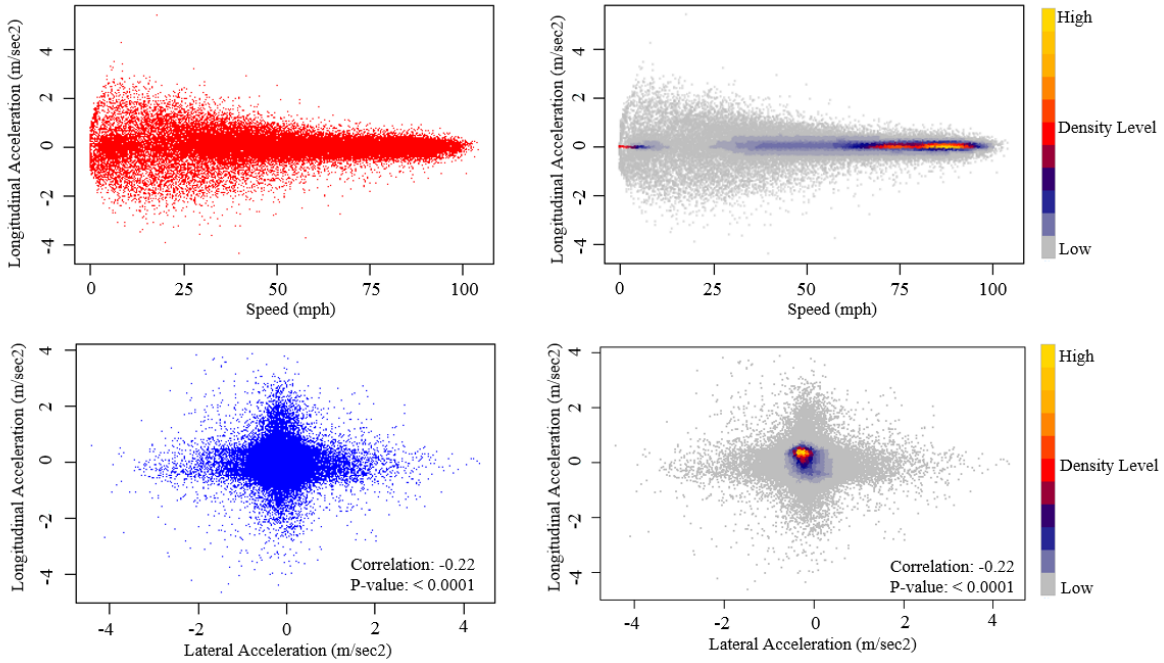

Figure 2.3 Distributions of speed, longitudinal, and lateral accelerations

2.5.2 Modeling Results

Data are used from 38 trips for further analyses[19], the total duration of which is 19.83 hours i.e. it is approximately half of the trip durations for overall 184 trips. As discussed in section 2.4.1, the data is aggregated at a frequency of 1 Hz (i.e., one BSM per second). Thus, in the present study, the regimes (s_t) are same for all 38 trips i.e., regime 1, and regime 2 in two-regime models, and regime 1, regime 2, and regime 3 in three-regime Markov switching models, and that the regimes (s_t) can change every one second. For ease of discussion, we first systematically present the results of two-regime dynamic Markov-switching models in section 2.6.1 followed by presenting results for the three-regime dynamic Markov-switching models in section 2.6.2.

2.5.2.1 Two-Regime Dynamic Markov Switching Models

We estimated 76 Markov switching regression models to analyze each trip separately, i.e. 38 constant-only instantaneous driving decision models for each trip and 38 instantaneous driving decision models with all explanatory variables. The analyses are conducted as:

- First, to observe the relationships and correlations, for each trip, we estimated simple Ordinary Least Square (OLS) regression models for modeling instantaneous driving decisions (response variable) as a function of number of objects around host vehicle and distance to closest object. Both explanatory variables were statistically significantly associated with modeling instantaneous driving decisions (response variable) at 95% confidence level.

[19] As mentioned earlier, detailed analysis is conducted for 38 trips (out of 43 trips) as 5 trips were excluded from the analysis due to relatively shorter duration (i.e. less than 2 minutes) and no objects around the host vehicle were recorded by Mobile Eye sensor for such trips.

- Second, to capture the evolution of driving behavior followed by time series, constant-only two-regime Markov Switching Dynamic Regression (MSDR) models were estimated for each trip. In the constant-only models, the intercept terms and variances[20] could switch between regimes. In other words, Eq. (4) was estimated. Constant-only models were developed to observe two regimes, regime-dependent means and the associated variances or volatilities. Table 2.3 illustrates the results of two-regime constant-only models for six trips, whereas Figure 2.4 illustrates the summary for constant-only models for all 38 trips. In Table 2.3, the regime-dependent means and variances are reported. Also, mean transition probabilities[21] (1→1, 1→2, 2→1, 2→2) are reported for the selected six trips, where 1→1 can be interpreted as estimated transitional probability of staying in regime 1 in the next period given the driver is observed in regime 1 in current period. Finally, mean durations of each regime are reported in Table 2.3 and Figure 2.4.
- For ease of discussion, we divide 38 trips (after estimating separate models) into two categories: 1) Category 1: trips on freeways, state routes, and freeway and state routes, and 2) Category 2: trips on local and state routes, and local routes.
- Finally, we estimate full two-regime Markov switching dynamic regression models with full specification as of Equation 2.6 i.e. $\boldsymbol{\theta} = [\mu_1, \mu_2, {\sigma_1}^2, {\sigma_2}^2, p_{1-2}, p_{2-1}, \beta_{s_t=1}, \beta_{s_t=2}]$. In this model, all estimable parameters (μ, σ, β) can switch between the two regimes of a specific driving cycle. Regarding regime-dependent variance term for the full models, we

[20] Intuitively, it would be unreasonable to assume that the variance in acceleration be equal to variance in deceleration. Thus, as a first step, two-regime constant-only models were developed with switching intercept-term only. Next, the variances were also allowed to switch between states. Finally, the model with switching intercept and variance term was selected as final model if variance terms were observed to be different in two regimes and statistically significant at 95% confidence level (Hamilton, 1994).

[21] Note that P(1→1) = 1 - P(1→2) and P(2→1) = 1 - P(2→2).

estimated models both with regime-dependent and regime-independent variance terms, and the model that resulted in best fit was selected (discussed later) (Hamilton, 1994). Table 2.4 illustrates the results of full models (including regime-dependent explanatory variables) for the same trips for which constant-only models are presented in Table 2.3. Furthermore, Table 2.5 and 2.6 summarizes the results of all specified two-regime models, for category 1 and category 2 trips, respectively. For all model parameters as identified in Equation 2.6, to summarize the distribution of estimated parameters for all trips, Table 2.5 and 2.6 present the mean, minimum, and maximum parameter estimates (βavg, βmin, βmax), standard deviation (Std.dev), and several percentile values (25^{th}P, 50^{th}P, 75^{th}P, and 90^{th}P), for category 1 and category 2 trips, respectively.

Table 2.3 Two-Regime Constant-Only Markov Switching Regression Models (six selected trips)

Constant-only Models		Freeway	Freeway	Freeway & State Route	Freeway & State Route	Local Route	Local Route
Acceleration-Regime 1	β	0.149	0.104	1.1297	0.147	0.2568	0.141
	z-score	16	5.23	26.01	12.61	6.01	7.93
Deceleration-Regime 2	β	-1.019	-1.104	-0.0163	-0.739	-1.412	-1.194
	z-score	-24.86	5.23	-2.69	-17.04	-11.19	-15.5
Regime 1 - Variance Parameter	β	0.4422	0.467	0.11635	0.377	0.6646	0.453
	Std. Error	0.0063	0.014	0.0021	0.007	0.028	0.012
Regime 2 - Variance Parameter	β	0.5811	0.341	0.1163	0.5323	0.6891	0.443
	Std. Error	0.0225	0.035	0.0021	0.0222	0.0715	0.05
Transition prob: 1→2	β	0.017	0.0144	0.0926	0.0284	0.0215	0.062
	Std. Error	0.0027	0.005	0.0506	0.0048	0.009	0.004
Transition prob: 2→2	β	0.8834	0.873	0.9979	0.8682	0.8763	0.866
	Std. Error	0.0179	0.04	0.0011	0.0213	0.0473	0.037
Expected Duration: Regime 1	β	58.58	69.12	10.7922	35.096	46.505	61.38
	95% Conf. Interval	43.0,79.9	34.6,139.0	4.0,32.8	25.1,49.0	20.0,109.5	34.4,110.1
Expected Duration: Regime 2	β	8.582	7.891	71.31	7.589	8.08	7.464
	95% Conf. Interval	6.3,11.6	4.3,15.2	59.1,81.1	5.5,10.4	4.0,17.7	4.4,13.2

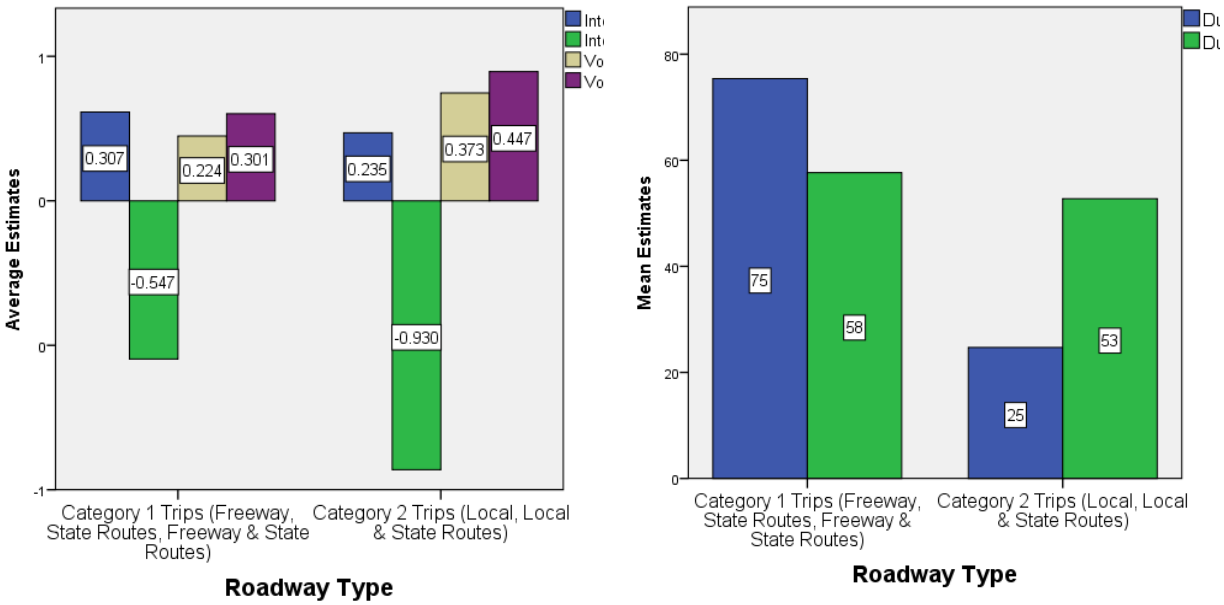

Figure 2.4 Summary of two-regime constant-only Markov switching regression models (all 38 trips).

Table 2.4 Two-Regime Full Markov Switching Regression Models (for six selected trips)

Full Models		Freeway	Freeway	Freeway & State Route	Freeway & State Route	Local Route	Local Route
Acceleration-Regime 1	Constant (std. error)	0.0666 (0.0159)	0.077 (0.031)	1.47 (0.082)	0.161 (0.019)	0.273 (0.051)	0.1172 (0.025)
	Objects indicator (std. error)	0.146 (0.020)	-0.083 (0.035)	-0.328 (0.086)	0.030 (0.015)	-0.320 (0.322)	0.229 (0.056)
	Range (std. error)	0.032 (0.017)	0.279 (0.131)	-0.349 (0.106)	-0.138 (0.037)	-0.084 (0.158)	0.041 (0.021)
Deceleration-Regime 2	Constant (std. error)	-1.494 (0.073)	-1.002 (0.094)	-0.051 (0.0124)	-0.806 (0.057)	-1.603 (0.180)	-1.183 (0.096)
	Objects indicator (std. error)	0.513 (0.080)	-0.063 (0.102)	0.0154 (0.006)	0.090 (0.051)	1.3707 (0.614)	0.559 (0.102)
	Range (std. error)	0.162 (0.073)	-0.546 (0.592)	0.041 (0.012)	-0.258 (0.099)	0.227 (0.097)	-0.169 (0.129)
Regime 1 - Variance Parameter	β	0.2265	0.466	0.229	0.402	0.665	0.401
	Std. Error	0.003	0.014	0.004	0.007	0.072	0.011
Regime 2 - Variance Parameter	β	0.2265	0.338	0.1145	0.201	0.655	0.456
	Std. Error	0.003	0.035	0.002	0.0035	0.072	0.033
Transition prob: 1→2	β	0.015	0.013	0.098	0.026	0.0206	0.017
	Std. Error	0.002	0.005	0.053	0.004	0.008	0.005
Transition prob: 2→2	β	0.846	0.878	0.997	0.845	0.8755	0.899
	Std. Error	0.022	0.04	0.001	0.024	0.048	0.027

Table 2.5 Summary of specified two-regime models for all trips taken on freeways, state routes, and freeway and state routes (Category 1 trips)

	Variable	βavg	Std.dev	βmin	βmax	25P	50P	75P	90P
Acceleration - Regime 1	Constant	0.366	0.457	0.013	1.475	0.055	0.129	0.518	1.240
	Objects indicator	-0.003	0.164	-0.328	0.460	-0.078	0.013	0.062	0.146
	Range	0.065	0.218	-0.330	0.608	-0.026	0.017	0.216	0.279
	Duration-Acc	49.659	38.157	10.180	150.713	19.100	40.060	72.494	105.312
	Sigma-Acc	0.203	0.119	0.074	0.466	0.121	0.150	0.248	0.461
Deceleration - Regime 2	Constant	-0.568	0.486	-1.494	-0.052	-0.994	-0.451	-0.109	-0.071
	Objects indicator	0.076	0.237	-0.272	0.548	-0.059	0.034	0.090	0.538
	Range	0.095	0.287	-0.546	0.665	0.025	0.064	0.162	0.658
	Duration-Dec	80.900	123.787	5.040	462.590	7.119	11.768	152.030	245.900
	Sigma-Dec	0.271	0.244	0.074	1.109	0.123	0.178	0.347	0.445
Transition Probabilities	1→1	0.918	0.065	0.802	0.998	0.859	0.915	0.993	0.995
	2→1	0.039	0.029	0.007	0.098	0.013	0.028	0.056	0.085

Notes: Objects indicator: 1 if ≥3 number of objects, 0 otherwise; Range: Distance to closest object in hundreds of feet; "Sigma" refers to variance of each regime i.e. $\sigma_1{}^2$ for regime-acceleration and $\sigma_2{}^2$ for regime-deceleration. 25P, 50P, 75P, 90P refers to 25th, 50th, 75th, and 90th percentile values of estimated parameters for all trips. βavg , βmin , βmax refers to mean, minimum, and maximum parameter estimate for all trips. Std. dev refers to standard deviation of mean parameter estimates (βavg).

Table 2.6 Summary of specified two-regime models for all trips taken on local and state, and local routes (Category 2 trips)

	Variable	βavg	Std.dev	βmin	βmax	25P	50P	75P	90P
Acceleration - Regime 1	Constant	0.344	0.441	-0.006	1.692	0.113	0.174	0.333	1.092
	Objects indicator	0.114	0.621	-1.519	2.122	-0.033	0.058	0.267	0.419
	Range	0.031	0.312	-0.814	0.701	-0.100	0.017	0.102	0.460
	Duration-Acc	43.443	33.034	5.558	146.36	19.76	38.10	54.40	80.490
	Sigma-Acc	0.337	0.147	0.112	0.615	0.216	0.333	0.429	0.551
Deceleration - Regime 2	Constant	-0.776	0.509	-1.604	-0.102	-1.189	-0.802	-0.228	-0.138
	Objects indicator	0.019	0.675	-2.167	1.371	-0.133	0.117	0.322	0.575
	Range	0.109	0.465	-1.077	1.028	-0.154	0.102	0.328	0.697
	Duration-Dec	29.255	42.197	5.472	147.32	8.061	10.34	23.31	110.60
	Sigma-Dec	0.424	0.248	0.112	1.018	0.226	0.401	0.538	0.812
Transition Probabilities	1→1	0.912	0.053	0.817	0.993	0.876	0.903	0.955	0.991
	2→1	0.043	0.043	0.007	0.180	0.018	0.026	0.055	0.097

Notes: Objects indicator: 1 if ≥3 number of objects, 0 otherwise; Range: Distance to closest object in hundreds of feet; "Sigma" refers to variance of each regime i.e. σ_1^2 for regime-acceleration and σ_2^2 for regime-deceleration. 25P, 50P, 75P, 90P refers to 25th, 50th, 75th, and 90th percentile values of estimated parameters for all trips. βavg , βmin , βmax refers to mean, minimum, and maximum parameter estimate for all trips. Std. dev refers to standard deviation of mean parameter estimates (βavg).

2.5.2.2 Three-Regime Dynamic Markov Switching Models

As discussed in detail in section 2.3.1., real-world driving is a complex task and we can anticipate existence of more than two regimes, say three regimes in a typical driving cycle. Thus, it is plausible to also investigate a more generic model specification that may capture common driving regimes, and thus can help in extracting important information related to instantaneous driving decisions embedded in real-world connected vehicle data. Having said this, we estimated 76 three-regime Markov switching regression models to analyze each trip separately, i.e., 38

constant-only three-regime instantaneous driving decision models for each trip and 38 three-regime instantaneous driving decision models with all explanatory variables i.e., full specification. The analyses are conducted as:

Like the two-regime Markov switching models, for ease of discussion in three-regime specification, we divide the trips (after estimating separate models) into two categories: 1) Category 1: trips on freeways, state routes, and freeway and state routes, and 2) Category 2: trips on local and state routes, and local routes.

To capture the evolution of driving behavior followed by time series, constant-only three-regime Markov Switching Dynamic Regression (MSDR) models are estimated for each trip. Specifically, the regimes are not observed i.e., we do not a-priori what are the three assumed regimes in a typical driving cycle. Like the two-regime constant only models, the intercept terms and variances can switch between the three regimes. In other words, Equations 2.7 and 2.8 are estimated. Constant-only models are developed to observe the three regimes, regime-dependent means and the associated variances or volatilities associated with each regime. Table 2.7 summarizes the results of three-regime constant-only models for all trips, whereas Figure 2.5 graphically illustrates the mean intercepts and the associated volatilities associated with each of the three regimes for all the trips. For all model parameters in three-regime constant only models, to summarize the distribution of estimated parameters for all trips, Table 2.7 also presents the mean, minimum, and maximum parameter estimates (βavg, βmin, βmax), standard deviation

Table 2.7 Summary of three-regime constant only models for all category 1 and category 2 trips.

	Regimes	Parameters	βavg	Std.dev	βmin	βmax	25P	50P	75P	90P
Freeway, State Routes, Freeway & State Routes (N = 14).[a]	High Rate Acc - Regime 1	Intercept	0.542	0.336	0.065	0.965	0.113	0.639	0.829	0.953
		Sigma (Volatility)	0.501	0.316	0.049	1.245	0.336	0.454	0.672	1.081
		Duration	10.006	3.503	5.903	16.589	6.889	8.833	12.913	15.772
	High Rate Dec - Regime 2	Intercept	-0.666	0.414	-1.576	-0.129	-0.936	-0.646	-0.264	-0.138
		Sigma (Volatility)	0.302	0.218	0.049	0.690	0.107	0.282	0.475	0.635
		Duration	7.651	3.241	3.749	15.489	4.987	7.143	8.866	14.020
	Cruise - Regime 3	Intercept	0.012	0.034	-0.059	0.059	-0.014	0.022	0.035	0.057
		Sigma (Volatility)	0.143	0.080	0.049	0.260	0.066	0.131	0.227	0.254
		Duration	33.991	35.978	9.422	138.165	15.717	18.400	41.081	110.32
Local, State and Local Routes (N = 14).[a]	High Rate Acc - Regime 1	Intercept	0.792	0.186	0.507	1.237	0.679	0.785	0.867	1.108
		Sigma (Volatility)	0.544	0.092	0.433	0.794	0.480	0.526	0.593	0.713
		Duration	9.566	2.575	5.946	13.139	7.464	8.940	12.495	12.908
	High Rate Dec - Regime 2	Intercept	-0.824	0.216	-1.310	-0.586	-0.945	-0.807	-0.624	-0.587
		Sigma (Volatility)	0.580	0.096	0.398	0.790	0.532	0.555	0.650	0.749
		Duration	9.050	2.081	5.364	12.895	7.147	9.594	10.588	12.132
	Cruise - Regime 3	Intercept	0.014	0.013	-0.019	0.038	0.007	0.012	0.021	0.033
		Sigma (Volatility)	0.137	0.061	0.056	0.312	0.106	0.127	0.160	0.245
		Duration	21.280	14.680	6.472	57.200	11.603	14.377	34.665	47.258

Notes: (a) Four category 1 and six category 2 trips are dropped due to failure in convergence of three-regime constant only models.

See footnote 23 for details

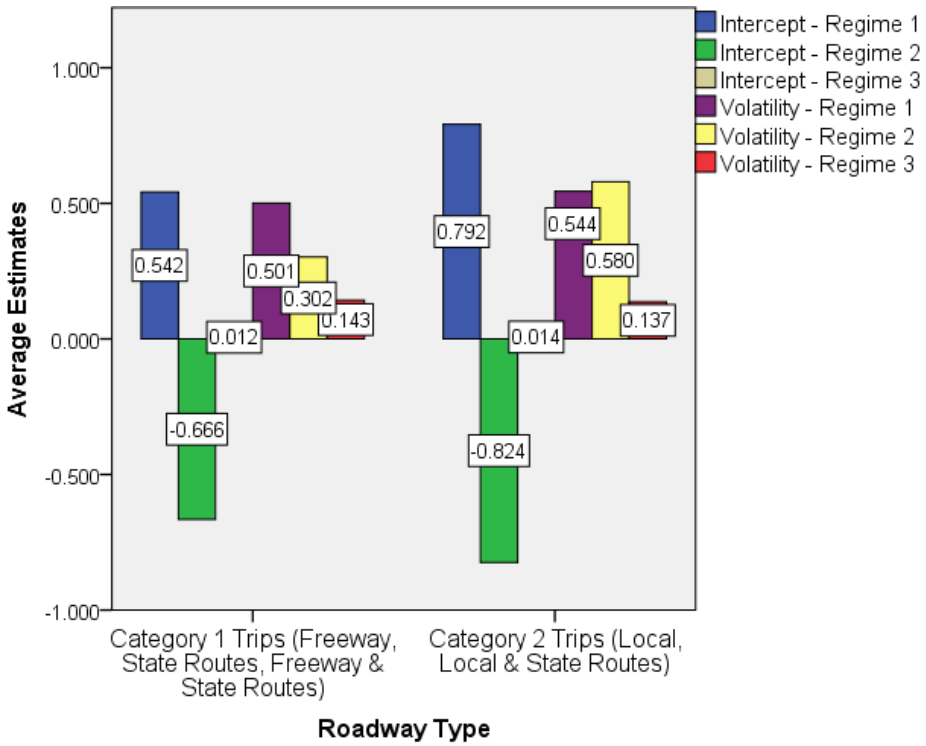

Figure 2.5 Summary of three-regime constant-only Markov switching regression models (all 38 trips).

(Std.dev), and several percentile values (25thP, 50thP, 75thP, and 90thP), for category 1 and category 2 trips, respectively[22,23]. Finally, for all the trips, we estimate full three-regime Markov switching dynamic regression models with full specification as of Equation 2.9 i.e., $\boldsymbol{\theta} = [\mu_1, \mu_2, \mu_3, \gamma_{s_t=1}, \gamma_{s_t=2}, \gamma_{s_t=3}, {\sigma_1}^2, {\sigma_2}^2, {\sigma_3}^2, p_{1-1}, p_{1-2}, p_{2-1}, p_{2-2}, p_{3-1}, p_{3-2}]$. In this model, all estimable parameters (μ, σ, β) can switch between the three regimes of a specific driving cycle. Regarding regime-dependent variance term for the full models, we estimated models both with

[22] The default algorithm we used for maximizing the likelihood functions for all trips in two-regime as well as in three-regime models is modified or quasi Newton-Raphson (NR) algorithm. The three-regime constant only models readily converged for 28 trips, however, for four category 1 trips and six category 2 trips, the three-regime constant only models did not converge. For these trips, we also tried other maximization algorithms such as Berndt-Hall-Hall-Hausman (BHHH), Davidon, Fletcher-Powell (DFP), and Broyden-Fletcher-Goldfarb-Shanno (BFGS) algorithms, however, the models did not converge. The failure of the quasi NR optimization (and other optimization methods) imply that the parameters of the specified three-regime models are not identified by the data, and this is common when attempting to fit a model with too many regimes (Stata, 2016).

[23] As such, 10 trips are dropped from the estimation sample which corresponds to 20,669 seconds (or 0.206 million BSMs) of driving data i.e., 29% of the data in total sample is dropped for the three-regime constant only models.

regime-dependent and regime-independent variance terms, and the model that resulted in best fit was selected.

Table 2.8 and 2.9 summarizes the results of full three-regime models (including regime-dependent explanatory variables) for category 1 and category 2 trips, respectively. Also, Table 2.8 and 2.9 present the mean, minimum, and maximum parameter estimates (β_{avg}, β_{min}, β_{max}), standard deviation (Std.dev), and several percentile values (25^{th}P, 50^{th}P, 75^{th}P, and 90^{th}P), for three-regime category 1 and category 2 trips, respectively[24]. Also, regime durations and mean transition probabilities[25] are reported (as in Equation 2.12) for all the trips, where for example, 3→1 can be interpreted as estimated transitional probability of staying in regime 3 in the next period given the driver is observed in regime 1 in current period.

[24] For fully-specified three-regime models (i.e., including regime dependent explanatory variables), the models did not converge for 14 trips (five category 1 trips and nine category 2 trips). As such, 14 trips are dropped for the estimation sample which corresponds to 14,830 seconds of driving data i.e., 21% of the data in total sample.

[25] Note that P (1→3) = (1 - P(1→1) – P(1→2)), P(2→3) = (1 - P(2→1) – P(2→2)), and P(3→3) = (1 - P(3→1) – P(3→2)).

Table 2.8 Summary of specified three-regime models for all trips taken on freeways, state routes, and freeway and state routes (Category 1 trips)

	Regimes	Parameters	βavg	Std.dev	βmin	βmax	25P	50P	75P	90P
Freeway, State Routes, Freeway & State Routes (N = 14). *	High Rate Acc - Regime 1	Intercept	0.693	0.393	0.040	1.239	0.383	0.788	0.943	1.200
		# of objects	-0.277	0.659	-2.359	0.184	-0.242	-0.075	0.011	0.155
		Range	-0.104	0.278	-0.549	0.423	-0.334	-0.126	0.027	0.382
		Sigma (Volatility)	0.330	0.202	0.061	0.676	0.109	0.345	0.512	0.638
		Duration	10.643	4.041	5.930	18.784	7.563	9.972	13.496	17.837
	High Rate Dec - Regime 2	Intercept	-0.811	0.569	-2.326	-0.147	-1.128	-0.686	-0.429	-0.162
		# of objects	0.164	0.450	-0.272	1.561	-0.018	0.055	0.216	1.050
		Range	0.206	0.534	-0.767	1.575	-0.080	0.188	0.430	1.160
		Sigma (Volatility)	0.324	0.178	0.061	0.578	0.124	0.387	0.450	0.560
		Duration	8.142	1.950	4.983	11.877	7.108	7.806	9.168	11.667
	Cruise - Regime 3	Intercept	-0.011	0.043	-0.070	0.078	-0.049	-0.001	0.019	0.057
		# of objects	-0.001	0.050	-0.144	0.054	-0.010	0.002	0.030	0.053
		Range	0.084	0.202	-0.116	0.694	-0.006	0.018	0.089	0.517
		Sigma (Volatility)	0.231	0.351	0.049	1.322	0.068	0.134	0.235	0.997
		Duration	37.969	36.668	8.152	128.455	16.128	17.742	59.744	113.23
	Transition Probabilities	1→1	0.029	0.039	0.000	0.126	0.002	0.019	0.028	0.114
		1→2	0.212	0.310	0.030	0.939	0.063	0.100	0.134	0.913
		2→1	0.810	0.220	0.084	0.915	0.842	0.871	0.890	0.913
		2→2	0.096	0.040	0.002	0.144	0.070	0.106	0.129	0.139
		3→1	0.090	0.250	0.003	0.920	0.010	0.025	0.034	0.567
		3→2	0.823	0.335	0.046	0.992	0.938	0.944	0.983	0.991

Note: (*) Five category 1 trips are dropped due to failure in convergence of three-regime fully specified models. See footnote 24 for details.

Table 2.9 Summary of specified three-regime models for all trips taken on local and state, and local routes (Category 2 trips)

	Regimes	Parameters	βavg	Std.dev	βmin	βmax	25P	50P	75P	90P
Local, State and Local Routes (N = 14). *	High Rate Acc - Regime 1	Intercept	0.764	0.156	0.499	0.948	0.612	0.852	0.887	0.936
		# of objects	-0.259	0.690	-1.859	0.251	-0.226	0.005	0.150	0.249
		Range	-0.121	0.265	-0.825	0.085	-0.188	-0.025	0.056	0.084
		Sigma (Volatility)	0.503	0.125	0.280	0.792	0.459	0.486	0.552	0.754
		Duration	9.756	2.874	5.588	13.237	7.111	8.985	12.654	13.186
	High Rate Dec - Regime 2	Intercept	-0.771	0.273	-1.039	-0.166	-1.018	-0.789	-0.650	-0.223
		# of objects	0.058	0.210	-0.221	0.403	-0.167	0.078	0.204	0.379
		Range	0.013	0.450	-1.031	0.808	-0.183	0.059	0.194	0.721
		Sigma (Volatility)	0.552	0.098	0.393	0.787	0.497	0.538	0.561	0.758
		Duration	9.345	1.721	6.876	11.947	7.842	9.964	10.727	11.863
	Cruise - Regime 3	Intercept	0.020	0.052	-0.006	0.176	-0.001	0.003	0.018	0.145
		# of objects	-0.079	0.212	-0.697	0.072	-0.092	-0.005	0.010	0.063
		Range	-0.022	0.107	-0.335	0.067	-0.014	0.005	0.019	0.061
		Sigma (Volatility)	0.111	0.034	0.054	0.158	0.095	0.111	0.142	0.155
		Duration	17.606	10.541	7.322	37.475	10.235	14.665	24.588	37.220
	Transition Probabilities	1→1	0.021	0.024	0.000	0.080	0.000	0.020	0.029	0.071
		1→2	0.089	0.033	0.033	0.150	0.076	0.083	0.114	0.144
		2→1	0.889	0.021	0.855	0.916	0.872	0.900	0.906	0.916
		2→2	0.062	0.019	0.032	0.086	0.038	0.063	0.078	0.086
		3→1	0.042	0.019	0.021	0.087	0.024	0.040	0.051	0.081
		3→2	0.926	0.035	0.863	0.973	0.902	0.932	0.959	0.973

Note: (*) Nine category 1 trips are dropped due to failure in convergence of three-regime fully specified models. See footnote 24 for details.

2.6 DISCUSSION

In this section, we discuss the results of two-regime and three-regime dynamic Markov switching models. First, the results of two-regime (constant only and models including all explanatory factors- Tables 2.3 through 2.6 are discussed followed by a discussion on three-regime Markov switching models (Tables 2.7 through 2.9).

2.6.1 Two Regime Dynamic Markov Switching Models

2.6.1.1 Two-Regime Constant-Only Models (Table 2.3 and Figure 2.4)

The constant-only models are developed to investigate whether the volatility of entire driving cycle is sensitive to regimes, i.e. single estimate of variance for the entire driving cycle or is volatility (variance terms) regime dependent? The modeling results (Table 2.3 and Figure 2.4) reveal an important finding—that two distinct yet unobserved regimes, acceleration and deceleration, exist and the empirical data strongly favor Markov switching dynamic regression models[26]. Wald tests of linear restrictions were conducted for all 38 constant-only models (for 38 trips), testing the coefficients for intercepts in two regimes for equality (null hypothesis). For all 38 trips, with 99.5% confidence, the null hypothesis was rejected in favor of alternative

[26] Note that the two-regimes were unobserved in the sense that we did not assume a-priori before estimation that acceleration and deceleration are two distinct regimes of a typical driving cycle. Instead, we let the Markov switching framework identify two distinct regimes from data. As an example, some possibilities regarding the two regimes could be, acceleration and deceleration, low and high rate acceleration, low and high rate deceleration, and so on. After estimating the Markov switching models, we eventually learned that acceleration and deceleration are the two typical regimes that characterize a typical driving cycle. Similar to the original Hamilton's Markov switching application to US gross national product data (Hamilton, 1994), we reached this conclusion based on the positive and negative statistically significant intercept terms in the two regimes (Figure 2.4). However, a positive intercept in regime 1 does not necessary mean that regime 1 is wholly characterized by positive values (i.e., acceleration values). It may be the case that regime 1 (which is identified as acceleration) still contain acceleration values near to zero or negative values near to zero, however, the average intercept term is positive and which makes us conclude that on-overage acceleration is regime 1, and vice versa for regime 2 (i.e., deceleration) (Hamilton, 1994). The concept of unobserved yet distinct regimes will become further clearer in case of three-regime models which are discussed later.

hypothesis, i.e. the differences in intercept values in two regimes are non-zero (Kodde and Palm, 1986). The existence of two distinct regimes in typical driving cycles (both for category 1 and 2 trips) is shown by the mean positive coefficients for regime 1 (Figure 2.4), and mean negative coefficient for regime 2 for the same trips (Figure 2.4). Relevant findings are listed below:

- While Table 2.3 presents results of Markov switching models for six trips as illustration, similar results were obtained for all 38 sampled trips. By examining the results for all 38 trips in Figure 2.4, for category 1 trips, the mean acceleration (for all 18 trips) is 0.307 m/sec^2 as opposed to mean deceleration of -0.547 m/sec^2. Note that for all sampled trips (38 trips), the coefficients for intercept terms were consistently positive and negative, for the two regimes, indicating the existence of two distinct regimes in typical driving cycles. Results show that compared to acceleration, drivers decelerate at a higher rate (intercepts of 0.307 m/sec^2 vs -0.547 m/sec^2). However, for category 2 trips (Figure 2.4), the difference between magnitudes of mean acceleration (regime 1) and mean deceleration (regime 2) is relatively large, i.e., mean acceleration (for all 20 trips) is 0.235 m/sec^2 whereas mean deceleration is -0.930 m/sec^2. This finding indicates that on local routes, drivers may decelerate frequently (and at higher rates) due to presence of traffic controls, i.e., signals, stop signs, and yield signs.
- Importantly, for both category 1 and category 2 trips (Figure 2.4), deceleration is statistically significantly more volatile than acceleration, noting mean ${\sigma_1}^2$ of 0.224 vs. mean ${\sigma_2}^2$ of 0.301 for category 1 and mean ${\sigma_1}^2$ of 0.373 vs mean ${\sigma_2}^2$ of 0.417 for category 2 (Figure 2.4). One explanation for this important finding can be that drivers react faster to hazardous or difficult situations, e.g. obstruction or a hard-braking car in

front, by decelerating harder as compared to their reaction to more non-hazardous conditions, e.g., an open road with no other vehicles.

- Figure 2.4 also summarizes the mean duration that driver stays in each regime. For example, for category 1 trips, on average, drivers spend more time accelerating (75 seconds) as compared to decelerating (58 seconds). Finally, referring to Table 2.3, as expected, it can be observed that both regimes i.e. acceleration and deceleration are highly persistent i.e. mean $1 \rightarrow 1$ probabilities of 0.91 and 0.88 for category 1 and 2 trips respectively (Table 2.3).

2.6.1.2 Two-Regime Specified Models (Table 2.4 to 2.6)

The number of objects and distance to the closest object were added as potential regime-dependent explanatory variables. Like constant-only models, implementation of Markov switching dynamic regression with explanatory variables still support the existence of two distinct regimes. The results in Table 2.4 suggest that the associations of explanatory variables are significantly different and distinct in two regimes. Drivers respond differently to increasing objects in the acceleration regime as they respond to such a situation during deceleration regime. Wald tests of linear restriction for all 38 trips confirmed this finding[27] (Kodde and Palm, 1986).

Note that a positive sign of the mean parameter estimate in the acceleration regime (Table 2.4) indicates that an increasing magnitude of acceleration is associated with an increase in explanatory variable, e.g., presence of greater than three objects around the host vehicle.

[27] Wald tests of linear restrictions for all 38 full models were conducted. Specifically, the coefficients for intercepts and β for explanatory variables in two regimes were tested for equality (null hypothesis). For all 38 trips, at 99.5% confidence level, the null hypothesis was rejected in favor of alternative hypothesis i.e. the differences in intercept and β terms in two regimes are non-zero (Kodde and Palm, 1986).

However, a positive sign of the parameter estimate in the deceleration regime indicates decrease in absolute magnitude of deceleration with increase in explanatory variable, e.g., presence of more objects. This association is characterized by a ↓ sign (negative association) in Table 2.10, which summarizes the associations (accounting for statistical significance at 95% confidence level) of explanatory variables with two regimes for all trips. A negative sign of parameter estimates in Table 2.4 in the deceleration regime indicates increase in absolute magnitude of deceleration (i.e. a negative value added with negative response value) with unit increase in explanatory variable. This association is conceptualized with ↑ sign (positive association) in Table 2.10.

2.6.1.2.1 Category 1 trips undertaken on freeways, state, and freeway and state routes

The results of full models for category 1 trips are summarized in Table 2.5, while summary of direction of effects for all trips is presented in Table 2.10. The results suggest that deceleration is high rate regime (as compared to acceleration) with mean intercept estimate of -0.368 m/sec^2. Furthermore, similar to the results from constant-only models, deceleration is observed statistically significantly more volatile than acceleration (mean ${\sigma_1}^2$ of 0.203 for acceleration vs mean ${\sigma_2}^2$ of 0.271 for deceleration) (Table 2.5).

Turning to the estimation results for category 1 trips (Table 2.5), in the acceleration regime, on average the number of objects is positively associated with driver propensity to accelerate; note that 50th Percentile β is 0.013 in Table 2.5. Moreover, the association between Objects indicator and acceleration-regime is statistically significantly positive for 8 trips, whereas it is statistically

significantly negative for 6 trips[28] (Table 2.10). The difference in associations of Objects indicator (positive for 44.44% and negative for 33.33% of trips) on driver's propensity to accelerate in the regime 1 may be an outgrowth of drivers having different perceptions regarding their surrounding and thus may make different decisions that match their preferences. However, if a driver is observed to be in the deceleration regime, then the Objects indicator (on average) is negatively associated with driver propensity to decelerate, or indirectly driver is observed to decelerate at a lower rate or even accelerate (i.e. βavg = 0.076 in Table 5). For the association between Objects indicator and deceleration-regime, it is statistically significantly negative for 11 (61.11%) trips, and positive for only 3 (16.66%) trips, and statistically insignificant for 4 (22.22%) trips (Table 2.10). Both above findings suggest drivers' tendency (on-average) to get out of crowded situations (characterized by greater than or equal to 3 number of objects around host vehicle) by accelerating (if driver is in acceleration regime) or to decelerate at a lower rate or even accelerate, if a driver is in deceleration regime.

An increase in distance (in feet) to closest object (Range) is associated with an increase in acceleration, noting that βavg = 0.065 in the acceleration regime (Table 2.5). Drivers tend to accelerate when they have more space around them and can freely maneuver their vehicle. Despite the heterogeneity in associations of the Range variable in the deceleration-regime (Ahmed et al., 2017, Khattak et al., 2016, Li et al., 2017, Mannering and Bhat, 2014, Mannering et al., 2016, Wali et al., 2017a, Wali et al., 2018b, Wali et al., 2018c, Wali et al., 2018d, Wali et

[28] We remind that results presented throughout hold for the two categories of trips, category 1 and 2, and not for specific roadway types per se. For example, among all the 18 trips in category 1, four trips are undertaken on a mixture of freeway and state routes. Thus, the results presented may not be entirely generalizable for trips on freeways only.

al., 2018e), it is generally statistically significantly negative for 10 trips (55.55%) and positive association for only 5 trips (27.77%) (Table 2.10).

2.6.1.2.2 Category 2 trips undertaken on local and state, and local only routes

Table 2.6 presents specified models for category 2 trips, and the direction of associations for all trips is presented in Table 2.10. Similar to category 1 trips where deceleration is the observed high rate regime compared to acceleration, for category 2 trips (i.e. particularly trips on lower functional classification roads), the mean intercepts for acceleration- and deceleration-regime vary significantly i.e., 0.344 m/sec^2 vs. -0.776 m/sec^2. Likewise, deceleration is more volatile than acceleration as indicated by ${\sigma_1}^2$ of 0.337 for acceleration and ${\sigma_2}^2$ of 0.424 for deceleration (Table 2.6).

Table 2.6 shows that parameter estimates for object indicator and range are all significantly different between two regimes for category 2 trips. The magnitudes of differences are reasonable, and partly attributable to the fluctuating traffic conditions due to traffic signals and stop or yield signs on lower classification roads. In the acceleration regime, Object indicator and the Range variable are associated with an increase in acceleration, with βavg of 0.114 and 0.031 for Objects indicator and Range, respectively (Table 2.6). The positive associations between objects indicator and acceleration are fairly consistent across sampled trips in sense that for object indicators, the association is positive for 7 (35%) trips and negative for only 2 trips (10%) and statistically insignificant for the rest of the trips (Table 2.10). The consistent finding for Object indicator is that drivers (on-average) prefer to accelerate given more objects around them on local routes. This finding agrees with the one in category 1 trips, showing that drivers (on-

average) tend to get out of crowded situations. For trips on local roads, the finding that increase in Range is associated with drivers' tendency to accelerate is also intuitive, as larger space around the host vehicle will enable drivers to maneuver the vehicles freely. However, this finding is not conclusive in the sense that the association between range and acceleration is positive for 30% of sampled trips whereas it is negative for 25% of the sampled trips, and this requires further investigation.

In the deceleration regime, the Objects indicator is negatively associated with deceleration, i.e. with three or more objects around them, drivers on-average tend to accelerate as indicated by βavg of 0.019. This finding is again in agreement with the ones observed for category 1 trips. Also, in deceleration regime, the negative association between objects indicator and deceleration holds true for 9 trips while it is positive for only 4 trips (Table 2.10). Finally, in the deceleration regime, increase in Range is associated with drivers' propensity to accelerate, as expected, and the finding seems conclusive in the sense that drivers in 60% of the sampled trips accelerated with increasing distance to the nearest object (Table 2.10).

Table 2.10 Two-Regime Markov Switching Models - Summary of direction of effects for all trips

Roadway Type	**Driving Regimes**	**Variable**	↑	↓	**Not Significant at 95% CL**
Freeways & State Routes (N = 18 trips)	Acceleration	Constant	18 *(100%)*	0 *(0%)*	0 *(0%)*
		Objects indicator	8 *(44.44%)*	6 *(33.33%)*	4 *(22.22%)*
		Range	10 *(55.55%)*	5 *(27.77%)*	3 *(16.66%)*
	Deceleration	Constant	0 (0%)	18 *(100%)*	0 *(0%)*
		Objects indicator	3 *(16.66%)*	11 *(61.11%)*	4 *(22.22%)*
		Range	2 *(11.11%)*	11 *(61.11%)*	5 *(27.77%)*
Local, State & Local Routes (N = 20 trips)	Acceleration	Constant	19 *(95%)*	0 *(0%)*	1 *(5%)*
		Objects indicator	7 *(35%)*	2 *(10%)*	11 *(55%)*
		Range	6 *(30%)*	5 *(25%)*	9 *(45%)*
	Deceleration	Constant	0 *(0%)*	20 *(100%)*	0 *(0%)*
		Objects indicator	4 *(20%)*	9 *(45%)*	7 *(35%)*
		Range	5 *(25%)*	12 *(60%)*	3 *(15%)*

Note: Row-wise percentages sum up to 100.

2.6.2 Three Regime Dynamic Markov Switching Models

2.6.2.1 Three-Regime Constant-Only Models (Table 2.7 and Figure 2.5)

The three-regime constant-only models are developed to identify the three regimes in a typical driving cycle, volatilities associated with each regime, and whether the volatility of entire driving cycle is sensitive to regimes, i.e. single estimate of variance for the entire driving cycle or is volatility (variance terms) regime dependent?

For Category 1 trips, i.e., trips on freeways, state routes, and freeway and state routes, the modeling results (in Table 2.7 and Figure 2.5) reveal that the mean intercepts for regime 1, 2, and 3 are 0.542, -0.666, 0.012 respectively. Based on these average intercept values, and its higher magnitudes, regime 1, 2, and 3 can be conceptualized as high rate acceleration, high rate

deceleration, and constant/cruise state respectively[29,30]. Moreover, drivers' on-average tend to decelerate at a higher rate than their rate of acceleration (βavg of -0.666 vs 0.542). Note that for all sampled trips (38 trips), the coefficients for intercept terms were statistically significant, and were consistently positive, negative, and near zero for the three regimes, indicating the existence of three distinct regimes in typical driving cycles. Regarding the volatility associated with each regime in category 1 trips, high rate acceleration is the most volatile ($\sigma_1{}^2$ = 0.501) followed by high rate deceleration ($\sigma_2{}^2$ = 0.302) and cruise/constant regime ($\sigma_3{}^2$ = 0.143). Overall, this finding intuitively suggests that compared to cruise/constant regime, drivers instantaneous driving decisions are more volatile both in "high-rate" acceleration as well as "high-rate" deceleration regime.

For Category 2 trips, i.e., trips on local, local & state routes, the modeling results (in Table 2.7 and Figure 2.5) reveal that the mean intercepts for regime 1, 2, and 3 are 0.792, -0.824, 0.014 respectively. Based on these statistics, we identify the three regimes as high-rate acceleration, high-rate deceleration, and cruise/constant regime. Again, and intuitively, drivers tend to decelerate at higher rates than their rates of acceleration (Figure 2.5). However, in case of

[29] Note that the mean intercept values for acceleration and deceleration (0.542 and -0.666) in three-regime specification are higher than the mean intercept values for acceleration and deceleration (0.307 and -0.547) in two-regime specification.

[30] Like the two-regime specification, the regimes in three-regime specification are unobserved i.e., by simply observing our dependent variable (column vector containing acceleration/deceleration values) directly we cannot know a-priori what the three regimes are. Note that in the two-regime case, it happened to be that by directly observing our response outcome, one could have expected acceleration and deceleration as two regimes. However, in case of three regimes, by visually inspecting the response outcome, it is impossible to infer exactly what the three regimes are and the cut-off points where the regimes change or switch. There can be several possibilities: e.g., 1) cruise state, low rate acceleration, and high rate acceleration, 2) cruise state, low rate deceleration, and high rate deceleration, and so on. It is only after application of Markov-switching models that we can mathematically quantify the three regimes by a data-driven approach, and the average cut-off points associated with each regime from the data at hand. Once the regimes are identified, the correlations between response outcome in each regime and explanatory factors are modeled separately in each regime. The concept of unobserved regimes in Markov switching framework is explicitly explained by (Hamilton, 1994).

category 2 trips, high-rate deceleration ($\sigma_2{}^2$ = 0.580) is the most volatile regime followed by high-rate acceleration ($\sigma_1{}^2$ = 0.544), and cruise/constant regime ($\sigma_3{}^2$ = 0.137). Also, for category 2 trips, the magnitudes of the high rate acceleration and high rate deceleration regimes are higher than the corresponding magnitudes for trips on freeways, state routes, and freeway and state routes (Category 1 trips) (Figure 2.5). This shows that, given high rate regimes, drivers accelerate and decelerate at higher rates on local roads compared to high rate accelerations and decelerations on freeways.

2.6.2.2 Three-Regime Specified Models (Table 2.8 and 2.9)

For the specified three-regime models, number of objects surrounding the host vehicle and distance to the closest object are added as potential regime-dependent explanatory variables. Overall, the results in Table 2.8 and 2.9 support the existence of three distinct driving regimes for category 1 and category 2 trips, after controlling for context specific explanatory factors. Like the constant-only three-regime models, the three regimes in specified models can be conceptualized as high-rate acceleration, high-rate deceleration, and constant/cruise regime (Table 2.7 and 2.8). Also, the correlations between explanatory factors and instantaneous driving decisions are significantly different and distinct in the three-regime specified models (Table 2.8 and 2.9). Wald tests of linear restriction for all the trips confirmed this finding where the coefficients for intercepts and $\beta's$ for explanatory variables in the three regimes were tested for equality (null hypothesis) and the null hypothesis was rejected for all the trips at 99.5% confidence level (Kodde and Palm, 1986).

Finally, Table 2.11 summarizes the correlations (accounting for statistical significance at 95% confidence level) between explanatory factors and the instantaneous driving regimes. A positive sign of the mean parameter estimate in the high-rate acceleration regime (Table 2.8) will indicate drivers' tendency to accelerate (on-average) with an increase in value of explanatory variable. However, a positive sign of the parameter estimate in the high-rate deceleration regime (Table 2.8) will indicate a decrease in absolute value of deceleration with increase in a value of explanatory value. This association is characterized by a ↓ sign (negative association) in Table 2.11. Likewise, a negative sign of parameter estimate in the high-rate deceleration regime (Table 2.8) will indicate an increase in absolute magnitude of deceleration (i.e. a negative value added with negative response value) with unit increase in explanatory variable. This association is thus conceptualized with ↑ sign (positive association) in Table 2.11.

2.6.2.2.1 Category 1 trips undertaken on freeways, state, and freeway and state routes

Before discussing the results of specified three-regime models, we note that five category 1 trips and nine category 2 trips were dropped from the sample due to non-convergence in model estimation. As discussed in section 2.5.5.2, 21% of the data in total sample is lost. However, for the trips for which the individual models converged, the results provide deeper insights (compared to two-regime models) into the correlation mechanism between instantaneous driving regimes and context-specific situational factors. The results of specified three-regime models (Table 2.8) suggest that in high-rate acceleration regime, the number of objects surrounding the host vehicle and the distance to the nearest object on average are negatively correlated with driver's propensity to stay in high-rate acceleration at next instant of time (βavg of -0.257 and -0.121 respectively). This seems intuitive as drivers on average, irrespective of their surroundings, may not stay in high-rate acceleration regime given that they are already in high-rate acceleration

Table 2.11 Three-Regime Markov Switching Models - Summary of direction of effects for all trips

Roadway Type	**Driving Regimes**	**Variable**	↑	↓	**Not Significant at 95% CL**
Freeways & State Routes (N = 13 trips)	High Rate Acceleration-Regime 1	Constant	13 *(100%)*	0	0
		Objects indicator	2 *(15.4%)*	6 *(46.2%)*	5 *(38.5%)*
		Range	3 *(23.1%)*	7 *(53.8%)*	3 *(23.1%)*
	High Rate Deceleration - Regime 2	Constant	0	13 *(100%)*	0
		Objects indicator	3 *(23.1%)*	6 *(46.2%)*	4 *(30.8%)*
		Range	2 *(15.4%)*	8 *(61.5%)*	3 *(23.1%)*
	Constant/Cruise around 0 - Regime 3	Constant	3 *(23.1%)*	6 *(46.2%)*	4 *(30.8%)*
		Objects indicator	4 *(30.8%)*	2 *(15.4%)*	7 *(53.8%)*
		Range	8 *(61.5%)*	1 *(7.7%)*	4 *(30.8%)*
Roadway Type	**Driving Regimes**	**Variable**	↑	↓	**Not Significant at 95% CL**
Local, Local & State Routes (N = 11 trips)	High Rate Acceleration-Regime 1	Constant	11 (100%)	0	0
		Objects indicator	2 *(18.2%)*	4 *(36.4%)*	5 *(45.5%)*
		Range	1 *(9.1%)*	4 *(36.34%)*	6 *(54.5%)*
	High Rate Deceleration - Regime 2	Constant	0	11 *(100%)*	0
		Objects indicator	1 *(9.1%)*	4 *(36.3%)*	6 *(54.5%)*
		Range	1 *(9.1%)*	6 *(54.5%)*	4 *(36.4%)*
	Constant/Cruise around 0 - Regime 3	Constant	1 *(9.1%)*	1 *(9.1%)*	9 *(81.8%)*
		Objects indicator	3 *(27.2%)*	4 *(36.3%)*	4 *(36.3%)*
		Range	3 *(27.2%)*	2 *(18.1%)*	6 *(54.5%)*

regime, and/or the ability to accelerate more at higher rates may be limited. Furthermore, the association between objects indicator and high-rate acceleration regime is statistically significantly negative for 46.2% (as opposed to positive correlation for 15.4% of trips) of the trips. Likewise, the association between range and high-rate acceleration is negative for 53.8% of category 1 trips (compared to only 23.1% of trips where the correlation is positive) (Table 2.11). Likewise, given that driver is in high-rate deceleration regime at current instant of time, the results suggest that with increase in number of objects and distance to the nearest object, drivers on-average are less likely to decelerate further at next instant of time, or drivers indirectly decelerate at a lower rate or can even accelerate at next instant of time.This result is intuitive and

is reflected by the positive βavg of 0.058 and 0.013 for object indicator and range respectively (Table 2.8). Moreover, the relationship between object indicator and high-rate deceleration is negative for 46.2% of the trips (compared to 23.1% of trips with positive correlation), whereas the relationship between range and high-rate deceleration is negative for 61.5% of the trips (compared to only 15.4% of trips with positive association). These findings collectively suggest that in high-rate deceleration regime, drivers (on-average) tend to get out of crowded situations (characterized by greater number of objects around host vehicle) by decelerating at a lower rate or even accelerate at next instant of time.

Finally, and intuitively, if a driver is in cruise/constant regime at current instant of time, with increasing number of objects around host vehicle and/or with increasing distance to the nearest object s(he) is more likely to accelerate (on average) at next instant of time. Moreover, the statistically significant positive associations between range and constant/cruise regime hold for 61.5% of the sampled trips, compared to only 7.7% of the trips where the correlation between range and cruise/constant regime is negative Table 2.11).

2.6.2.2.2 Category 2 trips undertaken on local, local and state routes

- Similar to the results for category 1 trips, the results for category 2 trips suggest that in high rate acceleration regime, increase in both object indicator and range are on-average negatively associated with drivers' tendency to stay in high-rate acceleration regime at next instant of time. As discussed earlier, this may be attributed to the fact that vehicle's ability to accelerate further may be constrained given that vehicle is already in high rate regime.

- For high-rate deceleration regime, our results suggest that increase in number of objects around host vehicle and increase in distance to the nearest object are both negatively associated with drivers' tendency to decelerate further at next instant of time. This is reflected in the average βs of 0.058 and 0.013 for object indicator and range respectively (Table 2.9). Furthermore, the negative association between object indicator and high-rate deceleration regime holds for 36.3% of the sampled trips whereas the negative association between range and high-rate deceleration regime holds for 54.5% of the sampled trips (Table 2.11). Note that the associations between the explanatory factors and high-rate deceleration regime are positive only for 9.1% of the sampled trips (Table 2.11).

2.6.3 Short-Term Regime Predictions

Markov switching models have a flexible structure for predicting unobserved regimes. Driving regimes can be predicted during each time period (Hamilton, 1993). For details regarding forecasting Markov-switching models by different probability estimation methods, interested readers are referred to (Hamilton, 1993). For demonstration, we use the two-regime model specification for estimating smoothed probabilities that predict the regimes at each time period using all sample data (Hamilton, 1993)(Figure 2.6). The switching model considers different regime-specific correlations, i.e. instantaneous driving contexts. Figure 2.6 illustrates the key elements of short-term regime predictions for a 25-minutes trip undertaken on I-94 freeway in Ann Arbor, Michigan. The first panel illustrates the time-series acceleration/deceleration cycle for the entire trip; the second panel illustrates the regime-specific variance; and the last panel illustrates the smoothed probabilities of observing a process in a specific regime at any instant of time. Note that the lowest magnitudes of variance shown in circles correspond to the acceleration

regime and vice versa, indicating that deceleration regime is more volatile than acceleration. While the results for all other trips are not presented, they are largely similar.

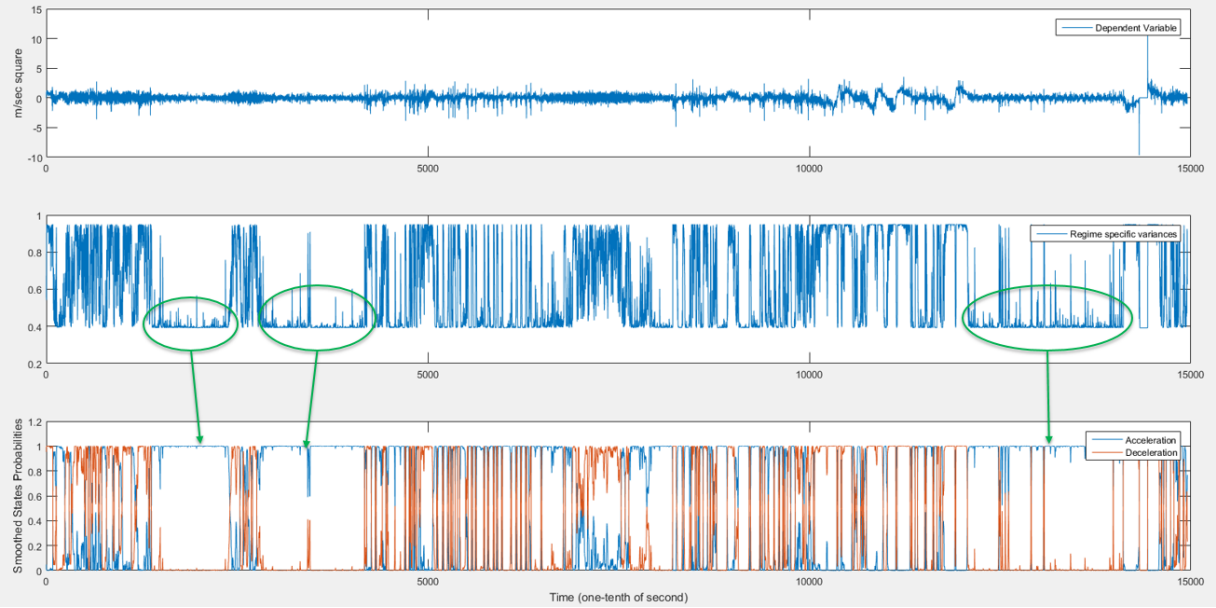

Figure 2.6 Short term prediction of driving regimes

2.7 LIMITATIONS/FUTURE WORK

The study is based on a limited number of trips. It is important to note that this study analyzes micro time-series instantaneous driving decisions during trips, but the application makes it difficult to use the entire large-scale database. Moreover, to extract critical information at the micro-level, each trip should be analyzed separately with two- and three-regime model specifications. Utilization of data from all trips for individual analysis is computationally demanding coupled with the difficulty of interpreting the results in a concise and effective manner. However, once the relationships are established at the microscopic level, it should be easier to predict short-term decisions. Even though the analyzed trips (N = 43) are randomly selected, one-day sample data may not be sufficient for conclusive results. While a two-month SPMD sample dataset is available through the Research Data Exchange (RDE, https://www.its-

rde.net/home) website, that data cannot be used due to a substantial number of missing observations about instantaneous driving contexts, i.e. number of objects surrounding host vehicles. Also, the model specification is limited, but it can be enhanced by exploring correlates with other variables when such data become available. Also, we acknowledge that if the "type" of the nearest object could be identified, it could have helped in extracting richer insights. In future, with availability of more detailed data about the type of nearest object, the methodology proposed in this study can be extended to understand how different types of nearest objects may influence the instantaneous driving decisions of host vehicle's driver.

Another important consideration relates to the positions of the vehicles surrounding the host vehicle. Conceptually, both greater number of vehicles around the host vehicle as well as the placement/direction of the vehicles surrounding the host vehicle can influence the drivers' instantaneous driving decisions. To further elaborate the potential influence of vehicles' placement surrounding the host vehicle (social envelope) on the instantaneous driving decisions of the host vehicle, Figure 2.7 is presented below (Khattak et al., 2015). For details about social interaction and/or gossip algorithms for modeling large-scale behavioral systems, see (Karan and Chakraborty, 2016, Srinivasan et al., 2017, Karan and Chakraborty, 2015). The overall driver behavior estimation can be conceptualized as a Markov Decision Process (MDP) (Khattak et al., 2015). Throughout a typical driving task, the driver is required to optimize his/her policy of instantaneous driving decisions (acceleration/deceleration) based on the number of vehicles surrounding the host vehicle and their placement. For simplicity, assume that the host vehicle is traveling on a three lanes roadway segment. Figure 2.7a illustrates the time complexity of the driver's policy optimization process. Depending on the number of features (slots around the host

vehicle where a vehicle can be present or otherwise) considered, the MDP states grow in the order of 2^n, where n is the number of features considered. With eight features considered (Figure 2.7a), the possible number of MDP states are 256. Figure 2.7c through 2.7e present few of the possible MDP states. When the host vehicle is surrounded by greater number of vehicles, one can expect that the host driver will accelerate (as our analysis suggests) but only if the slot in front of the host vehicle is empty (Figure 2.7c and 2.7d). Contrarily, if the host vehicle is in a situation where the front slot is occupied by another vehicle (Figure 2.7e), the driver must decelerate no matter he/she is surrounded by greater number of objects or otherwise. Due to the data unavailability about the placements of vehicles surrounding the host vehicle, the driver behavioral models presented in this study cannot capture the influence of "positions" of the surrounding vehicles on the instantaneous driving decisions of the host vehicle. As more detailed data become available in the future, accounting for this dimension in the overall driver behavior estimation can yield in more realistic driver behavioral models in a connected vehicles environment.

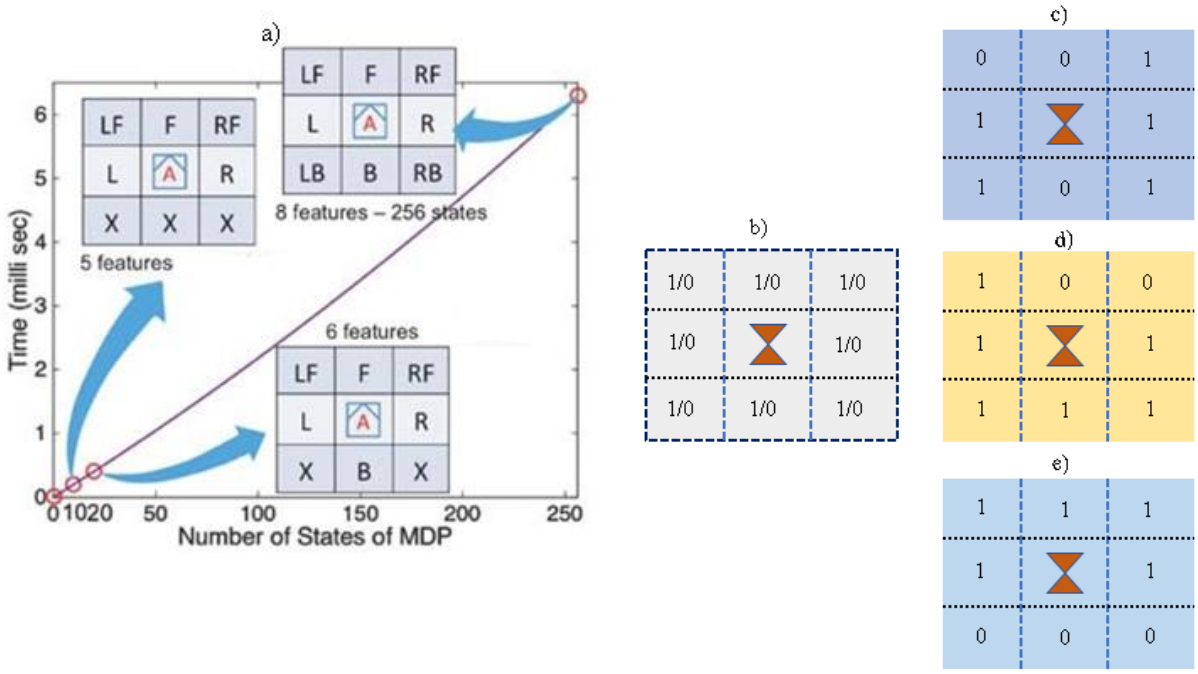

Figure 2.7 Illustration of time complexity of the drivers' policy optimization process as a function of number of surrounding vehicles and their placement.
(Notes: MDP is Markov Decision Process; 1/0 indicates if the slot surrounding the host vehicle is occupied or not; L is left; R is right; LF is left front; RF is right front; F is front; LB is left back; RB is right back; B is back; X is slot/feature blocked/not considered.)

2.8 CONCLUSION/IMPLICATIONS

This study focuses on utilizing large-scale high frequency data generated by data acquisition systems (DAS) that are installed in vehicles to facilitate V2V and V2I infrastructure communications via state-of-the-art communication and sensor technologies such as dedicated short-range communications. As part of USDOT Safety Model Pilot Deployment program, real-world large-scale empirical data transmitted between connected vehicles and infrastructure are used to investigate instantaneous driving decisions and its variation with respect to the ecosystem of mapped local traffic states in close proximity surrounding the host vehicle. To achieve the objectives, state-of-the-art time-series methods such as Markov-switching dynamic regression models were applied.

By conducting a detailed analysis of 43 randomly chosen trips that were undertaken on various roadway types, the study explores important questions related to instantaneous driving decisions in connected vehicle environment. Note that, the sampled trips account for 52% of the total one-day sample (714, 340 BSM packets out of total N = 1, 399, 084 BSM packets). To facilitate more meaningful conclusions, the entire vehicle trajectories for 43 randomly selected trips were visualized in Google Earth to identify the roadway functional classification on which the trips were undertaken. As such, significant efforts went into classifying the trips with respect to roadway type, and in processing the large-scale connected vehicle data. Altogether, the 43 trips are undertaken by 34 vehicles whereas few vehicles undertook two or more than two trips. The new proposed methodology helps in understanding instantaneous driving decisions in detail, and for providing answers to the following questions:

- How can driving regimes be characterized in a typical driving cycle?
- What is the level of volatility in each driving regime?
- When do the regimes change or how long do they last?
- Are driver decisions consistent across trips undertaken by different drivers?
- Do correlates vary across the regimes?

To answer the afore-mentioned questions, Expectation Maximization algorithm based on maximum likelihood was used for estimating Markov Switching Dynamic Regression models. First, for simplicity, the study categorized instantaneous short-term driving performance into two unobserved regimes and as such two-regime Markov Switching Dynamic Regression models were estimated for all trips. The results reveal that acceleration and braking are two distinct regimes in a typical driving cycle, with braking showing substantially greater volatility.

Compared to braking, acceleration regime typically lasts longer i.e. 75 seconds (switching time on average) for trips on freeways, state routes, and freeway and state routes. In addition, analysis reveals that driver decisions are not consistent across different trips as some drivers show greater volatility than others, especially on local and state, and local roads as expected. Importantly, when more objects surround a vehicle, the tendency is to accelerate even more if a driver is in acceleration regime, and to accelerate or lower the intensity of their braking if driver is in braking regime. Lastly, the magnitudes of associations between key correlates and instantaneous driving behavior vary significantly across the two regimes.

Real-world driving is a complex task and we can anticipate existence of more than two regimes. Thus, we allowed for a more generic dynamic Markov switching model specification where the instantaneous driving decision process was modelled as a three-regime process. The results suggest existence of three distinct and unobserved regimes, which are identified as high-rate acceleration, high-rate deceleration, and cruise/constant regime. Moreover, given in a high-rate regime, drivers on-average tend to decelerate at a higher rate than their rate of acceleration. Importantly, we observed that compared to cruise/constant regime, drivers instantaneous driving decisions are more volatile both in "high-rate" acceleration as well as "high-rate" deceleration regime. Finally, the three-regime specification suggested that in high-rate deceleration regime, drivers (on-average) tend to get out of crowded situations by decelerating at a lower rate or even accelerate at next instant of time.

The results obtained from this study has important implications. First, the study presents an appropriate analytical framework that can help in understanding instantaneous driving decisions

and key correlates. Driving decisions primarily depend on surrounding traffic states. An in-depth analysis of such factors is important for understanding driver specific behavior and for developing customized driver based safety applications. For instance, researchers and practitioners can implement the proposed methodology to connected vehicle data generated by specific driver for several trips. For a specific driver, quantification of the associations between instantaneous driving decisions and driving contexts can help us understand driver-specific instantaneous volatility, and to develop hazard anticipation and notification systems if a driver is observed to deviate from his/her normal driving patterns. Furthermore, given a specific driver and keeping in view his/her historical instantaneous driving decisions with respect to local traffic states, alerts and warnings can be provided well in advance to driver specifically if he/she is decelerating. Given that deceleration is consistently observed to be more volatile, such alerts and warnings can potentially help in improving safety and traffic flow disturbances. Finally, an important aspect of developing such hazard anticipation and notification systems is the need to be able to perform short term driving regime predictions. Thus, we demonstrate the potential of dynamic Markov switching models in terms of short-term instantaneous regime prediction at specific instances in time. While the current study focused on instantaneous driving decisions in longitudinal direction only, as part of future work, it would be interesting to develop a methodology for simultaneous analysis of instantaneous driving decisions in longitudinal as well as lateral direction. Such a methodology can potentially help in understanding the correlations between instantaneous driving decisions in longitudinal and lateral directions, and how such decisions can be mapped to surrounding traffic environment.

2.9 ACKNOWLEDGEMENT

The research is supported by National Science Foundation (Award number: 1538139). The authors would extend special thanks to the following entities at The University of Tennessee for their support: Transportation Engineering & Science Program and Initiative for Sustainable Mobility. The data used in this study were obtained from Research Data Exchange program maintained by Federal Highway Administration, US DOT. Software Packages R, MATLAB, Google Earth, and Stata 14.1 are used for data cleaning, linkage, processing, and modeling. The views expressed in this paper are those of the authors, who are responsible for the facts and accuracy of information presented herein. The corresponding author would like to dedicate his part of the effort to his mother, for her mentor-ship and ever-deepening support.

CHAPTER 3 CAN DATA GENERATED BY CONNECTED VEHICLES ENHANCE SAFETY? A PROACTIVE APPROACH TO INTERSECTION SAFETY MANAGEMENT

This chapter presents a modified version of two articles to which Behram Wali made extensive contributions to. *Can Data Generated by Connected Vehicles Enhance Safety? A proactive approach to intersection safety management* by Mohsen Kamrani, Behram Wali, and Asad J. Khattak. Peer-review conference paper: Presented in a podium session at the 96th Transportation Research Board Annual Meeting 2017, Washington D.C. Journal article: Published in Transportation Research Record: Journal of Transportation Research Board, 2659 (2017): 80-90.

- 2017 TRB Outstanding Paper Award for the paper "Can Data Generated by Connected Vehicles Enhance Safety? Proactive Approach to Intersection Safety Management" Awarded by TRB Safety Data, Analysis and Evaluation Committee.

ABSTRACT

Traditionally, evaluation of intersection safety has been largely reactive, based on historical crash frequency data. However, the emerging data from Connected and Automated Vehicles (CAVs) can complement historical data and help in proactively identify intersections which have high levels of variability in instantaneous driving behaviors prior to the occurrence of crashes. Based on data from Safety Pilot Model Deployment in Ann Arbor, Michigan, this study developed a unique database that integrates intersection crash and inventory data with more than 65 million real-world Basic Safety Messages logged by 3,000 connected vehicles, providing a more complete picture of operations and safety performance of intersections. As a proactive safety measure and a leading indicator of safety, this study introduces location-based volatility (LBV), which quantifies variability in instantaneous driving decisions at intersections. LBV represents the driving performance of connected vehicle drivers traveling through a specific intersection. As such, by using coefficient of variation as a standardized measure of relative dispersion, LBVs are calculated

for 116 intersections in Ann Arbor. To quantify relationships between intersection-specific volatilities and crash frequencies, rigorous fixed- and random-parameter Poisson regression models are estimated. While controlling for exposure related factors, the results provide evidence of statistically significant (5% level) positive association between intersection-specific volatility and crash frequencies for signalized intersections. The implications of the findings for proactive intersection safety management are discussed in the paper.

3.1 INTRODUCTION

There is considerable evidence about vehicle conflicts at intersections resulting in crashes, making them among the most dangerous locations on roadways (Abdel-Aty and Haleem, 2011, Persaud and Nguyen, 1998). Traditionally, intersection safety evaluations are done based on historical data and they are largely reactive i.e. the state-of-the-art methods characterize unsafe intersections based on historical and expected crash frequencies (Persaud and Nguyen, 1998, Kamrani et al., 2014). Safety treatments can then be applied to intersections based on historical crash data methodology. Variability in instantaneous driving behaviors can be leading indicators of occurrence of unsafe outcomes such as crashes/incidents. In this study, we posit that expanding the concept of driving volatility (Khattak et al., 2015, Khattak and Wali, 2017, Wang et al., 2015) to specific locations (termed as Location-Based Volatility) by using real-world large-scale connected vehicle data has a significant potential in unveiling critical relationships between extreme driving behaviors (and its fluctuations) and safety outcomes at specific intersections.

The Safety Pilot Model Deployment (SPMD) offers detailed and relevant data. This pilot is underway in Ann Arbor, Michigan, intended to demonstrate vehicle-to-vehicle (V2V) and vehicle-to-infrastructure (V2I) communication in a real-world environment. Within SPMD, Basic Safety Messages (BSMs) contain rich information packets (exchanged at the frequency of 10 Hz) that describe a vehicle's position, motion, its component status, and other relevant information exchanged between vehicles/infrastructure through V2V and V2I applications (Henclewood, 2014). Such emerging data has been used for creating trip-based driving volatilities for drivers, capable of identifying abnormal or extreme behaviors prior to unsafe outcomes such as crashes/incidents (Liu and Khattak, 2016b). Important in this aspect is the concept of "driving volatility" that captures the extent of variations in driving, especially hard accelerations/braking, jerky maneuvers, and frequent switching between different driving regimes (Khattak and Wali, 2017). Specifically, Wang et al. (Wang et al., 2015) and Liu and Khattak (Liu and Khattak, 2016b) examined the relationships between trip-based driving volatility and several factors such as demographics, trip purpose, duration, and detailed vehicle characteristics (Liu and Khattak, 2016b, Wang et al., 2015). The potential of driver-specific trip-based volatilities for developing advanced traveler information systems, driving feedback devices, and alternative fuel vehicle purchase decision tools were concluded (Liu and Khattak, 2016b, Wang et al., 2015).

This study focuses on developing an analytic methodology to examine instantaneous driving behaviors at specific locations, and its variability. The paper explores how variability in driving can be mapped to historical safety outcomes such as crashes at specific locations. Such an analysis is fundamental towards proactive intersection safety management.

3.2 LITERATURE REVIEW

There are different branches of ongoing research topics in the connected vehicles (CV) area. Several major directions of research can be identified. Topics such as network robustness and information propagation efficiency (Osman and Ishak, 2015) are still under investigation in order to establish a better vehicle to vehicle (V2V) and vehicle to infrastructure (V2I) connection (Osman and Ishak, 2015). Another is the systems and algorithms whose ultimate goal are the reduction of the gap between vehicles in order to increase roads capacity and reduction in fuel consumption through different methods such as speed harmonization (Ghiasi et al., 2017), trajectory optimization, and platooning as discussed in Bergenhem et al. (Bergenhem et al., 2012).

Also, there are a number of studies (not necessarily in CV area) trying to characterize aggressive, reckless or risky driving style (NHTSA, 2000). Among them, speed limits are usually the threshold that determines a driver's performance (Wali et al., 2017b, Haglund and Åberg, 2000). While characterizing driver's performance, the important finding is that risky driving behaviors have been found to be positively correlated with the likelihood of crashes or near-crash events (Paleti et al., 2010). This said, a broad spectrum of studies related to connected vehicle systems have proposed mechanisms for warnings or alerts to drivers using the CV applications and their effect on safety. For instance, Chrysler *et al.* (Chrysler et al., 2015) investigated the effect of warning messages on drivers' ability to handle primary and secondary threats. The results showed an improved detection time for the primary threat while increased reaction time to the secondary threat which was placed after the primary threat. In another study (Genders and Razavi, 2015), the impacts of dynamic route guidance on work zone safety under different

market penetration of CV were explored. Per the interesting results, 40% penetration of CV and below improves safety while above that leads to decreased safety of work zones. However, these benefits are dependent on the information dissemination delay (Du and Dao, 2015). Although, positive effects of warning messages have been investigated, the way those warning should be created from BSMs is still under explored.

One approach is trying to link the generation of warning messages to drivers' behavior. In some recent studies, the authors have initiated efforts to extract useful information from BSMs to understand the drivers' behavior. For instance, a measure of driving performance in connected vehicles network has been defined as "driving volatility" (Wang et al., 2015). As such, trip-based driving volatility was introduced (Wang et al., 2015) to account for the variation of driving behaviors under different conditions using objective driving performance evaluation matrix i.e. vehicular jerk. More succinctly, Liu *et al.* (Liu et al., 2014) studied extreme driving behaviors (trip-based volatility) using exhaustive high frequency connected vehicle data, and the analysis demonstrated framework for the generation of warnings/alerts for connected vehicles informing drivers about potential hazards. Also another study (Liu and Khattak, 2016a) proposed a way to identify abnormal or extreme behaviors (i.e., hard acceleration and decelerations) from BSMs, and warn drivers through the V2V, V2I, or other connected vehicle applications. In this paper, the authors believe that expanding the concept of driving volatility in connected vehicles environment to specific locations has significant potential in identifying hazardous roadway segments. Such a perspective of location-specific driving behavior in connected vehicle systems has not been identified and analyzed. Therefore, this paper is aimed at developing the new concept of location-based driving volatility (LBV) via using BSMs exchanged between

connected vehicles in real-world and linking it to historical crash data with the purpose of identifying hazardous spots proactively. Although the novelty of this study is in using high volume and high velocity connected vehicle data, the significance of works done by other researchers on crash frequency cannot be overlooked, given the emergence of new approaches, e.g., see Lord & Mannering (Lord and Mannering, 2010). Also random parameter and/or varying coefficient models have become popular as opposed to fixed parameter for their capability to address unobserved heterogeneity (Anastasopoulos and Mannering, 2009, Li et al., 2017, Khattak et al., 2016).

3.2.1 Research Objective and Contribution

The objectives of this study are to:

1) Quantify instantaneous driving decisions and its variability in intersection-specific Basic Safety Messages (BSMs).
2) Understand the relationship between intersection-specific volatility with crash frequencies, while controlling for other variables, using rigorous statistical tools.

The present study contributes by analyzing real-world large-scale connected vehicle data to extract critical driving behavior information embedded in raw BSMs. Such an analysis is important because driving actions and behaviors are believed to be the main cause of traffic crashes, and understanding the relationship between location-based volatility and historical crash data can provide fundamental knowledge regarding proactive safety countermeasures. A unique aspect of this study is that significant efforts have been undertaken to integrate large-scale connected vehicle data (more than 65 million BSMs) with intersection crash and inventory data

in order to provide providing a more complete picture of operations and safety performance of intersections. The assembled database allows investigation of correlations between potentially leading indicator of safety (location-based volatility) and historical crash frequencies. By taking the first step towards proactive safety using large-scale connected vehicle data, the current study is original and timely in sense that real-world data has been processed and used to understand the phenomena under discussion.

3.3 METHODOLOGY

3.3.1 Conceptual Framework

The two-month connected vehicle data from Safety Pilot Model Deployment (SPMD) (https://www.its-rde.net/home) contains rich information (i.e., basic safety messages in 10 Hz) that was exchanged between vehicles/infrastructure through vehicle-to-vehicle (V2V) and vehicle-to-infrastructure (V2I) applications. Such data provide us with an opportunity to scrutinize the mechanisms that lead to unsafe events on roadways. However, the methods of making a good use of such high-volume and high-resolution data need further development. SPMD collects Basic Safety Messages (BSMs) that describe a vehicle's position, motion, its component status, and other relevant travel information (Henclewood, 2014). However, BSMs are not informative to drivers when they need to make decisions based on information received through V2V or V2I applications. Most BSMs describe normal driver behaviors while abnormal and highly fluctuating driver behaviors determine the safety of driving in the short-term.

This study is focused on developing an innovative methodology for estimating location-based volatility for specific intersections and comparing it with their observed crashes. We

hypothesized that the nature of extreme instantaneous driving behaviors at intersections can be correlated with their crash history. Such correlations can help us understand instantaneous driving behaviors and how they relate to transportation safety. Location-based volatility (LBV) represents the driving performance of a substantial number of users traveling through a specific location. LBV may play a critical role in highway safety management, as it will highlight locations where many drivers behave differently from other locations. Proactive countermeasures can be considered in such locations. If many drivers make extreme driving behaviors or if driving behaviors are highly fluctuating at certain locations, the reasons of such extreme behaviors may be related to factors such as the road conditions. Such information can be disseminated to connected vehicle drivers through roadside equipment (RSE) which are able to send information to vehicles, and thus drivers may be alerted about potential hazards (e.g. conflicts/intersection sight distance) while traveling through certain intersections.

First, the connected vehicle data consisting of geo codes and longitudinal acceleration were cleaned. In the next step, 116 intersections were identified in Ann Arbor, Michigan (discussed later). Crash data along with other geometric elements (provided in Table 3.1) were collected. Then, four different coefficients of variation ($C_{V_{AL}}, C_{V_{AH}}, C_{V_{DL}}, C_{V_{DH}}$) are calculated and used as measures of location-based volatility (LBV) for each intersection (150 ft. from the center of each intersection). Given the hypothesis that higher LBV is likely to be positively correlated with historical crash data at intersections, appropriate statistical models are developed to investigate the correlation between LBV (among other traffic exposure factors) and crash frequency. The knowledge generated from the modeling results can identify intersections where drivers, on average, show higher volatility in their instantaneous driving decisions (e.g. longitudinal

acceleration), and where such volatilities are found to be correlated with crash frequency. By carefully analyzing high-resolution real-world data transmitted between connected vehicles and applying appropriate statistical methods, we can ultimately generate proactive (rather than the traditionally reactive safety approach) alerts and warnings given to vehicle drivers at intersections. Such proactive warning and alerts can be disseminated through roadside equipment to vehicles approaching specific intersections to warn them regarding the chance or ranking of intersection in terms of crash occurrence. In the next section, the computation of LBV is discussed.

3.3.2 Location Based Volatility

Understanding instantaneous driving volatility at specific intersections is one of the most challenging aspects of the current study. To calculate location-based volatility, different instantaneous driving measures can be used such as accelerations, steering angles or position of brakes (Liu and Khattak, 2016b). As explicitly discussed in Liu and Khattak (Liu and Khattak, 2016b), volatility in trip-based instantaneous driving decisions should be captured by considering both longitudinal and lateral accelerations. Considering longitudinal acceleration as the only measure of driving volatility can mask important information embedded in instantaneous driving data. For instance, at moments longitudinal acceleration can be low and thus considered normal, but the driver could still be volatile due to large magnitudes of lateral accelerations.

To calculate LBV, the authors intended to use longitudinal and lateral acceleration as they are direct outcomes of vehicle maneuvering. However, due to a considerable amount of questionable lateral acceleration data (see Data Accuracy section), only longitudinal acceleration data were

used. The longitudinal acceleration data is reasonable and available for all BSMs and has been error checked by estimating accelerations from speed trajectories of the vehicles. Given the data limitation, this study only focuses on capturing location-based volatility by using longitudinal accelerations. There are two reason for this decision: First, excluding lateral acceleration does not seem to be affecting the results drastically since lateral acceleration is more informative in trip based volatility calculation where curvature of the road changes and where the length of the trip allows several lane changes. Second, using the data with removed lateral acceleration reduces the amount of data for several intersections leading to reduction of sample size i.e. number of intersections.

3.3.3 Calculation of LBV

The present study uses a standardized measure of dispersion called Coefficient of Variation (C_V) (also known as the ratio of relative standard deviation) for quantifying the fluctuations in longitudinal acceleration /decelerations at a specific intersection. Note that different measures such as range, interquartile range, variance or standard deviation can be used for capturing variability in longitudinal accelerations. Although standard deviation and variance are preferable as whole information embedded in the data is used for calculation of variability, both measures are insensitive to magnitude of acceleration values in the data. Thus, we prefer the relative measure of dispersion (Coefficient of Variation), where the dispersion in accelerations or decelerations can be quantified as the proportion of their means. This approach can capture the variability (e.g. standard deviation) in instantaneous driving decisions with respect to the mean accelerations or decelerations undertaken by different drivers at a specific intersection.

To compute volatility for each intersection, two speed bins (see Figure 3.1a), one from minimum observed speed to the mean and one from the mean to maximum speed were considered. The rationale behind considering speed bins is that the acceleration capability of a vehicle depends on current vehicle speed i.e. at larger speeds the capability to accelerate decrease as compared to acceleration capability at lower speeds. For each bin within an intersection, acceleration and deceleration values are separated, and the means and standard deviations are computed. Finally, C_V as a measure of LBV is obtained by dividing standard deviations of accelerations to the mean. For each intersection, four C_Vs are reported as shown in Figure 3.1a. The calculated C_Vs for a specific intersection provide the relative measure of dispersion of longitudinal accelerations with respect to their means, and thus different intersections can be compared based on their C_Vs.

3.3.4 Modeling Approach

After quantification of volatility for each intersection, we investigate the correlations between location-based volatility (for each intersection), crash data, and other traffic related factors. Appropriate modeling can provide an empirical evidence as of how intersection location-based volatility relates to historical crash data. Given the count nature of crashes, Poisson and/or Poisson-gamma models (Negative Binomial) can be estimated depending on the mean and variance of crash data.

For a Poisson model, the probability of having a specific number of crashes "*n*" at intersection "*i*" can be written as (Greene, 2003):

$$P(n_i) = \frac{\exp(-\lambda_i)\lambda_i^n}{n_i!} \qquad \text{Equation 3.1}$$

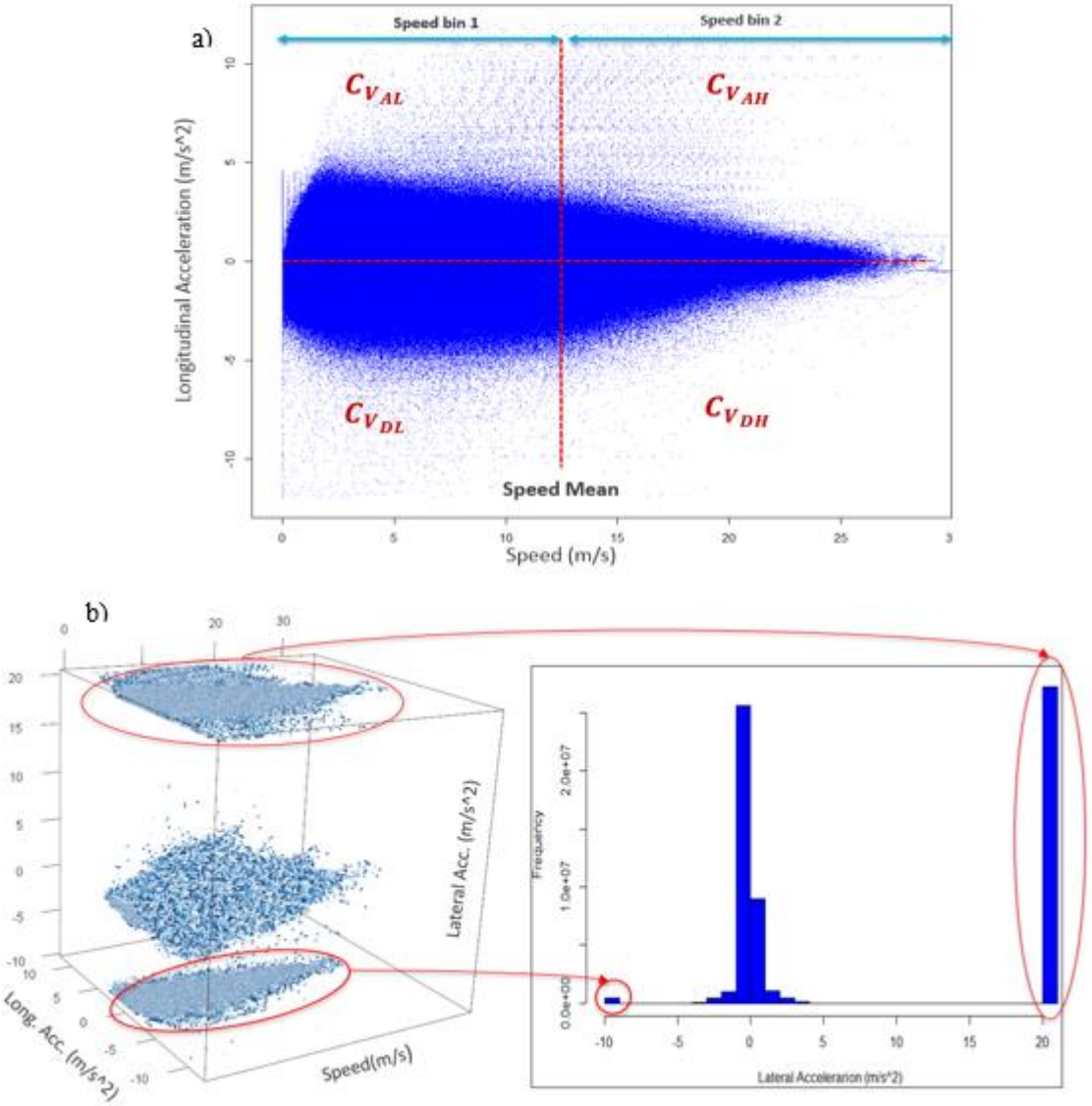

Figure 3.1 a) Four quadrants used to calculate coefficients of variation (standard deviation divided by mean) for each intersection, b) Plot of used data (left)/ Histogram of lateral acceleration (right)

Where: $P(n_i)$ is probability of crash occurring at intersection "*i*", "*n*" times per specific time-period; and λ_i is Poisson parameter for intersection "*i*" which is numerically equivalent to intersection "*i*" expected crash frequency per year $E(n_i)$. The regression can be fitted to crash data by specifying λ_i as a function of explanatory variables such as location-based volatility, Annual Average Daily Traffic, and speed limits on major and minor approach. Formally, λ_i can be viewed as a log link function of a set of independent variables (Greene, 2003):

$$\ln(\lambda_i) = \beta(X_i) \qquad \text{Equation 3.2}$$

Where X_i is a vector of explanatory variables and β is a vector of estimable parameters. Application of Poisson regression to over-dispersed crash data can result in inappropriate results. If mean and variance of crash data are not equal, corrective measures are applied to Equation 3.2 by adding an independently distributed error term $\in$. While presence of over-dispersion can be indicated by the mean and variance of crash data (Greene, 2003), formally a Lagrange multiplier can be performed to statistically test the existence of over- dispersion in Poisson model (Greene, 2003). The test statistic is defined as:

$$LM = \left[\frac{\sum_{i=1}^{n}[(y_i - \mu_i)^2 - y_i]}{2\sum_{i=1}^{n}\mu_i{}^2}\right]^2 \qquad \text{Equation 3.3}$$

Where: y_i are actual crash frequency for intersection "*i*", μ_i is expected crash frequency for intersection "*i*" as predicted by Poisson model, and n are number of observations. The null hypothesis is that Poisson regression is appropriate for the crash data at hand. Under this hypothesis, the LM test statistic should have chi-square distribution with degree of freedom equal one. If the asymptotic chi-square distribution obtained from Equation 3.3 is less than

critical chi-square of 3.84 at 95% level of confidence, Poisson regression should be favored, otherwise Negative Binomial regression can be more appropriate (Greene, 2003).

Finally, it is likely that the associations between key explanatory variables and crash frequency may not be consistent across intersections. The intrinsic unobserved heterogeneity can arise due to several observed and unobserved factors related to intersection crash frequency, which may not be available in the data at hand. This is referred to omitted variable bias in safety literature (Greene, 2003). Furthermore, if key variables are omitted from analysis and too few variables are included in the model, it is likely that location-based volatility (explanatory factor) can capture those effects and may not be the true association between location-based volatility and crash frequency. One way to address this issue is to allow parameter estimates to vary across observations (Greene, 2003). As such, random parameters can be included in the estimation framework as:

$$\beta_i = \beta + \varphi_i \qquad \text{Equation 3.4}$$

Where φ_i is randomly distributed term with any pre-specified distribution such as normal distribution with mean zero and variance σ^2.With Equation 3.4, the Poisson parameter in Equation 3.2 becomes:

$$\lambda_i|\varphi_i = e^{BX} \qquad \text{Equation 3.5}$$

And, the Poisson parameter in Equation 3.2 in Poisson-Gamma model becomes:

$$\lambda_i|\varphi_i = e^{BX+\epsilon} \qquad \text{Equation 3.6}$$

Finally, the following likelihood function for random-parameter model can be maximized through maximum simulated likelihood technique (Anastasopoulos and Mannering, 2009):

$$LL = \sum_i ln \int_{\varphi_i}^{i} g(\varphi_i) P(n_i|\varphi_i) d\varphi_i \quad \text{Equation 3.7}$$

Where: g(.) is the probability density function of randomly distributed term with pre-specified distribution such as normal distribution with mean zero and variance σ^2. More details on random parameter models can be found in (Anastasopoulos and Mannering, 2009).

3.4 DATA

The data used in this study (retrieved from https://www.its-rde.net/home) are BSMs from vehicles participating the SPMD in Ann Arbor, Michigan. SPMD is a comprehensive data collection effort, under real-world conditions, at Ann Arbor test site with multimodal traffic hosting approximately 3,000 connected vehicles equipped with V2V and V2I communication devices. BSMs are frequently transmitted messages (usually at 10Hz) that is meant to increase vehicle's situational awareness. At its core, the dataset contains vehicle's instantaneous driving statuses of vehicle's position (latitude, longitude, and elevation) and motion (heading, speed, accelerations).

To examine correlations, location-based volatility (LBV) data for each intersection (as explained earlier) are linked with historical crash data, annual average daily traffic (AADT) data for major and minor approaches, speed limits on major and minor approaches, and number of approaches at each intersection. Such data are publicly available at the website of the Metropolitan Planning

Organization: http://semcog.org/Data-and-Maps. Out of all intersections in the Ann Arbor area, 116 intersections are identified for which connected vehicle data are available, i.e. connected vehicles pass through such intersections and generating enough data for calculation of LBV. Finally, five years of crashes (2011-2015) along with geometric factors and flows were extracted and linked to LBV for each intersection. Note that the data are not available in spreadsheet format, and thus significant efforts went into carefully extracting data manually and linking it to LBV for 116 intersections.

3.4.1 Data Accuracy

Based on the distributions of key variables provided in Table 3.1, the data seems to be of reasonable quality. To assure the accuracy of intersection data, after initial collection, another person checked 10% of intersection data randomly and no discrepancies were observed. Also, the descriptive statistics of intersection data in Table 3.1 provide reasonable difference between signalized and un-signalized intersections. The major inaccuracy of data is from the lateral acceleration as it is shown in Figure 3.1b. Since 27,240,788 data points (42% of the data) had the maximum allowable value that can be recorded in DSRC devices (2g), lateral acceleration data was not used in the analysis.

Table 3.1 Description of Key Variables and Descriptive Statistics

Variables	All Intersections (N = 116)			Signalized (N = 53)			Un-signalized (N=63)		
	Mean	SD	Min/Max	Mean	SD	Min/Max	Mean	SD	Min/Max
Average crashes (5 years)	7.56	7.64	0/44	12.94	8.03	1/44	3.04	2.95	0/14
Average rear-end crashes (5 years)	4.28	4.56	0/24	7.07	5.24	1/24	1.93	1.79	0/9
$C_{V_{AL}}$ (In percent)	143.7	56.0	69/239	182.4	57.5	83/329	111.1	26.12	69/191
$C_{V_{AH}}$ (In percent)	84.9	13.7	56/121	77.93	12.7	59/113	90.77	11.8	57/121
$C_{V_{DL}}$ (In percent)	137.5	43	71/287	168.6	41.1	87/287	111.2	21.94	71/181
$C_{V_{DH}}$ (In percent)	96.29	12.9	57/155	99.44	14.8	76/155	93.64	10.39	57/115
AADT major road	20805	8326	3100/45400	22747	8209	3600/45400	19171	8131	3100/38900
AADT minor road	9396	4138	1100/27400	9994	5706	3100/27400	8893	1972	1100/13400
Ln (AADT major road)	9.84	0.49	8.03/10.72	9.96	0.39	8.18/10.72	9.74	0.54	8.03/10.56
Ln (AADT minor road)	9.05	0.47	7/10.21	9.07	0.52	8.03/10.21	9.03	0.42	7/9.50
Speed limit major	35.34	7.24	25/45	35.94	7.34	25/45	34.84	7.18	25/45
Speed limit minor	30.47	3.95	25/45	30.84	5.16	25/45	30.15	2.53	25/40
4-legged intersection	0.4	0.49	0/1	0.622	0.48	0/1	0.22	0.41	0/1
Total through lanes	4.45	1.28	2/8	5.13	1.35	2/8	3.38	0.9	2/6
Total left turn lanes	1.53	1.32	0/6	2.26	1.4	0/6	0.92	0.88	0/3
Total right turn lanes	0.93	0.78	0/4	1.11	1.01	0/4	0.79	0.48	0/2

Notes:$C_{V_{AL}}$: Coefficient of variation of acceleration below mean speed of intersection;$C_{V_{AH}}$: Coefficient of variation of acceleration above mean speed of intersection;$C_{V_{DL}}$: Coefficient of variation of deceleration below mean speed of intersection;$C_{V_{DH}}$: Coefficient of variation of deceleration above mean speed of intersection; AADT: Annual Average Daily Traffic; SD is standard deviation; Min is minimum value; Max is maximum value.

3.5 RESULTS

3.5.1 Descriptive Statistics

Table 3.1 presents the descriptive statistics of key variables used in modeling. The mean, standard deviation, minimum and maximum values are given for each variable which can help conceptualizing the distributions. Descriptive statistics are given for all the intersections (N=116) as well as for signalized intersections (N=53) and un-signalized intersections (N=63) separately. For all intersections, signalized, and un-signalized intersections, the mean five-year crash frequency is 7.56, 12.94, and 3.04. As expected, signalized intersections have significantly higher crash frequency (on average) than un-signalized intersections. This finding is in agreement with Abdel Aty and Keller (Abdel-Aty and Keller, 2005) who found approximately 9.6 crashes per year at signalized intersections as opposed to only 2 crashes per year on un-signalized intersections (Abdel-Aty and Keller, 2005). There can be several factors which may contribute to occurrence of crashes at signalized intersections such as conflicting movements as well as different intersection-specific design variables (Abdel-Aty and Keller, 2005). This said, investigating instantaneous driving actions at such locations, and higher volatility (if any) may help us design appropriate proactive strategies from preventing an "accident waiting to happen" (Schneider et al., 2004).

Regarding location-based volatility, all C_V statistics suggest that signalized intersections on average have higher variability in longitudinal accelerations/decelerations compared with unsignalized intersections, and thus can be more volatile (this is the case for all C_V's except $C_{V_{AH}}$). One reason for higher $C_{V_{AH}}$ (volatility of acceleration above mean speed) of un-signalized

intersections as compared to signalized intersections can be due to uninterrupted traffic of un-signalized intersections.

In order to avoid omitted variable bias in modeling (Mannering and Bhat, 2014), data on other variables such as five-year average AADT (major and minor approach), speed limits (major and minor approaches), and number of approaches were collected. Regarding the number of approaches, 40% of all intersections, 62.2% of signalized intersections, and 22% of un-signalized intersections are four-legged intersections (Table 3.1). In terms of exposure on major and minor roads, signalized intersections have higher (on average) AADT than un-signalized intersections (22,747 vs. 19,171 for major roads and 9,994 vs. 8,893 for minor roads). Regarding number of lanes, number of through and left turns for signalized intersection are considerably higher as compared to un-signalized intersections.

3.5.2 Modeling Results

For examining the correlations between crash frequency and location-based volatility (as measured by C_Vs), count data models are estimated given the count nature of crash frequency. Separate count data regression models are estimated for all intersections, signalized intersections and un-signalized intersections. Specifically, fixed-parameter Poisson regressions are estimated for total crash frequency as a function of location based volatility, major and minor road AADT, major and minor road speed limits, and total number of through lanes. It should be noted that the descriptive statistics for crash frequencies in Table 3.1 apparently reveal the existence of over-dispersion in the data where Negative Binomial model should be preferred over Poisson model (Washington et al., 2010).Thus, statistical tests are conducted to confirm the existence of over-dispersion (Greene, 2003). As explained in methodology section, Lagrange Multiplier tests were

conducted for all three Poisson models. By using Equation 3.3, the Lagrange Multiplier (LM) values were 0.05, 0.031, and 0.15 for all intersections, signalized intersections, and un-signalized intersections respectively. The LM values are much smaller than critical Chi-square value of 3.84 for one degree of freedom at 95% confidence level. Thus, the null hypothesis that Poisson regressions are more appropriate is failed to reject, and it would be more appropriate to use Poisson regressions (Washington et al., 2010).

Due to the likely presence of unobserved heterogeneity in crash data (Anastasopoulos and Mannering, 2009) which may arise due to several unobserved factors, random-parameter Poisson models are also estimated. Fixed parameter models are estimated with standard maximum likelihood whereas random parameter models are estimated through simulated maximum likelihood with 200 Halton draws used for random-held parameters (Anastasopoulos and Mannering, 2009). Regarding functional form of random-parameters, log-normal, Weibull, uniform, and triangular distributions are tested with normally distributed random parameters giving the best fit and shown in this study. The results obtained from fixed and random parameter Poisson model are presented in Table 3.2. Marginal effects are also provided for the random parameter models that translate unit change in crash frequency with unit change in explanatory variable. Compared to fixed-parameter models, random-parameter models resulted in better fit as of improved log-likelihood at convergence and McFadden's ρ^2 (Table 3.2) (Washington et al., 2010). While this study does not focus on methodological approaches for modeling intersection crash data, the predicted vs. actual values of crashes (Figure 3.2) are plotted and reveal statistical superiority of random parameter models in fitting the data at hand.

Table 3.2 Modeling results of fixed- and random-parameter Poisson regressions

Variables	Signalized and Un-signalized					Signalized Intersections					Un-signalized Intersections				
	Fixed Par.		Random Par.			Fixed Par.		Random Par.			Fixed Par.		Random Par.		
	□	t-stat	□	t-stat	ME	□	t-stat	□	t-stat	ME	□	t-stat	□	t-stat	ME
Constant	-7.752	-6.6	-7.786	-7.237	---	-7.21	-4.97	-7.35	-6.95	---	-10	-3.574	-9.61	-3.23	---
*Standard deviation**	---	---	---	---	---	---	---	---	---	---	---	---	0.488	6.155	---
$C_{V_{AL}}$	0.006	4.152	0.004	2.902	0.025	0.009	3.434	0.01	5.34	0.125	-0.014	-2.831	-0.016	-2.91	-0.035
Standard deviation	---	---	---	---	---	---	---	0.0002	1.99	---	---	---	---	---	---
$C_{V_{AH}}$	-0.003	-0.776	-0.007	-1.983	-0.038	0.009	1.453	0.01	1.95	0.118	0.005	0.683	0.004	1.28	0.01
Standard deviation	---	---	0.005	11.856	---	---	---	---	---	---	---	---	---	---	---
$C_{V_{DL}}$	0.002	1.243	0.005	2.827	0.027	-0.003	-1.541	-0.004	-2.22	-0.057	0.015	2.698	0.0153	3.186	0.036
Standard deviation	---	---	---	---	---	---	---	0.0009	4.36	---	---	---	---	---	---
$C_{V_{DH}}$	0.02	6.449	0.021	6.33	0.11	0.008	1.872	0.007	1.98	0.089	-0.0007	-0.09	0.0001	0.05	0.0004
Standard deviation	---	---	0.0007	2.182	---	---	---	---	---	---	---	---	---	---	---
Ln (Major Road AADT)	0.547	4.899	0.527	5.322	2.694	0.55	3.716	0.565	5.56	6.575	0.866	4.801	0.757	4.106	1.823
Standard deviation	---	---	0.011	3.376	---	---	---	---	---	---	---	---	0.488	6.155	---
Ln (Minor Road AADT)	0.123	1.656	0.15	1.97	0.767	0.191	2.083	0.207	2.03	2.413	0.231	1.004	0.292	1.25	0.704
Standard deviation	---	---	0.006	2.152	---	---	---	---	---	---	---	---	---	---	---
Speed limit major road	-0.009	-1.736	-0.014	-2.497	-0.073	0.004	0.576	0.008	1.22	0.097	---	---	---	---	---
Speed limit minor road	---	---	---	---	---	-0.016	-1.444	-0.023	-1.62	-0.271	---	---	---	---	---
Total through lanes	0.61	1.733	0.107	3.223	0.547	---	---	---	---	---	---	---	---	---	---

Notes: ME: Average Marginal Effects from Random Parameter Model. $C_{V_{AL}}$: Coefficient of variation of acceleration below mean speed of intersection; $C_{V_{AH}}$: Coefficient of variation of acceleration above mean speed of intersection; $C_{V_{DL}}$: Coefficient of variation of deceleration below mean speed of intersection; $C_{V_{DH}}$: Coefficient of variation of deceleration above mean speed of intersection; AADT: Annual Average Daily Traffic; *Standard deviation of normally distributed random parameters.

Table 3.2 Modeling results of fixed- and random-parameter Poisson regressions (Continued)

	Signalized and Un-signalized		**Signalized Intersections**		**Un-signalized Intersections**	
	Fixed Par.	**Random Par.**	**Fixed Par.**	**Random Par.**	**Fixed Par.**	**Random Par.**
Summary Statistics						
Log-lik. at Zero *L(0)*	-578.31	-578.31	-226.73	-226.73	-158.18	-158.18
Log-lik. at Convergence *L(□)*	-336.72	-305.02	-159.43	-154.91	-138.26	-130.44
McFadden □^{2}	0.417	0.831	0.31	0.893	0.125	0.59
Sample Size (N)	116		53		63	

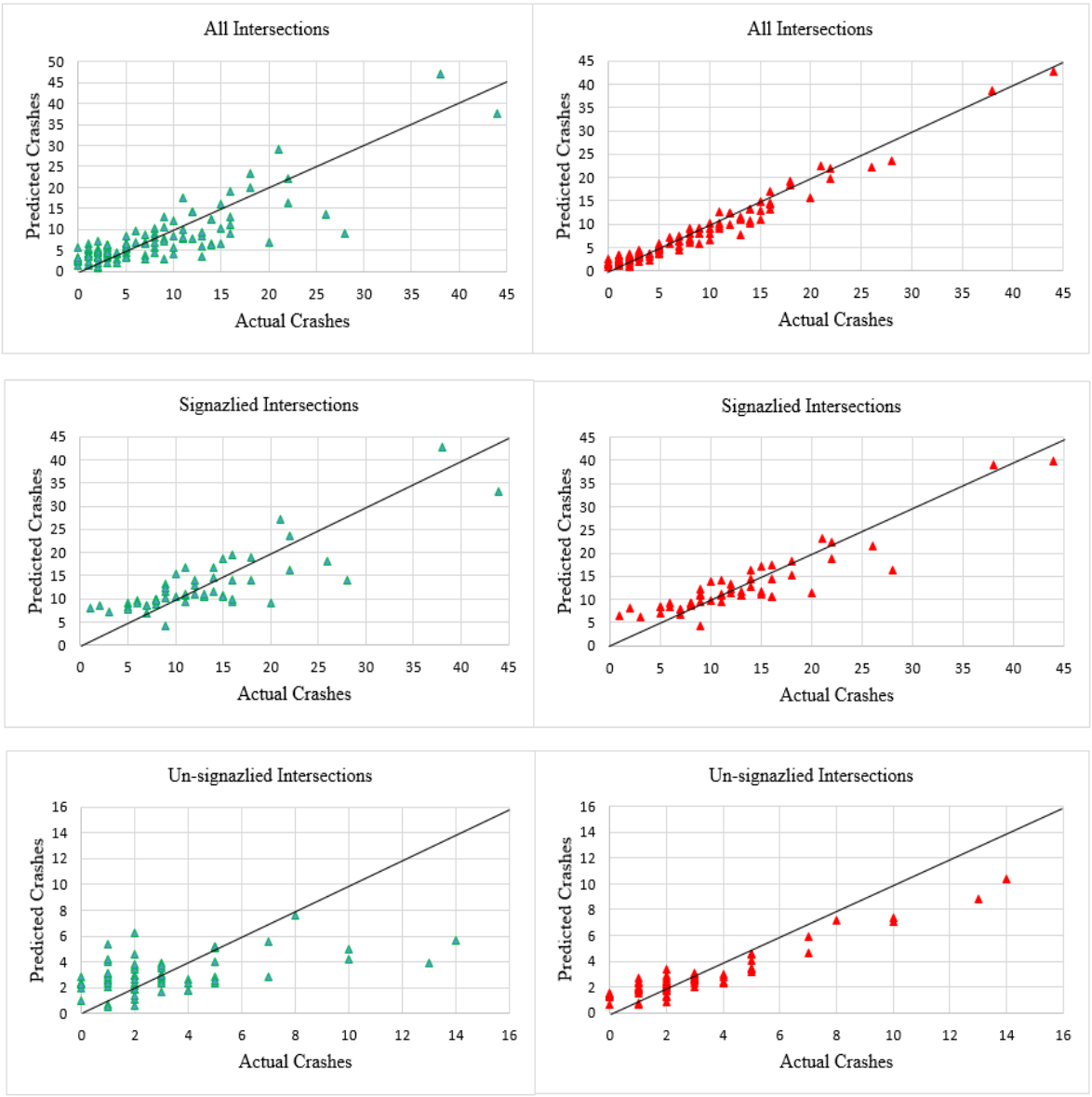

Figure 3.2 Mean-expected over actual number of crashes for fixed and random-parameter Poisson models (Green: fixed parameter models; Red: random parameter models)

3.6 DISCUSSION

Coming to the fixed-parameter estimation results for all intersections (Table 3.2), the results provide evidence that $C_{V_{AL}}$,$C_{V_{DL}}$, and $C_{V_{DH}}$ are positively associated (statistically significant at 95% confidence level) with crash frequency. However, $C_{V_{AH}}$ is negatively associated with crash frequency (at 90% confidence interval). It can be concluded, overall, volatility of deceleration regardless of speed range is positively associated with crash frequency. However, when it comes to acceleration, volatility at lower speed is more a significant factor as compared to volatility at higher speeds.

At signalized intersections, the association between $C_{V_{AL}}$, $C_{V_{AH}}$ and $C_{V_{DH}}$ and crash frequency is also positive and statistically significant. $C_{V_{DL}}$ for signalized intersection; however, it is negatively correlated with crash frequency.

Referring to marginal effects for random parameter model in Table 3.2, on average one-percent increase in $C_{V_{DH}}$ is associated with 0.11 increase in crash frequency for all intersections and 0.089 increase in crash frequency for signalized intersections. These findings have implications for proactive intersection-related safety strategies. In addition, it is interesting to note the significantly higher marginal effect of acceleration C_Vs for signalized intersections, implying that higher variability in acceleration at signalized intersections may potentially result in more crashes. Given that signalized intersections are typically observed to have more crashes (Abdel-Aty and Keller, 2005), proactive intersection-customized strategies can be designed. For instance, proactive warnings and alerts can be generated about potential hazards at specific intersections and transmitted to drivers via connected vehicle technologies such as road-side

equipment. This can in turn increase drivers' situational and safety awareness, and help drivers in undertaking safer driving behaviors.

Regarding un-signalized intersections, as shown in Table 3.2, $C_{V_{AL}}$ and $C_{V_{DL}}$ are statistically significant. We found negative association between $C_{V_{AL}}$ and crash frequency. This finding is seemingly counter intuitive and needs further investigation. Possibly, for un-signalized intersection, due to their uninterrupted traffic in major approach (78% of them are T-intersections), separation of 3-leg and 4-leg intersection might shed more clarification in future studies. However, the finding that $C_{V_{DL}}$ (Coefficient of variation of deceleration below mean speed of intersection) is positively associated with crash frequency is intuitive i.e. larger the volatility/variation in decelerations at low speeds, the more crash frequency at a particular intersection.

The estimation results quantify associations between major and minor road AADT and crash frequency. Referring to marginal effects from the random-parameter model, one-log unit increase in major road AADT is associated with 2.69, 6.57, and 1.82-unit increase in crash frequency for all intersections, signalized intersections, and un-signalized intersections, respectively. Minor road AADT is statistically significant in the random-parameter model for signalized intersections, but the relationships are not statistically significant for un-signalized intersections (Table 3.2). Speed limit on major roads is negatively associated with crash frequency for all intersections. These findings are consistent with past studies on this topic (Ye et al., 2009, Abdel-Aty and Haleem, 2011). Notably, the total number of through lanes is positively

associated with crash frequency. From Table 3.2, it can be observed that one added through lane is correlated with 0.547 more crashes.

Figure 3.3 illustrates how the study results can assist in proactive intersection safety management. The black, green and red circles in the figure are scaled crashes, volatility of acceleration, and volatility of deceleration at lower speeds, respectively. The intersection in the center is a known hotspot because it has more crashes and proportionately high levels of volatility. However, two other intersections shown in dashed ellipses have relatively low crashes but high volatility levels ($C_{V_{AL}}, C_{V_{DL}}$). In such locations (hotspots), although crash frequencies are low, drivers show proportionately more volatile driving behavior. In other words, at such locations crashes may be waiting to happen. Proactive countermeasures can be taken in those locations depending on the real cause of driving volatility, e.g., by studying speed limits, signal timing, geometric design, dilemma zone, and lines of sight.

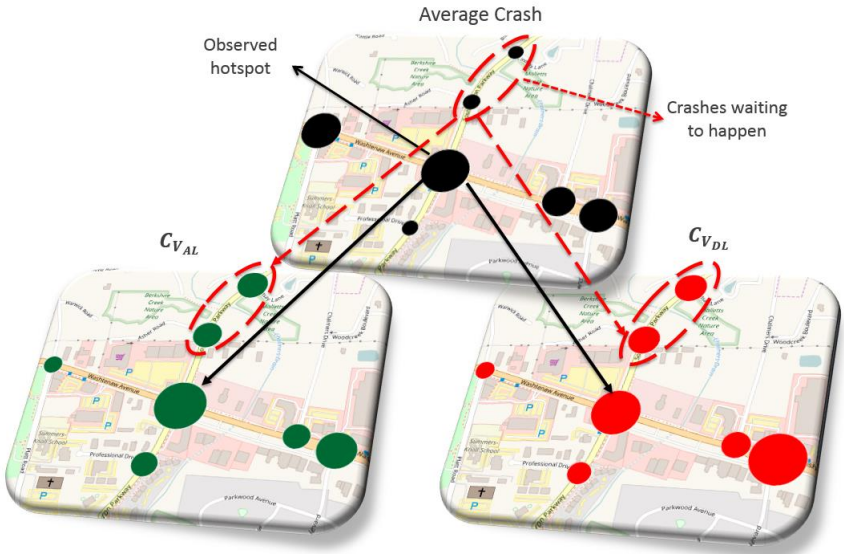

Figure 3.3 Known hotspots and spots where crashes are waiting to happen.

3.7 LIMITATIONS

The study captures variability in longitudinal acceleration/deceleration as a measure of intersection-specific volatility, which only partially capture the true volatility exhibited by drivers. As explained in the methodology section, due to data limitations, the study could not incorporate lateral acceleration/deceleration in estimation of intersection-specific volatility. While the results from this study provide evidence between crash frequency and intersection-specific volatility, more robust measures such as vehicular jerk and combination of longitudinal and lateral accelerations can be used in future studies for quantifying volatility at specific intersections. Also, the results and conclusions of this study are dependent on the sample-size. Another limitation is that one month data were used to explain 5-year average crash. While the current sample size may not be enough to draw robust conclusions, the authors have used all available data for 116 intersections.

3.8 CONCLUSIONS

This study contributes by developing and demonstrating a proactive intersection safety methodology using real-world large-scale connected vehicle data. The study quantifies volatility in instantaneous driving decisions using intersection-specific Basic Safety Messages (BSMs) and its relationship with observed crash frequencies, while controlling for other variables. Such a method can complement the state-of-the-art in evaluating intersection safety, which is largely reactive, based on observed and expected crash frequencies. The emerging data from Connected and Automated (CAVs) are increasingly becoming available, which can help us understand the detailed nature of instantaneous driving behaviors prior to the occurrence of unsafe outcomes

such as crashes/incidents. This study proposes the concept of location-based volatility that captures the extent of variations in instantaneous driving decisions.

A unique database that provides a more complete picture of operations and safety performance was created by combining more than 65 million Basic Safety Messages transmitted between connected vehicles and roadside units at 116 intersections in Ann Arbor, Michigan, with crash and inventory data. The geo-coded raw BSMs were allocated to each intersection and the connected vehicles trajectories extracted from raw BSMs were plotted, revealing reasonable data precision and coverage. A simple and standardized measure of dispersion called Coefficient of Variation (C_V) (also known as the ratio of relative standard deviation) was used to quantify the fluctuations in longitudinal acceleration and/or decelerations at specific intersections. Five-year crash frequencies, AADT, speed limits, and number of approaches for all intersections are extracted and linked with location-based volatilities. Significant efforts went into data processing, collection, and linkage.

Rigorous fixed and random parameter Poisson regression models are estimated that allow consideration of unobserved heterogeneity in crash data. The modeling results reveal that most of computed C_Vs (as measures of volatilities) are positively associated with crash frequency. The study has implications for proactive intersection safety management. Importantly, the magnitude of association between location-based volatility and crash frequency is significantly higher for signalized intersections, implying that higher variability in instantaneous driving decisions at signalized intersections may potentially result in more crashes. This finding is important in the sense that if many drivers behave in a volatile manner at a specific intersection (exhibit higher

variability in longitudinal accelerations), then such intersections can be identified before accidents happen. Of course, the reasons for volatile behaviors may be related to intersection and environmental conditions, vehicles' and drivers' conditions. Given that signalized intersections are typically observed to have more crashes (Abdel-Aty and Keller, 2005), intersection-customized strategies can be designed to improve safety. Proactive warnings and alerts can be generated about potential hazards at specific intersections and transmitted to drivers via connected vehicle technologies such as road-side equipment; these can in turn increase drivers' situational and safety awareness, and help them pursue safer driving at dangerous intersections.

3.9 ACKNOWLEDGEMENT

This paper is based upon work supported by the US National Science Foundation under grant No. 1538139. Additional support was provided by the US Department of Transportation through the Collaborative Sciences Center for Road Safety, a consortium led by The University of North Carolina at Chapel Hill in partnership with The University of Tennessee. Any opinions, findings, and conclusions or recommendations expressed in this paper are those of the authors and do not necessarily reflect the views of the sponsors.

CHAPTER 4 HOW IS DRIVING VOLATILITY RELATED TO INTERSECTION SAFETY? A BAYESIAN HETEROGENEITY-BASED ANALYSIS OF INSTRUMENTED VEHICLES DATA

This chapter presents modified versions of two research papers by Behram Wali, Asad J. Khattak, Hamparsum Bozdogan, and Mohsen Kamrani. These papers include:

Journal Paper - "How is Driving Volatility Related to Intersection Safety? A Bayesian Heterogeneity-Based Analysis of Instrumented Vehicles Data." Wali. B., Khattak, A.J., Bozdogan, H, Kamrani, M. Accepted for publication in Transportation Research Part C: Emerging Technologies.

Peer-Reviewed Conference Paper – "How is Driving Volatility Related to Intersection Safety in a Connected Vehicles Environment?" Wali, B., Khattak, A. J., Bozdogan, H. (2018). Presented at the 97th Annual Meeting of the Transportation Research Board, Washington DC, USA. TRB PAPER # 18-00058.

ABSTRACT

Driving behavior in general is considered a leading cause of intersection related traffic crashes. However, due to unavailability of real-world driving data, intersection safety performance evaluations are largely reactive where state-of-the-art methods are applied to analyze historical crash data. In this regard, the emerging connected vehicles technology provides a promising opportunity for investigating intersection safety more from a proactive perspective. Driving volatility captures the extent of variations in instantaneous driving decisions when a vehicle is being driven. This study develops a fundamental understanding of microscopic driving volatility and how it relates to unsafe outcomes at intersections. Using high resolution driving data from a real-world connected vehicle testbed, Safety Pilot Model Deployment, in Ann Arbor, Michigan, a methodology is presented to quantify driving volatility at 116 intersections by analyzing more than 230 million real-world Basic Safety Messages. For proactive intersection safety evaluation,

the large-scale connected vehicle data is then linked to detailed intersection data containing crashes, traffic exposure, and other geometric features. By using vehicular speed, acceleration/deceleration, and vehicular jerk based eight different volatility measures, descriptive analysis is performed to spot differences between driving volatility at signalized and un-signalized intersections. Then, in-depth statistical analysis is conducted separately for all intersections (signalized and un-signalized) and signalized intersections only. Importantly, not all factors that may influence crash frequency can be observed in the data. If unobserved factors could be included in a model, then correlations between driving volatility and crash frequency can change, e.g., the relationship can become statistically insignificant. Given the important methodological concerns of unobserved heterogeneity and potential omitted variable bias, hierarchical fixed- and random-parameter Poisson and Poisson log-normal models are estimated. Full Bayesian estimation via Markov Chain Monte Carlo (MCMC) based Gibbs sampling is performed, providing more efficient results. For all intersections, after controlling for traffic exposure, geometrics, and unobserved factors, a one-percent increase in intersection-level volatility calculated through two standard deviations threshold for acceleration/deceleration, passing level volatility captured through coefficient of variation of speed, and mean absolute deviance of vehicular jerk results in a 1.25%, 0.25%, and 0.35% increase in crash frequencies respectively. However, the relationships between intersection-specific volatility and crash frequencies are different for signalized intersections. Several of the exogenous factors are found to be normally distributed random parameters, suggesting that the effects of such variables vary across different intersections. The implications of the findings for proactive safety management are discussed.

4.1 INTRODUCTION

Intersections are believed to be the most dangerous locations on roadways potentially due to the complex traffic movements that result in large number of vehicular conflicts, and the diverse set of operational and geometric features associated with them (Zheng and Liu, 2017, Persaud and Nguyen, 1998, Hashimoto et al., 2016, Rakha and Kamalanathsharma, 2011, Rakha et al., 2007). As such, improving roadway intersection safety is of high interest to the profession. Through application of diverse set of advanced empirical methods, researchers since decades have come up with intersection targeted safety performance models (Quddus et al., 2001, Muralidharan et al., 2016, El-Basyouny and Sayed, 2013). Typically, intersection safety performance evaluations are largely reactive, where state-of-the-art methods are applied to link historical crash data with crash specific, operational, and geometric related features, to name a few (Lord and Mannering, 2010). Given information about the afore-mentioned characteristics specific to each intersection, crashes can then be predicted based on which appropriate safety treatments are developed and recommended (Braitman et al., 2007, Tay and Rifaat, 2007).

Driving behavior and/or human factors in general are considered a leading cause of intersection traffic crashes (Akamatsu et al., 2003, Zimmerman and Bonneson, 2004). Importantly, volatility in instantaneous driving decisions can be a leading indicator for understanding the occurrence of unsafe outcomes such as incidents or crashes (Wali et al., 2018d, Khattak and Wali, 2017). The concept of driving volatility captures the extent of variations in instantaneous driving decisions (such as variations in speed) when a vehicle is being driven at a specific roadway location (Khattak and Wali, 2017). Such information can help in identification of intersection locations where crashes may not have happened yet but are perhaps waiting to happen (Schneider et al.,

2004). In this regard, connected vehicles technology provides a promising avenue for investigating intersection safety, more from a proactive perspective. With monitoring, processing, and adequate integration of connected vehicle data with historical crash data, the generated large-scale empirical data from connected vehicle systems have significant potential in facilitating deeper understanding of instantaneous driving decisions, and to link microscopic driving decisions to unsafe safety outcomes. The Safety Pilot Model Deployment (SPMD) offers detailed instantaneous driving data generated by connected vehicles in real-world environment. This pilot, sponsored by US-DOT, is currently on-going in Ann Arbor, Michigan, and intends to display vehicle-to-vehicle (V2V) and vehicle-to-infrastructure (V2I) communication systems in real-life environment. Of specific interest are the Basic Safety Messages (BSMs) that provide high-frequency (usually ten times per second) information packets containing detailed data on vehicle's motion, location, driving context, and instantaneous driving decisions (e.g., speed).

This study focuses on extending the concept of driving volatility to specific intersections, thus termed as Intersection-Based Volatility, by using real-world large-scale connected vehicle data. Given that navigating through an intersection is a complex task, we posit that the concept of intersection-based volatility can provide critical insights regarding the correlations between driving behaviors (its extent and variation) at a specific intersection and key safety outcomes. Using large-scale real world microscopic driving data, a methodology for conceptualizing and quantifying driving volatility at individual intersections is presented. Then, for proactive intersection safety management, driving volatilities at specific intersections are linked to detailed intersection data containing crashes, traffic exposure, and other geometric features. From a methodological perspective, appropriate count data models are developed within Full Bayesian

framework, and which accounts for the important issues of omitted variable bias and unobserved heterogeneity (discussed later in detail).

4.2 LITERATURE REVIEW

A careful review of literature reflects the prompt response by government agencies, automotive industry and academia to such disruptive yet beneficial connected and automated vehicles innovation. This innovation has an unquestionable potential to significantly improve the current transportation systems (Ghiasi et al., 2017a, Wali et al., 2018d, Liu and Khattak, 2016, Khattak and Wali, 2017, Zeng et al., 2017), with some recent studies showing benefits in form of comprehensive crash savings, fuel efficiency, parking benefits, and travel time reduction to approach $4000 per year for each CAV operated on road (Fagnant and Kockelman, 2015). From a research perspective, a wide range of reliable transportation connectivity solutions are explored to address real world safety challenges, mobility issues, and environmental challenges (Khattak and Wali, 2017, Zulkefli et al., 2017, Zulkefli et al., 2014, Liu and Khattak, 2016a, Wali et al., 2018e, Letter and Elefteriadou, 2017).

Connected vehicle solutions can potentially help in addressing transportation challenges by primarily targeting the human factor involved in surface transportation. From safety perspective, driving behavior and/or human factors in general are considered a leading cause of traffic crashes (Akamatsu et al., 2003, Zimmerman and Bonneson, 2004, Kamrani et al., 2014, Arvin et al., 2017). Since decades, by analyzing traditional crash, roadway, and geometric data, researchers have developed safety performance models for designing effective safety countermeasures. However, the intersection safety countermeasures in particular and road safety countermeasures

in general are typically reactive in nature, i.e., roadway or intersection geometric improvements are developed once crashes happen, and are not specifically designed based on the driver's behavior which in turn is a major cause of unsafe outcomes at intersections. This largely can be attributed to the intrinsic limitations of traditional crash data which do not provide detailed information about drivers' performance, and typically surrogate measures such as speed limits or controlled simulation experiments are used to evaluate drivers' performance (Aarts and Van Schagen, 2006, Bao and Boyle, 2008, Haglund and Åberg, 2000, Shah et al., 2018, Wali et al., 2017a, Wali et al., 2017b). On the other hand, the rapid technological sensor and driving surveillance advancements in recent years have enabled collection of huge amounts of spatiotemporal data about vehicle and human movement (Ghasemzadeh et al., 2018). For example, by using Global Positioning System (GPS) based taxi data, Pei et al. (2012) investigated relationships between traveling speeds (as a measure of driving behavior) and safety outcomes for road segments in Hong Kong (Pei et al., 2012). Likewise, for proactive safety management, Quddus (2013) investigated relationship between traveling speeds and unsafe outcomes on motorways (freeways) by using segment-based 1 hour average speed data (Quddus, 2013).

As opposed to traditional GPS and loop-detector based data, the state-of-the-art has further advanced where human movements can be recorded by recent innovations that enable realization of V2V and V2I communication such as DSRC, Wi-Fi, Bluetooth, and cellular networks (Cheng et al., 2007, Chou et al., 2009, Sugiura and Dermawan, 2005, Kamrani et al., 2018c). The Safety Pilot Model Deployment (SPMD) provides an exciting opportunity by using state-of-the-art technologies to generate Basic Safety Messages (BSMs) that describe vehicle's instantaneous

position, vehicle maneuvering, and instantaneous driving contexts (Henclewood, 2014, Khattak and Wali, 2017). Important in this respect is the concept of "driving volatility" which is a measure of driving performance in connected vehicles network (Khattak et al., 2015, Khattak and Wali, 2017, Wali et al., 2018e, Wali et al., 2018d), and captures the extent of variations in driving, especially hard accelerations/braking and jerky maneuvers (Khattak et al., 2015, Khattak and Wali, 2017, Wali et al., 2018e, Wali et al., 2018d, Wang et al., 2015). The basic idea is to monitor instantaneous driving decisions (threshold based vehicular jerk, accelerations/decelerations), identify abnormal and extreme behaviors, and to generate proactive warnings in case unsafe driving maneuver is anticipated (Wang et al., 2015, Khattak et al., 2015, Khattak and Wali, 2017, Wali et al., 2018d).

Collectively, the potential of "trip-level" driving volatility in developing advanced traveler information systems, driving feedback devices, and alternative fuel vehicle purchase frameworks for consumers was documented (Khattak and Wali, 2017, Wang et al., 2015, Liu et al., 2017, Kamrani et al., 2018a). However, several gaps exist. First, all the afore-mentioned studies focused on trip-level driving volatility, i.e., driving volatility across a specific trip was conceptualized. Second, the earlier studies did not link trip-level volatility to unsafe outcomes such as traffic crashes. Third, from a methodological perspective, unobserved heterogeneity and omitted variables bias has not been dealt with adequately in the literature (discussed later in detail). The present study focuses on these issues and extending the concept of trip-level volatility to specific intersections, termed intersection-specific volatility. Specifically, a methodology is developed to quantify microscopic driving volatility in real-world high frequency microscopic driving data. The real-world driving volatility indices are then linked with

key safety outcomes to examine the relationships between intersection-specific volatility and unsafe outcomes (such as crashes). We believe that expanding the concept of driving volatility in connected vehicles environment to specific locations (i.e., intersections) has significant potential in identifying hazardous locations and which can have important implications for proactive safety management.

4.2.1 Research Objective and Contribution

The objectives of this study are:

1. To develop a methodology for quantifying driving volatility (magnitude and variations in instantaneous driving decisions) in CAV based Basic Safety Messages.
2. To understand correlations between driving volatility and traffic crashes at specific intersections.
3. To fully account for unobserved heterogeneity by developing full Bayesian hierarchical random parameter Poisson and Poisson log-normal models.

To achieve these objectives, significant efforts went into processing large-scale real-world connected vehicles microscopic driving data for generating intersection-specific driving volatility indices. In particular, more than 230 million Basic Safety Messages are analyzed to examine intersection-specific driving volatility. The volatility indices are then linked with intersection crash, exposure, and geometrics data that is collected for a sample of intersections in Ann Arbor, Michigan. As a key focus, the study aims at analyzing correlation between driving volatility and intersection crashes. Once the driving volatility indices are estimated, descriptive analysis is performed to spot differences between driving volatility at signalized and un-signalized intersections. The volatility indices for intersections are then visually compared to

historical crashes and meaningful patterns are spotted. Next, as signalized intersections often experience higher crash frequencies, in-depth statistical analysis is performed separately for all intersections (signalized plus un-signalized) and signalized intersections only. From a technological and data analytics standpoint, this study contributes by making sense of large-scale seemingly unstructured driving data collected in a connected vehicles environment. The raw data generated by sensors is of limited use to drivers when presented in raw form. Emerging large-scale data from connected vehicles, sensors, and telematics have recently become available, however, the methods to extract useful information from such data are not well established. Thus, a methodology is proposed in the current study that extracts patterns from the microscopic driving data that may be relevant to safety performance of intersections (discussed later in detail).

From a methodological standpoint, the interactions between driving behavior and traffic crashes are very complex involving driver responses to different stimuli, as well as interactions between driver, vehicle, roadway, and traffic factors. Given that the integrated connected vehicles and inventory data is assembled manually; it is obvious not all factors that may influence crash frequency are observed. In presence of such unobserved factors, it may happen that any correlation that is established between driving volatility and crash frequency is not real and in fact is an outgrowth of some other factors that are not observed in the data. If this happens, the traditional statistical models will have serious specification issues, and can lead to inconsistent, erroneous or unreliable, and biased correlations between driving volatility and crash frequency (Mannering et al., 2016). These methodological concerns are generally referred to unobserved

heterogeneity and omitted variable bias in the literature[31] (Mannering and Bhat, 2014). Thus, from a methodological perspective, for relating connected vehicles based driving volatility with unsafe safety outcomes at intersections, the study contributes by developing Full Bayesian fixed- and hierarchical random-parameter count data models via Markov Chain Monte Carlo (MCMC) based Gibbs updates. Specifically, hierarchical fixed- and random-parameter Poisson regression models are estimated in a Full Bayesian setup. While random-parameter Poisson regression models can capture the over-dispersion in crash data (Washington et al., 2010), recent studies have also shown that any variance/over-dispersion in crash data left behind in random-parameter Poisson model can be effectively captured with random parameter Poisson log-normal distributions (El-Basyouny and Sayed, 2009a). Thus, to better capture unobserved heterogeneity and to reduce its negative implications, we also test Poisson log-normal regression models in Full Bayesian context. The motivation behind using Full Bayesian estimation methods is discussed later.

[31] Statistically, leaving out one or more important explanatory factors can lead to omitted-variable bias (Mustard, 2003). One of the implication of omitted-variable bias is that the estimated model will tend to over- or underestimate the effects of observed variables. Alternatively, this suggests that in presence of such unobserved factors, it may happen that any correlation that is established between driving volatility and crash frequency is not real and in fact is an outgrowth of some other factors that are not observed in the data. These omitted factors (and which constitute heterogeneity due to unobserved factors) can lead to variation in the effects of observed explanatory factors on crash frequency (Mannering et al., 2016). To account for these issues, we employ a Bayesian version of random parameter modeling technique that can guard us from the severe implications of omitting important variables from the model specification. However, we emphasize that the statistical methods used in this paper do not "explicitly" address omitted variable bias. In our case, the potential omitted explanatory factors that are likely to be associated with crash frequency become a portion of the unobserved heterogeneity. As such, the statistical methods used in this study that account for unobserved heterogeneity can mitigate the adverse impacts of omitted variables bias (Mannering et al., 2016). However, as noted in Mannering et al. (2016), we acknowledge that the parameter estimates obtained from the Bayesian heterogeneity-based models may not track the unobserved heterogeneity (due to omitted variables) as good as if we could have included all the important omitted variables in the model specification (Mannering et al., 2016).

4.3 METHODOLOGY

4.3.1 Conceptual Framework

To understand driving volatility at intersections, detailed microscopic data on instantaneous driving decisions are needed. In this regard, the currently on-going connected vehicles Safety Pilot Model Deployment program provides relevant data. However, the generated data regarding instantaneous driving decisions is high-resolution and highly microscopic in nature, and is of little use if presented to drivers in raw form. Thus, a methodology needs to be developed first by which we can meaningfully process and combine microscopic driving data and use it for generation of volatility indices at aggregate level, e.g., intersection-level. The concept of driving volatility captures the extent of variations in instantaneous driving decisions (such as variations in speed, acceleration, or vehicular jerk) when a vehicle is being driven at a specific roadway location (Kamrani et al., 2017, Khattak and Wali, 2017, Wali et al., 2018e). Such volatility indices can represent, on-average, the driving performance of majority of drivers traversing through a specific intersection. For intersection safety management, such information is crucial as it can highlight intersection locations where behaviors of drivers may differ, compared to their behaviors at other intersection locations. With real-world driving data based volatility indices, proactive safety countermeasures can be planned for hazardous intersection locations. Another dimension to this is to investigate potential correlations between intersection-specific driving volatility and historical crashes. We posit a positive correlation between variations in instantaneous driving decisions and crash frequency at a specific intersection. Any correlation, if exists, can shed light on microscopic driving decisions, and how such decisions influence intersection safety.

4.3.2 Intersection Based Volatility

For development of volatility indices, different instantaneous driving measures may be used such as vehicle speeds, accelerations/decelerations, vehicular jerk, and/or steering angles (Kamrani et al., 2017, Liu and Khattak, 2016b, Quddus, 2013a, Wali et al., 2018e). For instance, Liu and Khattak (Liu and Khattak, 2016) quantified trip-level driving volatility by using acceleration/deceleration based thresholds in connected vehicle environment. Likewise, Khattak and Wali (2017) used acceleration/deceleration based profiles to examine volatility in driving regimes in a connected vehicles environment (Khattak and Wali, 2017). Vehicular jerk is also recently introduced for conceptualizing instantaneous driving volatility in trips (Wang et al., 2015). Compared to acceleration/deceleration based volatility measures, vehicular jerk can better capture the variations in driving behavior (Wang et al., 2015). Likewise, Kamrani et al. (2017) used acceleration/deceleration based measures to quantify driving volatility at intersections (Kamrani et al., 2017).

Keeping in view the previous work, we propose several microscopic speed, acceleration/deceleration, and vehicular jerk based measures derived from high-resolution driving data to develop intersection-specific volatility indices. Given that acceleration capabilities vary across different speeds (low and high), the acceleration/deceleration based volatility indices used are made sensitive to traveling speeds. The present study differs from the study by Kamrani et al. (2017) both methodologically and conceptually (Kamrani et al., 2017). From a methodological perspective, this study employs Full Bayesian (FB) methodology (compared to empirical Bayes or maximum likelihood estimation) for proactive safety evaluation. Compared to other methods, FB estimation technique builds upon using prior

distributions which has many advantages such as accounting for temporal and spatial variations, the flexibility of allowing estimation of models with smaller sample sizes, allowing models with several hierarchies, and more detailed insights such as parameter distributions and credible intervals (Dong et al., 2014). To fully account for unobserved heterogeneity, we employ and test a broader set of appropriate count data models in the FB setup. From a conceptual stand-point, Kamrani et al. (2017) used accelerations/decelerations as a measure of driving volatility, whereas instantaneous driving speed, acceleration/deceleration, and vehicular jerk based measures are used in the current study for quantifying driving volatility. Compared to other measures, speed profiles are also used for calculation of volatility because the relationship between safety outcomes and speed is more direct, i.e., speed (its magnitude and variation) is widely believed to directly influence safety outcomes (Aarts and Van Schagen, 2006, Quddus, 2013, Fildes et al., 1991). While simultaneously accounting for magnitude and heterogeneity (variance) in instantaneous driving decisions, we introduce several statistical measures to capture heterogeneity in instantaneous driving decisions at specific locations (discussed later in detail).

4.3.3 Calculation of Volatility

The data provides geo-coded information about vehicle position and motion characteristics such as instantaneous speeds and accelerations. Thus, the connected vehicle data from the SPMD were processed and cleaned. Next, we identified 116 intersections in Ann Arbor, Michigan, the details of which are discussed later. Figure 4.1 (upper panel) illustrates the sampled intersections in Ann Arbor area. To process and assign geocoded instantaneous trajectory data to individual intersections, a threshold of 150 feet was established from the center of each intersection and any geocoded BSM packet within 150 feet from the center of specific intersection was assigned to

that intersection[32]. For each intersection, polygons were drawn based on the 150 feet threshold from the center of intersection to all the intersection approaches. These geocoded polygons are then used to appropriately filter the Basic Safety Message data applicable to each of the sampled intersections. As such, a total of more than 230 million Basic Safety Messages were processed and linked to 116 intersections in Ann Arbor, Michigan. The bottom panel of Figure 4.1 illustrates the example for one of the signalized intersection. For each of the 116 intersections, the relevant microscopic driving behavior measures (speed, acceleration/deceleration, and vehicular jerk) are linked to particular intersection and volatility indices calculated. Note that the microscopic speed profiles include the zero speed data, i.e., when vehicle is stopped at an intersection. If this "mean speed" at signalized intersections includes the speed data when the vehicle is stopped, it can be expected that the driving volatility definition will be highly different between signalized and un-signalized intersections[33]. As such, we removed the zero speeds from the BSM data. While the magnitudes of driving volatilities calculated using data including zeros and excluding zeros varied, our overall conclusion regarding the extent of driving volatility at signalized and un-signalized intersections *(i.e., greater volatility on signalized intersections compared to un-signalized intersections)* remained the same (discussed later in detail).

The methodology used for quantification of driving volatility is explained next.

[32] The crash and road inventory data used in this study are manually downloaded from the Metropolitan Planning Organization (MPO) in Ann Arbor, Michigan (see http://semcog.org/Data-and-Maps.) Note that the 150 feet threshold (from the center of intersection) for linking Basic Safety Messages with intersections is employed because the intersection crash data are allocated to individual intersections based on a 150 feet threshold from the center of the intersection. Further details can be found at http://semcog.org/Data-and-Maps.

[33] We thank the anonymous reviewer for bringing up this conceptual concern to our attention.

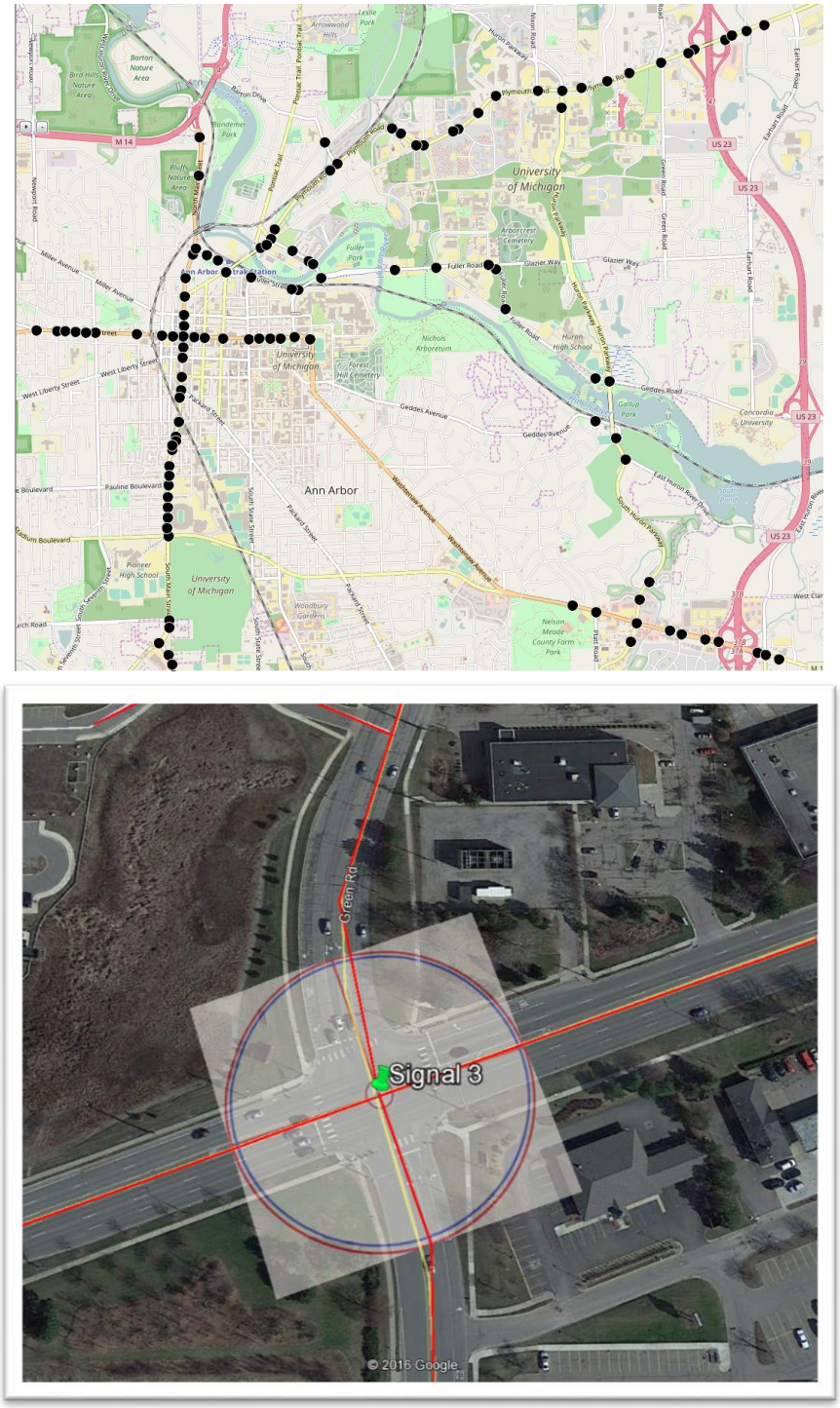

Figure 4.1 Sampled intersections in Ann Arbor area and method for calculating intersection specific volatilities. Notes: Black dots represent individual intersections in Ann Arbor, Michigan

From a data analytic standpoint, intersection-specific driving volatility indices are calculated from BSM data at two levels using:

1. Aggregate intersection level data
2. Trip level data.

Figure 4.2 illustrates the two levels used in the analysis. In particular, the driving volatility indices calculated at the first level (aggregate intersection level) are derived from considering the intersection-specific BSM data as a bulk and ignores the individual trips[34], i.e., vehicle passings at each intersections. At the second level (trip/passing level data), volatility indices are calculated for each vehicle passing and not bulk intersection-specific BSM data. To identify individual vehicle passings at each intersection, the time and device IDs provided in the SPMD BSM file are used. Once the volatility indices are calculated for each passing at a particular intersection, the average of the volatility indices for all the passings are calculated and reported as intersection-specific volatility measures. Compared to the passing level calculations, the calculations using aggregate data are relatively simpler and faster. Nonetheless, keeping in view the huge large scale BSM data (N > 230 million BSMs), the computations took considerable time on a work station level computer (Dell Precision T7600, 3.1 GHZ (32 CPUs)).

Finally, based on speed, acceleration/deceleration, and vehicular jerk, a total of eight different volatility measures at the two levels are calculated.

[34] Note that the notion of individual trips in our context refers to individual vehicle passings at each intersection, and are not necessarily entire trips undertaken by the instrumented vehicles. From this point onward, for the sake of convenience, we will use the words trips and passings interchangeably.

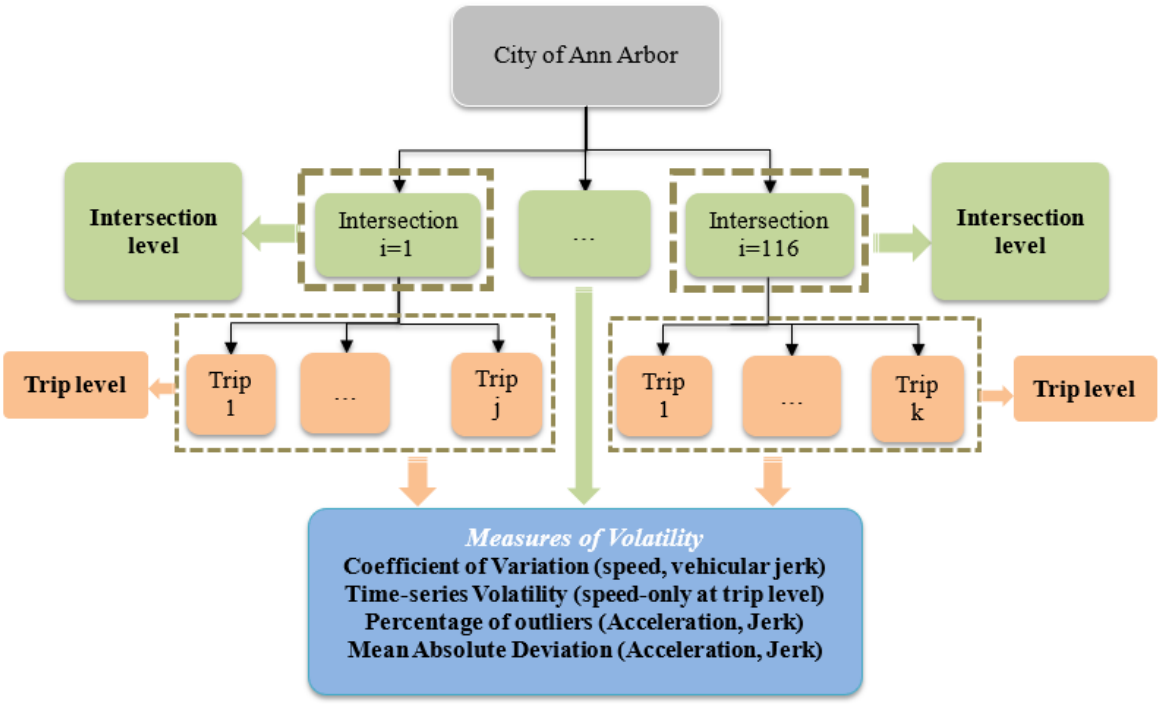

Figure 4.2 Measures of driving volatility calculated at trip and intersection level

4.3.3.1 Coefficient of variation:

The first statistical measure used is coefficient of variation in order to simultaneously account for the magnitude and heterogeneity (variance) in microscopic driving decisions. Specifically, compared to standard deviation or variance, coefficient of variation is scale in-sensitive and this property allows meaningful comparisons between the volatility in instantaneous driving decisions at different intersections. In particular, coefficient of variations are calculated using speed data (both at aggregate level and passing level) as well as vehicular jerk data. Note that vehicular jerk cannot be calculated using the aggregate data as vehicular jerk is a derivative of acceleration profiles, and as such requires identification of the trajectories of vehicles passing through the intersections. For each of the 116 intersections, average and standard deviations of speed and vehicular jerk are calculated. Note that the positive and negative values of vehicular jerk are separated and coefficients of variations are computed separately. Finally, coefficient of

variation, as a measure of intersection-specific volatility, is calculated by dividing the standard deviation of the driving measure (speed, vehicular jerk) by the average of the driving measure, i.e.,σ/μ.

4.3.3.2 Mean absolute deviation around mean:

This measure quantifies the average of difference of each individual observations from the mean. MAD is very similar to standard deviation but it is simpler and more intuitive (Huber, 2005).

$$MAD_{mean} = \frac{1}{n}\sum_{i=1}^{n}|x_i - \bar{x}| \qquad \text{Equation 4.1}$$

As a measure of driving volatility, the mean absolute deviance is calculated for vehicular jerk at passing level.

4.3.3.3 Percentage of outliers:

Another potential way of quantifying the extent of volatility in microscopic driving decisions is to obtain the ratio of outlier observations to total number of observations (Liu et al., 2015b):

$$V_O = \frac{count\ of\ obs.beyond\ the\ threshold}{n} * 100 \qquad \text{Equation 4.2}$$

Where: n is the total of number of observations. In this study, we have defined threshold as $\bar{x} \pm 2 * S_{dev}$. In case of applying the above equation to speed data, there would be two threshold as upper and lower bounds, and the speed observations falling outside the two bounds can be counted as outliers. However, in case of acceleration/deceleration, the capability of a vehicle to accelerate/deceleration vary significant at different traveling speeds, i.e., at higher speeds the

possible values of maximum acceleration and minimum deceleration are considerably smaller than the ones observed at lower speed. Therefore, instead of having two fixed upper and lower bounds, it would be more appropriate to define speed bins where each of them has their own upper and lower bound. The concept of is shown in Figure 4.3. Note that the driving volatility indices using this method are calculated both at intersection and passing level (see Figure 4.2).

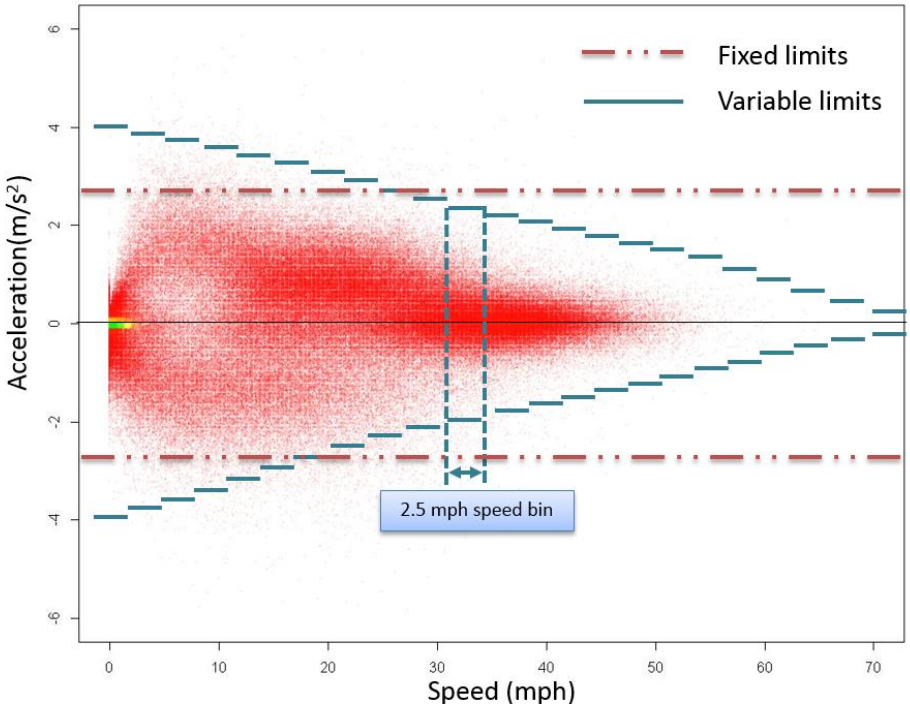

Figure 4.3 Dynamic speed varying thresholds for calculating volatility in acceleration/deceleration using BSM data.

4.3.3.4 Time dependent dynamic volatility:

This volatility measure is commonly used in Finance to analyze volatility in financial markets (Figlewski, 1994). This measure takes into account the time-series dependencies in the instantaneous driving data by calculating the standard deviation of the logarithms of the ratios of current observations x_i to x_{i-1} as follow (Kamrani et al., 2018, Figlewski, 1994):

$$V_f = \sqrt{\frac{1}{n-1}\sum_{i=1}^{n}(\mathrm{r_i} - \bar{r})^2} \quad \text{from } i = 1 \text{ to } n$$ Equation 4.3

Where:

$$\mathrm{r_i} = \ln\left(\frac{x_i}{x_{i-1}}\right) * 100$$ Equation 4.4

Note that the time dependent dynamic volatility can only be calculated at passing/trip-level and not using the aggregate data for each intersection (Figure 4.2). Overall, at intersection level, all the observations from different vehicles are placed back to back of each other and then overall intersection volatilities are calculated. Contrarily, at trip/passing level, the volatility of each trip is obtained and the average of trip volatilities are reported as the intersection volatility.

4.3.4 Statistical Models

Once the intersection-specific volatilities are calculated, we investigate the correlations between crashes and location-based volatility, after controlling for other traffic and geometric related factors. Appropriate statistical models can shed light on microscopic driving decisions i.e., intersection-specific volatility, and how such decisions influence intersection safety.

As the number of crashes occurring at a specific intersection have count nature, count data models can be estimated (Washington et al., 2010, Kamrani et al., 2017). In particular, the dependent variable is average number of crashes over a five-year period. Regarding the distributional forms, we consider Poisson and Poisson-lognormal regressions to model

intersection crashes as a function of intersection-specific volatilities and other factors (El-Basyouny and Sayed, 2009a, Kamrani et al., 2017).

4.3.4.1 Poisson regression

Let N_i denote the number of crashes at intersection i, where $i = 1,2,3, \ldots \ldots, N$. The probability of observing N crashes at intersection i, $(P(N_i))$, then can be formulated as:

$$P(N_i) = \frac{\exp(-\lambda_i)\lambda_i^N}{N_i!} \qquad \text{Equation 4.5}$$

Where: λ_i is Poisson parameter for intersection i, and is mathematically equal to expected crash frequency at intersection i, $E(N_i)$. Typically, λ_i is a log-link function of a set of explanatory factors (Washington et al., 2010, Kamrani et al., 2017):

$$E(N_i) = \ln(\lambda_i) = \beta_o + \beta_1 X_{i1} + \beta_2 X_{i2} + \cdots \ldots + \beta_N X_{iN} \qquad \text{Equation 4.6}$$

In Equation 4.6, X is a matrix of explanatory factors such as intersection-specific volatility, traffic and geometric factors, and $\beta's$ are model parameters.

4.3.4.2 Poisson-lognormal regression

Crash data is often characterized by over-dispersion i.e., mean is greater than variance. As an alternative to negative binomial/Poisson-gamma models (which accounts for over-dispersion), researchers have recently proposed to use Poisson-lognormal models for modeling crash frequency. For N_i number of crashes at intersection i, Poisson-lognormal model assumes that crashes at i intersections are independent and distributed as:

$$N_i|\theta_i \sim \text{Poisson}(\theta_i) \quad \text{Equation 4.7}$$

As opposed to Poisson regression where the mean and variance of crash data are constrained to be equal (Poch and Mannering, 1996), one may also address over-dispersion for the unmeasured heterogeneity in Poisson log-normal model as (El-Basyouny and Sayed, 2009a):

$$\theta_i = \lambda_i \exp(\lambda_i) \quad \text{Equation 4.8}$$

And, where: $\exp(\lambda_i)$ indicates a multiplication random effect (El-Basyouny and Sayed, 2009a). λ_i can then be regressed, as a log-link function, on a set of explanatory factors following the same specification in Equation 6. Specifically, $\exp(\lambda_i)$ is now assumed to be log-normally distributed with mean 0 and variance σ_λ^2.

Unlike the coefficients in a linear regression, the coefficients in Poisson/Poisson log-normal regression cannot be interpreted as marginal effects. To better interpret the results, elasticities of each variable are examined. Generally, elasticity can be calculated as (Washington et al., 2010):

$$E_{x_{iN}}^{\lambda_i} = \frac{\partial \lambda_i}{\partial x_{iN}} \frac{x_{iN}}{\lambda_i} = \beta_N x_{iN} \quad \text{Equation 4.9}$$

Where: E is the elasticity, x_{iN} is the value of the N^{th} explanatory factor for observation i, β_N is the parameter estimate for N^{th} explanatory factor, and λ_i is the expected crash frequency for observation i (Washington et al., 2010). Following (Washington et al., 2010), we compute the elasticities for each observation i, and report a single elasticity as an average elasticity for all i.

Note that the elasticity obtained through Equation 4.9 holds for continuous variables and not discrete. For dummy variables, we examine pseudo-elasticity. To examine the change in crash frequency with dummy variable switching from 0 to 1, the pseudo-elasticity can be computed as:

$$E_{x_{iN}}^{\lambda_i} = \frac{\exp(\beta_N) - 1}{\exp(\beta_N)} \quad \text{Equation 4.10}$$

4.3.4.3 Unobserved Heterogeneity in Poisson and Poisson log-normal Models

Given that the integrated CAV and intersection inventory data is assembled manually, not all factors that may influence crash frequency can be observed. Due to such unobserved factors, the associations between independent variables (such as intersection-specific volatility) and crash frequency may be varying across intersections. This is referred to as unobserved heterogeneity in the literature (Anastasopoulos and Mannering, 2009, Anastasopoulos et al., 2012, Khattak et al., 2016, Li et al., 2017, Mannering and Bhat, 2014, Mannering et al., 2016, Wali et al., 2017a, Wali et al., 2018b, Wali et al., 2018c, Wali et al., 2018d, Wali et al., 2018e), and in presence of which reliable and unbiased correlations between crash frequency and other factors (driving volatility in our case) cannot be established (Anastasopoulos and Mannering, 2009, El-Basyouny and Sayed, 2009a). Also, if important variables are omitted from the models (e.g., key geometric variables), it may happen that the observed correlation between location-based volatility (independent variable) and crash frequency may be an outgrowth of those omitted factors, and not true correlation between volatility and crash frequency. Given these issues, we account for unobserved heterogeneity by allowing the model parameters ($\beta's$) to vary across intersections in the Poisson and Poisson log-normal models as:

$$E(N_i) = \ln(\lambda_i) = \beta_{i,o} + \beta_{i,1}X_{i1} + \beta_{i,2}X_{i2} + \cdots \ldots + \beta_{i,N}X_{iN} \quad \text{Equation 4.11}$$

Where: $\beta_{i,j} \sim \text{Normal}(\beta_j, \sigma_j^2)$ and where $j = 0,1,2, \ldots . N$. We have considered different distributions for the regression parameters ($\beta_{i,j}$), however, normal distribution is observed to result in best fit (Dong et al., 2016). Further details can be found in (El-Basyouny and Sayed, 2009a, Dong et al., 2014).

4.3.5 Parameter Estimation

4.3.5.1 Prior Distributions

For the estimation of fixed- and random-parameter count data models, we have employed a full Bayesian estimation method. As such, it is essential to specify prior distributions for the regression parameters ($\beta's$) and variance parameters (σ_j^2). Strong informative priors can be used for estimable parameters when good prior information (e.g. from past research) is available, otherwise, non-informative (or vague) priors can be used. For regression parameters in Equation 4.6 (i.e., fixed parameter models), we use flat priors (similar to frequentist approach). For random parameter models, the following priors were used: $\beta_{i,j} \sim \text{Normal}(0, 100^2)$ and $\sigma_j^{-2} \sim \text{Gamma}(0.001, 0.001)$ or $\sigma_j^{-2} \sim \text{Gamma}(1, 0.001)$(Dong et al., 2016). These prior specifications are consistent with the literature (Qin et al., 2005). A regression parameter was considered random if the posterior estimate of $\hat{\sigma_j^2}$ was statistically significantly greater than zero. All the 95% credible intervals for location and shape parameters are constructed using the 2.5th percentiles and the 97.5th percentiles of the corresponding posterior distributions.

4.3.5.2 Markov Chain Monte-Carlo Methods

To quantify the uncertainty estimates for $\beta_{i,j}$ and σ_j^{-2}, posterior distributions are needed which are obtained using MCMC Gibbs Sampler techniques. Repeated samples are obtained from joint posterior distributions until the generated chains of random draws converge to the target posteriors. For the estimation process, a sub-sample of the random draws is used to monitor convergence and then discarded as burn-in sample. The remaining random draws are used to summarize parameter estimates, establish credible intervals, and inference. Proper convergence should be established before parameter estimation. To check convergence, for the fixed- and random-parameter Poisson and Poisson log-normal models, two chains are initiated each with 100,000 draws (in two updates of 50,000 draws) with 50,000 random draws used as burn-in samples. Following literature, we use Brooks-Gelman-Rubin (BGR) statistic for assessment of convergence. In our case, the BGR statistic was less than 1 for all parameter estimates, indicating convergence (Spiegelhalter et al., 2003).

Finally, for evaluating model performance and for comparing competing models, a Bayesian generalization of Akaike's Information Criteria (AIC) (Bozdogan, 1987), Deviance Information Criteria (DIC), is used. The criteria accounts for model complexity and fit, and is calculated as (Spiegelhalter et al., 2003):

$$\mathrm{DIC} = \mathrm{D_{bar}} + \mathrm{D_{bar}} - \mathrm{D_{hat}} \qquad \text{Equation 4.12}$$

Where: $\mathrm{D_{bar}}$ is the posterior mean of the unstandardized deviance of the model, D, and $\mathrm{D_{hat}}$ is the point estimate obtained by substituting $\mathrm{D_{bar}}$ in D. Following (Spiegelhalter et al., 2003), a

difference of more than 10 in DICs of two competing models may certainly rule out the model with higher DIC, whereas differences between 5 and 10 are substantial (El-Basyouny and Sayed, 2009a). However, if the difference in DICs of the competing models is less than 5, and the models suggest very different results, then it is essential to report both of the models (Spiegelhalter et al., 2003).

The likelihoods for estimable models are coded and evaluated in Stata's MATA language and MCMC Gibbs sampling performed in WinBUGS software which provides efficient tools for complex Bayesian inference.

4.3.6 Spatial Correlation Analysis

The modeling framework described earlier can capture unobserved heterogeneity in the observed relationships due to systematic variations in the unobserved factors. However, the random parameter modeling framework considers intersections independent of each other, i.e., the safety performance of one intersection is independent of the safety performance of another intersection in close proximity (Zeng et al., 2017, El-Basyouny and Sayed, 2009c). In recent years, several studies have shown that a micro-level spatial correlation can exist among segments/intersections in the sense that intersections nearer to each other will tend to be more similar (Guo et al., 2010, Quddus, 2008, Quddus, 2013a, El-Basyouny and Sayed, 2009c). In our case, the hypothesis is that the micro-level correlation may represent a second order variation that could not be reasonably explained by the explanatory factors alone. In order to examine the possibility of spatial autocorrelation, we conduct Moran's I test on the residuals of the estimated models for all

intersections as well as signalized intersections only (Guo et al., 2010, Quddus, 2008). Following Banerjee (2014)(Banerjee et al., 2014), the statistic is defined as (Black and Thomas, 1998):

$$\text{Moran's I statistic} = \frac{n\sum_i\sum_j w_{ij}(Y_i - Y')(Y_j - Y')}{\left(\sum_{i\neq j} w_{ij}\right)\sum_i (Y_i - Y')^2} \qquad \text{Equation 4.13}$$

Where: n is the total number of intersections indexed by i and j, Y_i and Y_j are the average crashes at intersections i and j, Y' is the global average of crashes at all intersections, and w_{ij} is the spatial proximity matrix that captures the spatial correlations among the intersections i and j. A common approach (especially in case of road segments) is to construct a contiguity matrix: setting the diagonal entries in this matrix as 0 and off-diagonal elements as 1, i.e., 1 if two intersections are neighbors, and 0 otherwise (Banerjee et al., 2014, Zeng et al., 2017, El-Basyouny and Sayed, 2009c). However, the w_{ij} in our case is populated as a function of the distance between the sample intersections as (Quddus, 2013a):

$$w_{ij} = \begin{pmatrix} c(d_{ij}) & \text{if } i \neq j \\ 0 & \text{if } i = j \end{pmatrix} \qquad \text{Equation 4.14}$$

Where: $c(d_{ij})$ is a decreasing function of the distances between intersections (d_{ij}) so that nearby intersections are more similar than the distant ones (Drukker et al., 2013). In this study, an inverse distance function is adopted, i.e., $c(d_{ij}) = \frac{1}{d_{ij}}$. For details, see (Quddus, 2013a, Drukker et al., 2013, Banerjee et al., 2014, Black and Thomas, 1998). Finally, a positive statistically significant Moran's I statistic will suggest that the crashes are positively spatially correlated and vice versa.

4.4 DATA

The connected vehicles data used in this study comes from the US-DOT sponsored Safety Pilot Model Deployment (SPMD) in Ann Arbor, Michigan. We retrieved the data from the official website of US-DOT Research Data Exchange program: https://www.its.dot.gov/data/. This pilot intends to display vehicle-to-vehicle (V2V) and vehicle-to-infrastructure (V2I) communication systems in a multi-modal real-life traffic environment with approximately 3,000 connected vehicles. Of specific interest are the Basic Safety Messages (BSMs) that provide high-frequency (usually ten times per second) information packets containing detailed data on vehicle's motion (heading, accelerations, speed), location (latitude, longitude, elevation), and driving context related factors. Specifically, the entire two months (October and April, 2012) publicly available connected vehicles data are used in this study. By using more than 230 million geo-coded BSMs aggregated to each intersection, intersection-specific volatilities are then calculated for all 116 intersections (53 signalized and 63 un-signalized intersections) using the methods described earlier. Next, for analyzing correlations between crashes and intersection volatility, historical crash data (2011-2015) are manually collected. As discussed earlier, the correlation between intersection-specific volatility and crashes cannot be established without accounting for the simultaneous effects of other traffic and/or geometric characteristics (Imprialou et al., 2016, Mannering and Bhat, 2014). Thus, significant data collection effort was undertaken to manually collect traffic and intersection inventory data for all intersections considered in this study (Kamrani et al., 2017). Specifically, data on annual average daily traffic (AADT) on major and minor approaches, number of intersection legs, total through lanes, total left turn lanes, and total right turn lanes were collected. All this data is publicly available on the website of Metropolitan Planning Organization (MPO) in Ann Arbor, Michigan: http://semcog.org/Data-and-Maps,

however is manually extracted as data are not available in analysis ready format (spreadsheet form). Out of all the intersections in Ann Arbor, 116 intersections are identified and considered in this study. This is because enough connected vehicle data for calculation of intersection-specific volatilities were available for these intersections. To ensure data accuracy, the distributions of key variable used in calculation of intersection volatilities were examined (discussed later in Results section). Also, to ensure accuracy and reliability of the manual data collection effort, another team member randomly selected 20% of the intersections and matched the manually collected data with the one on Ann Arbor MPO website. Doing so resulted in 100% correct matching.

4.5 RESULTS

4.5.1 Descriptive Statistics and Concept Illustration

First, we present the descriptive statistics of the BSM data used in this study. In particular, two-months of connected vehicles data (sample size of more than 230 million BSMs) are used including information on latitude and longitude, speed, and acceleration. Before excluding zero speeds, more than 2 million BSMs on-average are available for each intersections that translates to an average of 3337 minutes and more than 55 hours of real world driving data per intersection (Table 4.1). As shown in Table 1, a total of 6453.17 hours of driving data is used. However, after removal of zero speeds, it reduces to 4832.2 hours of driving data with average of 41.6 hours of driving data for each intersection (Table 4.1). In terms of vehicle passings, a total of 3291707

passings occurred at the 116 intersections, with an average of 28376.8 passings per intersection[35].

Table 4.1 Descriptive Statistics of BSM Data

Variable	Mean	SD	Min	Max	Sum
Before removal of zero speeds					
Number of Basic Safety Messages	2002708	2235865	171193	1.48E+07	2.32E+08
Minutes of driving data	3337.85	3726.44	285.322	24650.27	3.87E+05
Hours of driving data	55.63	62.11	4.76	410.84	6453.17
After removal of zero speeds					
Number of Basic Safety Messages	1499648	1402152	167816	9098974	1.74E+08
Minutes of driving data	2499.41	2336.92	279.693	15164.96	2.90E+05
Hours of driving data	41.66	38.95	4.66	252.75	4832.20
Number of passings	28376.8	26185	3745	148419	3291707

Notes: The column "mean" shows the average number of BSMs or the average minutes/hours of driving data available per intersection.

Next, Table 4.2 presents the descriptive statistics of key variables used in this study. Key distributional parameters are provided for each variable and for total intersections (N = 116), signalized intersections (N = 53), and un-signalized intersections (N = 63). Regarding volatility related variables, the mean speed at all intersections, signalized, and un-signalized intersections is 22.59, 15.95, and 28.19 mph respectively (Table 4.2). This is expected as traveling speeds at intersections are generally lower than on roadway segments and given that the sampled intersections are in a dense urban area. This suggests that, compared to signalized intersections, un-signalized intersections (on-average) have high traveling speeds.

[35] We sincerely thank the anonymous reviewer for suggesting to examine the ratio of time when the intersection have these CAV based BSMs. That is, if the ratio is not big, speed data based on the basic safety messages may not represent the real speed data. An earlier version of this paper used 62 million Basic Safety Messages as analysis of the CAV BSM data required significant computational resources. However, the entire 2 months CAV BSM data are now used (N > 230 Million BSMs). Considering the statistics and sample sizes in Table 4.1, the vehicle kinematics data can be considered to reasonably represent the real vehicle kinematics data at the sampled intersections.

Table 4.2 Descriptive Statistics of Key Variables

	Variable	All intersections				Signalized Intersections				Unsignalized Intersections			
		Mean	*Std. Dev.*	*Min*	*Max*	*Mean*	*Std. Dev.*	*Min*	*Max*	*Mean*	*Std. Dev.*	*Min*	*Max*
Volatility Related Factors	***Volatility 1****	56.35	24.35	12.77	101.40	76.48	13.94	35.90	101.40	39.41	17.30	12.77	84.03
	Volatility 2 *	6.67	1.12	2.69	8.77	7.28	0.64	5.16	8.50	6.16	1.18	2.69	8.77
	Volatility 3 *	4.12	3.28	0.31	11.88	6.82	2.62	0.71	11.88	1.84	1.63	0.31	7.75
	Volatility 4 *	19.37	14.16	1.34	52.83	30.71	10.85	5.20	52.83	9.84	8.41	1.34	40.47
	Volatility 5 *	2.43	0.50	0.93	3.61	2.68	0.44	1.72	3.61	2.22	0.46	0.93	3.36
	Volatility 6 *	78.10	5.53	68.23	96.17	81.69	4.49	73.32	92.87	75.08	4.42	68.23	96.17
	Volatility 7 *	76.59	4.40	68.60	93.52	78.45	3.99	71.93	93.52	75.02	4.14	68.60	87.78
	Volatility 8 *	0.85	0.12	0.57	1.16	0.85	0.11	0.65	1.01	0.84	0.13	0.57	1.16
	Mean Speed	22.59	8.93	8.55	43.89	15.95	4.96	8.55	33.01	28.19	7.59	12.13	43.89
	Standard deviation of speed	10.71	2.19	4.74	15.14	11.58	1.56	7.62	14.98	9.99	2.39	4.74	15.14
Crash history	Average crashes over five year period	6.78	6.67	0	40	11.66	6.80	1	40	2.68	2.52	0	12
	Crash rate (Per million entering vehicles)	0.57	0.49	0	2.18	0.96	0.44	0.12	2.18	0.24	0.19	0	0.9
Exposure	Major road AADT (in thousands)	20.8	8.32	3.1	45.4	22.74	8.2	3.6	45.4	19.17	8.13	3.1	38.9
	Minor road AADT (in thousands)	9.39	4.13	1.1	27.4	9.99	5.7	3.1	27.4	8.89	1.97	1.1	13.4
	Log form: Major road AADT in thousands	2.94	0.49	1.13	3.82	3.06	0.40	1.28	3.82	2.84	0.54	1.13	3.66
	Log form: Minor road AADT in thousands	2.15	0.47	0.10	3.31	2.16	0.52	1.13	3.31	2.13	0.43	0.10	2.60

Notes: (*) ***Volatility 1:*** Intersection level: Coefficient of variation of speed (%); ***Volatility 2:*** Intersection-level: Two standard deviations threshold for acceleration/deceleration; ***Volatility 3:*** Passing level: Time stochastic volatility; ***Volatility 4:*** Passing level: Coefficient of variation of speed (%); ***Volatility 5:*** Passing-level: Two standard deviations threshold for acceleration/deceleration; ***Volatility 6:*** Passing-level: Coefficient of variation of positive vehicular jerk; ***Volatility 7:*** Passing-level: Coefficient of variation of negative vehicular jerk; ***Volatility 8:*** Passing level: Mean absolute deviance of vehicular jerk; Std. Dev. is standard deviation.

Table 4.2 Descriptive Statistics of Key Variables (Continued)

	Variable	All intersections				Signalized Intersections				Unsignalized Intersections			
		Mean	*Std. Dev.*	*Min*	*Max*	*Mean*	*Std. Dev.*	*Min*	*Max*	*Mean*	*Std. Dev.*	*Min*	*Max*
Geometric Factors	Speed limit major road	35.34	7.24	25	45	35.94	7.34	25	45	34.84	7.18	25	45
	Speed limit minor road	30.47	3.96	25	45	30.85	5.16	25	45	30.16	2.53	25	40
	Signalized Intersections	0.46	0.50	0	1	1	0	1	1	0	0	0	0
	Four legged intersections	0.41	0.49	0	1	0.62	0.49	0	1	0.22	0.42	0	1
	Total number of through lanes	6.93	2.51	3	15	8.51	2.68	4	15	5.60	1.31	3	9
	Total number of right turn lanes	0.94	0.78	0	4	1.11	1.01	0	4	0.79	0.48	0	2
	Total number of left turn lanes	1.53	1.33	0	6	2.26	1.40	0	6	0.92	0.89	0	3

Notes: Std. Dev. is standard deviation.

As can be seen, the mean speeds at signalized and un-signalized intersections are very different. Likewise, the average speed at signalized intersections is 15.95 mph which is lower than the mean speed of 28.19 mph at un-signalized intersections. Based on these distributions, the connected vehicle data seem to be of reasonable quality.

Interestingly, the (mean) standard deviations of speeds for signalized intersections is little higher than un-signalized intersections (11.58 vs 9.99) (Table 4.2), suggesting that the variability in instantaneous driving speeds at signalized intersections is a bit higher than un-signalized intersections. However, in our case mean speeds at signalized and un-signalized intersections are significantly different (15.95 vs 28.19 mph), and in such case comparing the degree of variation (driving volatility) at signalized and un-signalized intersections by using standard deviation can often produce misleading and inaccurate conclusions (Wander and D'Vari, 2003). Thus, coefficient of variation can be used which represents the ratio of standard deviation to the mean, and is a useful statistic for comparing the variability in instantaneous driving decisions between signalized and un-signalized intersections even if the mean speeds (or other driving measure) differ significantly (Washington et al., 2010, Weber et al., 2004). In fact, coefficient of variation is widely used as a measure of heterogeneity in organizational demography research (Knight et al., 1999, Pelled et al., 1999). Having said this, the distributions of coefficient of variation (COV) of speed (as a measure of intersection-specific volatility) at intersection level shows that signalized intersections have in fact greater volatility (mean volatility 1 of 76.48 vs. 39.41 for signalized and un-signalized intersections) (Table 4.2). Likewise, coefficient of variation of speed calculated at passing level also reveals instantaneous driving speeds at signalized intersections to be more volatile (Table 4.2).

Coming to the driving volatility calculated using the percentage of outliers method, the results show that instantaneous accelerations/decelerations at signalized intersections are more volatile compared to un-signalized intersections, both at intersection as well as passing level (see volatility 2 and volatility 5 in Table 4.2). Likewise, the results of time-dependent dynamic volatility (volatility 2) reveals a significantly higher volatility in speeds at signalized intersections (6.82 for signalized intersections vs. 1.84 for un-signalized intersections). Overall, all of the volatility measures reveal signalized intersections to be more volatile (Table 4.2).

Regarding unsafe outcomes and traffic exposure, signalized intersections have higher (on-average) crash frequency and higher traffic exposure than their un-signalized counterparts (Table 4.2). As signalized intersections often have higher traffic volumes, crash rates are also reported in Table 4.2 in order to better compare the occurrence of unsafe outcomes at signalized and un-signalized intersections[36]. However, the crash rate comparison reveals that signalized intersections on-average have 0.96 crashes per million entering vehicles compared to 0.24 crashes per million entering vehicles at un-signalized intersections (Table 4.2). Compared to un-signalized intersections, the higher crash rates at signalized intersections is in agreement with the literature (Hazel, 2015). The data also reveals that speed limits on major and minor approaches are approximately similar for signalized and un-signalized intersections (Table 4.2). Likewise, 62% and 22% of the signalized and un-signalized intersections are four-legged respectively (Table 4.2). Based on the above statistics and the fact that the crash, traffic, and inventory data is

[36] Following the guidelines provided by U.S. Federal Highway Administration (Golembiewski and Chandler, 2011), crash rates at intersection are calculated using the formula $R = \frac{1{,}000{,}000 * C}{365 * N * V}$, where R is the crash rate for the intersection expressed as accidents per million entering vehicles (MEV), C is total number of intersection crashes in the study period, N is number of years of data, and V is traffic volumes entering the intersection daily (Golembiewski and Chandler, 2011).

extracted from a well-maintained publicly available database (Southeast Michigan Council of Governments – SEMCOG), the data is of reasonable quality. Furthermore, to visualize the relationship between intersection-specific volatilities and crash frequency, Figure 4.4A shows the historical crash frequencies (orange bubbles on the left) and intersection-specific volatilities (blue bubbles on the right) for the sampled 116 intersections. For illustration, intersection level driving volatilities based on percentage of outliers of acceleration/deceleration (as illustrated in Figure 3 earlier) are used in Figure 4.4A. As discussed earlier, the intersection-specific volatilities capture the extent of variations in instantaneous driving decisions when a vehicle is being driven at a specific intersection. Broadly, for the encircled intersections in Figure 4.4A, crash frequencies are generally lower while intersection-specific volatilities are relatively larger. To further elaborate the point, the bottom panel (Figure 4.4B) focuses on a subset of intersections which are highlighted in top panel. Here, the differences are clearer in the sense that some intersections can be termed "known hot-spots" (highlighted in solid circles) i.e., both crash frequencies and volatilities are higher and approximately similar, whereas the intersections highlighted in dashed circles have lower crash frequencies but significantly higher intersection-specific volatilities. This implies that the observed crash frequency is lower but perhaps crashes are waiting to happen as instantaneous driving decisions are consistently more volatile at such intersections (Schneider et al., 2004). For intersection safety management, such information is crucial as it can highlight intersection locations where behaviors of drivers may differ, compared to their behaviors at other intersection locations. Thus, safety managers may consider proactive countermeasures at such locations, e.g., providing proactive alerts and warnings to drivers through connected vehicle roadside equipment (RSE) (Kamrani et al., 2017, Khattak and Wali, 2017, Wali et al., 2018e).

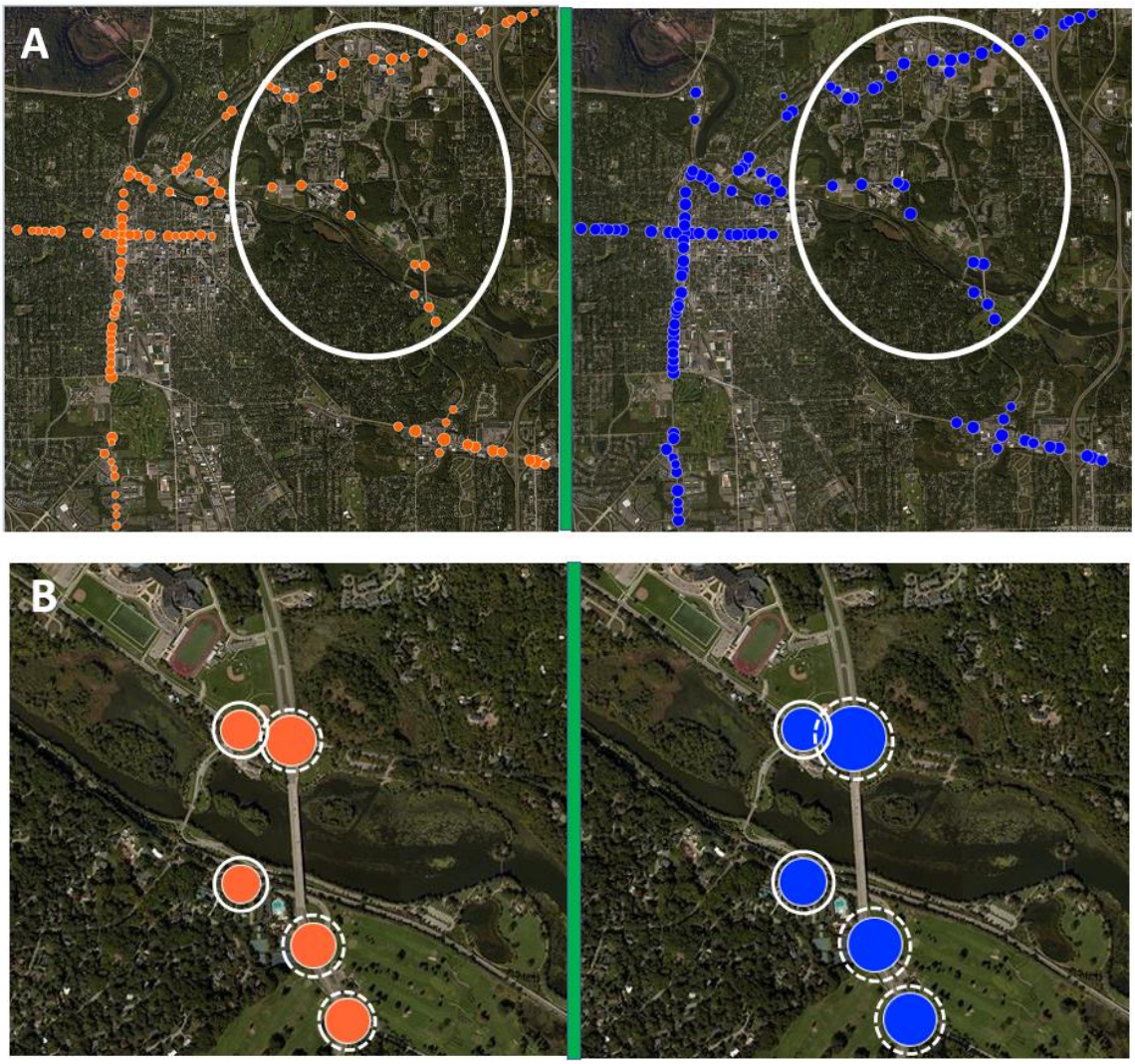

Figure 4.4 Visual Illustration of Relationship between Intersection-Specific Volatility and Crash Frequency
(Orange bubbles indicate average crash frequency and blue bubbles indicate intersection-specific volatility; Bubbles scaled equivalently for comparison purposes).

4.5.2 Modeling Results

The descriptive statistics and simple visualizations presented earlier helped in spotting meaningful relationships between crash frequency and intersection-specific volatilities. However, without controlling for important traffic exposure and/or geometric related factors, the descriptive or visual relationships are not conclusive (Imprialou et al., 2016). Given the count data nature of crashes, appropriate count data models in a Full Bayesian setting are estimated.

Specifically, average of yearly crashes over a five years period at intersections is modelled as a function of intersection-specific volatilities, and other factors (Table 4.2). The results of statistical models are presented and discussed next that quantify the correlations between crashes and intersection-specific volatilities, after controlling for other traffic and geometric related factors.

All the models (for all intersections and signalized) are derived from a systematic process to include most important variables (available in the data) based on intuition, statistical significance, and specification parsimony. Initially, a series of full Bayes fixed-parameter pooled Poisson models were estimated for all intersections by controlling for signalized vs. un-signalized intersections through a dummy variable (see Table 4.2). All the variables shown in Table 4.2 were tested and the statistically significant explanatory factors were retained. Among all the factors available, the focus was on examining the relationships between intersection-specific volatilities and crash frequency. As discussed in detail in the methodology section, unobserved heterogeneity is suspected and in presence of which the correlations obtained in full Bayes fixed parameter models may be biased and inefficient. As such, random-parameter Poisson model is estimated in full Bayesian context. Compared to random-parameter Poisson models, random-parameter Poisson log-normal models can help in accounting for extra over-dispersion in crash data, if any is left behind. Thus, random parameter Poisson log-normal model is also estimated. A parameter estimate for a particular explanatory variable is treated as random if the parameter estimates exhibited 1) only statistically significant standard deviations, or 2) exhibited both statistically significant means and standard deviations. If a parameter estimate exhibited only statistically significant standard deviations, the information criteria statistic was

examined to compare the model treating the specific variable as random parameter (with only statistically significant standard deviation) with the alternative model treating the parameters for the same variable as fixed parameter (Fountas and Anastasopoulos, 2017). Further details about the implications of statistical significance of mean and variance parameters in random parameter modeling framework can be found in (Behnood and Mannering, 2017b, Wali et al., 2018e, Wali et al., 2018b). Table 4.3 presents the results of fixed parameter Poisson (base model), hierarchical random parameter Poisson model, and hierarchical random parameter Poisson log-normal model. Compared to the fixed-parameter Poisson model, both hierarchical random parameter Poisson and hierarchical random parameter Poisson log-normal model resulted in better fit (as shown by the DIC values in Table 4.3). However, the hierarchical random parameter Poisson log-normal performed better than the hierarchical random parameter Poisson model (DIC values of 546.871 vs. 552.969). This suggests that there exists extra over-dispersion in crash data beyond the one captured in random parameter Poisson regression. However, the extra-Poisson variance in hierarchical random parameter Poisson log-normal model is not substantial (see Table 4.3).

Table 4.3 Full Bayes Gibbs Sampler Random Parameter Estimation of Crash Models (All Intersections)

Variables	Fixed Parameter Poisson Model	Hierarchical Random Parameter Poisson (HRPP) Model	Hierarchical Random Parameter Poisson Log-Normal (HRP-PLN) Model
Mean effects (location parameters)			
Volatility Related Factors			
Volatility 2[a]	0.19	0.258	0.188
	(0.0742, 0.3052)	(0.0741, 0.3920)	(0.0984, 0.2806)
Volatility 4[b]	0.011	0.0123	0.013
	(0.0041, 0.0188)	(0.0027, 0.0218)	(0.0225, 0.0246)
Volatility 8[c]	0.392	0.772	0.414
	(-0.339, 1.134)	(0.1549, 1.7190)	(0.0847, 0.8961)
Other factors			
Major road AADT (log form)	0.763	0.748	0.732
	(0.5501, 0.9845)	(0.5223, 0.9609)	(0.4846, 0.9659)
Minor road AADT (log form)	0.201	0.148	0.160
	(0.0518, 0.3589)	(0.0657, 0.3795)	(0.0812, 0.3788)
Signalized intersection	0.73	0.680	0.733
	(0.4859, 0.9744)	(0.4650, 0.9498)	(0.3228, 1.0711)
Four leg intersection	0.319	0.277	0.298
	(0.154, 0.489)	(0.0462, 0.5075)	(0.0520, 0.5445)
Constant	-3.4 (-4.7390,-1.9690)	-4.042 (-5.732, -3.826)	-3.298 (-4.561, -2.2011)
Unobserved effects (standard deviations/scale parameters)			
Signalized intersection	---	0.053 (0.0164, 0.1821)	0.048 (0.0167, 0.1521)
Volatility 2[a]	---	0.037 (0.0184, 0.0574)	0.032 (0.0163, 0.0521)
Volatility 8[c]	---	0.053 (0.0161, 0.212)	0.047 (0.0162, 0.1705)
Major road AADT (log form)	---	0.048 (0.0169, 0.1071)	0.042 (0.0161, 0.0931)
Extra-Poisson variance	---	---	0.0311 (0.0007, 0.123)
Goodness of Fit			
Dbar	577.353	499.818	497.691
Dhat	569.294	446.667	448.511
pD	8.058	53.151	49.18
DIC	585.411	552.969	546.871

Notes: (a) Volatility 2 is Intersection-level: Two standard deviations threshold for acceleration/deceleration, (b) Volatility 4 is Passing level: Coefficient of variation of speed, (c) Volatility 8 is Passing level: Mean absolute deviance of vehicular jerk. All the 95% credible intervals for location and shape parameters are constructed using the 2.5th percentiles and the 97.5th percentiles of the corresponding posterior distributions; Included in the parenthesis are the 95% credible intervals for location and shape parameters.

Next, separate regression models (un-pooled) are estimated for quantifying the relationship between intersection volatility and crash frequency for signalized intersections. For signalized intersections, the results of full Bayes fixed parameter Poisson, hierarchical random parameter Poisson, and hierarchical random parameter Poisson log-normal models are presented in Table 4.4. As can be seen, hierarchical random parameter Poisson model resulted in best fit[37] (lowest DIC value of 305.366) (Table 4.4). Note that the DIC of hierarchical random parameter Poisson log-normal model is 306.226 which is slightly more than the DIC of random parameter Poisson model. As the differences in DIC is negligible, and given that the parameter estimates in both of the models do not differ significantly, a random parameter Poisson model is preferable. Also, the extra variance in random parameter Poisson log-normal model is negligible.

Finally, to better interpret the results, elasticities for continuous variables and pseudo-elasticities for dummy variables are provided for all the estimated models in Table 4.5. In particular, the mean, standard deviations, minimum, and maximum elasticities are provided for all the variables to spot the differences. With all other variables controlled at average values, average elasticities translate to percentage increase/decrease in crash frequency with a one percent increase in corresponding continuous variable from its mean value (switching from 0 to 1 for dummy variable). Whereas, maximum elasticities translate to percentage increase/decrease in crash frequency with a one percent increase in the maximum value of corresponding continuous variable (Table 4.5). As hierarchical random parameter Poisson log-normal model and random

[37] Given the possibility of spatial autocorrelation among the sampled intersections (as discussed earlier), Moran I tests are conducted on the residuals of models for all intersections as well as signalized intersections only. For all intersections, the calculated Moran's I for the error terms of the Poisson model is 0.044 with a corresponding z-statistic of 1.33. Likewise, for signalized intersections, the estimated Moran's I statistic of the error terms of Poisson regression is 0.081 with a z-statistic of 1.42. Given the small and statistically insignificant Moran's I statistics, a lack of significant positive spatial autocorrelation in the data can be concluded at a 99% confidence level.

Table 4.4 Full Bayes Gibbs Sampler Random Parameter Estimation of Crash Models (Signalized Intersections Only)

Variables	Fixed Parameter Poisson Model	Hierarchical Random Parameter Poisson Model	Hierarchical Random Parameter Poisson Log-Normal Model
Mean effects (location parameters)			
Volatility Related Factors			
Volatility 2[a]	0.011	0.075	0.136
	(-0.0211, 0.2413)	(-0.0031, 0.2693)	(-0.0498, 0.3433)
Volatility 4[b]	0.012	0.0014	0.014
	(0.0036, 0.0203)	(0.0024, 0.0261)	(0.0014, 0.0262)
Other factors			
Major road AADT (log form)	0.660	0.573	0.581
	(0.4079, 0.91140	(0.2917, 0.9205)	(0.0171, 0.9655)
Minor road AADT (log form)	0.020	0.164	0.165
	(0.0416, 0.3595)	(0.0509, 0.4056)	(-0.0785, 0.3987)
Four leg intersection	0.3429	0.335	0.313
	(0.1475, 0.5424)	(0.0529, 0.6181)	(0.0267, 0.5987)
Constant	-1.482	-0.9574	-1.416
	(-2.5512, -0.4075)	(-2.5860, 0.7146)	(-2.9140, 0.1474)
Unobserved effects (standard deviations/scale parameters)			
Major road AADT (log form)		0.044	0.040
	---	(0.0166, 0.0987)	(0.0161, 0.0911)
Volatility 4		0.045	0.031
	---	(0.0187, 0.0549)	(0.0162, 0.0518)
Extra-Poisson variance			0.0289
	---	---	(0.0008, 0.1171)
Goodness of Fit			
Dbar	329.556	276.811	275.447
Dhat	323.525	248.256	244.669
pD	6.031	28.555	30.778
DIC	335.588	305.366	306.226

Notes: (a) Volatility 2 is Intersection-level: Two standard deviations threshold for acceleration/deceleration, (b) Volatility 4 is Passing level: Coefficient of variation of speed. All the 95% credible intervals for location and shape parameters are constructed using the 2.5th percentiles and the 97.5th percentiles of the corresponding posterior distributions; Included in the parenthesis are the 95% credible intervals for location and shape parameters.

Table 4.5 Elasticity Estimates for Explanatory Variables

Variables	All Intersections											
	Poisson Model				HRPP Model				HRP-PLN Model			
	μ	***SD***	***Min***	***Max***	***μ***	***SD***	***Min***	***Max***	***μ***	***SD***	***Min***	***Max***
Volatility Related Factors												
Volatility 2[a]	1.27	0.21	0.51	1.67	1.72	0.29	0.70	2.26	1.25	0.21	0.51	1.65
Volatility 4[b]	0.21	0.16	0.01	0.58	0.24	0.17	0.02	0.65	0.25	0.18	0.02	0.69
Volatility 8[c]	0.33	0.05	0.22	0.46	0.65	0.09	0.44	0.90	0.35	0.05	0.24	0.48
Other factors												
Major road AADT (log form)	2.24	0.37	0.86	2.91	2.20	0.37	0.85	2.85	2.15	0.36	0.83	2.79
Minor road AADT (log form)	0.43	0.09	0.02	0.67	0.32	0.07	0.01	0.49	0.34	0.08	0.02	0.53
Signalized intersection	0.52	0	0.52	0.52	0.49	0	0.49	0.49	0.52	0	0.52	0.52
Four leg intersection	0.27	0	0.27	0.27	0.24	0	0.24	0.24	0.26	0	0.26	0.26
	Signalized Intersections											
	Poisson Model				HRPP Model				HRP-PLN Model			
	μ	***SD***	***Min***	***Max***	***μ***	***SD***	***Min***	***Max***	***μ***	***SD***	***Min***	***Max***
Volatility Related Factors												
Volatility 2[a]	0.08	0.01	0.06	0.09	0.55	0.05	0.39	0.64	0.99	0.09	0.70	1.16
Volatility 4[b]	0.37	0.13	0.06	0.63	0.04	0.02	0.01	0.07	0.43	0.15	0.07	0.74
Other factors												
Major road AADT (log form)	2.02	0.26	0.85	2.52	1.75	0.23	0.73	2.19	1.78	0.23	0.74	2.22
Minor road AADT (log form)	0.04	0.01	0.02	0.07	0.36	0.09	0.19	0.54	0.36	0.09	0.19	0.55
Four leg intersection	0.29	0	0.29	0.29	0.28	0	0.28	0.28	0.27	0	0.27	0.27

Notes: (a) Volatility 2 is Intersection-level: Two standard deviations threshold for acceleration/deceleration, (b) Volatility 4 is Passing level: Coefficient of variation of speed, (c) Volatility 8 is Passing level: Mean absolute deviance of vehicular jerk. HRPP is Hierarchical Random Parameter Poisson Model; and HRP-PLN is Hierarchical Random Parameter Poisson Log-Normal Model; μ indicates mean/average value.

parameter Poisson model resulted in best fit for all intersections and signalized intersection respectively, we focus our discussion of the results obtained from these two model only.

4.6 DISCUSSION

4.6.1 Safety Effect of Intersection Volatility

Coming to the results of fixed-parameter Poisson model for all intersections in Table 4.3, crash frequency is found associated with three of volatility related factors, 1) Intersection-level: Two standard deviations threshold (Volatility 2) , 2) Passing-level: coefficient of variation of speed (Volatility 4), and 3) Passing-level: mean absolute deviance of vehicular jerk (Volatility 8). While the relationship between passing-level mean absolute deviance of vehicular jerk (volatility 8) and crash frequency is statistically insignificant in fixed parameter model, the other volatility related factors are statistically significantly positively associated with crash frequency. The fixed-parameter model suggests that the associations between intersection-specific volatilities and crash frequency are fixed across all the intersections.

However, the best-fit hierarchical random parameter Poisson log-normal suggests that the effects of intersection-specific volatilities on crash frequency are not fixed, and are normally distributed random parameters (Table 4.3). For instance, the intersection level volatility variable calculated based on two standard deviations threshold for acceleration/deceleration (volatility 2) is a normally distributed random parameter with a mean of 0.188 and standard deviation of 0.032 (Table 4.3). This translates to a 1.25 percent increase, on average, in crash frequency with a one-percent increase in intersection volatility calculated based on two standard deviations threshold for acceleration/deceleration (see elasticities for volatility 2 variable in Table 4.5). Likewise, a one-percent increase in passing-level mean absolute deviance of vehicular jerk (volatility 8)

increases crash frequency by 0.35 percent (see estimation results and elasticities in Table 4.3 and 4.5). However, the effects vary across the sampled intersections with a mean of 0.414 and standard deviation of 0.047 (Table 4.3). Finally, volatility 4 (i.e., passing-level coefficient of variation of speed) is positively correlated with crash frequency – a one-percent increase in passing-level coefficient of variation of speed increases crash frequency by 0.25 percent. Also note that, for intersection with the highest passing-level coefficient of variation of speed (i.e., maximum value of volatility 4 variable equals 52.83 in Table 4.2), the crash frequency is observed to increase by 0.69% (see maximum elasticity in Table 4.5).

To see if the relationships between intersection volatilities and crash frequency are significantly different for signalized intersections, Table 4.4 summarizes the results for signalized intersections only. In particular, among all the volatility related variables considered, volatility 2 (Intersection-level: two standard deviations threshold for acceleration/deceleration) and volatility 4 (Passing level: coefficient of variation of speed) are found to be positively correlated with crash frequency (Table 4.4). For instance, a one-percent increase in volatility 4 is associated with a 0.55% increase in crash frequency at signalized intersections (Table 4.5). However, the effects of this variable on crash frequency varies between 0.39% and 0.64% depending on the values of volatility 4 at signalized intersections (Table 4.5). Finally, volatility 2 variable that captures intersection volatility at passing level through coefficient of variation of speed is also positively correlated with crash frequency (Table 4.4). A one-percent increase in volatility 2 increases crash frequency at signalized intersections by 0.55% (Table 4.5). However, the maximum elasticity is around 0.64, suggesting that for the maximum value of volatility 2 variable, crash frequency can increase by 0.64%. This variable is normally distributed random parameter with mean of 0.075

and standard deviation of 0.045. As such, the effect of volatility 2 on crash frequency is positive for 95.2% of the signalized intersections and negative for the rest.

4.6.2 Safety Effect of Traffic Exposure & Other Variables

For traffic exposure related factors, the hierarchical random parameter Poisson log-normal model for all intersections suggests that a one percent increase in major road AADT and minor road AADT (in log scales) translate to 2.15% and 0.34% increase in crash frequencies respectively (Table 4.5). However, the parameter estimates for major road AADT are normally distributed random parameters suggesting that the effects of this variable on crash frequency varies across the sampled intersections. In terms of geometric factors, a signalized intersection and four leg intersection are both associated with significantly higher crash frequencies. For instance, referring to elasticities for hierarchical Poisson log-normal random parameter model in Table 4.3, at signalized and four legged intersections, the crash frequencies increased by 52% and 26% respectively[38]. Again, the variable for signalized intersections is found to have normally distributed random parameters suggesting heterogeneity in the effects of this variable on crash frequencies at all intersections (Table 4.3).

For signalized intersections (Table 4.4), a one-percent increase in major road AADT and minor road AADT (in log scales) translate to 1.75% and 0.36% increase in crash frequency respectively (Table 4.4 and 4.5). Likewise, at four legged intersection, the crash frequencies increased by 28% (see elasticities for HRPP model for signalized intersection in Table 4.5). These findings are

[38] For indicator variables, such as dummy variable for signalized intersection and four-legged intersection, the interpretation of elasticity is different (Washington et al., 2010). That is, the estimated elasticities quantify the change in crash frequency given the existence (indicator variable = 1) of specific condition (Washington et al., 2010).

intuitive as greater exposure is generally associated with higher crash frequencies (Quddus et al., 2001). Note that the parameter estimates and elasticities for traffic exposure factors (major), both for pooled and un-pooled model, vary significantly across the sampled intersections, suggesting significant heterogeneity in the effects of exposure-related factors (Table 4.5).

Overall, as discussed above, several variables are found to have random parameters suggests that the effects of these variables vary across different intersections, and is not fixed/constant for all intersections. While the direction of effects is consistent among the fixed- and random-parameter models, the magnitudes (in some cases) vary widely.

4.7 LIMITATIONS/FUTURE WORK

This study used several vehicle speed, acceleration, and jerk based measures to quantify volatility at intersections. In future, it will be interesting to explore more measures such as steering angles for quantifying intersection-specific volatility. Given the connected vehicle data availability and the significant manual data collection and data mining efforts involved, this study analyzed a sample of 116 intersections. Thus, the results are dependent on the sample size and with availability of more data, the methodology should be extended. From a methodological perspective, this study examined the relationships between average number of crashes (irrespective of crash types) and intersection-specific volatility measures. However, recent studies have shown that different crash outcomes at roadway entities can exhibit significant dependencies (El-Basyouny and Sayed, 2009b, El-Basyouny and Sayed, 2011). Methodologically, taking the potential dependencies among correlated response outcomes can lead to more efficient parameter estimates (Wali et al., 2018a). In future, by collecting additional

data on crash types, the proposed methodology should be extended to a Bayesian multivariate modeling framework where relationships between different categories of crashes (such as fatal, serious, injury, and property-damage only) and intersection-specific volatility can be sought. That is, different crash types can be modeled simultaneously in order to capture the dependencies/correlations between different crash outcomes at intersections/segments (El-Basyouny and Sayed, 2009b, El-Basyouny and Sayed, 2011, Barua et al., 2016, Ma et al., 2008, Barua et al., 2014). Such an extension would be relevant because the effects of driving volatility (and other factors) on fatal crashes can be expected to be different from the effects of volatility (and other factors) on PDO crash frequency. We also acknowledge that signal timing/cycle phase information is important for the analysis of safety performance at signalized intersections. However, the present study could not incorporate signal timing related variables as such data are not publicly available for the study area under consideration. Incorporating signal timing information in future efforts can help extract deeper insights. Finally, the present study considered microscopic driving data based volatility measures while several researchers have introduced other mature safety surrogates such as time to collision and post-encroachment time (Saunier et al., 2010, Tarko et al., 2009, Ismail et al., 2009, Ismail et al., 2010). These measures are important in the sense that it provides insights about driving behavior (for example acceleration/deceleration) immediately prior to involvement in a crash. While the volatility measures discussed in this study captures variations in speeds, acceleration/deceleration, and vehicular jerk, the volatilities cannot be linked to specific crashes given that the high resolution driving behavior and crash data are not necessarily for the same vehicles. This precludes analysis of investigating impacts of driving volatility in time to collision on key safety outcomes. However, with other recent advances in video analytic and naturalistic driving based data

streams, the role of human (driver) behavior or the volatility therein immediately prior to involvement in safety-critical events can be better sought, e.g., see (Ismail et al., 2010, Wali et al., 2018e).

4.8 CONCLUSIONS

Driving behavior in general is considered a leading cause of intersection related traffic crashes. However, due to unavailability of real-world driving data, intersection safety performance evaluations are largely reactive where state-of-the-art methods are applied to analyze historical crash data. The emerging connected and automated vehicles (CAV) technology provides a promising opportunity for investigating intersection safety more from a proactive perspective. Driving volatility captures the extent of variations in instantaneous driving decisions when a vehicle is being driven. This study develops a fundamental understanding of microscopic driving volatility and how it relates to unsafe outcomes at intersections. The key research objectives are:

1) To develop a methodology for quantifying driving volatility (magnitude and variations in instantaneous driving decisions) in CAV based Basic Safety Messages.
2) To understand correlations between driving volatility and traffic crashes at specific intersections.
3) To fully account for unobserved heterogeneity by developing full Bayesian hierarchical random parameter Poisson and Poisson log-normal models.

To achieve the objectives, real-world connected vehicle data from the Safety Pilot Model Deployment (SPMD) in Ann Arbor, Michigan are used. Specifically, by using data mining

techniques, several intersection-specific volatility indices are created for 116 intersections in Ann Arbor, Michigan. Altogether, more than 230 million real-world Basic Safety Messages (BSMs) are processed and analyzed to quantify intersection volatility. Intersection-specific driving volatility indices are created from BSM data at two levels using aggregate intersection level data and trip/passing level data. To better quantify intersection-specific volatility, eight different measures are introduced to capture volatility in vehicle speeds, acceleration/deceleration, and vehicular jerk.

For proactive intersection safety evaluation, the large-scale connected vehicle data is then manually linked to detailed intersection data containing crashes, traffic exposure, and other geometric features. Significant efforts went into data processing, collection, and linkage. By using the eight newly created volatility measures, descriptive analysis is performed and visualizations developed to observe the relationships between intersection volatility and historical crashes. As signalized intersections often experience higher crash frequencies, in-depth statistical analysis is then performed to quantify correlations between intersection volatility and traffic crashes, separately for all intersections and signalized intersections only.

Given that the integrated CAV and inventory data is assembled manually, it is obvious not all factors that may influence crash frequency are observed. In presence of such unobserved factors, it may happen that any correlation that is established between driving volatility and crash frequency is not real and in fact is an outgrowth of some other factors that are not observed in the data. As such, owing to the presence of unobserved heterogeneity, hierarchical fixed- and random-parameter Poisson and Poisson log-normal models are estimated in Full Bayesian

context via Markov Chain Monte Carlo (MCMC) based Gibbs updates. Specifically, hierarchical random-parameter Poisson log-normal regression and hierarchical random-parameter Poisson regression models were observed to provide the best-fit for all intersections and signalized intersections respectively. Among the volatility, traffic exposure, and other factors tested, parameter estimates for several variables were found to be normally distributed random parameters, suggesting that the effects of explanatory factors on crash frequency vary significantly across the intersections.

For all intersections, after controlling for traffic exposure, geometrics, and unobserved factors, the results show that a one-percent increase in intersection-level volatility calculated through two standard deviations threshold for acceleration/deceleration (volatility 2), passing level volatility captured through coefficient of variation of speed (volatility 4), and mean absolute deviance of vehicular jerk results in a 1.25%, 0.25%, and 0.35% increase in crash frequencies respectively. However, the relationships between driving volatility indices and crash frequency are significantly different for signalized intersections, i.e., a one-percent increase in coefficient of variation of speed at passing level (volatility 4) is associated with a 0.04% increase in crash frequency. Likewise, a one-percent increase in intersection-level volatility calculated through two standard deviations threshold for acceleration/deceleration increases crash frequency by 0.55%. However, for a signalized intersection with the highest volatility, the crash frequency is observed to increase by 0.64%. This finding is important in the sense that increase in signalized intersection-specific volatility may result in more crashes. Also, for many intersections, it is found that observed crash frequency is lower but perhaps crashes are waiting to happen as instantaneous driving decisions are consistently more volatile at such intersections (Schneider et

al., 2004). For intersection safety management, such information is crucial as it can highlight intersection locations where behaviors of drivers may differ, compared to their behaviors at other intersection locations. Thus, safety managers may consider proactive countermeasures at such locations, e.g., providing proactive alerts and warnings to drivers through connected vehicle roadside equipment (RSE). The associations between other traffic exposure factors, geometric factors, and crash frequency are also quantified and discussed, and shows that greater traffic exposure is generally associated with higher crash frequencies.

4.9 ACKNOWLEDGEMENT

This paper is based upon work supported by the US National Science Foundation under grant No. 1538139. Additional support was provided by the US Department of Transportation through the Collaborative Sciences Center for Road Safety, a consortium led by The University of North Carolina at Chapel Hill in partnership with The University of Tennessee. Any opinions, findings, and conclusions or recommendations expressed in this paper are those of the authors and do not necessarily reflect the views of the sponsors. The authors would like to recognize the contributions of Ms. Ali Boggs and Ms. Megan Lamon in proof-reading several versions of the manuscript. Finally, the authors acknowledge the helpful comments of two anonymous reviewers on an earlier version of the paper.

CHAPTER 5 EXPLORING MICROSCOPIC DRIVING VOLATILITY IN NATURALISTIC DRIVING ENVIRONMENT PRIOR TO INVOLVEMENT IN SAFETY CRITICAL EVENTS

This chapter presents a modified versions of a research article by Behram Wali, Asad J. Khattak, and Thomas Karnowski. *"Exploring Microscopic Driving Volatility in Naturalistic Driving Environment Prior to Involvement in Safety Critical Events."* The manuscript is currently under second-stage review in Accident Analysis and Prevention.

ABSTRACT

The sequence of instantaneous driving decisions and its variations, known as driving volatility, prior to involvement in safety critical events can be a leading indicator of safety. This study extends the concept of driving volatility to specific normal and safety-critical events, thus named "event-based volatility." The research issue is characterizing volatility in instantaneous driving decisions in longitudinal and lateral directions, and how it varies across drivers involved in normal driving, crash, and/or near-crash events. To explore the issue, a rigorous quasi-experimental study design is adopted to help compare driving behaviors in normal vs unsafe outcomes. Using a unique real-world naturalistic driving database from the 2nd Strategic Highway Research Program (SHRP), a test set of 9,593 driving events featuring 2.2 million temporal samples of real-world driving are analyzed. This study features a plethora of kinematic sensors, video, and radar spatiotemporal data about vehicle movement and therefore offers the opportunity to initiate such exploration. By using information related to longitudinal and lateral accelerations and vehicular jerk, 24 different aggregate and segmented measures of driving volatility are proposed that captures variations in extreme instantaneous driving decisions. In doing so, careful attention is given to the issue of intentional vs. unintentional volatility. The volatility indices are then linked with safety critical events, crash propensity, and other event specific explanatory variables. Owing to the presence of unobserved heterogeneity and omitted variable bias, fixed- and random-parameter discrete choice models are developed that relate crash propensity to driving volatility and other factors. Statistically significant evidence is found that driver volatilities in near-crash and crash events are significantly greater than volatility in normal driving events. After controlling for traffic, roadway, and unobserved factors, the results suggest that greater intentional volatility increases the likelihood of both crash and near-crash

events. A one-unit increase in intentional volatility associated with positive vehicular jerk in longitudinal and lateral direction increases the probability of crash outcome by 5.21 and 8.91 percentage points, respectively. Importantly, intentional volatility in longitudinal negative jerk (braking) has more negative consequences than intentional volatility in positive vehicular jerk. Compared to acceleration/deceleration, vehicular jerk can better characterize the volatility in microscopic instantaneous driving decisions prior to involvement in safety critical events. Finally, the magnitudes of correlations exhibit significant heterogeneity, and that accounting for the heterogeneous effects in the modeling framework can provide more reliable and accurate results. The study demonstrates the value of quasi-experimental study design and big data analytics for understanding extreme driving behaviors in safe vs. unsafe driving outcomes.

5.1 INTRODUCTION

The Global Status Report on Road Safety indicates that an estimated 1.25 million people annually die in road traffic crashes (RTCs) and approximately 50 million sustain injuries (WHO 2015). This high toll of annual RTCs imposes substantial costs on our societies, with annual crash costs totaling to $240 billion within the United States (NHTSA 2015). Among other factors, driving behavior and/or human factors in general are considered a leading cause of RTCs (Dingus et al. 2006, Liu and Khattak 2016, FHWA 2017). Recent statistics suggest that more than 90 percent of crashes are influenced in a major way by driver behavior (FHWA 2017). Thus, for several decades researchers have attempted to understand the behavioral correlates of crash risk or crash propensity. For the most part, the analysis of behavioral factors correlated with crash propensity mainly builds upon questionnaire surveys and/or controlled experiments (Schneider et al. 2001, Schneider et al. 2004, Machin and Sankey 2008, Ivers et al. 2009,

Antonopoulos et al. 2011, Qu et al. 2014, Scott-Parker and Oviedo-Trespalacios 2017b). While analysis of such a nature is important for identifying driver-related factors associated with higher crash risk, it does not shed light on the actual driving tasks and/or decisions that typically precede drivers' involvement in a crash (Kim et al. 2016). As such, it is crucial to gain insights regarding the sequence of microscopic instantaneous driving decisions (e.g., acceleration/deceleration) preceding drivers' involvement in a near-crash or crash situation. However, an analysis of such a nature was not possible until very recent mainly due to data unavailability.

The rapid technological advancements in recent years have enabled collection of huge amounts of spatiotemporal data about vehicle and human movement. With recent innovations ranging from realization of vehicle-to-vehicle (V2V) and vehicle-to-infrastructure (V2I) technologies such as Dedicated Short Range Communication (DSRC) and WI-FI, to continuous video and radar surveillance, the collection of countless terabytes of real-world driving data is now a reality (Campbell 2012, Henclewood 2014). The generated large-scale empirical data by such technologies has significant potential in facilitating deeper understanding of instantaneous driving decisions prior to occurrence of unsafe outcomes, such as crashes (Kamrani et al., 2017). Relevant in this regard is the concept of "driving volatility" that captures the extent of variations in driving, especially hard accelerations/braking and jerky maneuvers (Khattak et al., 2015, Wang et al., 2015, Liu and Khattak, 2016b). Broadly, through monitoring and analysis of real-world driving data, proactive safety approaches can be formulated by giving warnings and alerts to drivers and which can reduce such volatility potentially improving safety.

With these forethoughts in mind, the main objective of this study is to investigate correlations between driving volatility and crash propensity. Crash propensity is usually defined as the tendency of a driver to get involve in an unsafe outcome, and which is mostly defined as a crash (Abdel-Aty and Pande 2005, Christoforou et al. 2011). However, an important goal within this broader unsafe outcome perspective is to identify and analyze situations resulting in near-crashes (or near misses), as such "close calls" may foreshadow actual future crashes. Thus, in this study an unsafe outcome is defined as a crash or near-crash event. To explore the issue, a tight quasi-experimental study design is adopted to help compare driving behaviors in normal vs unsafe outcomes. Such a study design is crucial to understanding the microscopic extreme driving behaviors in unsafe events and normal driving events. As such, the study builds upon a unique Naturalistic Driving Study (NDS) database of thousands of driving events in which a driver was involved in a safe driving event (baseline or normal event), crash event, or a near-crash event. For all such driving events, large-scale microscopic instantaneous driving decision data prior to involvement in both safe and unsafe outcomes are analyzed and volatility indices created based on different driving performance measures. The volatility indices are then linked with crash propensity, event specific variables such as drivers' pre-event maneuvers and behaviors, secondary tasks, roadway and traffic flow related factors. Both simple and advanced statistical methods are employed to generate new knowledge critical to formulation of proactive warnings and alerts in case an unsafe outcome is anticipated. From a methodological perspective, discrete choice models are estimated for modeling crash propensity as a function of several variables including driving volatility, and which accounts for important issues of unobserved heterogeneity and omitted variable bias (discussed later in detail).

5.2 LITERATURE REVIEW

5.2.1 Crash frequency, crash rate and associated factors

At an aggregate level, a broad spectrum of studies have established relationships between crash frequency (or crash rates) and traffic related factors (Ivan et al. 2000, Martin 2002, Qin et al. 2004, Anastasopoulos et al. 2008, Ma et al. 2017, Sarker et al. 2017), roadway factors (Qin et al. 2004, Anastasopoulos et al. 2008, Dong et al. 2014, Ma et al. 2017), built-environment factors (Ivan et al. 2000, Lee et al. 2014, Chen 2015), weather related factors (Anastasopoulos et al. 2008, Dong et al. 2014, Hassan et al. 2017), and driver behavior (Lee et al. 2014, Hassan et al. 2017). Among other factors, driver behavior (or risky driving) is concluded to be the main contributing factor for crashes (Neyens and Boyle 2007, Boyle et al. 2008, Lee and Abdel-Aty 2008, Yan et al. 2008, Lee et al. 2014, Hassan et al. 2017). As a surrogate of driving behavior, aggregate measures such as residence characteristics of drivers, socio-economic and age-related factors, and/or ticket violations are usually used to relate driving behavior with crash frequency (Ivan et al. 2000, Weng and Meng 2012, Lee et al. 2014, Mitchell et al. 2014, Liu et al. 2015b, Hassan et al. 2017). Traditional police crash report forms do not typically include detailed information about driving behavior related factors. As such, studies have also used self-reported questionnaire surveys to investigate (or infer) links between driving behavior and crash risk (Mannering 2009, Tronsmoen 2010, Smorti and Guarnieri 2014, Hassan et al. 2017, Scott-Parker and Oviedo-Trespalacios 2017a). Different driver related factors (age, gender, nationality), vehicle types, mobile-phone use, drink driving, risk perception, and safety attitudes are found correlated with crash involvement (Tronsmoen 2010, Hassan et al. 2017, Scott-Parker and Oviedo-Trespalacios 2017a).

As opposed to using crashes as a safety tool, near-crash traffic events are usually acknowledged but not used as safety tools. This is primarily due to the degree of subjectivity involved in identification of such events (Hayward 1972). However, for drawing a complete picture, it is important to analyze situations that may result in near-crashes as such events are typically precursors to actual crashes. Collectively, while the previous studies provided information about important variables related to crash occurrence and/or crash rates, crucial information is missing regarding pre-safety critical vehicle maneuvers or operation. An understanding of the actual driving mechanism related with occurrence of crash or near-crash event is crucial for designing actionable proactive behavioral countermeasures.

5.2.2 Real-world driving data and concept of driving volatility

Emerging technologies such as vehicle-to-vehicle and vehicle-to-infrastructure communication, and naturalistic driving studies facilitate the collection of high frequency real-world driving data. Towards this end, recent studies utilized real-world driving data integrated with sensor and radar technologies to propose the concept of "driving volatility", which is a measure of driving practice for characterizing instantaneous driving decisions, importantly extreme driving behaviors, and the dynamics of regimes in a typical driving profile (Khattak and Wali, 2017)(Liu et al. 2015a, Wang et al. 2015). Specifically, such sensing captures the extent of variations in driving, especially hard accelerations/braking and jerky maneuvers (Khattak and Wali, 2017)(Khattak et al. 2015, Wang et al. 2015)(Liu et al. 2015a, Liu and Khattak 2016). The fundamental idea is to capture the magnitudes and amount of variations in driving decisions as larger variations (or heterogeneity) in microscopic decisions by the driver cannot only influence their own safety but also the operations of sorrounding traffic. For instance, a recent study

developed a fundamental understanding of instantaneous driving decisions, and to distinguish normal from anomalous driving (Khattak and Wali, 2017). By conceptualizing microscopic driving decisions into distinct yet unobserved regimes, the focus was to quantify volatility in each regime and how driving regime allocation can be probabilistically mapped to the surrounding traffic contexts (Khattak and Wali, 2017). A dynamic Markov regime switching methodology was presented to predict what a driver will do in short term in a connected vehicles environment, and which is fundamental to the development of driving feedback devices and control assist systems (Khattak and Wali, 2017). Compared to traditional behavioral measures (such as age, education, gender, socio-economics), the concept of individual level driving volatility provides personalized and actionable information for developing driving feedback devices, warning and control assists systems (Khattak and Wali, 2017)(Wang et al. 2015, Liu and Khattak 2016).

5.2.3 Driving volatility and Unsafe Outcomes

While the afore-mentioned studies characterized driving practices by using rigorous data analytic methodologies (Liu et al. 2015a, Wang et al. 2015, Liu and Khattak 2016)(Khattak and Wali, 2017), the volatility was not linked with unsafe outcomes such as crashes. In this regard, recent studies by Kamrani et al. (2017) and Wali et al. (2018) extended the concept of driving volatility to specific locations (location-based volatility) and demonstrated how high resolution connected vehicles based driving data can be linked with historical crashes for designing proactive safety management tools (Kamrani et al., 2017, Wali et al., 2018d). Furthermore, in simulation-assisted frequentist as well as in Full-Bayesian setup, the studies demonstrated that the relationship between driving volatility and crashes vary across different locations (unobserved

heterogeneity), and that it is necessary to control for omitted variables while establishing relationships between driving volatility and crash outcomes (Kamrani et al., 2017, Wali et al., 2018d). Furthermore, different statistical measures of location (intersection) specific volatilities were proposed to quantify location-based volatilities in connected (instrumented) vehicles environment (Wali et al., 2018d).

In similar work, Kim et al. (2016) conducted an exploratory study to analyze the association between rear-end crash propensity and micro-scale driving behavior (Kim et al. 2016). Simple correlational statistics were studied and spatial distributions explored (Kim et al. 2016). All the three studies concluded that hard deceleration rates are associated with rear-end crashes on freeway ramps (Kim et al. 2016) and total crashes at signalized intersections (Kamrani et al., 2017, Wali et al., 2018d), and innovative proactive safety strategies were discussed (Kamrani et al., 2017, Kim et al., 2016, Wali et al., 2018d).

5.2.4 Research Gap

The aforementioned studies contributed by providing data analytic and Bayesian statistical methodologies to link large-scale driving behavior data with historical crashes. However, important research gaps exist. First, these studies were aggregated level in the sense that location specific (intersections or freeway on/off ramps) driving behavior data were used to explain historical crashes at such locations (Kamrani et al., 2017, Kim et al., 2016, Wali et al., 2018d). Thus, insights regarding how individual driver's instantaneous driving decisions can be related to his/her crash involvement cannot be obtained. Second, due to data unavailability, short duration of high frequency driving data (two months' data in (Kamrani et al., 2017, Kim et al., 2016) and

three months' data in (Kim et al. 2016)) were used to explain multi-year crashes. Third, only crashes were used as tools for characterizing safety and near-crashes were not considered (Kamrani et al., 2017, Kim et al., 2016, Wali et al., 2018d). However, an important goal within this broader unsafe outcome perspective should be to identify and analyze situations resulting in near-crashes (or near misses), and which may be considered forerunners to actual future crashes. Given these research gaps, this study extends the concept of driving volatility to specific normal and safety-critical events, thus named "event-based volatility."

Finally, the authors believe that methodological issues related to unobserved heterogeneity and omitted variable bias should be properly accounted for in analyses of such a nature. That is, it is important to control for unobserved factors that may influence unsafe outcomes but are not observed in data. If such unobserved factors could be included in a model, the correlations between driving volatility and unsafe outcomes can change, e.g., the magnitude or statistical significance of the relationship can change. The study by (Kim et al. 2016) was descriptive in nature and did not account for unobserved heterogeneity.

5.2.5 Research Objective and Contribution

Given the prevalent gaps in the literature, the objectives of this study are:

- To characterize volatility in instantaneous driving decisions in normal driving events, crash events, and near-crash events.
- To examine how volatility in instantaneous driving decision vary across drivers involved in normal, crash, and/or near-crash events.

- To understand correlations between driving volatility (intentional and unintentional) and crash propensity after controlling for other factors, unobserved heterogeneity and omitted variable bias.

These objectives seek to gain a fundamental understanding of instantaneous short-term driving decisions prior to involvement in unsafe outcomes, and therefore reveal how we can map driving volatility to drivers' involvement in different possible safety outcomes, i.e., concept of "event-based volatility" is introduced. We define it as event-based volatility because the driving volatility indices provide insights about microscopic driving decisions in different possible safety-critical events. Crash propensity is defined as likelihood of drivers' involvement in crash- or near-crash events, compared to normal (baseline) driving events. Such an analysis is critical for designing proactive behavioral countermeasures as it can highlight moments of volatile (potentially unsafe) instantaneous driving decisions prior to involvement in an unsafe outcome.

For thousands of driving events in naturalistic driving studies, large-scale microscopic instantaneous driving decision data prior to involvement in both safe and unsafe outcomes are analyzed and volatility indices created based on different driving performance measures. Careful attention is given to the issue of intentional vs. unintentional volatility (discussed later in detail). The volatility indices are then linked with crash propensity, event specific variables such as drivers' pre-event maneuvers and behaviors, secondary tasks, roadway and traffic flow related factors. Simple correlational and ANOVA analysis is first conducted to spot statistically significant differences (if any) among driving volatilities in different safety events. Next, advanced statistical methods are employed to relate different driving volatility measures to crash propensity to generate new knowledge critical to formulation of proactive warnings and alerts in

case an unsafe outcome is anticipated. Given the important methodological concerns of unobserved heterogeneity and omitted variable bias (Kamrani et al., 2017, Lord and Mannering, 2010, Savolainen et al., 2011), fixed- and random-parameter discrete choice models are developed to reach reliable conclusions.

5.3 METHODOLOGY

5.3.1 Conceptual Framework

To understand driving volatility prior to involvement in safety critical events, detailed microscopic data on instantaneous driving decisions are needed (Liu and Khattak 2016). The recently concluded SHRP2 Naturalistic Driving Study provides relevant data (TRB 2013). Figure 5.1 presents a conceptual framework that describes the overall study structure. The "Event Detail Table" in the framework consists of a table of critical safety events and baseline events, ranging from 20 seconds long to 30 seconds long. Specifically, 20 seconds of microscopic driving data are available for baseline events, whereas, 30 seconds data are available for safety-critical events (such as near-crashes and crashes). These events have been manually reviewed and categorized into a set of 74 descriptive variables (VTTI Insight Web Site). Each event is also accompanied by a set of measurements from the NDS sensors, sampled at 10 frames / second. The EDT used in this work was obtained in September 2014.

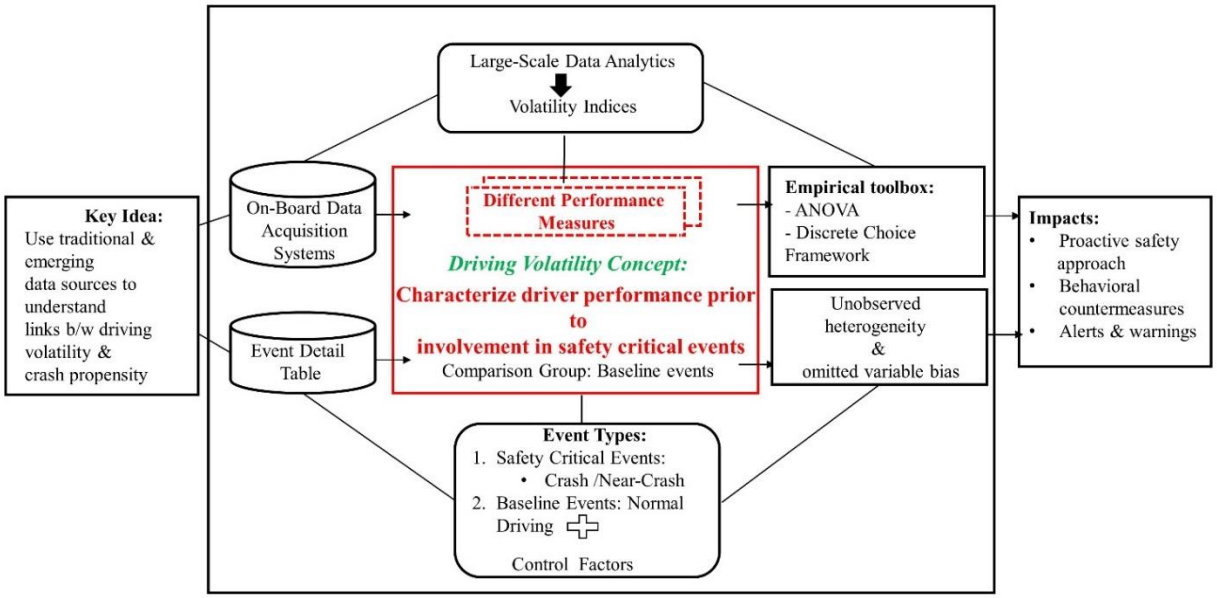

Figure 5.1 Conceptual framework

By using large-scale data analytic techniques, a unique aspect of the current study is to combine traditional and emerging data sources in a meaningful way critical to development of proactive safety tools and behavioral countermeasures. In this study, both safety critical events (crash/near-crash) and baseline events (normal driving) are considered[39]. This is important because understanding driving behavior in safety critical events vis-à-vis normal driving events can help determine meaningful behavioral differences. By using several performance measures, the magnitudes and extent of variations (termed as driving volatility) in driver's performance prior to involvement in safety critical and/or baseline events are quantified (Figure 5.1). With real-world driving data based volatility indices, proactive behavioral countermeasures can be planned for drivers that are consistently more volatile. As a next step, the microscopic driving volatility

[39] Crash is defined as any contact that the subject instrumented vehicle has with an object (moving or fixed) at any speed in which kinetic energy is measurably transferred or dissipated (Hankey et al., 2016). Whereas, SHRP2 NDS defines near-crash as any circumstance that requires a rapid evasive maneuver by the subject vehicle, or any other vehicle, pedestrian, cyclist, or animal, to avoid a crash (Hankey et al., 2016). Baseline events are samples of "normal" driving and the goal is to provide an estimate of what constitutes "normal driving" and/or "typical driver behavior" (Hankey et al., 2016). Further details are discussed in later sections.

information is then linked with data in the event detail table that provides event specific data such as pre-crash maneuvers, road inventory, weather factors, and traffic factors. By using simple and advanced statistical methods, correlations between driving volatility and crash propensity are then explored. We hypothesis a positive correlation between driving volatility and crash propensity. Any correlation, if exists, can shed light on microscopic driving decisions, and how such decisions influence roadway safety (Figure 5.1).

5.3.2 Data

Data from an on-going national Naturalistic Driving Study conducted as part of the 2nd Strategic Highway Research Program (SHRP) were used in this study (TRB 2013). In this largest naturalistic driving study performed to date, the driving behaviors of approximately 3,400 participant drivers were recorded with over 4,300 years of naturalistic driving data collected between 2010 and 2013 (Hankey et al. 2016). The study data was collected from six naturalistic driving sites around the United States, with largest data collection sites in New York, Tampa, Seattle, Washington, Florida, and Buffalo (Hankey et al. 2016). The study used approximately 3,300 participant vehicles (TRB 2013, Hankey et al. 2016), using a data acquisition system (DAS) that collected four video views (driver's face, driver's hand, forward roadway, and rear roadway), vehicle network and status information (speed, brake, acceleration), and information from additional sensors networked with the DAS (e.g., accelerometers) (TRB 2013).

Out of the many data categories collected in the SHRP 2 project, the data used in this study are "event data" and "continuous data". Event data provides detailed information regarding the different safety events in which a participant driver was involved. A notable feature of the SHRP 2 NDS data is the inclusion of three categories designated as events: crash, near-crash, and

baseline events. Information about crash and near-crash events can provide richer estimates of prevalence and risk from different driver behaviors, roadway characteristics, and environmental conditions, whereas, baseline events are necessary for comparison purposes (TRB 2013). Following (Hankey et al. 2016), the definitions of the three event types are provided for reference:

- Crash event: "Any contact that the subject vehicle has with an object, either moving or fixed, at any speed in which kinetic energy is measurably transferred or dissipated is considered a crash. This also includes non-premeditated departures of the roadway where at least one tire leaves the paved or intended travel surface of the road, as well as instances where the subject vehicle strikes another vehicle, roadside barrier, pedestrian, cyclist, animal, or object on or off the roadway." (Hankey et al. 2016).
- Near-Crash event: "Any circumstance that requires a rapid evasive maneuver by the subject vehicle, or any other vehicle, pedestrian, cyclist, or animal, to avoid a crash is considered a near-crash. A rapid evasive maneuver is defined as steering, braking, accelerating, or any combination of control inputs." (Hankey et al. 2016).
- Baseline events: Baseline events are samples of "normal" driving and the goal is to provide an estimate of what constitutes "normal driving" and/or "typical driver behavior".

A case-cohort type sampling design is used for selection of baseline events where a random sampling scheme was conducted stratified by participant and proportion of time vehicle was driven. Proportion of time driven is defined as to include only vehicle speeds above 5 mph so as to eliminate the effect of long stopping times, and to focus on time periods where the vehicle was

actually at risk of a crash or near-crash (Hankey et al. 2016). Regardless of whether involved in a crash or near-crash, all participants are included in the sample for baseline events to ensure that a minimum of one baseline event is included for each driver. Further details regarding the sampling design can be found in Hankey et al. (2016) (Hankey et al. 2016). The combination of crashes and near-crashes are referred to as safety-critical events (SCEs). Regarding identification of SCEs, SHRP 2 NDS used multiple methods such as, 1) Data collection site report, 2) Automatic Crash Notification (ACN), 3) Critical Incident (CI) button, 4) Analyst identified, and 5) Trigger execution. For example, the most systematic approaching to identifying an SCE was the method of trigger execution, which included post hoc processing of incoming data via custom algorithms called "triggers." These algorithms are characterized by different kinematic and behavioral signatures that have a highly probability of being present during specific SCEs. The SHRP 2 NDS used different thresholds based on project resources (as detailed in (Hankey et al., 2016)). Among many of other trigger types, longitudinal deceleration and lateral acceleration were also used. For instance, the initial trigger for lateral acceleration was specified if the lateral acceleration was greater than or equal to 0.75 g or less than or equal to -0.75g, and that this threshold was exceeded for at least 0.2 seconds. For details about other trigger types, see (Jovanis et al., 2011, Hankey et al., 2016). Finally, once a SCE was identified through trigger execution method, video verification was then used to determine if an SCE occurred. Details about other methods used for identifying SCEs can be found in (Hankey et al., 2016). As can be seen, all the aforementioned techniques used in SHRP 2 NDS for identification of SCEs are rigorous. On top of that, the fact that majority of the SCEs identified through any of the aforementioned methods were video verified at the end further increases our confidence in the data.

A total of 9,593 driving events are considered in this study, out of which 7,589 are baseline, 673 are crashes, and 1295 are near-crash events. Note that the term "event" does not imply "trips". A participant along a single trip can have several events, e.g., baseline, crash, and/or near-crash. The 9,593 events involve 1580 unique participants with some participants appearing more than once (i.e., involvement in more than one safety critical events). For each of the three event types, time-series data on vehicle motion (continuous data) is provided, i.e., 30 seconds instantaneous driving data (frequency of 10 Hz) for safety critical events (crashes and near-crashes) and 20 seconds instantaneous driving data with a frequency of 10 Hz for baseline events (Hankey et al. 2016). The time-series data contains information about longitudinal and lateral accelerations, speeds, gas pedal and steering wheel position, and wiper status.

As such, a total of 2.2 million records of real-world driving are analyzed in this study. By using information related to longitudinal and lateral accelerations and vehicular jerk, 24 different measures of driving volatility are calculated using the methods described next (Table 5.1). Finally, the event table provides detailed information on pre-incident maneuvers[40], legality of maneuvers, driver behavior, secondary tasks[41], start and end times, if applicable, of first, second, and third secondary events. Also included in the data is information about front-seat and rear-seat passengers, intersection and roadway type indicators, and traffic flow related factors. The

[40] For Baseline events, this is the driving maneuver or action that the driver is engaged in for the last 2-6 seconds prior to the baseline anchor point (the point in video where the 20 seconds baseline driving data starts).

[41] Observable driver engagement in any of secondary tasks, and which begins at any point during the 5 seconds prior to the event start (crash, near-crash) through the end of the event (TRB, 2013). Secondary tasks primarily refer to distractions related to non-driving related glances away from the direction of vehicle movement (TRB, 2013). Some examples include radio adjustments, seat-belt adjustments etc. For Baselines, secondary tasks are coded for the last 5-6 seconds of the baseline epoch, which includes 5 seconds prior to baseline event start through one second after (to the end of the baseline). For further details, refer to (TRB, 2013).

detailed event data are finally linked with the event-specific volatility indices for subsequent analyses.

Table 5.1 Different Volatility Measures Considered In this Study

Direction	Performance Measure	Entire 30-seconds data[1]	First 20-seconds data[2]	First 25-seconds data[3]
Longitudinal Direction	Positive vehicular jerk	✓	✓	✓
	Negative vehicular jerk	✓	✓	✓
	Acceleration	✓	✓	✓
	Deceleration	✓	✓	✓
Lateral Direction	Positive vehicular jerk	✓	✓	✓
	Negative vehicular jerk	✓	✓	✓
	Acceleration	✓	✓	✓
	Deceleration	✓	✓	✓

Notes: (1) Entire time series data, i.e., 20-seconds for baseline and 30-seconds for crash/near-crash events; (2) Of the 30-seconds data, the initial 20 seconds data are used while the 10 seconds data immediately prior to crash/near-crash are not used; (3) The initial 25 seconds data are used while the 5 seconds data immediately prior to crash/near-crash are not used.

5.3.3 Components of Volatility

Figure 5.2 shows a 30-seconds longitudinal and lateral acceleration/deceleration (vehicular jerk) profiles prior to involvement in a crash event. By using large-scale data analytic techniques, driving volatility can be characterized for each of the events (i.e., baseline, crash, or near-crash events). Broadly speaking, the volatility indices for each event can be regarded as microscopic measures of driving performance (or erratic behavior) in normal or safety-critical events. The driving volatility indices developed using the entire 30-seconds data (for crash and near-crash events) can shed light on microscopic driving decisions that the driver undertook prior to involvement in safety-critical events.

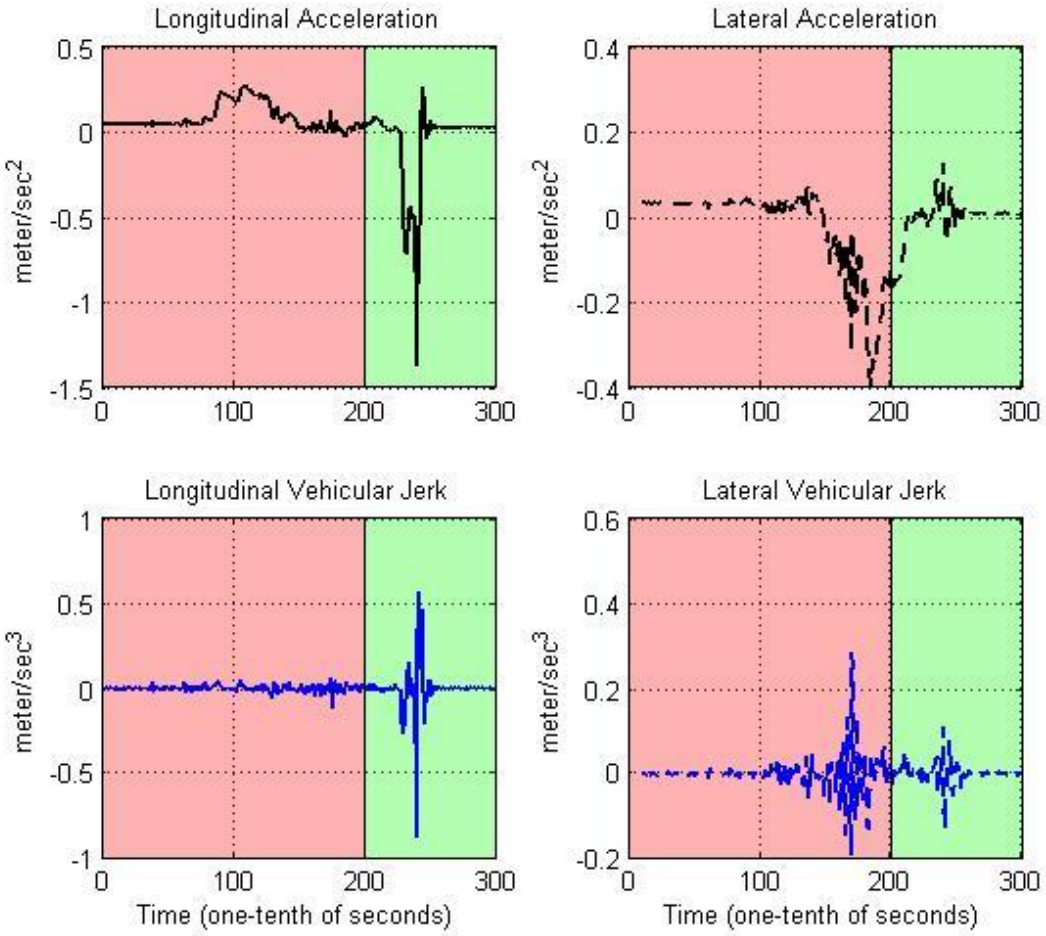

Figure 5.2 Profiles of instantaneous driving decisions prior to involvement in a sample crash event

Note: First portion of series in pink background indicate actual driving behavior and second portion of series in light green background may indicate driving decisions due to situational factors – see text for explanation.

With real-world driving data based volatility indices (Figure 5.2), proactive behavioral countermeasures can be planned for drivers that are consistently more volatile.

However, as explained in Wali et al. (2018), using the entire 30-seconds driving data for crash and near-crash events aggregates the different components of volatility in instantaneous driving decisions prior to unsafe outcomes (Wali et al., 2018e). For instance, Figure 5.2 illustrates the microscopic driving decisions in longitudinal and lateral direction prior to a crash event. However, in case of crash and near-crash events, the series can be divided into two series, where the first portion of the series will indicate the driver's speed choice (or acceleration, vehicular jerk) regardless of the event outcome, while the second portion of the series would indicate the "adjustments" or drivers' reaction to the event. That is, the volatility in the first component of the series is likely to reflect the actual driver behavior, and can be regarded as "intentional volatility" by the driver, i.e., due to aggressive self-driving when the driver is in control. As shown in Figure 5.2, the intentional volatility may be reflected in instantaneous driving data 20 to 30 seconds before the crash/near-crash (see the first part of the profile in Figure 5.2 – indicated in pink background). Whereas, the second component may reflect "unintentional volatility" in the sense that the driver undertook evasive maneuvers to avoid the crash or near-crash event, or lost the control. The unintentional volatility can be reflected in driving data immediately before the unsafe outcome (such as 5 to 10 seconds before the crash/near-crash event), as highlighted in light green background in Figure 5.2. We call it "unintentional volatility" as the driver may have already anticipated the crash/near-crash in this case and is undertaking preventive measures to avoid the crash, i.e., evasive maneuvers. Also, the volatility 5 to 10 seconds before the crash is likely to contain volatility due to loss of control before the crash (Wali et al., 2018e).

The fundamental objective of this study is to explore the links between driving volatility and crash propensity. As is evident, combining the two sources of volatility (intentional vs. unintentional) to explain the unsafe outcomes can lead to bias due to reverse causation, i.e., the volatility measures using 30-seconds data will not only reflect the actual driving behavior but also volatile driving behaviors due to risky situations/external events. Conversely, by aggregating the different components of volatility, evasive maneuvers that allowed a driver to avoid a crash would also be interpreted as increasing volatility. In this case, high volatility may then be associated with near-miss outcomes, again not due to driver behavior in general but due to a driver's reaction to unobserved situational variables. In this case, the first portion of the time series, i.e., intentional volatility can be used to explain the occurrence of unsafe outcomes (Wali et al., 2018e). As illustrated in Figure 5.2, much of this bias may be eliminated by censoring data used to calculate different volatility measures in the time period immediately before a crash or near-crash outcome occurs; i.e., censoring to remove the influence of driver reactions immediately prior to a crash from the volatility measures while retaining volatility derived from driver behavior in the seconds leading up to, but not immediately before, a crash or near-rash event. As such, we also consider generating segmented volatility indices based on different time bins, and which can separate out how volatility in time to crash (or near-crash) relates to crash propensity (Figure 5.2).

5.3.4 Calculation of Volatility

Driving volatility captures the extent of variations in driving, especially hard accelerations/braking and jerky maneuvers (Wali et al., 2018d, Wali et al., 2018e, Khattak and Wali, 2017, Khattak et al., 2015, Kamrani et al., 2017). Different instantaneous driving

performance measures such as vehicle speeds, accelerations/decelerations, and/or steering angles can be used for estimation of volatility indices in longitudinal directions (Quddus 2013, Kim et al. 2016, Liu et al. 2016, Liu and Khattak 2016). For instance, acceleration/deceleration based thresholds in connected vehicle environment are used for quantifying volatility in instantaneous driving decisions (Kamrani et al., 2017, Liu and Khattak, 2016b, Wali et al., 2018d). Also, deceleration and acceleration profiles differ with larger variation observed in deceleration (Kim et al., 2016, Kamrani et al., 2017, Wali et al., 2018d). As such, separate volatility measures are usually defined for acceleration and deceleration (Kamrani et al., 2017, Liu and Khattak, 2016b, Wali et al., 2018d). Another important driving decision is in the lateral dimension, e.g., lane change decisions. Larger volatility in lateral dimension may also be associated with unsafe outcomes (Wali et al., 2018d). For instance, Wali et al. (2018) used both longitudinal and lateral accelerations to better characterize driving volatility in time to collision and its relationship with injury outcomes in a naturalistic driving environment (Wali et al., 2018d).

Another measure recently introduced in the literature for characterizing driving volatility is vehicular jerk (Wali et al., 2018d)(Wang et al. 2015). Vehicle jerk is basically defined as the rate of change of vehicle acceleration with respect to time. Compared to accelerations/decelerations, vehicular jerk represents drivers' decisions to change marginal rate of acceleration or deceleration, and may better characterize driving volatility in instantaneous driving decisions (Wali et al., 2018d). In relevance to the current study, Feng et al. (2017) concluded the better potential of longitudinal vehicular jerk to identify "aggressive" drivers (Feng et al. 2017). However, vehicular jerk measures in lateral direction are not widely used (Wali et al., 2018d).

To fully characterize volatility in instantaneous driving decisions, we use both acceleration and vehicular jerk based performance measures (Figure 5.2). As deceleration profiles usually have higher variations (Kamrani et al., 2017), separate volatility measures for acceleration and deceleration are used. Likewise, separate volatility indices are generated for positive and negative jerk values. While doing so, both longitudinal and lateral dimensions are considered in calculation of volatility prior to involvement in safety critical events, and which can better characterize the complex mechanism of instantaneous driving decisions in longitudinal and lateral directions (Figure 5.3). Figure 5.3 illustrates the methodology for characterizing driving volatility. For the sake of completeness, the formulae for velocity, acceleration, and vehicular jerk are shown in Equations 5.1-5.4:

$$r = Position \quad \text{Equation 5.1}$$

$$Velocity = v = \frac{\partial r}{\partial t} \quad \text{Equation 5.2}$$

$$Acceleration = a = \frac{\partial v}{\partial t} = \frac{\partial^2 r}{\partial^2 t} \quad \text{Equation 5.3}$$

$$Vehicular\ Jerk = j = \frac{\partial a}{\partial t} = \frac{\partial^2 v}{\partial^2 t} = \frac{\partial^3 r}{\partial^3 t} \quad \text{Equation 5.4}$$

Where: $\frac{\partial}{\partial \mathrm{t}}$ indicates derivative of a performance measure (velocity, acceleration, etc.) with respect to time, and $\partial \mathrm{t}$ is a small change in time "t" (set to 0.1 seconds in our case).

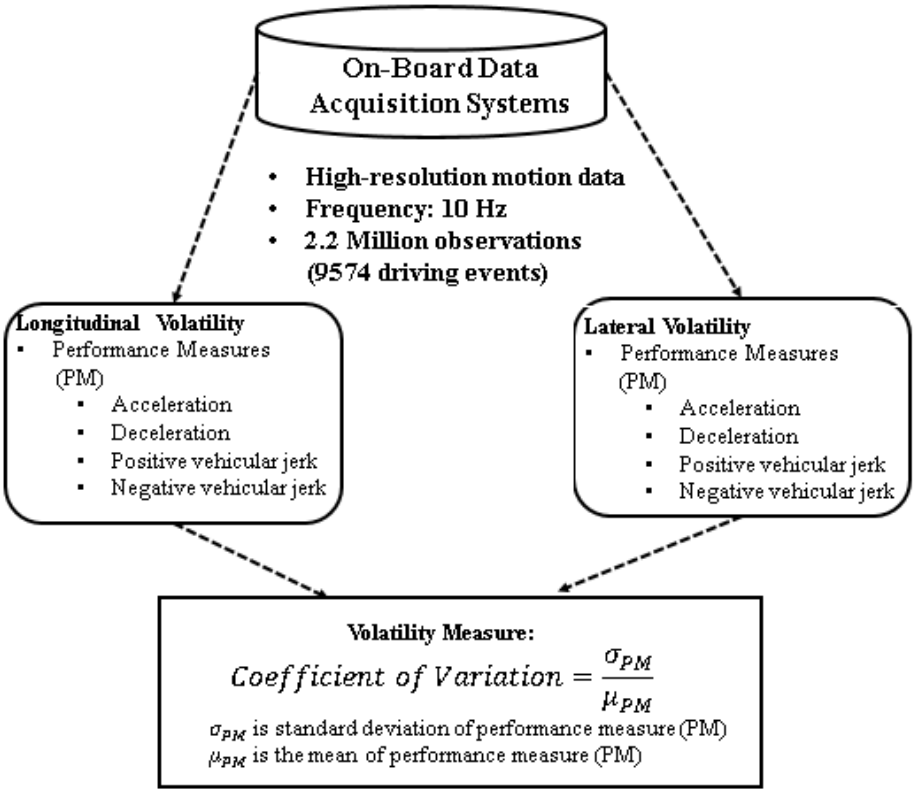

Figure 5.3 Methodology for characterizing driving volatility prior to involvement in safety critical events.

Specifically, the on-board data acquisition systems installed in vehicles provide high-resolution motion data at a frequency of 10 Hz (TRB, 2013). Instantaneous longitudinal and lateral acceleration profiles are recorded for the entire trip. However, compared to drivers' performance throughout the entire trip, instantaneous driving decisions immediately prior to involvement in safety critical events are more relevant and crucial. As such, the EDT provides instantaneous motion data, 30 seconds for every safety critical event (crash/near-crash) and 20 seconds for every baseline event (TRB, 2013). The 30-second driving behavior data can be interpreted as driving decisions undertaken immediately before the occurrence of crash or near-crash event.

A total of 2.2 million observations are used in this study for calculation of volatility indices for 9574 driving events (discussed later in detail). As shown in Figure 5.3, for each event, acceleration and deceleration values are separated, and mean and standard deviations calculated for each. As a measure of volatility, coefficient of variation is used in the present study[42] , i.e., the standard deviation(s) are then divided by mean values to get an estimate of relative variability in instantaneous driving decisions across different events. Similar procedure is repeated for acceleration/decelerations in lateral direction, and for vehicular jerk (both positive and negative) in longitudinal and lateral directions (Figure 5.3). Finally, considering the discussion on different components of volatility (see section 5.3.3), 24 different volatility measures are considered in this study based on the whether the entire 30 seconds, starting 20 seconds, or 25 seconds data are used (Table 5.1).

Note that the SHRP 2 NDS provides 30-seconds microscopic vehicle trajectory data for each of the safety-critical events (crashes/near-crashes), and which were used in this study. In addition, 29-30 seconds videos are also available for majority of the safety-critical event. However, note that the safety-critical event does not need to occur exactly at the end of the 30-seconds trajectory data or at the end of the corresponding video files. In other words, the safety-critical event can take place before the end of the event data/video file, e.g., after 20 seconds while the event data is provided for the entire 30-seconds. Using the entire 30-seconds data in this case will distort the results, especially with respect to intentional vs. unintentional volatility. While it is not practical to manually check all of the video files for safety-critical events (as there are

[42] Kamrani et al. (2017) introduced coefficient of variation as a measure for characterizing driving volatility in connected vehicles environment. Compared to standard deviation or variance, coefficient of variation is scale in-sensitive and this property allows meaningful comparisons between the volatility in instantaneous driving decisions in different safety critical and baseline events (Kamrani et al., 2017).

thousands of events), we manually checked the video files of a completely random sample of 100 crashes to exactly record the time at which the event occurred during the 30 seconds. For the decision of using all the 30 seconds data to be reasonable, we would expect the distribution of the event occurrence times to be left-skewed, i.e., majority of the event occurrence times would be expected to occur at the end of the trajectory/video files. Out of the 100 randomly sampled crashes, videos were available for 59 of them. For these 59 crashes, the video duration was 29 seconds for all except two crashes (16 seconds for one and 13 seconds for the other). After extracting the event (crash) occurrence time from these 59 videos, we conducted a descriptive analysis to see the distribution of the data. The resulting distribution of event occurrence time (in seconds) was highly skewed to the left with a skewness parameter of -1.92 (skewness of less than -1 indicates heavily skewed distribution to the left) and kurtosis parameter of 10.887 (kurtosis value for a normal distribution is exactly 3). The mean event occurrence time was 24.70 seconds with a small standard deviation of 2.39 seconds. This analysis highlights that the decision to use the entire trajectory data for calculation of intentional vs. unintentional volatilities is reasonable and the un-intentional volatility indices appropriate. However, out of the 59 crash events, we did find two shorter duration videos of 16 and 13 seconds for two crash events respectively. That is, 2% of the crashes in the sample may be like these if we have the event videos for all of them. Strictly speaking, this may also imply that we may not have some creep from unintentional volatility due to the crash. However, the extent of this would be low given that only 2% of the cases had shorter durations.

5.3.5 Statistical Models

Once the event specific volatilities (eight different volatility measures) are calculated for each event, the correlations between crash propensity and driving volatility are explored. Appropriate statistical models can shed light on microscopic driving decisions i.e., driving volatility, and how such decisions may be related to involvement in safety critical events. The potential outcomes related to crash propensity are baseline events, crash events, crash-relevant events, near-crash events, and non-subject conflict events. As can be seen, the response outcome is discrete and un-ordinal in nature, and thus un-ordinal discrete framework can be used. Following McFadden et al. (McFadden, 1973), a crash propensity function determining the outcome "i " of a specific event "j" can be defined as:

$$CP_{ij} = \boldsymbol{\beta_i X_{ij}} + \varepsilon_{ij} \qquad \text{Equation 5.5}$$

Where: CP_{ij} is a crash propensity function determining the safety outcome *"*i*"* (if event was baseline, crash, crash-relevant, near-crash, or non-subject conflict) for event "j"; $\mathbf{X_{ij}}$ is the matrix of explanatory variables (driving volatility related variables, pre-crash maneuvers, weather, or traffic factors); $\boldsymbol{\beta_i}$ is the vector of estimable parameters related to each explanatory factor in $\mathbf{X_{ij}}$, and ε_{ij} are the error terms. Following McFadden (1973) (McFadden, 1973) and Train (Train, 2003), if ε_{ij} are assumed to be generalized extreme value distribution, the multinomial logit model can be formulated as:

$$P_j(i) = \frac{\exp\left[\boldsymbol{\beta_i X_{ij}}\right]}{\sum_I \exp\left[\boldsymbol{\beta_i X_{Ij}}\right]} \qquad \text{Equation 5.6}$$

Where: $P_j(i)$ is the probability of specific outcome "i " (from the super-set of all possible categories "I" defined earlier) for event "j". Following (Train, 2003), the following log-likelihood function can be solved to get estimates of $\boldsymbol{\beta_i}$:

$$LL = \sum_{j=1}^{J}\left(\sum_{i=1}^{I} \aleph_{ij}\left[\beta_i X_{ij} - LN\sum_{\forall I}\exp(\beta_i X_{Ij})\right]\right) \quad \text{Equation 5.7}$$

Where: $\aleph_{ij}$ is an indicator equal to 1 if observed response outcome for event "j" is "i", and 0 otherwise (Train, 2003). For further details about the fundamentals of the statistical methods used, see (Wu and Jovanis, 2012).

5.3.5.1 Unobserved Heterogeneity

The key focus of this study is to investigate correlations between driving volatility related measures and crash propensity. Crash propensity can be influenced by different factors, some of which are observed while other factors are unobserved in the data at hand. Given such unobserved factors, the correlation between explanatory factors (such as driving volatility indices) and crash propensity may vary across different events, and which is referred to unobserved heterogeneity in the literature (Train, 2003). In addition, the issue of possible omission of relevant and important explanatory factor(s) from the modeling framework has also serious implications (Jovanis et al., 2011, Washington et al., 2010). For example, if important explanatory factor (e.g., education, age, gender etc.) that may influence driver's performance is omitted from the model, it may happen that the observed correlation between driving volatility indices (observed explanatory factor) and crash propensity may be an outgrowth of those omitted factors, and not true correlation between volatility and crash propensity (Washington et al., 2010). Note that, the unobserved factors need not to be only driver-related but can also include

other omitted and important variables, such as situational variables (Jovanis et al., 2011). For instance, while the SHRP 2 NDS database contains very detailed context-specific data, information on certain situational variables such as more complex situations, shorter sight distances, erratic driving be other motorists may not be available. These omitted situational factors may also be correlated with crash propensity. In our case, all such unobserved factors (driver-specific, vehicle-specific, environment-specific, and situation-specific, to name a few) that are likely to be correlated with crash propensity become a portion of the unobserved heterogeneity. As such, the statistical methods used in this study account for all different types of unobserved variables. To reach reliable conclusions about the correlation between driving volatility and crash propensity, it is crucial to account for the afore-mentioned methodological concerns. To account for these issues (Kamrani et al., 2017, Savolainen et al., 2011), a random parameter framework is adopted where the $\boldsymbol{\beta_i}$ are allowed to vary across different events according to some pre-specified distribution. Following (Train, 2003), a mixing distribution is introduced in random parameters logit model, where the logit framework now becomes:

$$P_j(i) = \int \frac{\exp\left[\boldsymbol{\beta_i X_{ij}}\right]}{\sum_I \exp\left[\boldsymbol{\beta_i X_{Ij}}\right]} f(\beta|\varphi)d\beta \qquad \text{Equation 5.8}$$

Where: $f(\beta|\varphi)$ is the density function of β conditional on the vector of parameters for the density function denoted φ. With the random parameter logit model in Equation 5.8, β can now account for driver-specific variations of the effect of $\mathbf{X_i}$ on probabilities of different crash propensity outcomes, and with β determined by approximating the integral in Equation 5.8 by drawing from a pre-specified density function $f(\beta|\varphi)$ (Train, 2003). The estimation proceeds with Maximum Simulated Likelihood procedures where Halton draws (compared to random draws) are used in the simulation process. In this study, 1000 Halton draws are used for parameter estimation,

nonetheless, 200 Halton draws are reported to produce accurate parameter estimates (Train, 2003, Bhat, 2003). Regarding function form of the parameter density functions, we have tested normal, lognormal, triangular, uniform, and Weibull distributions. Further details can be found in (Kamrani et al., 2017, Train, 2003).

Although crash propensity function in all the estimated random parameter logit models are expressed in linear form, the logit transformation restricts direct interpretation of parameter estimates (Naik et al., 2016). To intuitively interpret the modeling results, marginal effects are estimated for the fixed- and random-parameter logit model (Naik et al., 2016). For a certain change in value of explanatory factor, marginal effect suggests an instantaneous change in the probability of a crash propensity outcome while keeping all other factors at constant. Separate marginal effects are estimated for continuous and binary indicator variables. Following (Train, 2003), as marginal effects can be different at different levels of explanatory factors, therefore the average marginal effects over the sampled events are estimated.

5.4 DESCRIPTIVE ANALYSIS

5.4.1 Concept Illustration and Descriptive Statistics

To understand how microscopic driving decisions vary across different events, Figure 5.4 illustrates the distributions of longitudinal acceleration against speed for baselines/normal driving events, crash events, and near-crash events. As can be seen, high speeds (>50-60 kph) are associated with smaller magnitudes of acceleration/deceleration as well as smaller dispersion in acceleration/deceleration values, i.e., lower volatility.

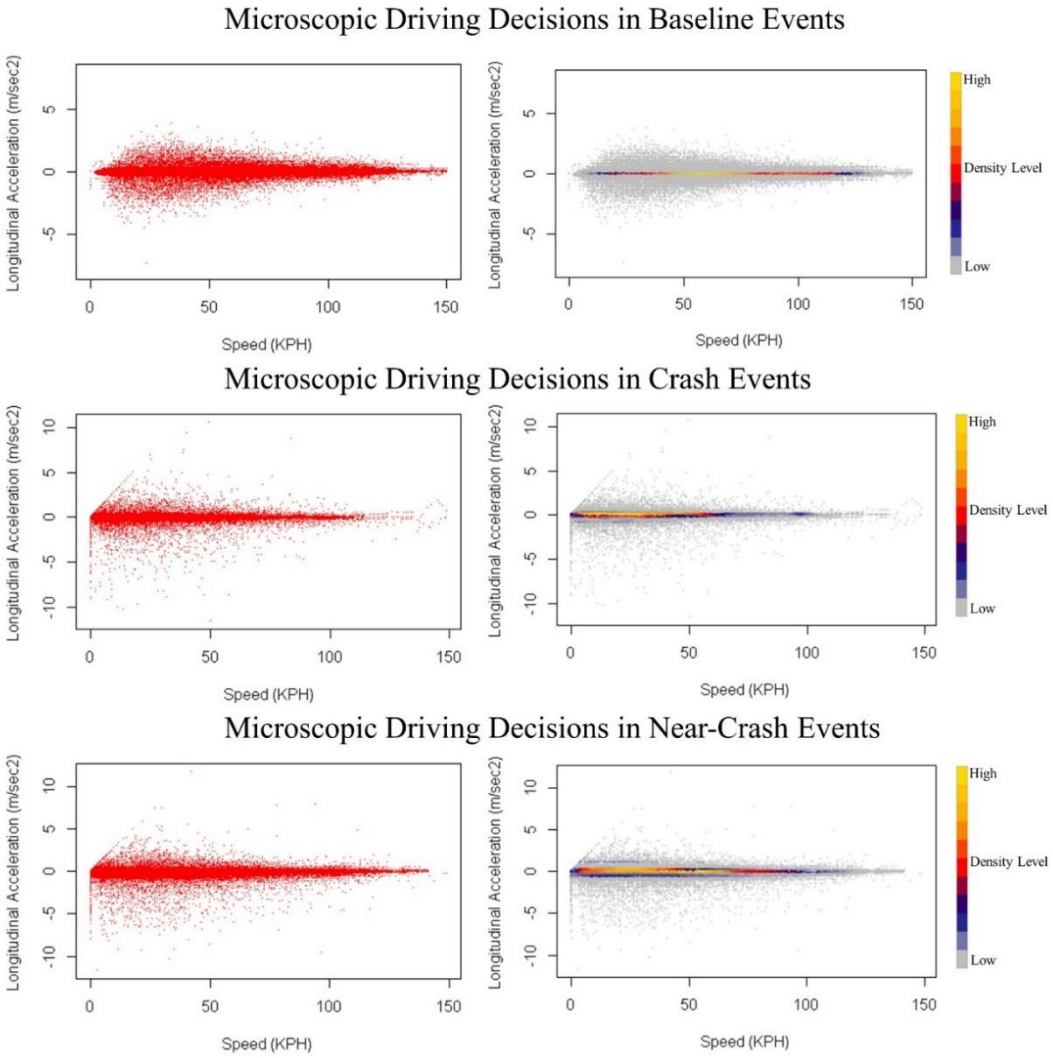

Figure 5.4 Scatter and density plot distributions of longitudinal acceleration and speed in baseline, crash, and near-crash events

Likewise, for each of baseline, crash, and near-crash events, Figure 5.4 provides the density scatter plot of the relationship between longitudinal acceleration and speed. It can be seen that the bandwidth of acceleration values at high speeds is tighter than the bandwidth of acceleration values at low speeds. This finding corresponds with our understandings of basic Physics principles according to which the ability to accelerate a vehicle naturally decreases at higher traveling speeds (Figure 4) (Khattak and Wali, 2017, Liu and Khattak, 2016b).

Importantly, Figure 5.4 also reveals a smaller dispersion in microscopic driver decisions in baselines events, compared to significantly greater dispersion in case of crash and/or near-crash events (Figure 5.4). This finding suggests that drivers on-average are more volatile in crash and near-crash events.

Next, Figure 5.5 presents the distributions of eight volatility measures considered in this study. For brevity, the distributions of volatility measure calculated using the entire data (20 seconds for baseline and 30 seconds for crashes/near-crashes) are shown (Figure 5.5). All eight volatility measures are not normally distributed and in fact skewed to the right, with mean volatility statistic greater than the median. Recall that coefficient of variation (Figure 5.3) is used as a measure to capture volatility in instantaneous driving decisions. Interestingly, the four volatility measures based on longitudinal and lateral accelerations (top two plots in Figure 5.5) exhibit similar patterns, whereas, the volatility measures based on longitudinal and lateral vehicular jerks have greater magnitudes as well as range. Broadly, this suggests that vehicular jerk based measures may also better characterize the volatility in instantaneous driving decisions as it accounts for the sharp rate of change (within one-tenth of a second) in acceleration values (Wali et al., 2018d, Wali et al., 2018e, Liu and Khattak, 2016b, Feng et al., 2017).

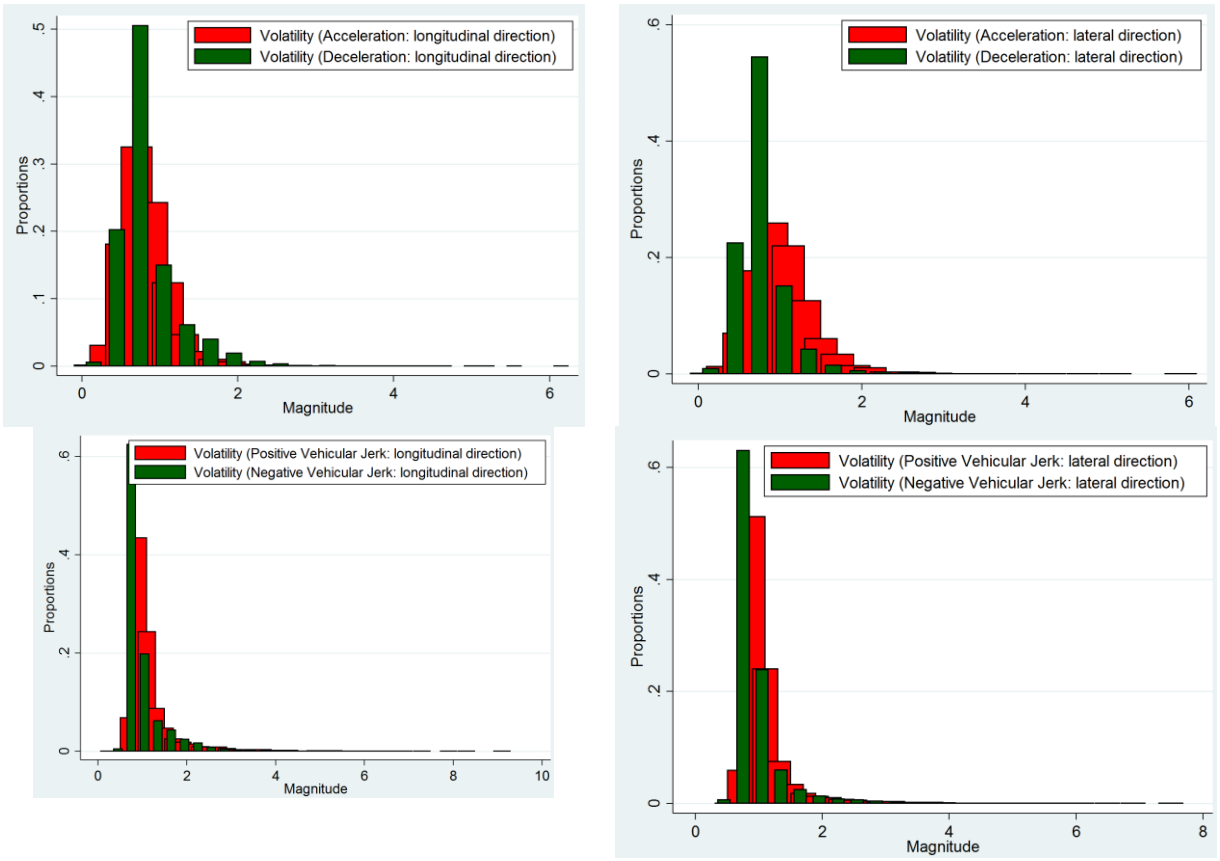

Figure 5.5 Distributions of volatility measures in naturalistic driving environment calculated using the entire data

Next, to see if there are statistically significant differences between driving volatility in safety critical events (crash, near-crash) and baseline events, ANOVA analysis is performed and results shown in Table 5.2. Our a-priori hypothesis is that compared to baseline (normal) driving events, drivers may exhibit greater volatility in crash and/or near-crash events.

Table 5.2 Descriptive and ANOVA Analysis of Driving Volatility Measures in Naturalistic Driving Environment

	Longitudinal Volatility								**Lateral Volatility**							
PM*	**Positive vehicular jerk**		**Negative vehicular jerk**		**Acceleration**		**Deceleration**		**Positive vehicular jerk**		**Negative vehicular jerk**		**Acceleration**		**Deceleration**	
Event Type	*Mean*	*SD*	*Mean*	*SD*	*Mean*	*SD*	*Mean*	*SD*	*Mean*	*SD*	*Mean*	*SD*	*Mean*	*SD*	*Mean*	*SD*
Baseline	0.99	0.18	0.82	0.15	0.80	0.29	0.71	0.19	0.97	0.17	0.84	0.18	0.99	0.33	0.71	0.20
Crash	2.41	1.28	1.98	1.04	1.03	0.52	1.21	0.62	2.24	1.05	1.85	0.76	1.37	0.61	1.20	0.55
Near-Crash	1.77	0.77	1.50	0.47	0.87	0.31	1.42	0.45	1.30	0.46	1.06	0.33	1.14	0.46	0.92	0.36
	Analysis of Variance															
	B	**W**	**B**	**W**	**B**	**W**	**B**	**W**	**B**	**W**	**B**	**W**	**B**	**W**	**B**	**W**
SS	1754.4	2131.2	1238	1184.0	35.2	946.3	656.7	792	1048.2	1224.5	653.5	775.1	104.2	1328.7	175.9	667.3
DF	2	9556	2	9553	2	9426	2	9337	2	9,555	2	9,553	2	9409	2	9446
MS	877.2	0.2	619.1	0.1	17.6	0.1	328.4	0.1	524.1	0.1	326.8	0.1	52.1	0.1	88.0	0.1
F	3933.3	---	4995	---	175.5	---	3870	---	4089	---	4027.6	---	369.0	---	1245	---
Prob > F	0	---	0	---	0	---	0	---	0	---	0	---	0	---	0	---

Notes: (*) PM is performance measures; For definitions of volatility measures, refer to Figure 2; SD is standard deviation; SS is Sum of Squares; DF is degrees of freedom; MS is mean of squares and is calculated as SS/DF; F is the corresponding F-statistic; B refers to between groups variance; W refers to within group variance; (---) means Not-Applicable; Unit for volatility in jerk is $\frac{m}{sec^3}$; Unit for volatility in acceleration and deceleration is: $\frac{m}{sec^2}$.

Note that the below descriptive findings relate to driving volatility indices calculated using the entire time-series (20 seconds for baselines, and 30 seconds for crashes/near-crashes) and not the segmented time series data (see section 5.3.3 for details). The rigorous statistical analyses presented in next section carefully addresses the issue of intentional vs. unintentional volatility and how it relates to crash propensity.

The top panel in Table 5.2 presents the summary statistics for all eight volatility measures (calculated using the entire data – refer to the third column in Table 5.1) and for each of the three event types. Whereas, the bottom panel summarizes the within- and between-group variances across the three event types. The within- and between-group variances are obtained from one-way ANOVA analysis (Stata, 2016). In particular, the grouping variable is event type, and which can be a baseline, near-crash, and crash. The motivation behind using event type as a grouping unit is that we are interested in examining the magnitudes and variations in volatilities across different normal and/or safety-critical events. Of course, the one-way ANOVA analysis of driving volatilities can also be performed by considering other grouping units such as driver gender, age-groups, or education status, etc. However, we use the variable event type given the primary focus of characterizing extent of variations in microscopic driving decisions within and across different event types. The following observations can be made from Table 5.2:

- For all eight volatility measures (except one) tested, compared to baseline events, drivers on-average exhibit higher volatility in near-crash situations, whereas drivers' volatility in crash events is further greater than in near-crash situations.
- Interestingly, for near-crash events, the volatility in deceleration in longitudinal direction

is greater than volatility in crash events (mean of 1.42 and 1.21 for near-crash and crash events respectively). This may be since drivers, in near-crash events, may react quickly (and with high volatility) to avoid an actual crash, and thus observed as near-crash.

- For volatility in longitudinal direction based on acceleration/deceleration measure, it is observed that drivers exhibit greater volatility in deceleration as compared to their volatility in acceleration (see mean values in top panel of Table 5.2 under longitudinal volatility). This is intuitive as drivers may react quickly to potential safety hazards in front of them and thus decelerate harder.
- For all volatility measures, compared to between-group variances, within-group variances are greater, suggesting larger variance in volatilities exhibited by different drivers involved in same event type. This is intuitive given the driver-specific differences and that different drivers may respond differently even in same situations.
- Finally, for all the eight volatility measures, there is statistically significant evidence that driver volatilities in baseline, near-crash, and crash events are significantly different (see F-statistics and corresponding p-values in bottom panel of Table 5.2), with volatilities in near-crash and crash events significantly greater than volatility in baseline events.

Next, Table 5.3 provides the descriptive statistics of the significant variables in subsequent statistical models. The descriptive statistics of volatility related variables using the data (30-seconds for crash and near-crash and 20 seconds for baseline events) are presented in Table 5.3. Furthermore, driving volatility prior to involvement in safety-critical events can contain different components, i.e., intentional and unintentional volatility (section 5.3.3).

Table 5.3 Descriptive Statistics of Key Variables

Variable	Mean	Std. Dev.	Min	Max	VIF
Key Volatility Indicators (entire 30 seconds driving data)					
Volatility (Positive vehicular Jerk: longitudinal direction)	1.195	0.638	0.28	9.13	4.75
Volatility (Negative vehicular Jerk: longitudinal direction)	0.997	0.503	0	6.59	4.73
Volatility (Positive vehicular Jerk: lateral direction)	1.107	0.488	0.47	7.43	4.72
Volatility (Negative vehicular Jerk: lateral direction)	0.942	0.387	0.43	5.90	4.46
Volatility (Acceleration: longitudinal direction)	0.827	0.323	0	5.17	1.14
Volatility (Deceleration: longitudinal direction)	0.849	0.394	0	6.09	1.65
Volatility (Acceleration: lateral direction)	1.037	0.390	0	5.92	1.28
Volatility (Deceleration: lateral direction)	0.776	0.299	0	4.27	1.26
Key Volatility Indicators (first 20 seconds driving data)					
Volatility (Positive vehicular Jerk: longitudinal direction)	1.024	0.270	0.28	5.70	2.15
Volatility (Negative vehicular Jerk: longitudinal direction)	0.836	0.184	0	3.30	1.86
Volatility (Positive vehicular Jerk: lateral direction)	1.012	0.309	0.47	14.07	2.36
Volatility (Negative vehicular Jerk: lateral direction)	0.854	0.202	0	4.03	2.20
Volatility (Acceleration: longitudinal direction)	0.800	0.303	0	4.16	1.03
Volatility (Deceleration: longitudinal direction)	0.721	0.211	0	2.41	1.12
Volatility (Acceleration: lateral direction)	0.986	0.365	0	6.99	1.07
Volatility (Deceleration: lateral direction)	0.717	0.211	0	2.47	1.16
Key Volatility Indicators (first 25 seconds driving data)					
Volatility (Positive vehicular Jerk: longitudinal direction)	1.168	0.600	0.28	9.06	4.09
Volatility (Negative vehicular Jerk: longitudinal direction)	0.984	0.491	0	6.46	4.08
Volatility (Positive vehicular Jerk: lateral direction)	1.093	0.476	0.47	8.72	4.01
Volatility (Negative vehicular Jerk: lateral direction)	0.930	0.370	0.43	5.62	3.85
Volatility (Acceleration: longitudinal direction)	0.822	0.322	0	5.17	1.07
Volatility (Deceleration: longitudinal direction)	0.840	0.386	0	6.08	1.74
Volatility (Acceleration: lateral direction)	1.029	0.392	0	7.27	1.16
Volatility (Deceleration: lateral direction)	0.767	0.294	0	5.25	1.52
Drivers' Secondary Task Durations					
Secondary Task 1 (duration in seconds)	2.092	2.720	0	24.12	1.16
Secondary Task 2 (duration in seconds)	0.357	1.259	0	14.22	1.12
Secondary Task 3 (duration in seconds)	0.047	0.465	0	15.00	1.07

Notes: Sample size is N = 9593; SD is standard deviation; and VIF is Variance Inflation Factor.

Table 5.3 Descriptive Statistics of Key Variables (Continued)

Variable	Mean	Std. Dev.	Min	Max	VIF
Secondary Tasks					
Adjusting/monitoring other devices, 0 otherwise	0.008	0.092	0	1	1.03
Engaged with cell-phone, dialing hand-held	0.002	0.040	0	1	1.04
Cell-phone, Texting	0.023	0.149	0	1	1.06
Looking at pedestrian	0.004	0.061	0	1	1.09
Pre-Incident Maneuvers					
Changing lanes	0.038	0.190	0	1	1.06
Making U-turn	0.002	0.046	0	1	1.03
Merging	0.003	0.059	0	1	1.03
Passing or overtaking	0.005	0.071	0	1	1.09
Legality of Maneuvers					
Maneuver is safe and legal	0.893	0.309	0	1	1.83
Maneuver is safe but illegal	0.021	0.142	0	1	1.44
Maneuver is unsafe but legal	0.027	0.162	0	1	1.31
Driver Behavior					
Unfamiliar/inexperience with roadway	0.003	0.050	0	1	1.45
Aggressive Driving	0.002	0.046	0	1	1.65
Drowsy, sleepy, fatigued	0.013	0.112	0	1	2.12
Angry	0.005	0.069	0	1	1.12
Number of occupants					
Front Seat Passengers	1.279	0.449	1	3	1.12
Rear Seat Passengers	0.106	0.416	0	5	1.08
Intersection-Roadway Influence					
Intersection influence: Traffic Signal	0.124	0.329	0	1	1.13
Intersection influence: Uncontrolled	0.034	0.181	0	1	1.05
Intersection influence: Stop sign	0.034	0.181	0	1	1.08
Divided Roadway	0.400	0.490	0	1	2.10
Not Divided - 2 way Traffic	0.431	0.495	0	1	2.05
Traffic Flow Factors					
Level of Service: A1	0.406	0.491	0	1	1.78
Level of Service: A2	0.300	0.458	0	1	1.56
Unstable Flow	0.021	0.142	0	1	1.07
Dead Flow	0.010	0.100	0	1	1.04

Notes: Sample size is N = 9593; SD is standard deviation; and VIF is Variance Inflation Factor.

To that effect, Table 5.3 also presents the descriptive statistics of volatility measures calculated using the first 20 seconds and 25 seconds driving data (as listed earlier in Table 5.1). Compared to volatility measures calculated using entire data, the volatility measures computed using the censored data are more likely to reflect the actual driving behavior and not the evasive maneuvers undertook by driver due to situational factors.

Several important insights can be obtained. First, the distributions of aggregate volatility measures (calculated using entire data) and volatility measures (calculated using censored data) are on-average similar (see the descriptive statistics in Table 5.3). For instance, the mean coefficient of variation for positive vehicular Jerk in longitudinal direction is 1.195 (for the entire data) compared to the mean coefficient of variation of 1.168 computed using the first 25-seconds data. Similar observations can be made for other volatility performance measures in longitudinal and lateral directions. This indicates that for the sampled events, drivers were not just volatile immediately before a crash (i.e., 5 seconds before the crash/near-crash) but also exhibited erratic or volatile behavior well before the crash (as reflected in volatility measures computed using first 20-seconds or 25-seconds data). Based on the discussion presented in earlier sections, *the critical question then becomes how intentional volatility may be associated with crash propensity?* Or in other words, is the relationship between aggregate driving volatility measures and crash propensity significantly different than the relationship between censored driving volatility measures and crash propensity. Note, however, that irrespective of the empirical results, the censoring of driving behavior data for eliminating the bias due to reverse causality is conceptually critical.

Regarding other factors, the average durations of first, second, and third secondary tasks are 2.09, 0.35, and 0.047 seconds respectively. Regarding secondary tasks, driver was observed to be texting while driving and looking at pedestrians in approximately 2.3% and 0.4% of the events (221 and 39 events). In 3.8% of the events, drivers changed lanes prior to getting involved in one of the three events. Interestingly, driver maneuver was observed to be safe but illegal in 201 events, whereas, maneuver was unsafe but legal in 259 events. The average number of front-seat (including driver) and rear-seat passengers are 1.279 and 0.106 respectively. Most of the events (around 70%) happened under free-flow traffic conditions. To check for multicollinearity, variance inflation factors are reported for all the explanatory variables. A VIF value of less than 10 indicates lack of problematic multicollinearity. In our case, VIF values for all explanatory factors are less than 5 (Table 5.3).

5.5 MODELING RESULTS

This section presents the results of fixed- and random-parameter logit models, where crash propensity is modeled as a function of driving volatility related measures and other factors. In particular, owing to the issue of intentional and unintentional volatility (as discussed in section 5.3.3), two sets of statistical models are estimated. The first set of statistical models contain the aggregate volatility measures (calculated using the entire time series data) as explanatory factors in addition to other factors. The use of aggregate volatility measures for explaining crash propensity can provide insights regarding how driving volatility relates to occurrence of unsafe outcomes. However, as noted earlier, driving volatility can contain separate components where the first component can be regarded as actual driving behavior (or intentional volatility) whereas the second component may reflect unintentional volatility (or volatility not due to the driver per

se but due to the external situational factors). The use of aggregate volatility measures will not allow us to relate how "intentional volatility" may be linked with crash propensity. In this regard, the second set of statistical models contain segmented volatility measures (calculated using censored time series data) as explanatory factors. For convenience, we first present the results of statistical models with aggregate volatility measures followed by presentation of results of statistical models with segmented volatility measures.

5.5.1 Modeling Scheme

Before presenting the results, we briefly present the overview of the modeling scheme. As mentioned earlier, the first set of models use aggregate driving volatility measures that are computed using the entire driving behavior time series data (30 seconds for crash/near-crash and 20 seconds for baseline events). Under this setting, for computing driving volatility, two sets of performance measures are considered, i.e., acceleration/deceleration and vehicular jerk. The statistical models with aggregate vehicular jerk or acceleration/deceleration based volatility measures as explanatory variables are termed as Category 1 and Category 2 models, respectively (see Table 5.4). The rationale behind considering these two performance measures is to investigate if vehicular jerk based driving volatility (compared to acceleration/deceleration based) measures better explain crash propensity or vice versa. For each of the two performance measures, fixed and random parameter logit models are developed.

Next, to separate out the two components of driving volatility, i.e., intentional vs. unintentional volatility, second set of statistical models are developed (Table 5.4). Under this setting, two schemes of censoring mechanisms for time series driving behavior data are considered. In particular, only the first 20 seconds time series data are used for computing driving volatility

measures in the first censoring scheme (see Table 5.1 and 5.4). Whereas, in the second censoring scheme, the first 25 seconds time series data are used for computing volatility indices and the last 5 seconds driving data are not considered (Table 5.4). As explained in detail earlier, the censoring of time series data can help in removing the influence of driver reactions immediately prior to crash or near-crash outcomes from the volatility measures while retaining volatility derived from driver behavior in the seconds leading up to but no immediately before the crash/near-crash event. Thus, using the best-fit performance measure under Category 1 and 2 models, censored versions of volatility indices are considered in Category 3 and 4 models. For each of the two categories, fixed and random parameter logit models are estimated (Table 5.4).

Table 5.4 Overview of Statistical Models Considered in this Study

Category	**Key Volatility Variables as Correlates**	**Statistical Models**	
		Fixed Parameter Logit	**Random Parameter Logit**
	First set of models: Computed using Aggregate time series data		
Category 1	Acceleration/Deceleration based volatility measures	✓	✓
Category 2	Vehicular jerk based volatility measures	✓	✓
	Second set of models: Computed using censored time series data		
Category 3	Volatility measures computed using first 20 seconds time series data*	✓	✓
Category 4	Volatility measures computed using first 25 seconds time series data*	✓	✓

Notes: (*) the performance measures (vehicular jerk vs. acceleration/deceleration) that provided statistically better results in first set of models are used in the second set of models (category 3 and 4 models).

5.5.2 Estimation Results

The results of statistical models are discussed next that quantify the correlations between crash propensity and driving volatility (aggregate and segmented), after controlling for other traffic, crash, and unobserved factors. As mentioned earlier, the crash propensity quantifies the risk of a crash or near-crash event relative to a normal[43] (baseline driving event). First, a series of fixed-parameter logit models are estimated in which the parameter estimates were constrained to be fixed across all events. The fixed parameter multinomial logit models are derived from a systematic process to include most important variables (such as driving volatility related variables and others) on basis of statistical significance, specification parsimony, and intuition. For example, given the key focus, only aggregate volatility related variables were first inserted into the crash propensity functions to better understand the relationship between driving volatility and crash propensity. Driving volatility related variables that were statistically significant at 90% confidence level were retained in the corresponding crash propensity functions. Once this was done, other important variables as shown in Table 3 were inserted into the crash propensity functions in a step wise fashion. In doing so, variance inflation factors (VIF) of explanatory factors were examined to avoid multicollinearity issue. As discussed in detail in methodology section, unobserved heterogeneity and omitted variable bias is suspected and in presence of which accurate correlations between driving volatility related measures and crash propensity cannot be established. Therefore, random-parameter logit models are estimated where all the parameter estimates were allowed (and tested) to vary across different events. Any

[43] According to the results of the manual video checking analysis discussed in section 5.3.4, we found that many of the randomly sampled crashes were probably not police reportable as they were quite minor (running over curb, side-walk, slight bumper touching in parking lot, etc.). These crashes in the NDS data may not even reach the crash reporting limit (USD 400 in Tennessee and USD 1000 in North Carolina and Virginia). Thus, the analysis presented includes minor crashes. This gives us the opportunity to look at some of the non-police reported crashes, even though they may be minor.

parameter estimate that resulted in statistically significant mean and/or standard deviation was retained as a random parameter in final model specification. Below, we briefly explain the key model comparison results from the first set of statistical models (using aggregate volatility measures) and the second set of statistical models (using segmented volatility measures). Note that the first set of models are briefly discussed for the sake of completeness and are treated as base models. As discussed in Section 5.3.3 in detail, a better way of quantifying the correlations between driving volatility and crash propensity is to eliminate the seconds of driving data immediately prior to crash/near-crash from the calculations of driving volatility, as done in the second set of statistical models below.

5.5.2.1 Statistical Models Using Aggregate Volatility Measures as Explanatory Factors

Under the first set of statistical models, eight different volatility measures based on acceleration/deceleration and vehicular jerk in longitudinal and lateral direction are considered (see Table 5.4). In particular, fixed and random parameter models with acceleration/deceleration based volatility indices are termed as Category 1 models, whereas models with vehicular jerk based measures are termed as Category 2 models (Table 5.4). In the models above, both longitudinal and lateral volatility are considered. Conceptually, we hypothesize that vehicular jerk based volatility measures may perform better than acceleration based measures as the earlier accounts for the sharp rate of change (within one-tenth of a second) in acceleration values. Table 5.5 summarizes the goodness-of-fit results of fixed- and random-parameter Category 1 and 2 logit models. It is seen that random-parameter models in the two categories clearly outperformed their fixed-parameter counterparts. This is evident from the significantly lower AIC and BIC values for random-parameter models (Table 5.5). Also, the results of likelihood-ratio test are

reported which suggest that random-parameter models are statistically superior to their fixed parameter counterparts at 99.5% confidence level (Table 5.5) (Washington et al., 2010). Specifically, the parameter estimates for eight variables each in Category 1 model, and six variables in Category 2 models are found to be normally distributed random parameters, suggesting significant heterogeneity in the effects of explanatory factors (including aggregate volatility measures) on crash propensity (Table 5.5). Importantly, both for fixed- and random-parameter approaches, vehicular jerk based longitudinal and lateral volatility measures (category 2 models) performed statistically superior to acceleration based volatility measures (category 1 models). After adjusting for the degrees of freedom differences, this is evident from the significantly lower AIC and BIC values for category 2 models against category 1 models (Table 5.5). This finding is intuitive and expected as hypothesized earlier.

Table 5.5 Model Comparison Using Aggregate Driving Volatility Measures

	Category 1 Models		Category 2 Models	
	Random Parameters	Fixed Parameters	Random Parameters	Fixed Parameters
Number of Parameters	45	37	39	33
Log-likelihood at zero	-6202.12	-6202.12	-6202.12	-6202.12
Log-likelihood at convergence	-2568.27	-2609.51	-2001.71	-2044.20
AIC	5226.54	5293.02	4081.418	4154.413
BIC	5546.02	5555.71	4403.683	4427.1
Likelihood Ratio Test	Random vs Fixed Parameters		Random vs Fixed Parameters	
Likelihood Ratio χ^2	82.48		84.98	
DF	8		6	
Prob > χ^2	0.000		0.000	

Notes: Category 1 models include acceleration/deceleration based volatility measures as explanatory factors; Category 2 models include vehicular jerk based volatility measures as explanatory factors; AIC is Akaike Information Criterion; BIC is Bayesian Information Criterion; DF is Degree of Freedom.

5.5.2.2 Statistical Models Using Segmented Volatility Measures as Explanatory Factors

To separate out the different components of driving volatility in time to crash/near-crash, this section briefly presents the results of statistical models with segmented driving volatility measures calculated either using first 20-seconds time series data (Category 3 models) or first 25-seconds time series data (Category 4 models). To account for unobserved heterogeneity and omitted variable bias, both fixed and random parameter logit models are estimated. As vehicular jerk based volatility indices significantly outperformed acceleration/deceleration based volatility indices (see earlier section), only vehicular jerk based volatility indices are considered in this set of statistical models. Table 5.6 summarizes the goodness-of-fit results of fixed- and random-parameter Category 3 and 4 logit models. Several insights can be obtained from the results presented in Table 5.6. First, models with vehicular jerk based volatility measures that are calculated using first 25 seconds time series data (Category 4 models) significantly outperformed the models with volatility measures calculated using the first 20-seconds time series data (Category 3 models). This can be seen from the significantly lower AIC/BIC values for Category 4 models. Second, owing to the presence of unobserved heterogeneity and potential omitted variable bias, the random-parameter models in the two categories clearly outperformed their fixed-parameter counterparts, as indicated by lower AIC/BIC values for random parameter models and likelihood ratio test statistics favoring random parameter models (Table 5.6).

Table 5.6 Model Comparison Using Segmented Driving Volatility Measures

	Category 3 Models		Category 4 Models	
	Random Parameters	Fixed Parameters	Random Parameters	Fixed Parameters
Number of Parameters	35	33	38	33
Log-likelihood at zero	-6202.12	-6202.12	-6202.12	-6202.12
Log-likelihood at convergence	-4522.30	-4533.75	-2411.88	-2475.94
AIC	9114.60	9133.50	4899.76	5017.88
BIC	9365.35	9369.92	5172.00	5254.30
Likelihood Ratio Test				
Likelihood Ratio χ^2	10.91		128.11	
DF	2		5	
Prob > χ^2	0.0043		0	

Notes: Category 3 models include vehicular jerk based volatility measures calculated using first 20-seconds time series data as explanatory factors; Category 4 models include vehicular jerk based volatility measures calculated using first 25-seconds time series data as explanatory factors; AIC is Akaike Information Criterion; BIC is Bayesian Information Criterion; DF is Degree of Freedom.

Table 5.7 shows the results of random parameter Category 4 model, i.e., models estimated with segmented vehicular jerk based volatility measures based on 25-seconds driving data. To contrast the differences, results of fixed parameter Category 4 model are also presented in Table 5.7. Finally, to better interpret the results, marginal effects are provided in Table 8 for the best-fit random parameter Category 4 model. To demonstrate the differences in the effects of explanatory factors on crash propensity, Table 5.8 also provides the marginal effects for fixed parameter Category 4 model. Given the conceptual motivation presented in Section 5.3.3, and the fact that Category 4 vehicular jerk based models with volatility measures calculated using 25-seconds data resulted in best-fit, we base our discussion on the results of Category 4 models only. Nonetheless, for completeness, the estimation results of random parameter Category 1 and 2 models and the marginal effects of best-fit Category 2 model (among the aggregate volatility models) are presented in Tables 5A.1 and 5A.2 in Appendix A.

Table 5.7 Estimation Results of Random Parameter Logit Models for Crash Propensity with Segmented Vehicular Jerk Based Driving Volatility Measures*

Variable	Category 4 Model: Fixed Parameter Logit[1]				Category 4 Model: Random Parameter Logit[1]			
	Crash		Near-Crash		Crash		Near-Crash	
	Coeff	z-score	Coeff	z-score	Coeff	z-score	Coeff	z-score
Constant	-12.95	-30.93	-8.80	-26.39	-27.12	-8.8	-9.73	-21.57
standard deviation	---	---	---	---	*4.52*	*6.85*	---	---
Key Segmented Volatility Indicators (Based on first 25 seconds data bin)								
Volatility (Positive vehicular Jerk: longitudinal direction)	1.92	8.82	1.88	9.17	2.21	4.26	2.15	8.64
standard deviation	---	---	---	---	*2.56*	*5.15*	---	---
Volatility (Negative vehicular Jerk: longitudinal direction)	5.51	20.73	5.37	21.56	7.18	10.72	6.71	19.08
Volatility (Positive vehicular Jerk: lateral direction)	2.41	8.14	1.95	6.84	5.76	5.79	1.65	4.62
Volatility (Negative vehicular Jerk: lateral direction)	1.51	4.9	-0.18	-0.63	5.62	5.08	-0.27	-0.75
Drivers' Secondary Task Durations								
Secondary Task 1 (duration in seconds)	0.27	12.64	0.22	12.97	0.51	6.67	0.24	11.43
Secondary Task 2 (duration in seconds)	0.17	4.26	0.15	4.55	0.29	2.52	0.18	4.43
Legality of Maneuvers								
Maneuver is safe and legal	-2.30	-13.39	-2.22	-16.27	-3.95	-6.44	-2.59	-14.84
standard deviation	---	---	---	---	*-0.79*	*-2.2*	---	---
Maneuver is safe but illegal	-2.23	-4.74	-3.59	-7.27	-2.67	-2.36	-4.71	-6.99
Driver Behavior								
Unfamiliar/inexperience with roadway	1.55	2.79	---	---	5.84	2.97	---	---
Aggressive Driving	---	---	2.85	3.24	---	---	3.09	3.2
Front Seat Passengers	-0.43	-2.74	-0.52	-4.48	-0.49	-2.27	-0.55	-3.94

Notes: (*) Baseline event is considered base category- all parameter estimates to be interpreted relative to baseline event; (1) refers to models with vehicular jerk based volatility measures calculated using first 25-seconds time series data.

Table 5.7 Estimation Results of Random Parameter Logit Models for Crash Propensity with Segmented Vehicular Jerk Based Driving Volatility Measures* (Continued)

Variable	Category 4 Model: Fixed Parameter Logit				Category 4 Model: Random Parameter Logit			
	Crash		Near-Crash		Crash		Near-Crash	
	Coeff	z-score	Coeff	z-score	Coeff	z-score	Coeff	z-score
Intersection-Roadway Influence								
Intersection influence: Traffic Signal	0.50	2.75	0.93	7.20	-2.46	-1.99	1.04	6.72
standard deviation	---	---	---	---	*-4.87*	*-3.45*	---	---
Intersection influence: Uncontrolled	1.89	7.57	2.19	11.06	2.97	4.21	2.61	10.84
Divided Roadway	-0.79	-4.88	---	---	-3.12	-4.54	---	---
Not Divided - 2 way Traffic	-0.76	-4.97	-0.34	-3.23	-2.02	-4.03	-0.67	-3.97
standard deviation	---	---	---	---	---	---	*1.26*	*5.45*
Traffic Flow Factors								
Level of Service: A1	---	---	-1.35	-12.65	---	---	-1.99	-11.88
Level of Service: A2	-0.35	-2.19	-0.73	-6.15	-1.14	-2.42	-0.96	-6.55
Unstable Flow	---	---	0.86	3.58	---	---	0.97	3.19

Notes: (*) Baseline event is considered base category- all parameter estimates to be interpreted relative to baseline event; (1) refers to models with vehicular jerk based volatility measures calculated using first 25-seconds time series data.

Table 5.8 Marginal Effects of Fixed- and Random-Parameter Best-Fit Category 4 Model

	Effects on probabilities of the event outcomes (multiplied by 100)					
	Fixed Parameter Logit Model			**Random Parameter Logit Model**		
Variable	**Baseline**	**Crash**	**Near-Crash**	**Baseline**	**Crash**	**Near-Crash**
Crash						
Volatility (Positive vehicular Jerk: longitudinal direction)	-3.15	3.47	-0.33	-3.53	5.21	-1.68
Volatility (Negative vehicular Jerk: longitudinal direction)	-9.02	9.95	-0.93	-9.03	13.86	-4.83
Volatility (Positive vehicular Jerk: lateral direction)	-3.95	4.36	-0.41	-6.05	9.81	-3.76
Volatility (Negative vehicular Jerk: lateral direction)	-2.47	2.73	-0.26	-5.78	9.44	-3.65
Secondary Task 1 (duration in seconds)	-0.44	0.48	-0.05	-0.27	0.55	-0.28
Secondary Task 2 (duration in seconds)	-0.28	0.31	-0.03	-0.14	0.30	-0.16
Front seat passengers	0.70	-0.77	0.07	0.22	-0.48	0.26
Maneuver is safe and legal	3.76	-4.14	0.39	2.89	-5.16	2.27
Maneuver is safe but illegal	3.65	-4.02	0.38	0.97	-2.25	1.28
Unfamiliar/inexperience with roadway	-2.54	2.80	-0.26	-6.17	9.98	-3.81
Intersection influence: Traffic Signal	-0.81	0.90	-0.08	-0.21	-0.56	0.77
Intersection influence: Uncontrolled	-3.09	3.41	-0.32	-2.09	3.81	-1.73
Divided Roadway	1.29	-1.42	0.13	1.30	-2.93	1.62
Not Divided - 2 way Traffic	1.24	-1.37	0.13	1.02	-2.10	1.07
Level of Service: A2	0.57	-0.63	0.06	0.52	-1.11	0.60
Near-Crash						
Volatility (Positive vehicular Jerk: longitudinal direction)	-15.41	-0.32	15.73	-10.74	-1.23	11.97
Volatility (Negative vehicular Jerk: longitudinal direction)	-43.99	-0.91	44.90	-60.61	-3.80	64.41
Volatility (Positive vehicular Jerk: lateral direction)	-16.02	-0.33	16.35	-7.43	-0.94	8.37
Volatility (Negative vehicular Jerk: lateral direction)	1.51	0.03	-1.54	0.83	0.14	-0.97
Secondary Task 1 (duration in seconds)	-1.80	-0.04	1.90	-0.82	-0.13	0.95
Secondary Task 2 (duration in seconds)	-1.30	-0.03	1.30	-0.59	-0.10	0.69
Front Seat Passengers	4.27	0.09	-4.35	1.59	0.29	-1.88
Maneuver is safe and legal	18.21	0.38	-18.58	13.49	1.43	-14.92
Maneuver is safe but illegal	29.39	0.61	-30.00	8.00	2.01	-10.00
Aggressive Driving	-23.34	-0.48	23.83	-18.76	-1.81	20.56
Intersection influence: Traffic Signal	-7.66	-0.16	7.82	-3.90	-0.58	4.47
Intersection influence: Uncontrolled	-17.92	-0.37	18.29	-14.15	-1.50	15.65
Not Divided - 2 way Traffic	2.75	0.06	-2.81	1.17	0.33	-1.50
Level of Service: A1	11.10	0.23	-11.33	6.06	1.11	-7.16
Level of Service: A2	6.01	0.12	-6.13	2.93	0.50	-3.44
Unstable Flow	-7.04	-0.15	7.18	-3.75	-0.54	4.29

Note: Marginal effects (multiplied by 100) rounded to nearest two decimals.

5.6 DISCUSSION

5.6.1 Safety Effects of Driving Volatility

As presented in earlier section, Category 4 vehicular jerk based models with volatility measures calculated using 25-seconds data resulted in best-fit. This suggests that volatility measures based on 25-seconds driving data best explain crash propensity, after accounting for the possible reverse causality that may arise due to the effects of unsafe outcomes on driving behavior immediately prior to involvement in unsafe outcomes. Thus, we discuss the key findings based on random parameter Category 4 model only, and contrast the results with fixed parameter Category 4 model to highlight the implications of ignoring unobserved heterogeneity and possible omitted variable bias. Furthermore, as the segmented volatility measures are likely to be reflecting the "intentional" driving behavior, we will refer to it as "intentional volatility" in interpreting the findings below.

For crash outcome, the parameter estimates for all four segmented vehicular-jerk based volatility measures in the random parameter model are positive and statistically significant at 95% confidence level (Table 5.7). This suggests that, compared to baseline events, greater "intentional" volatility is associated with higher likelihood of involvement in a crash event. For example, a one-unit increase in segmented volatility associated with positive vehicular jerk in longitudinal direction is associated with a 5.21% increase in probability of observing a crash outcome (Table 5.8). However, the parameter estimate for segmented volatility in positive vehicular jerk in longitudinal direction is normally distributed random parameter with a mean of 2.21 and standard deviation of 2.56 (Table 5.7). This suggests that the associations are not fixed and vary across different events.

To visualize the heterogeneity in the effects of random parameters, Figure 5.6 shows the distributions of all random parameters in Category 4 model, e.g., see box-plot 1 in Figure 5.6 for positive vehicular jerk in longitudinal direction. Likewise, a one-unit increase in volatility associated with positive vehicular jerk in lateral direction increases the probability of observing a crash outcome by 8.81 percentage points (Table 5.8).

These findings are important because it suggests that greater "intentional volatility" in positive vehicular jerk in time to crash and near-crash makes unsafe outcomes a more probable outcome. Regarding the effects of volatility in deceleration (both in longitudinal and lateral direction) on crash outcomes, the estimation results reveal important findings. For instance, as shown in Table 5.8, a one-unit increase in segmented volatility associated with negative jerk in longitudinal direction increases the probability of crash outcome by 13.86 percentage points (compared to only 5.21 percentage points increase for segmented volatility associated with positive jerk in longitudinal direction). This finding corroborates previous research finding by the authors which focused on correlations between volatility and crash frequency (Kamrani et al., 2017, Wali et al., 2018d). Likewise, a one-unit increase in volatility associated with negative jerk in lateral direction increases the probability of crash outcome by 9.44 percentage points (Table 5.8). The above findings show that intentional volatility in negative vehicular jerk (both lateral and longitudinal direction) has more negative consequences than volatility in positive vehicular jerk.

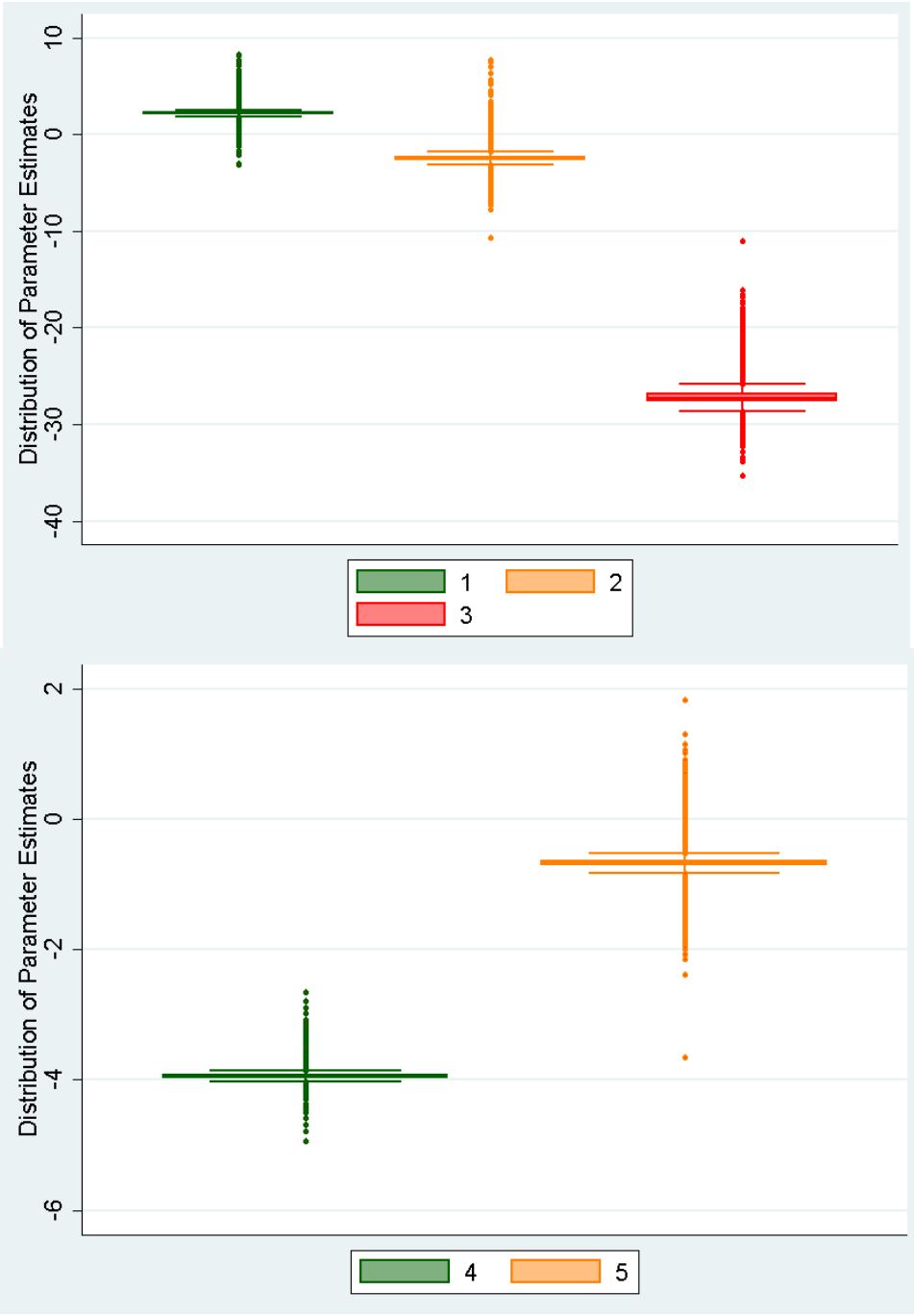

Figure 5.6 Distributions of random-parameters in category 4 model

Notes:

(1) Volatility (Positive vehicular Jerk: longitudinal direction) – utility function of crash outcome;
(2) Intersection influence: Traffic Signal – utility function of crash outcome;
(3) Intercept/Constant term – utility function of crash outcome;
(4) Maneuver is safe and legal - utility function of crash outcome;
(5) Not Divided – 2-way Traffic – utility function of near-crash outcome

Coming to the effects of volatility on near-crash outcome, the results intuitively suggest that increase in segmented volatilities (both longitudinal and lateral direction) increases the probabilities of observing near-crash events (Table 5.7). For example, a one-unit increase in segmented volatility associated with negative vehicular jerk in longitudinal direction increases the probability of near-crash outcome by 64.41 percentage points, compared to only 44.90 percentage points increase indicated by the fixed parameter counterpart (see marginal effects in Table 5.8). However, the parameter estimate for segmented volatility of negative vehicular jerk in lateral direction is statistically insignificant in utility function of near-crash outcome and deserves further investigation (see Table 5.7).

Finally, we point out that the associations between aggregate vehicular-jerk volatility measures and crash propensity are approximately similar in magnitude to the ones between segmented volatility measures and crash propensity (see Table 5.7 and Table 5A.1). In terms of probability statements, this is reflected in the marginal effects for the best-fit segmented vehicular jerk based random parameter model (Table 5.8) and the best-fit aggregate vehicular jerk based random parameter model (Table 5A.2). This suggests that the correlations between aggregate volatility measures and crash propensity observed in best-fit Category 2 model (as shown in Table 5A.1) are reliable, however, the volatility measures in Table 5A.1 are a mix of intentional as well as unintentional driving behavior components. Thus, given the theoretical reasoning presented in Section 5.3.3, we prefer and regard the results of Category 4 models (Table 5.7) as more appropriate as it provides insights about the relationships between “intentional volatility” (and which is preventable) and crash propensity.

5.6.2 Safety Effects of Secondary Task Durations, Passengers, & Legality of Maneuvers

The estimation results in Table 5.7 also shed light on the associations between secondary task durations, legality of maneuvers, and crash propensity. Secondary tasks in this study primarily refer to distractions related to non-driving related glances away from the direction of vehicle movement[44] (TRB, 2013). The results suggest that a one-second increase in the duration of the first secondary task increases the probability of crash outcome and near-crash outcome by 0.0055 and 0.009 units respectively (Table 5.8). Likewise, a one-second increase in the duration of the second secondary task increases the probability of crash and near-crash outcome by 0.30 and 0.69 percentage points respectively (Table 5.8). These findings are in agreement with previous studies (Klauer et al., 2006), and intuitive as any driver distraction for larger amount of time are likely to result in unsafe outcomes.

Regarding legality of maneuvers, some interesting findings surfaced from the analysis. It is found that if a maneuver is safe (irrespective of being legal or illegal), the likelihood of crashes and near-crashes decreases[45] (Table 5.7). However, the parameter estimate for maneuver being safe and legal in utility function of crash exhibits significant heterogeneity (see Figure 5.6). While the direction of effect is consistently negative, the magnitude of negative correlations, nonetheless, varies significantly (see box-plot 4 in Figure 5.6). Likewise, if the driver is unfamiliar with the roadway, the probability of crash outcome increases by 9.98 percentage points, compared to only 2.80 percentage points increase in fixed-parameter model (Table 5.8).

[44] Some examples of secondary tasks are radio adjustments, seatbelt adjustments, or looking outside at pedestrians. Note that secondary tasks do not include tasks that are critical to the driving task such as speedometer checks, mirror/blink spot checks, activating wipers/headlights, or shifting gears (TRB, 2013).

[45] Note that the maneuver is a vehicle-kinematic based measure, and is not related to driver's engagement in secondary tasks and/or distractions. For example, the variable related to legality of maneuvers refer to what the vehicle does (movement and position of the vehicle) such as going straight or changing lane, and is not related to what the driver is doing inside the vehicle (such as texting and driving).

This finding is in agreement with previous studies, e.g., (Klauer et al., 2006). Finally, Category 4 model suggests that a one-unit increase in number of front seat passengers decreases the probability of crash and near-crash outcome by 0.0048 and 0.0188 units respectively (Table 8). Again, the associations between passengers, legality of maneuvers, and crash propensity exhibit directional consistency in Category 2 (Table 5A.1) and Category 4 (Table 5.7) models. This is intuitive as accompanying front seat passenger may alert or warn the driver in case the driver is anticipated to undertake an unsafe maneuver or action.

5.6.3 Safety Effects of Roadway and Traffic Flow Factors

Compared to baseline events, the fixed parameter modeling results suggest that the probability of crashes or near-crashes increases at intersections (Table 5.7). Within intersections, the likelihood of near-crashes is higher on un-controlled intersections compared to intersections with traffic signals (Table 5.7). However, after accounting for potential unobserved heterogeneity, the results of random parameter model (Table 5.7) suggest that the relationship between an intersection with traffic signal and likelihood of crash outcome is in fact negative (β of -2.46 in random parameter model vs. β of 0.50 in fixed parameter model – see Table 5.7). Nonetheless, significant heterogeneity in the direction and magnitude of effect is also observed (see box-plot 2 in Figure 5.6), with negative correlation for 30.67% of the cases and positive for the rest, as opposed to a statistically significant and fixed positive correlation in fixed parameter counterpart. This finding is important in the sense that it indicates that ignoring unobserved heterogeneity can lead to inaccurate or misleading results.

Contrary to intersections which have higher likelihood of safety critical events, the likelihood of crashes or near-crashes is on-average lower on roadways (Table 5.7). These findings are intuitive

as intersections generally involve more complex movements and larger number of conflicts (Chin and Quddus, 2003, Kamrani et al., 2017, Poch and Mannering, 1996, Ye et al., 2009).

Coming to traffic related factors, the results suggest that the likelihood of crashes and/or near-crashes decreases in free-flow traffic either with no lead traffic present (Level of Service: A1) or with lead traffic present (Level of Service: A2) (Table 5.7). Contrarily, the likelihood of near-crashes increases in in unstable flow and/or dead-flow traffic conditions[46]. These findings are also intuitive as potential of conflict in unstable low and/or dead-flow traffic conditions is higher, and thus probability of near-miss may increase (Table 5.8).

5.7 LIMITATIONS/FUTURE WORK

The present study focused on exploring the links between event-based volatility and crash propensity irrespective of different types of crash events, such as rear-end, sideswipe, angled, roadway departure, etc. In future, a natural extension of the present study would be to examine how event-based driving volatility varies across different crash event types. Another natural extension of this work would be to analyze the links between event-based driving volatility and injury outcomes, given a crash.

5.8 CONCLUSIONS

Driving behavior in general is considered a leading cause of road traffic crashes. Relevant in this regard is the concept of "driving volatility" that captures the extent of variations in driving,

[46] The variables related to unstable flow and dead-flow traffic conditions were found statistically insignificant in utility function of crash outcome.

especially hard accelerations/braking and jerky maneuvers. To understand driving volatility prior to involvement in safety critical events, detailed microscopic data on instantaneous driving decisions and safety outcomes are needed. The present study extended the concept of driving volatility to specific events, thus termed as event-based volatility. The SHRP2 Naturalistic Driving Study provides relevant sensor, video, and radar based real-world microscopic driving data in this regard. The present study adopts a tight quasi-experimental study design to help compare driving behaviors in normal vs unsafe outcomes. Specifically, crash propensity is defined as likelihood of drivers' involvement in crash- or near-crash events, compared to normal (baseline) driving events. With these forethoughts in mind, the key objective of this study was to examine how driving volatility in time-to-crash or near-crash correlates with crash propensity? To achieve this, an innovative methodology is proposed for characterization of volatility in instantaneous driving decisions in normal and safety-critical events. A total of 2.2 million records of real-world driving for 9,593 driving events are analyzed in this study. By using information related to longitudinal and lateral accelerations and vehicular jerk, 24 different aggregate and segmented measures of driving volatility are proposed. In doing so, intentional as well as unintentional event-based driving volatility is characterized, i.e., the issue of actual driving behavior (and the volatility therein) and volatility due to evasive maneuvers of driver to avoid an unsafe outcome (reverse causality) is carefully addressed. Given the important methodological concerns of unobserved heterogeneity and omitted variable bias, fixed- and random-parameter discrete choice models were estimated to reach reliable conclusions.

For all eight aggregate volatility measures, there is statistically significant evidence that driver volatilities in baseline, near-crash, and crash events are significantly different, with volatilities in near-crash and crash events significantly greater than volatility in baseline events. Owing to the

issue of intentional vs. unintentional driving volatility, empirical evidence suggests that volatility measures based on censored 25-seconds driving data (where the last 5-seconds of entire 30-seconds driving data prior to unsafe outcomes are not considered) best explain crash propensity. After controlling for traffic, roadway, situational, and other unobserved factors, the results suggest that greater "intentional" volatility is positively correlated with both crash and near-crash events. Importantly, the findings show that greater intentional volatility in negative vehicular jerk (longitudinal direction) has more negative consequences than volatility in positive vehicular jerk. For example, a one-unit increase in (intentional) volatility of negative vehicular jerk in longitudinal direction increases the probability of crash and near crash outcome by 13.86 and 64.41 percentage points respectively, compared to only 5.21 and 11.97 percentage point increase in probability of crash and near crash outcome in case of a unit increase in positive vehicular jerk in longitudinal direction respectively. Compared to acceleration/deceleration based volatility measures, empirical evidence suggests that vehicular jerk based volatility models best explain crash propensity. Finally, the correlations established in this study exhibit significant heterogeneity, i.e., the effects of explanatory factors (such as driving volatility) varies across different events and that accounting for the heterogeneous effects in the modeling framework can provide more accurate and reliable results.

The above volatility related findings have important implications for proactive safety. For instance, instantaneous driving decisions can be monitored in real-time and warnings and alerts can be issued to drivers in case driver's decisions in longitudinal and lateral directions exhibit greater volatility (especially in braking). Given that instantaneous driving decisions during deceleration are more volatile and that the effect of volatility in deceleration on safety outcome is more severe, such alerts and warnings can potentially help in improving safety. From a

behavioral perspective, the findings originating from our analysis using segmented volatility indices indicates that it is not just the driving volatility immediately prior to crash/near-crash outcome that is critical, but more importantly the volatility in driving decisions when the driver is presumably in control of the vehicle. Given that the volatility in driving decisions well before the driver anticipated an unsafe outcome can be regarded as "intentional" volatility, proactive real-time warning and control assist applications can significantly enhance safety.

5.9 ACKNOWLEDGEMENT

The data for this study were provided through a collaborative effort between Virginia Tech Transportation Institute, the U.S. Federal Highway Administration (FHWA), and Oak Ridge National Laboratory (ORNL). The timely assistance and guidance of the ORNL team about data elements is highly appreciated. The contribution of Ali Boggs in proof-reading the manuscript is highly appreciated. This paper is based upon work supported by the US National Science Foundation under grant No. 1538139. Additional support was provided by the US Department of Transportation through the Collaborative Sciences Center for Road Safety, a consortium led by The University of North Carolina at Chapel Hill in partnership with The University of Tennessee. Any opinions, findings, and conclusions or recommendations expressed in this paper are those of the authors and do not necessarily reflect the views of the sponsors.

5.10 APPENDIX A

Table 5A.1: Estimation Results of Random Parameter Logit Models for Crash Propensity with Aggregate Driving Volatility Measures*

Variable	Category 1 Model (Random Parameters Logit)[1]				Category 2 Model (Random Parameters Logit)[2]			
	Crash		Near-Crash		Crash		Near-Crash	
	Coeff	z-score	Coeff	z-score	Coeff	z-score	Coeff	z-score
Constant	-15.15	-13.90	-10.40	-17.02	-29.07	-11.09	-13.10	-16.34
standard deviation	*1.73*	*4.38*	---	---	2.86	5.44	---	---
Key Volatility Indicators								
Volatility (Positive vehicular Jerk: longitudinal direction)	---	---	---	---	3.32	7.11	2.82	8.46
standard deviation	---	---	---	---	*1.23*	*4.19*	*0.83*	*5.11*
Volatility (Negative vehicular Jerk: longitudinal direction)	---	---	---	---	8.70	11.35	7.76	14.75
Volatility (Positive vehicular Jerk: lateral direction)	---	---	---	---	4.95	6.66	2.55	5.76
Volatility (Negative vehicular Jerk: lateral direction)	---	---	---	---	5.63	5.88	-0.20	-0.46
Volatility (Acceleration: longitudinal direction)	1.55	5.37	-0.50	-2.15	---	---	---	---
standard deviation	*0.81*	*3.59*	---	---	---	---	---	---
Volatility (Deceleration: longitudinal direction)	6.61	17.23	8.49	19.70	---	---	---	---
standard deviation	---	---	*0.8*	*3.58*	---	---	---	---
Volatility (Acceleration: lateral direction)	1.85	6.45	0.65	3.66	---	---	---	---
standard deviation	*1.06*	*3.66*	---	---	---	---	---	---
Volatility (Deceleration: lateral direction)	5.92	12.98	3.35	13.10	---	---	---	---
Drivers' Secondary Task Durations								
Secondary Task 1 (duration in seconds)	0.27	8.89	0.21	8.97	0.27	5.32	0.24	8.9
Secondary Task 2 (duration in seconds)	0.17	2.95	0.15	3.24	0.28	2.8	0.15	2.97
Legality of Maneuvers								
Maneuver is safe and legal	-2.67	-9.84	-2.45	-11.74	-4.16	-7.69	-2.85	-12.55
standard deviation	---	---	---	---	*2.93*	*6.37*	---	---
Maneuver is safe but illegal	-2.39	-4.40	-4.17	-6.18	-2.63	-2.61	-5.53	-6.45

Notes: (*) Baseline event is considered base category- all parameter estimates to be interpreted relative to baseline event; (1) refers to model with acceleration/deceleration based volatility measures as explanatory factors; (2) refers to model with vehicular jerk based volatility measures as explanatory factors.

Table 5A.1: Estimation Results of Random Parameter Logit Models for Crash Propensity with Aggregate Driving Volatility Measures (Continued)

Variable	Category 1 Model (Random Parameters Logit)[1]				Category 2 Model (Random Parameters Logit)[2]			
	Crash		Near-Crash		Crash		Near-Crash	
	Coeff	z-score	Coeff	z-score	Coeff	z-score	Coeff	z-score
Driver Behavior								
Unfamiliar/inexperience with roadway	2.18	2.23	---	---	3.46	2.06	---	---
Aggressive Driving	---	---	2.89	2.80	---	---	3.68	3.4
Front Seat Passengers	-0.31	-1.60	-0.44	-2.91	---	---	-0.49	-3.1
Intersection-Roadway Influence								
Intersection influence: Traffic Signal	0.84	3.64	1.50	8.72	---	---	1.09	6.05
Intersection influence: Uncontrolled	1.38	4.03	1.96	7.40	1.99	3.3	2.80	9.2
Intersection influence: Stop sign	0.82	2.21	1.07	3.47	---	---	---	---
Divided Roadway	-0.41	-2.28	-0.41	-2.28	-1.72	-3.34	-0.43	-2.14
Not Divided – 2-way Traffic	-0.83	-5.01	-0.37	-1.84	-1.13	-2.85	-0.28	-1.29
standard deviation	---	---	*0.85*	*2.36*	---	---	*1.01*	*3.72*
Traffic Flow Factors								
Level of Service: A1	---	---	-1.69	-7.38	---	---	-2.40	-8.81
standard deviation	---	---	*1.04*	*3.19*	---	---	*1.13*	*3.17*
Level of Service: A2	-1.13	-2.83	-0.83	-5.01	-0.71	-1.99	-0.93	-5.36
standard deviation	*1.39*	*2.20*	---	---	---	---	---	---
Unstable Flow	---	---	1.42	4.49	---	---	0.97	2.77
Dead Flow	---	---	1.19	2.32	---	---	0.78	1.61
standard deviation	---	---	*1.45*	*1.99*	---	---	---	---

Notes: (1) refers to model with acceleration/deceleration based volatility measures as explanatory factors; (2) refers to model with vehicular jerk based volatility measures as explanatory factors.

Table 5A.2: Marginal Effects of Fixed- and Random-Parameter Category 2 Model

	Effects on probabilities of the event outcomes (multiplied by 100)					
	Fixed Parameter Logit Model			**Random Parameter Logit Model**		
Variable	**1**	**2**	**3**	**1**	**2**	**3**
Crash						
Volatility 1[a]	-2.13	2.34	-0.21	-2.75	5.58	-2.83
Volatility 2[b]	-5.57	6.12	-0.55	-13.13	21.21	-8.07
Volatility 3[c]	-2.50	2.74	-0.25	-4.10	8.40	-4.30
Volatility 4[d]	-2.04	2.24	-0.20	-5.22	10.20	-4.98
Secondary Task 1 (duration in seconds)	-0.17	0.19	-0.02	-0.10	0.30	-0.19
Secondary Task 2 (duration in seconds)	-0.14	0.15	-0.01	-0.11	0.31	-0.20
Maneuver is safe and legal	2.03	-2.23	0.20	1.52	-4.51	2.99
Maneuver is safe but illegal	2.34	-2.57	0.23	0.70	-2.34	1.64
Unfamiliar/inexperience with roadway	-0.92	1.01	-0.09	-2.23	5.09	-2.86
Intersection influence: Uncontrolled	-1.64	1.81	-0.16	-0.98	2.50	-1.52
Divided Roadway	0.35	-0.39	0.04	0.56	-1.75	1.20
Not Divided – 2-way Traffic	0.44	-0.49	0.04	0.43	-1.24	0.80
Level of Service: A2	0.28	-0.31	0.03	0.25	-0.75	0.50
Near-Crash						
Volatility 1[a]	-17.99	-0.19	18.19	-13.57	-1.92	15.50
Volatility 2[b]	-47.57	-0.52	48.08	-59.26	-4.64	63.89
Volatility 3[c]	-18.71	-0.20	18.91	-10.16	-1.80	11.96
Volatility 4[d]	-1.02	-0.01	1.03	0.48	0.14	-0.62
Secondary Task 1 (duration in seconds)	-1.50	-0.02	1.50	-0.61	-0.17	0.78
Secondary Task 2 (duration in seconds)	-1.00	-0.01	1.00	-0.38	-0.11	0.49
Front Seat Passengers	2.50	0.03	-2.52	1.14	0.35	-1.49
Maneuver is safe and legal	17.98	0.19	-18.18	11.47	1.99	-13.46
Maneuver is safe but illegal	31.93	0.35	-32.27	7.26	3.38	-10.64
Aggressive Driving	-25.52	-0.28	25.79	-18.16	-2.55	20.70
Intersection influence: Traffic Signal	-5.78	-0.06	5.84	-3.13	-0.79	3.92
Intersection influence: Uncontrolled	-17.08	-0.19	17.27	-11.55	-1.98	13.54
Divided Roadway	-2.63	-0.03	2.66	-1.10	-0.31	1.41
Not Divided – 2-way Traffic	1.12	0.01	-1.13	0.28	0.19	-0.48
Level of Service: A1	11.23	0.12	-11.35	5.24	1.79	-7.03
Level of Service: A2	5.56	0.06	-5.62	2.23	0.66	-2.89
Unstable Flow	-7.01	-0.08	7.09	-2.84	-0.70	3.54
Dead Flow	-5.12	-0.06	5.17	-2.23	-0.56	2.79

Note: (a) Volatility 1 (Positive vehicular Jerk: longitudinal direction); (b) Volatility 2 (Negative vehicular Jerk: longitudinal direction); (c) Volatility 3 (Positive vehicular Jerk: lateral direction); (d) Volatility 4 (Negative vehicular Jerk: lateral direction); (1) is baseline; (2) is crash; (3) is near-crash; Marginal effects (multiplied by 100) rounded to nearest two decimals.

CHAPTER 6 THE RELATIONSHIP BETWEEN DRIVING VOLATILITY IN TIME TO COLLISION AND CRASH INJURY SEVERITY IN A NATURALISTIC DRIVING ENVIRONMENT

This chapter presents modified versions of two research papers by Behram Wali, Asad J. Khattak, Thomas Karnowski. These papers include:

Journal Paper (under-review) - *"How Driving Volatility in Time to Collision Relates to Crash Severity in a Naturalistic Driving Environment?."* Wali. B., Khattak, A.J., Karnowski, T. Under-review in Analytic Methods in Accident Research.

Peer-Reviewed Conference Paper – "How Driving Volatility in Time to Collision Relates to Crash Severity in a Naturalistic Driving Environment?" Wali, B., Khattak, A. J., Karnowski, T (2018). Presented at the 97th Annual Meeting of the Transportation Research Board, Washington DC, USA. TRB PAPER # 18-00060.

Wali. B., Khattak, A.J., Karnowski, T. (2017). How Driving Volatility in Time to Collision Relates to Crash Severity in a Naturalistic Driving Environment? Presented at the 5th Annual UTC Conference for the Southeastern Region, University of Florida, Gainesville, 2017.

ABSTRACT

The sequence of instantaneous driving decisions and its variations, known as driving volatility, can be a leading indicator of unsafe driving practices. The research issue is to characterize volatility in instantaneous driving decisions in longitudinal and lateral direction and to seek an understanding of how driving volatility relates to crash severity. By using a unique real-world naturalistic driving database from the 2nd Strategic Highway Research Program (SHRP), a test set of 671 crash events featuring around 0.2 million temporal samples of real-world driving are analyzed. Based on different driving performance measures, 16 different volatility indices are created. To explore correlations between driving volatility and crash severity outcomes, the volatility indices are then linked with individual crash events including information on crash severity, drivers' pre-crash maneuvers and behaviors, secondary tasks and durations, and other factors. As driving volatility prior to crash involvement can have different components, an in-depth analysis is conducted using the aggregate as well as segmented (based on time to collision) real-world driving data. To account for the issues of observed and unobserved heterogeneity, fixed and random parameter ordered models with heterogeneity in parameter means are estimated. The empirical results offer important insights regarding how driving volatility in time to collision may be related to crash severity outcomes. Overall, statistically significant positive correlations are found between the aggregate (as well as segmented) volatility measures and crash severity outcomes. The findings suggest that greater driving volatility (both in longitudinal and lateral direction) prior to crash occurrence increases the likelihood of police reportable or severe crash events. Importantly, compared to the effect of volatility in longitudinal acceleration on crash outcomes, the effect of volatility in longitudinal deceleration is significantly greater in magnitude. Methodologically, the random parameter models with heterogeneity-in-means

significantly outperformed both the fixed parameter and random parameter counterparts; underscoring the importance of accounting for both observed and unobserved heterogeneity. The relevance of the findings to the development of proactive behavioral countermeasures for drivers is discussed.

6.1 INTRODUCTION and BACKGROUND

The recent Traffic Safety Facts published by the National Highway Traffic Safety Administration (NHTSA) reported a total of 32,166 fatal traffic crashes and an additional 1,715,000 injury crashes in the U.S. (NHTSA, 2016). Of all the fatalities and injuries sustained by vehicle occupants, drivers sustained 73% of fatalities and 71% of injuries (NHTSA, 2016). As a result of extensive research over the decades (Mannering and Bhat, 2014), a broad spectrum of factors are known to be associated with the injury severity outcomes of drivers including drivers' characteristics, crash and roadway factors, vehicle features, weather, and environment-related factors (Quddus et al., 2002, Abdel-Aty, 2003, Behnood and Mannering, 2015, Khattak and Targa, 2004, Kockelman and Kweon, 2002, Mooradian et al., 2013, Zajac and Ivan, 2003). However, among other factors, driving behavior, in general, is considered a leading cause of road traffic crashes (RTCs) and the injuries involved therein. A better understanding of driving behavior prior to involvement in a crash is fundamental to the design of behavioral countermeasures. Thus, several studies have attempted to understand the behavioral correlates of injury severity, given a crash, e.g., (Paleti et al., 2010, Zhu and Srinivasan, 2011) (Abdel-Aty, 2003). Primarily, the focus has been on what is referred to as "aggressive" driving (such as driver was speeding, tailgating, improper lane changes, making obscene gestures, and so on), and

its correlation with injury outcomes[47] (Nevarez et al., 2009, Paleti et al., 2010, Richards and Cuerden, 2009, Weiss et al., 2014). By using "aggressive" driving as a latent construct, Paleti et al. (2010) quantified the moderating effect of aggressive driving in increasing injury severity outcomes (Paleti et al., 2010). Likewise, as surrogates of driving behavior, higher speeds or speed limits are known to be correlated with higher injury severity outcomes (Weiss et al., 2014, Abdel-Aty, 2003, Renski et al., 1999, Duncan et al., 1998, Klop and Khattak, 1999, Quddus et al., 2009).

For the most part, the analysis of driver-specific behavioral factors correlated with injury outcomes mainly builds upon data from traditional police crash reports or crash causation studies (Paleti et al., 2010, Mannering and Bhat, 2014) (Imprialou and Quddus, 2017). As acknowledged in the literature (Paleti et al., 2010, Mannering and Bhat, 2014) (Imprialou and Quddus, 2017), classifying "aggressive" driving based on information (such as speeds, maneuvers, etc.) in police crash reports is a subjective process and there exists the possibility of misclassification. Also, the extent to which the speed information in police crash reports, typically used as a measure of driving behavior, is accurate is unclear. Importantly, while analysis of such a nature has helped to formulate actionable strategies for development of behavioral countermeasures, it does not shed light on the actual microscopic driving tasks or decisions that typically precede drivers' involvement in a crash (Kim et al., 2016). Having said this, it is crucial to gain insights regarding the sequence of microscopic instantaneous driving decisions (e.g., acceleration/deceleration) preceding drivers' involvement in a crash, and which may determine the injury outcomes. An

[47] There exists extensive psychometrics-related literature regarding latent constructs for characterizing aggressive driving (Shinar, 1998). However, for brevity we focus on studies linking driving behavior explicitly to injury outcomes.

analysis of such a nature, however, was not possible until very recent mainly due to the data unavailability.

6.1.1 Concept of Driving Volatility

The rapid technological advancements in recent years have enabled collection of huge amounts of spatiotemporal data about the vehicle and human movement. With recent innovations ranging from the realization of vehicle-to-vehicle (V2V) and vehicle-to-infrastructure (V2I) technologies such as Dedicated Short Range Communication (DSRC) and WI-FI, to continuous video and radar surveillance, the collection of countless terabytes of real-world driving data is now a reality (Henclewood, 2014, Campbell, 2012). The real-world driving data generated by advanced technologies are large-scale and are not informative to drivers in the raw form (Khattak and Wali, 2017). However, by using appropriate data analytic techniques, a deeper and richer understanding of instantaneous driving decisions can be obtained (Khattak and Wali, 2017). Important in this regard is the concept of "driving volatility" that captures the extent of variations in driving, especially hard accelerations/braking and jerky maneuvers (Liu et al., 2015b, Liu et al., 2017, Liu and Khattak, 2016b, Wang et al., 2015). Driving volatility can be regarded as a measure of driving practice for characterizing instantaneous driving decisions, and importantly the extreme driving behaviors (Liu and Khattak, 2016b, Khattak and Wali, 2017). Compared to traditional surrogates of driving behavior (such as speed and driver demographics), the concept of individual-level driving volatility provides personalized and actionable information for developing driving feedback devices, warning and control assists systems[48] (Liu and Khattak,

[48] Note that real-world driving data generated by connected vehicles, radar sensors, or video surveillance are typically used for quantifying the extent of variations in instantaneous driving decisions (Liu and Khattak, 2016b, Liu et al., 2015b, Khattak and Wali, 2017). Extreme driving behaviors (based on information in police crash reports) are generally referred to as "aggressive driving" in the literature (Nevarez et al., 2009, Paleti et al., 2010). However,

2016b, Khattak and Wali, 2017).

6.1.2 Driving Volatility and Safety

A fundamental understanding of instantaneous short-term driving decisions prior to involvement in unsafe outcomes (such as crashes) can shed light on the actual mechanism in which a vehicle is maneuvered or operated before a crash. Such an understanding is crucial for designing actionable proactive behavioral countermeasures. The previous studies characterized driving volatility by using rigorous data analytic methodologies (Liu et al., 2015b, Liu et al., 2017, Liu and Khattak, 2016b, Wang et al., 2015, Khattak and Wali, 2017). However, the volatility was not linked with unsafe outcomes such as crashes. In this regard, a recent study by Kamrani et al. (2017) extended the concept of driving volatility to specific locations and proposed a methodology for linking high frequency microscopic connected vehicles driving data with historical crashes (Kamrani et al., 2017). In a similar zeal, Kim et al. (2016) conducted an exploratory study to analyze the association between rear-end crash propensity and micro-scale driving behavior (Kim et al., 2016). Both studies concluded that hard deceleration rates are associated with rear-end crashes on freeway ramps (Kim et al., 2016) and total crashes at signalized intersections (Kamrani et al., 2017). Innovative, proactive safety strategies were discussed (Kamrani et al., 2017, Kim et al., 2016). It seems reasonable to expect that the variations in microscopic driving behaviors *immediately* prior to crash involvement, termed as driving volatility, can be majorly correlated with crash outcomes, i.e., near-crash vs. crash or injury outcomes given a crash. The previous studies focused on crash frequency (propensity) and not on the outcomes of crashes per se (Kamrani et al., 2017, Kim et al.,

---

we prefer to use a neutral term, driving volatility, to refer to the variations in real-world microscopic driving performance and the extreme (potentially unsafe) behaviors therein.

2016). Also, the analysis in previous studies is aggregated in nature, i.e., location-specific driving behavior data are used to explain historical crashes at such locations. As such, insights regarding how driving volatility immediately prior to the crash may be related to driver's propensity of receiving injuries cannot be obtained.

6.1.3 Research Objective and Contribution

The main objective of this study is to investigate correlations between driving volatility and injury severity. To achieve this, a tight quasi-experimental study design is adopted to quantify real-world driving volatility immediately prior to involvement in a crash, and how it relates to injury outcomes sustained by drivers. In particular, the study uses a unique Naturalistic Driving database of drivers involved in crash events. For all the crash events, large-scale microscopic instantaneous driving data immediately prior to involvement in crashes are analyzed, and volatility indices created using different driving performance measures. To explore correlations between driving volatility and injury severity outcomes, the volatility indices are then linked with individual crash events including information on injury severity, event-specific variables such as drivers' pre-crash maneuvers and behaviors, traffic flow factors, secondary tasks and durations, roadway factors, and fault status (discussed later). Careful attention is given to the issue of both observed and unobserved heterogeneity (Mannering et al., 2016). From a methodological standpoint, fixed and random parameter discrete choice ordered models are estimated to account for both observed and unobserved heterogeneity. Unlike commonly-used random parameters models that typically assume the same mean for each random parameter, the present study also accounts for the possible heterogeneity in the means of the random parameters which vary as a function of several observed factors.

By using advanced modeling methods, the study contributes by seeking a fundamental understanding of short-term microscopic driving volatility, and how can we map driving volatility to injury severities sustained by drivers in crashes. Such an analysis is critical for designing proactive behavioral countermeasures as it can highlight moments of volatile (potentially unsafe) instantaneous driving decisions prior to involvement in crashes, and which may be linked with the drivers' injury outcomes.

6.2 METHODOLOGY

6.2.1 Conceptual Illustration

To understand the relationship between driving volatility and injury outcomes (given a crash), detailed microscopic instantaneous driving data are needed. The currently on-going SHRP2 Naturalistic Driving Study (NDS) provides relevant data (TRB, 2013). A key aspect of the SHRP2 NDS study is that it provides information on real-world driving decisions undertaken by drivers prior to involvement in a crash event. Crash is defined as any contact that the subject instrumented vehicle has with an object (moving or fixed) at any speed in which kinetic energy is measurably transferred or dissipated (Hankey et al., 2016). Figure 6.1 presents the conceptual framework describing the overall study structure. Importantly, the instantaneous driving data are event specific (in our case event is crash), and thus facilitate analysis of driving volatility and its correlation with injury outcomes while controlling for a wide variety of traffic, roadway, and behavioral factors in the event detail table (Figure 6.1).

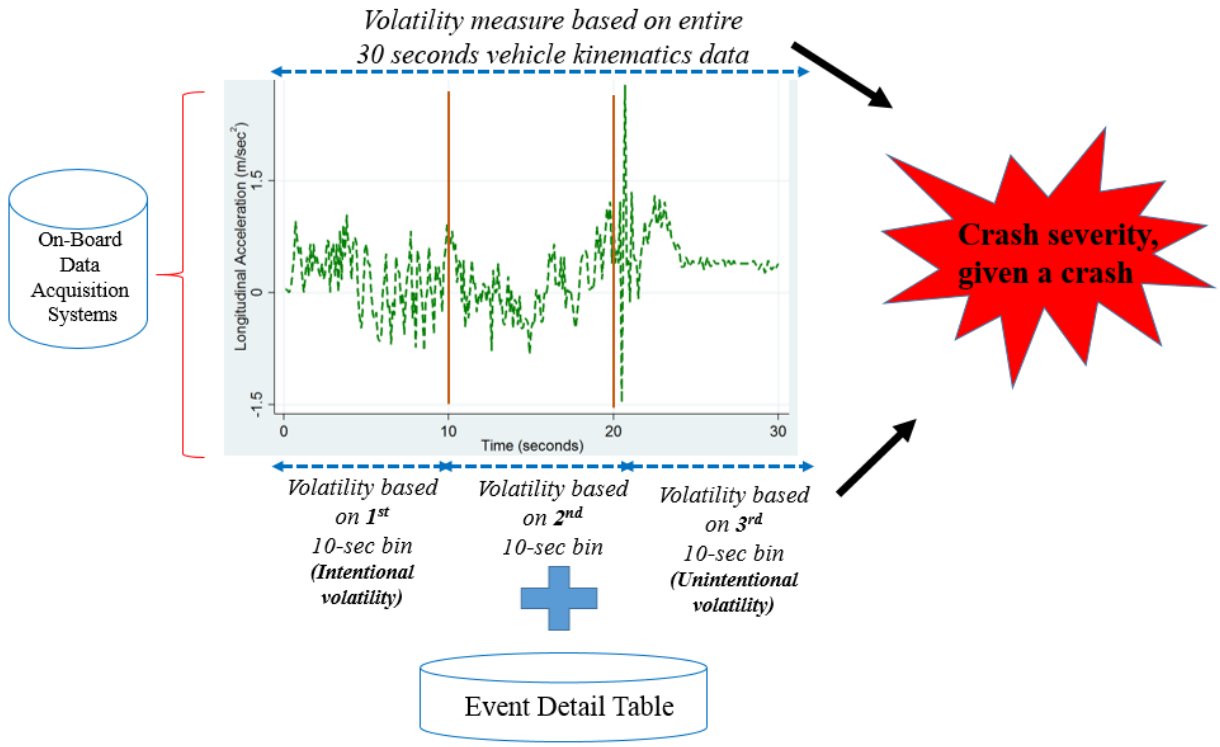

Figure 6.1 Conceptual framework
(Note: The original data resolution is 10 Hz, i.e., one-tenth of a second. However, the x-axis is labelled in seconds (1 Hz) for ease of presentation.)

The data from on-board data acquisition systems can be used to characterize volatility in instantaneous driving decisions (Figure 6.1). In particular, the on-board data acquisition systems installed in vehicles provide high-resolution motion data at a frequency of 10 Hz (Hankey et al., 2016). The on-board units collect data on instantaneous longitudinal and lateral acceleration profiles for the entire trip. However, compared to drivers' performance throughout the entire trip, instantaneous driving decisions immediately prior to involvement in safety-critical events are more relevant and crucial. Therefore, the SHRP2 NDS provides 30 seconds instantaneous motion data for every safety critical event (i.e., crash). The 30-second driving behavior data can be interpreted as driving decisions undertaken immediately before the occurrence of a crash (Figure 6.1).

6.2.2 Components of Volatility

Figure 6.1 shows a 30-seconds acceleration/deceleration profile prior to involvement in a crash. By using large-scale data analytic techniques, driving volatility can be characterized for each of the crash events. Broadly speaking, the volatility indices for each event can be regarded as measures of driving performance (or erratic behavior) before involvement in crash events. Linking driving volatility indices based on 30-seconds data can shed light on how instantaneous driving decisions are linked with injury outcomes. We hypothesize a positive correlation between driving volatility and injury outcomes. Any correlation, if exists, can provide fundamental knowledge about how driving decisions may influence crash outcomes. With real-world driving data based volatility indices (Figure 6.1), proactive behavioral countermeasures can be planned for drivers that are consistently more volatile.

However, using the entire 30-seconds driving data aggregates the driving volatility. For example, volatility in driving decisions prior to involvement in a crash may contain separate components, i.e., "intentional volatility" by the driver (due to aggressive self-driving when the driver is in control), and "unintentional" volatility due to evasive maneuvers or loss of control immediately before the crash. The earlier may be reflected in instantaneous driving data 20 to 30 seconds before the crash, and as such may be "intentional" volatility by the driver, i.e., the driver has not yet anticipated the crash but is undertaking erratic driving behavior. The later (unintentional or situational volatility) can be reflected in driving data immediately before the crash (e.g., 10 seconds before). We call it "unintentional volatility" as the driver may have already anticipated the crash in this case and is undertaking preventive measures to avoid the crash, i.e., evasive maneuvers. Also, the volatility 10-seconds before the crash is also likely to contain volatility due

to loss of control before the crash. As such, we also consider generating segmented volatility indices based on different time bins, and which can separate out how volatility in time to collision (bins) is related to injury outcomes (Figure 6.1).

6.2.3 Calculation of Volatility

Different instantaneous driving performance measures such as vehicle speeds, accelerations/decelerations, and/or steering angles can be used for estimation of volatility indices in longitudinal directions (Quddus, 2013b, Liu and Khattak, 2016b). The present study uses acceleration/deceleration profiles for generation of volatility indices. Typically, the deceleration profiles are known to exhibit larger variations (Kamrani et al., 2017, Kim et al., 2007). Thus, separate volatility indices are created for capturing variations in instantaneous longitudinal acceleration and deceleration profiles. In particular, coefficient of variation (C_v) is used as a measure for characterizing driving volatility prior to crash occurrence. Compared to standard deviation or variance, coefficient of variation (C_v) is scale insensitive, and this property allows meaningful comparisons between the volatility in instantaneous driving decisions in different crash events. To compute volatility for each crash event, acceleration and deceleration values are separated, and means and variances calculated for both. Then, C_v is obtained by dividing the standard deviations of accelerations (and decelerations) to the mean values, i.e., σ/μ. The process is repeated for all crash events, and both by using the entire 30-seconds data and bin-wise 10 seconds data (Figure 6.1). In total, eight volatility measures are computed for longitudinal direction (shown later).

Instantaneous driving decisions in the lateral dimension, such as lane change decisions, are also important as larger variations in lateral dimension may also be correlated with unsafe outcomes

(Wang et al., 2015). Having said this, separate volatility indices (for acceleration and deceleration) are also generated for instantaneous driving decisions in the lateral dimension. As shown in Figure 6.1, both aggregate and bin-wise data are used for calculation of volatility indices, and which can better characterize the complex mechanism of instantaneous driving decisions prior to involvement in a crash event. This resulted in a total of eight volatility measures in the lateral dimension.

6.2.4 Statistical Models

Once the volatilities indices (18 different volatility measures) are calculated for each crash event, the correlations between injury severity and driving volatility are explored while controlling for different observed and unobserved factors. Past research has extensively used a variety of methodological alternatives for modeling crash-related injury severity including multinomial or binary probit/logit models, ordered choice models, and nested logit models (Mannering and Bhat, 2014). For a detailed review of methodological alternatives, see Mannering and Bhat (2014) (Mannering and Bhat, 2014). Keeping in view the ordinal nature of the response outcome (crash severity), ordered probit framework is used to model injury severity as a function of driving volatility and other factors (Washington et al., 2010, Abdel-Aty, 2003, Khattak and Rocha, 2003, Quddus et al., 2002, Quddus et al., 2009). Following the work presented in (Washington et al., 2010, Duncan et al., 1998), consider:

$$Y_i^* = \beta \boldsymbol{X}_i + \varepsilon_i, \qquad \text{Equation 6.1}$$

Where: Y_i^* is the dependent variable coded as 0, 1, 2, and 3 for crash i; β is the vector of parameter estimates; $\boldsymbol{X}_i$ is the vector of independent variables; and ε_i is the normally distributed

error term with density function $\varphi(.)$ and cumulative distribution $\emptyset(.)$. Given a specific injury severity outcome, an individual crash falls in category n if $\mu_{n-1} < y < \mu_n$. The observed injury outcome data, Y, are related to the underlying latent variable Y_i^* through thresholds μ_n, where $n = 1,2,3$ (Duncan et al., 1998). In this context, the ordered probability of each different injury outcome for each crash i can be estimated as:

$$P(Y = n) = \emptyset(\mu_n - \beta \boldsymbol{X}) - \emptyset(\mu_{n-1} - \beta \boldsymbol{X}) \quad \text{Equation 6.2}$$

Where: $\mu_o = 0$, $\mu_3 = +\infty$, and $\mu_1 < \mu_2$ are the two thresholds between which the ordered responses are estimated (Wali et al., 2017b). To quantify the effects of the independent variables on the probability of each injury-severity level, and especially on the intermediate levels, marginal effects can be computed as:

$$\frac{\partial Prob(Y = n)}{\partial \boldsymbol{X}} = -[\varphi(\mu_n - \beta \boldsymbol{X}) - \varphi(\mu_{n+1} - \beta \boldsymbol{X})]\beta, \quad n = 1,2,3 \quad \text{Equation 6.3}$$

Following (Train, 2003), as marginal effects can be different at different levels of explanatory factors. Therefore, the average marginal effects over the sampled events are estimated.

6.2.4.1 Observed and Unobserved Heterogeneity

The key focus of this study is to investigate correlations between driving volatility related measures and crash-injury severity outcomes. Crash-injury severity outcomes can be influenced by different factors, some of which are observed while other factors are unobserved in the data at hand. Data extracted from police-reported crash forms, traffic and local weather stations, and in some cases highway-asset-management systems have been historically used to understand the factors associated with injury severity outcomes (Mannering and Bhat, 2014). However, with the

existing databases, there exists a real possibility that data on all the factors known to influence injury severity outcomes may not be available for analysis. For example, detailed information about driver-related behavioral variables is not usually available, and such variables may be correlated with crash-injury outcomes. Likewise, while safety-feature indicators (air-bags deployment, safety belts usage etc.) are typically available in traditional datasets, the effectiveness of these safety features in reducing crash-injury severity may vary across different crashes due to driver-specific characteristics such as height, health conditions, and bone density (to name a few), and such information is not typically available in traditional crash datasets (Mannering et al., 2016). These factors (potentially important) constitute what is referred to as "unobserved heterogeneity" in the safety literature (Mannering et al., 2016), and which is reflective of the possibility of systematic variations in the effects of explanatory factors across the sample population due to unobserved factors[49]. As explicitly noted in (Mannering et al., 2016), emerging data sources such as naturalistic driving (and which is used in this study) provide additional valuable data but still may not be enough to fully model the factors correlated with crash-injury severity outcomes (Mannering et al., 2016). Such unobserved factors can potentially introduce heterogeneity in the effects of observed explanatory factors on crash-injury severity. Recall that the focus of the current study is to understand the relationship between crash-injury severity and driving volatility. The driving volatility indices are calculated based on the vehicle kinematics data collected by on-board units installed in vehicles participating in the naturalistic driving study. As noted in Mannering et al. (2016), the kinematics data are vehicle-specific (and driver-specific), and can vary significantly across different vehicles and drivers, and which can introduce heterogeneity in the effects of "observed" driving volatility-related

[49] For a detailed discussion on why unobserved heterogeneity may make the effects of explanatory factors vary across the sample, interested readers are referred to Mannering et al. (2016).

variables on crash-injury severity. In addition, if important explanatory factors are omitted from the models, and appropriate methodological remedies not taken, it may happen that the "observed" correlation between driving volatility and crash-injury severity outcome may be an outgrowth of those omitted factors, and not "true" correlation between volatility and crash-injury severity outcomes.

Given this important methodological concern, statistical methods that can account for unobserved heterogeneity in the crash-injury severity analysis have fairly become a methodological standard (Mannering and Bhat, 2014, Mannering et al., 2016). By allowing the effects of exogenous explanatory factors to vary across individual crashes (or segments of population), more efficient, precise, and richer insights can be obtained. To account for unobserved heterogeneity, a broad spectrum of studies have successfully used different methodological alternatives including random parameter models (Anastasopoulos and Mannering, 2009, Zhao and Khattak, 2015, Alarifi et al., 2017, Bhat et al., 2017), random parameter models with heterogeneity in means (Behnood and Mannering, 2017b, Venkataraman et al., 2014), random parameter models with heterogeneity in means and variances (Behnood and Mannering, 2017a, Seraneeprakarn et al., 2017), latent-class models (Eluru et al., 2012, Yasmin et al., 2014, Shaheed and Gkritza, 2014), latent class models with random parameters (Xiong and Mannering, 2013), Markov-switching models (Malyshkina and Mannering, 2009, Malyshkina et al., 2009, Khattak and Wali, 2017), and Markov-switching models with random parameters (Xiong et al., 2014b). For a detailed discussion on the advantages and limitations of each of these methods, see Mannering et al. (2016). In the current study, we account for (possible) systematic variations in the effects of explanatory factors through random parameter modeling technique. To

account for the unobserved heterogeneity in the ordered outcome probability process, random parameters can be introduced as (El-Basyouny and Sayed, 2011, El-Basyouny and Sayed, 2009a, Li et al., 2017, Milton et al., 2008):

$$\beta_i = \beta + \boldsymbol{\Upsilon}\zeta_i \qquad \text{Equation 6.4}$$

Where: β is the mean of random parameter vectors, $\boldsymbol{\Upsilon}$ is the diagonal matrix with standard deviations for random parameters, and ζ_i is a randomly distributed random term that captures unobserved heterogeneity across crashes (Mannering et al., 2016, Tay, 2015). In particular, the distribution for ζ_i is specified by the analyst where different distributions can be tested (discussed later). The estimation proceeds with Maximum Simulated Likelihood procedures where Halton draws (compared to random draws) are used in the simulation process. In this study, 1000 Halton draws are used for parameter estimation, nonetheless, 200 Halton draws are reported to produce accurate parameter estimates (Bhat, 2003). Regarding function form of the parameter density functions, we have tested normal, lognormal, triangular, uniform, and Weibull distributions. Further details can be found in (Anastasopoulos and Mannering, 2009, Bhat, 2003).

While the mathematical formulation in Equation 6.4 accounts for unobserved heterogeneity by estimating different set of crash-specific parameter estimates β_i, nonetheless, the mean parameter estimate (β) is still fixed across all the crashes. Unlike commonly-used random parameters models shown above that typically assume the same mean for each random parameter, we also allow the means of random parameters to vary across crashes as a function of observed explanatory factors. Thus, Eq. 4 becomes (Venkataraman et al., 2014, Behnood and Mannering, 2017b):

$$\beta_i = \boldsymbol{\beta} + \boldsymbol{\xi Z_i} + \boldsymbol{\Upsilon}\zeta_i \qquad \text{Equation 6.5}$$

Where: β is the mean parameter estimate across all crashes i, $\boldsymbol{Z_i}$ is a vector of explanatory factors from crash i which influence the mean of β_i, $\boldsymbol{\xi}$ is the parameter vector associated with $\boldsymbol{Z_i}$, and $\boldsymbol{\Upsilon}\zeta_i$ are as defined earlier that accounts for unobserved heterogeneity across different crashes. In addition to accounting for unobserved heterogeneity, the formulation in Equation 6.5 now also accounts for observed heterogeneity by allowing the means of random parameters to vary as a function of specific observed factors. This can help extract richer insights from the data at hand[50].

6.3 DATA

This study uses data from an on-going Naturalistic Driving Study (NDS) conducted as part of the 2nd Strategic Highway Research Program (SHRP2) (TRB, 2013). The SHRP2 NDS is the largest naturalistic driving environment till date including 3,400 participant drivers with over 4,000 years of real-world naturalistic driving data collected between 2010 and 2013 (Hankey et al., 2016). In particular, this study uses the "event data" and "continuous" time-series data collected

[50] Compared to the traditional random parameter (with fixed-means) models, Behnood and Mannering (2017b) found that accounting for heterogeneity-in-means in logit models resulted in better fit and substantially difference inferences (Behnood and Mannering, 2017b). In addition, recent studies have extended the heterogeneity-in-means approach to also account for heterogeneity-in-variances (Behnood and Mannering, 2017a, Seraneeprakarn et al., 2017). In a random parameter model with both heterogeneity in means and variances, Equation 6.5 becomes $\beta_i = \boldsymbol{\beta} + \boldsymbol{\xi Z_i} + \boldsymbol{\sigma_i} \exp(\boldsymbol{\aleph_i B_i}) \boldsymbol{v_i}$ (Behnood and Mannering, 2017a). Where, $\mathbf{B_i}$ is a vector of explanatory factors that captures heterogeneity in the standard deviation of random parameter ($\boldsymbol{\sigma_i}$), $\boldsymbol{\aleph_i}$ is a parameter vector associated with $\mathbf{B_i}$, and $\boldsymbol{v_i}$ is the disturbance term. The study by Seraneeprakam et al. (2017) found significant differences in the magnitudes of direct marginal effects for random parameters logit models with no mean-variance heterogeneity, with mean-only heterogeneity, and with both mean-variance heterogeneity (Seraneeprakarn et al., 2017). Likewise, Behnood and Mannering (2017a) noticed that constraining the means and variances of random parameters without statistical validation can result in model specification error, further leading to misguided policies (Behnood and Mannering, 2017a). We discuss the results of our attempts to estimate random parameter models with heterogeneous means and variances later in the results section.

as part of the NDS. For drivers involved in crashes, the event data table provides detailed information on pre-incident maneuvers, legality of maneuvers, driver behavior, secondary tasks, start and end times, if applicable, of first, second, and third secondary events. Also included in the data is information about front-seat and rear-seat passengers, intersection and roadway type indicators, and traffic flow related factors. Secondary tasks are defined as any observable driver engagement other than the key driving tasks, and which may begin at any point during the 5 seconds prior to the event start, i.e., crash in this case, through the end of the event (TRB, 2013).

A total of 671 crash events are analyzed in this study in which 501 distinct drivers are involved, i.e., some participants had more than one crash during the study period. A notable feature of the NDS database is the availability of vehicle's motion data prior to involvement in a crash event. For the thousands of instrumented participant vehicles, advanced data acquisition systems (DAS) are used that collect four video views (driver's face, driver's hand, forward roadway, and rear roadway), vehicle network and status information (speed, brake, acceleration), and information from additional sensors networked with the DAS (e.g., accelerometers) (TRB, 2013). As discussed earlier, 30 seconds instantaneous motion data for every safety-critical event (i.e., crash) are provided. The 30-second driving behavior data can be interpreted as driving decisions undertaken immediately before the occurrence of a crash (Figure 6.1). The time-series data contain information about longitudinal and lateral accelerations, speeds, gas pedal and steering wheel position, and wiper status. As such, a total of 2.2 million records of real-world driving is processed and finally around 200,000 (i.e., crash-related motion data) instantaneous motion packets used for calculation of 16 different volatility measures. The detailed event data are finally linked to the event-specific volatility indices for subsequent analyses.

6.4 RESULTS

6.4.1 Descriptive Statistics

Table 1 presents the descriptive statistics of key variables used in this study. In the SHRP2 NDS database, the crash severity is coded into four categories: low-risk tire strike, minor crash, police-reportable crash, and most severe crash. For detailed definitions of the different response outcome categories, see Hankey et al. (2016) (Hankey et al., 2016). As shown in Table 6.1, approximately 40% and 38% of crashes resulted in low-risk tire strike and minor crash respectively. Whereas, 13.3% and 8.8% of crashes were police-reportable crashes and most severe crashes respectively (Table 6.1).

As discussed earlier, the study focuses on analyzing the correlations between crash severity and event-specific driving volatility. Thus, descriptive statistics of aggregate volatility measures calculated using the entire 30-seconds pre-crash motion data are presented (Table 1). Both for volatility measures in longitudinal and lateral direction, and for acceleration and deceleration, the volatility distributions on-average are highly dispersed, as shown by the coefficient of variation values of greater than one (Table 6.1). In addition, the coefficient of variations for all the four volatility measures exhibits significant standard deviations, suggesting considerable variations in volatilities across the different crash events (Table 6.1). An interesting finding is that the volatility in lateral acceleration is greater than the volatility in longitudinal acceleration (Table 6.1). This may reflect the evasive maneuvers (such as abrupt lane change) that drivers' may undertake to avoid the obstacle in front of them once they anticipate a crash.

Compared to aggregate volatility measures, the descriptive statistics for segmented volatility

indices are next presented in Table 6.1. Such a segmentation can separate out the different components of volatility (intentional vs. unintentional) and can shed light on how volatility in time to collision is related to the crash severity (Table 6.1).

Several important insights can be obtained. First, the distributions of segmented volatility measures (estimated based on time to collision) are on-average similar (see mean and standard deviations of bin-wise volatility indices in Table 6.1). It seems that for the sampled crashes, drivers were not just volatile immediately before a crash (i.e., third 10-second bin) but also exhibited erratic or volatile behavior 20-30 seconds before the crash. Based on the discussion presented in earlier sections, this also implies that intentional vs. unintentional volatility is on-average similar in magnitude. *Thus, the question then becomes how intentional volatility may be associated with crash severity outcomes?*

Second, for all the three bin-wise volatility indices, volatility in longitudinal deceleration on-average is greater than volatility in longitudinal acceleration. Given a crash, this suggests that drivers on-average are more volatile during deceleration immediately prior to crash occurrence. This finding is in agreement with the literature (Kamrani et al., 2017, Kim et al., 2007).
Third, similar to the aggregate volatility indices, the volatility in lateral acceleration is greater than the volatility in longitudinal acceleration for the bin-wise volatility measures too. This finding is intuitive and may be an outgrowth of the crash avoidance maneuvers undertaken by the drivers in the lateral direction.

The descriptive statistics of other variables are also presented in Table 6.1. For the sampled crash events, the mean speed is approximately 29 kilometers per hour. In 35.9% of the crashes, drivers did not engage in secondary tasks, whereas drivers were texting in 3.9% of the crashes (Table 6.1). Importantly, durations of secondary tasks are also available. On average, drivers spent 3.58, 0.77, and 0.14 seconds on first, second, and third secondary task respectively. In addition, drivers undertook safe and legal maneuver in 72% of the crashes, safe and illegal maneuver in 2.5% of the crashes, unsafe and illegal maneuver in 14.5% of the crashes, and unsafe but legal maneuvers in 10.4% of the crashes. For a detailed description of maneuver judgement related variables, see (Hankey et al., 2016).

To check for multicollinearity, variance inflation factors (VIF) are checked for all the explanatory variables. A VIF value of less than 10 indicates a lack of problematic multicollinearity. In our case, VIF values for all explanatory factors are less than 3; however, the values are not shown due to space constraints. Finally, the descriptive statistics of a variety of other variables can be interpreted in a similar way (Table 6.1).

Table 6.1 Descriptive Statistics of Key Variables

Category	Variable Name	N	Mean	SD	Min	Max
Dependent Variable: Crash severity	Low-risk tire strike	671	0.404	0.491	0	1
	Minor crash	671	0.376	0.485	0	1
	Police-reportable crash	671	0.133	0.339	0	1
	Most severe	671	0.088	0.283	0	1
Volatility based on entire 30-seconds driving data	Coefficient of variation: longitudinal acceleration	668	1.027	0.518	0.267	4.552
	Coefficient of variation: longitudinal deceleration	668	1.203	0.624	0.075	6.093
	Coefficient of variation: lateral acceleration	665	1.370	0.614	0.345	5.920
	Coefficient of variation: lateral deceleration	666	1.201	0.548	0.156	4.268
Speed	Mean Speed (KPH)	668	28.875	21.851	0	121.17
Volatility based on first 10-seconds bin	Coefficient of variation: longitudinal acceleration	665	0.980	0.453	0.163	4.497
	Coefficient of variation: longitudinal deceleration	666	1.145	0.545	0.074	4.240
	Coefficient of variation: lateral acceleration	661	1.273	0.560	0.347	5.918
	Coefficient of variation: lateral deceleration	659	1.122	0.529	0.160	3.723
Volatility based on second 10-seconds bin	Coefficient of variation: longitudinal acceleration	661	0.959	0.429	0.048	4.046
	Coefficient of variation: longitudinal deceleration	662	1.127	0.591	0.039	6.019
	Coefficient of variation: lateral acceleration	655	1.278	0.566	0.265	4.480
	Coefficient of variation: lateral deceleration	661	1.099	0.521	0.122	3.869
Volatility based on third 10-seconds bin	Coefficient of variation: longitudinal acceleration	643	0.969	0.447	0.263	4.171
	Coefficient of variation: longitudinal deceleration	648	1.118	0.542	0.042	6.008
	Coefficient of variation: lateral acceleration	642	1.278	0.577	0.289	6.566
	Coefficient of variation: lateral deceleration	644	1.096	0.509	0.031	4.821
Passengers	Number of front seat passengers (including driver)	671	1.250	0.434	1	2
	Number of rear seat passengers	671	0.103	0.430	0	3
Travel lanes	Number of through lanes	671	1.213	0.939	0	5
	Number of contiguous travel lanes*	671	3.3	1.58	1	9
Secondary tasks	Holding cell phone	671	0.028	0.166	0	1
	Talking on cell phone: hand-held	671	0.033	0.178	0	1
	Texting on cell phone	671	0.039	0.193	0	1
	No secondary task	671	0.359	0.480	0	1
Duration of secondary tasks	Duration in seconds of first secondary task	671	3.585	4.192	0	24.119
	Duration in seconds of second secondary task	671	0.772	2.031	0	14.221
	Duration in seconds of third secondary task	671	0.145	1.045	0	13.878
Incident maneuvers	Changing lanes	671	0.031	0.174	0	1
	Negotiating a curve	671	0.075	0.263	0	1

Notes: N is sample size; SD is standard deviation; KPH is kilometers per hour

Table 6.1 Descriptive Statistics of Key Variables (Continued)

Category	Variable Name	N	Mean	SD	Min	Max
Maneuver judgement	Maneuver is safe and legal	671	0.723	0.448	0	1
	Maneuver is safe and illegal	671	0.025	0.157	0	1
	Maneuver is unsafe and illegal	671	0.145	0.352	0	1
	Maneuver is unsafe but legal	671	0.104	0.306	0	1
Nature of events	Conflict with a following vehicle	671	0.054	0.225	0	1
	Conflict with lead vehicle	671	0.098	0.298	0	1
Driver Behavior	Exceeded safe speed but not speed limit	671	0.054	0.225	0	1
	Exceeded speed limit	671	0.037	0.190	0	1
	Distracted	671	0.311	0.463	0	1
	Made turn, cut corner on right	671	0.146	0.353	0	1
Roadway factors	Intersection influence: Traffic Signal	671	0.185	0.388	0	1
	Intersection influence: Uncontrolled	671	0.083	0.277	0	1
	Intersection influence: Stop sign	671	0.063	0.242	0	1
	Divided Roadway	671	0.219	0.414	0	1
	Not Divided – 2-way Traffic	671	0.484	0.500	0	1
Traffic factors	Level of Service: A1 (Free flow, no lead traffic)	671	0.562	0.497	0	1
	Level of Service: A2 (Free flow, leading traffic present)	671	0.180	0.385	0	1
	Level of Service: B (Flow with some restrictions)	671	0.180	0.385	0	1
	Level of Service: Stable flow, maneuverability and speed more restricted	671	0.049	0.216	0	1
Driver hand status	Both hands on wheels	671	0.465	0.499	0	1
	Left hand only	671	0.325	0.469	0	1
	Right hand only	671	0.143	0.350	0	1
	None	671	0.039	0.193	0	1
Seat-belt use	Lap/shoulder belt properly worn	671	0.900	0.300	0	1
	None used	671	0.085	0.279	0	1
Light conditions	Darkness, lighted	671	0.204	0.403	0	1
	Darkness, not lighted	671	0.046	0.210	0	1
	Daylight	671	0.708	0.455	0	1
Weather factors	Mist/Light rain	671	0.058	0.234	0	1
	No adverse weather	671	0.860	0.347	0	1
	Heavy rain	671	0.061	0.240	0	1
Locality	Business/industrial	671	0.463	0.499	0	1
	Moderate residential	671	0.204	0.403	0	1
	Open residential	671	0.049	0.216	0	1
	School	671	0.079	0.270	0	1
	Urban	671	0.079	0.270	0	1
Fault status	Other driver (Driver 2) on fault	671	0.088	0.283	0	1
	Subject driver on fault	671	0.854	0.353	0	1

Notes: N is sample size; SD is standard deviation.

6.4.2 Modeling Results

The empirical models focus on analyzing the correlations between crash severity and event-specific driving volatility, after controlling for a wide variety of observed factors (Table 6.1) and unobserved factors. Two different model specifications are presented: 1) the first specification models crash severity as a function of aggregate volatility indices and other factors, and 2) the second specification models crash severity as a function of segmented volatility indices and other factors. For ease of discussion, we will refer to the two specifications as specification 1 and 2.

6.4.2.1 Model Specification 1

For specification 1, Table 6.2 presents the model estimation results for the fixed parameter ordered probit, random parameter ordered probit, and random parameter ordered probit with heterogeneity-in-means. All the models are derived from a systematic process to include most important variables (such as driving volatility related factors and others) on the basis of statistical significance, specification parsimony, and intuition. First, fixed parameter ordered probit models are developed in which the parameter estimates were constrained to be fixed across all the crash events (Table 6.2). As discussed earlier, unobserved heterogeneity and omitted variable bias can be suspected, and in the presence of which precise and unbiased correlations cannot be established. Thus, random parameter ordered probit models are estimated that allowed the parameter estimates to vary across different crash events (Table 6.2). A variable is treated as random when the parameter estimates either exhibited only statistically significant standard deviations or exhibited both statistically significant means and standard deviations (Fountas and Anastasopoulos, 2017). In the earlier case, both likelihood ratio test and AIC statistic are examined to compare the model treating the specific variable (with only statistically significant standard deviation) as random parameter with the model treating the same variable as fixed

Table 6.2 Model Estimation Results for Crash Severity in Naturalistic Driving Environment (First-Specification)

Variable Name	Model 1		Model 2		Model 3	
	β	**t-stat**	**β**	**t-stat**	**β**	**t-stat**
Volatility based on entire 30-seconds driving data						
Coefficient of variation: longitudinal acceleration	0.267	2.75	0.476	4.04	0.391	3.18
Coefficient of variation: longitudinal deceleration	0.956	11.89	1.895	15.30	0.976	3.26
standard deviation	---	---	*0.817*	*14.97*	*0.715*	*14.17*
Coefficient of variation: lateral acceleration	0.207	2.42	0.304	3.13	0.308	3.16
Coefficient of variation: lateral deceleration	0.139	1.53	0.197	1.91	0.245	2.38
Mean Speed (KPH)	0.010	3.87	0.014	4.29	0.009	2.49
Heterogeneity in means						
Coefficient of variation (longitudinal deceleration): *Subject driver on fault*	---	---	---	---	1.102	3.46
Exceeded safe speed but not speed limit: *Unsafe and illegal*	---	---	---	---	1.982	3.43
Business/industrial: *Duration in seconds of first secondary task*	---	---	---	---	0.061	2.4
Divided Roadway: *Darkness but road lighted*	---	---	---	---	-1.002	-3.39
Divided Roadway: *Mean Speed (KPH)*	---	---	---	---	0.020	3.5
Secondary tasks and durations						
Texting on cell phone	0.503	2.20	0.676	2.24	0.716	2.35
Duration in seconds of first secondary task	0.033	2.88	0.059	4.45	0.032	1.93
Duration in seconds of second secondary task	0.047	2.12	0.080	2.99	0.078	2.88
Driver hand status						
Both hands on wheels	-0.147	-1.48	-0.236	-2.04	-0.259	-2.24
Maneuver judgement						
Maneuver is safe and legal	-0.352	-2.71	-0.534	-3.42	-0.551	-3.48
Maneuver is safe and illegal	-0.409	-1.29	-0.599	-1.69	-0.683	-1.88
Driver behavior						
Exceeded safe speed but not speed limit	0.162	0.70	0.434	1.55	*0.116*	*0.38*
standard deviation	---	---	*1.650*	*6.28*	*0.733*	*3.04*
Exceeded speed limit	0.19	0.72	0.434	1.41	*0.433*	*1.4*
standard deviation	---	---	*1.008*	*3.79*	*1.177*	*4.38*
Passengers and through lanes						
Number of rear seat passengers	0.131	1.24	0.271	2.1	0.272	2.11
Number of through lanes	0.129	2.03	0.093	1.24	0.062	0.84
standard deviation	---	---	*0.230*	*6.23*	*0.107*	*3.02*
Roadway factors						
Intersection influence: Traffic Signal	0.135	1.05	0.319	2.2	0.433	2.95
Intersection influence: Uncontrolled	-0.237	-1.40	-0.383	-1.89	-0.211	-1.05
Divided Roadway	-0.053	-0.40	-0.081	-0.51	-0.567	-2.05
standard deviation	---	---	*0.800*	*6.38*	*1.192*	*8.51*

Notes: (Model 1) Fixed Parameter Ordered Probit Model; (Model 2) Random Parameter Ordered Probit Model; (Model 3) Random Parameter Ordered Probit - Heterogeneity-in-Means Model; **β** is parameter estimate; (---) indicates not applicable; KPH is kilometers per hour.

Table 6.2 Model Estimation Results for Crash Severity in Naturalistic Driving Environment (First-Specification) (Continued)

Variable Name	Model 1		Model 2		Model 3	
	β	**t-stat**	**β**	**t-stat**	**β**	**t-stat**
Fault Status						
Other driver (Driver 2) on fault	0.9671	3.73	1.498	4.82	1.4787	4.7
Subject driver on fault	-0.6127	-2.96	-1.221	-4.72	-2.4926	-5.1
Locality						
Business/industrial	-0.1752	-1.79	-0.319	-2.78	-0.5475	-3.55
standard deviation (normally distributed)	---	---	*0.620*	*7.26*	*0.7356*	*8.36*
Summary statistics						
Constant	-1.2502	-3.81	-1.883	-4.69	-0.5268	-0.95
Threshold 1	1.5175	21.99	2.534	16.18	2.5249	16.03
Threshold 2	2.4314	25.75	4.308	18.27	4.2514	18.31
Number of parameters	24		30		35	
Log-likelihood at constant	-814.7498		-814.7498		-814.7498	
Log-likelihood at convergence	-599.119		-580.749		-569.4407	
McFadden R2	0.2646		0.2872		0.301	
AIC	1246.2		1221.5		1208.9	

Notes: (Model 1) Fixed Parameter Ordered Probit Model; (Model 2) Random Parameter Ordered Probit Model; (Model 3) Random Parameter Ordered Probit - Heterogeneity-in-Means Model; **β** is parameter estimate; AIC is Akaike Information Criteria.

parameter (Fountas and Anastasopoulos, 2017). With fixed **β**'s and varying $\boldsymbol{\Upsilon}$, the random parameter model accounts for the systematic variations in the effects of variables across the sample population due to unobserved factors. A total of six variables are found to be normally distributed random parameters suggesting that their effects vary across crash events. These variables are: Coefficient of variation: longitudinal deceleration, exceeded safe speed but not speed limit, exceeded speed limit, number of through lanes, divided Roadway, and business/industrial location (Table 6.2).

To also account for observed heterogeneity (discussed earlier), random parameter models with heterogeneity-in-means are estimated. The results of best-fit random parameter heterogeneity-in-means model are presented in Table 6.2. Importantly, in addition to accounting for unobserved

heterogeneity, the random parameter heterogeneity-in-means approach now also accounts for observed heterogeneity by allowing the means of random parameters to vary as a function of specific observed factors. Five of the six random parameters produced significant heterogeneity in the means as well (see Table 6.2). For the coefficient of variation in longitudinal direction, a subject driver at fault increased the mean making low-risk tire strike or minor crash less likely (Table 6.2). For indicator variable for exceeded safe speed but not speed limit (Table 6.2), crashes where driver undertook unsafe and illegal maneuver also increased the mean making lower order outcomes less likely. Evaluated at the mean duration of the first secondary task and mean speed, crashes occurring in business/industrial location and divided roadways also exhibited higher means suggesting a higher probability of severe crash outcome (Table 6.2). Finally, for divided roadway indicator, crash events occurring at dark but lighted roads exhibited lower means suggesting a higher likelihood of low-risk tire strike crash event.

To justify the use of different models, goodness-of-fit measures such as likelihood ratio test, AIC, and McFadden R^2 are used. After accounting for the degrees of freedom, random parameter ordered probit model outperformed its fixed parameter counterpart (Table 6.2), as reflected in lower AIC value, higher McFadden R^2, and likelihood ratio test favoring the random parameter model (see bottom panel of Table 6.2). Next, accounting for observed heterogeneity further resulted in better fit as shown by the relatively best goodness-of-fit statistics of random parameter heterogeneity-in-mean model[51] (Table 6.2). From an explanatory power standpoint,

[51] As discussed in methodology section and keeping in view the results of Behnood and Mannering (2017a*)* and Seraneeprakam et al. (2017), we tested both for heterogeneity in the means as well as variances of random parameters. The possible heterogeneity in the means and variances of random parameters was tested as a function of different explanatory factors shown in Table 1. While random parameter models with heterogeneity-in-means significantly outperformed the random parameter models with fixed-mean, almost all our attempts to estimate models with both heterogeneity-in-means and variances faced convergence issues. In some rare instances, the models with both heterogeneity-in-means and variances converged but with statistically insignificant variances or poor fit (in terms of log-likelihood at convergence and Akaike Information Criteria) compared to random parameter models with heterogeneity-in-means only. For example, compared to the best-fit random parameter model with

several variables that were statistically insignificant in fixed parameter model became statistically significant in random parameter counterparts. For example, a total of 21 explanatory factors is included, out of which only 11 variables are found to be statistically significant at 95% confidence level in the fixed parameter model. Whereas, 18 out of the 21 explanatory factors exhibited statistically significant means and/or standard deviations each in the random parameter and random parameter heterogeneity-in-means models respectively, with additional statistically significant heterogeneity in means parameter estimates in the later one (see Table 6.2). All of these findings demonstrate the significant potential of heterogeneity based models (both observed and unobserved) in extracting richer insights from the data at hand.

6.4.2.2 Model Specification 2

For specification 2, the results of the fixed parameter ordered probit, random parameter ordered probit, and random parameter ordered probit with heterogeneity-in-means are presented in Table 6.3. The main motivation behind the specification presented in Table 6.3 is to separate out the different components of volatility (intentional vs. unintentional), and which can shed light on how volatility in time to collision is related to crash severity (Table 6.3).

heterogeneity-in-means only (Table 6.2 - log-likelihood at convergence of -569.44, degrees of freedom = 35), the log-likelihood of heterogeneity-in-means and variances model was -569.12 (degrees of freedom = 41) indicating poor fit. As such, we present and discuss the results of random-parameter models with heterogeneity-in-means in this paper. The results of models with heterogeneity-in-means and variances can be obtained from the authors upon request.

Table 6.3 Model Estimation Results for Crash Severity in Naturalistic Driving Environment (Second-Specification)

Variable Name	Model 1		Model 2		Model 3	
	β	t-stat	β	t-stat	β	t-stat
Volatility based on first 10-seconds driving data						
Coefficient of variation: longitudinal acceleration	0.2918	2.12	0.620	3.35	0.690	3.45
Coefficient of variation: longitudinal deceleration	0.6212	4.46	1.597	8.16	1.774	8.21
Coefficient of variation: lateral acceleration	0.1872	1.59	0.473	3.02	0.582	3.45
Coefficient of variation: lateral deceleration	0.2321	2.14	0.502	3.44	0.601	3.8
Volatility based on second 10-seconds driving data						
Coefficient of variation: longitudinal acceleration	---	---	---	---	---	---
Coefficient of variation: longitudinal deceleration	0.2148	1.64	0.288	1.68	0.232	1.25
standard deviation	---	---	*1.431*	*14.8*	*1.661*	*14.42*
Coefficient of variation: lateral acceleration	0.2063	1.69	0.315	1.91	0.391	2.15
Coefficient of variation: lateral deceleration	---	---	---	---	---	---
Volatility based on third 10-seconds driving data						
Coefficient of variation: longitudinal acceleration	0.1368	1.04	0.349	1.99	0.417	2.17
standard deviation	---	---	*0.337*	*5.32*	*0.506*	*7.12*
Coefficient of variation: longitudinal deceleration	0.4275	3.35	1.272	6.94	1.593	7.8
Coefficient of variation: lateral acceleration	-0.3827	-3.12	-0.942	-5.41	-1.154	-6.07
Coefficient of variation: lateral deceleration	0.0747	0.66	0.233	1.56	0.694	3.61
standard deviation	---	---	*0.458*	*7.77*	*0.212*	*3.7*
Mean Speed (KPH)	0.0083	3.29	0.018	5.19	0.021	5.57
Heterogeneity in means						
Coefficient of variation (longitudinal acceleration): *Unsafe and illegal*	---	---	---	---	0.448	1.78
Coefficient of variation (lateral deceleration): *Darkness but road lighted*	---	---	---	---	-1.696	-4.91
Secondary tasks and durations						
Texting on cell phone	0.428	1.76	0.877	2.71	0.968	2.82
Duration in seconds of first secondary task	0.0313	2.58	0.065	3.97	0.073	4.16
Duration in seconds of second secondary task	0.0372	1.58	0.082	2.55	0.086	2.58
Driver hand status						
Both hands on wheels	-0.1552	-1.49	-0.510	-3.58	-0.668	-4.3
standard deviation	---	---	*0.819*	*7.55*	*1.213*	*9.42*
None	0.5014	1.85	1.401	3.53	1.763	4.17
Maneuver judgement						
Maneuver is safe and legal	-0.4480	-3.91	-0.902	-5.69	-0.710	-3.38
Maneuver is safe and illegal	-0.4505	-1.43	-0.762	-1.85	-0.605	-1.32
Through lanes						
Number of through lanes	0.1354	2.31	0.203	2.46	0.205	2.34
standard deviation	---	---	*0.664*	*11.4*	*0.76*	*11.58*
Roadway factors						
Intersection influence: Traffic Signal	0.2244	1.72	0.719	3.99	0.828	4.27

Notes: (Model 1) Fixed Parameter Ordered Probit Model; (Model 2) Random Parameter Ordered Probit Model; (Model 3) Random Parameter Ordered Probit - Heterogeneity-in-Means Model; β is parameter estimate; (---) indicates not applicable; KPH is kilometers per hour.

Table 6.3 Model Estimation Results for Crash Severity in Naturalistic Driving Environment (Second-Specification) (Continued)

Variable Name	Model 1		Model 2		Model 3	
	β	**t-stat**	**β**	**t-stat**	**β**	**t-stat**
Fault Status						
Subject driver on fault	-1.2617	-8.86	-3.239	-12.41	-3.6563	-12.31
Light and Weather						
Darkness, lighted	-0.15332	-1.27	-0.223	-1.38	1.613	3.88
Mist/Light rain	0.6581	3.29	1.176	3.95	1.3906	4.29
standard deviation	---	---	*2.491*	*7.24*	*3.1175*	*7.95*
Summary statistics						
Constant	-0.9518	-3.05	-1.613	-3.82	-2.5741	-5.24
Threshold 1	1.49	21.20	3.583	14.71	4.1188	14.14
Threshold 2	2.3755	25.24	6.082	15.92	7.0168	15.07
Number of parameters	26		32		34	
Log-likelihood at constant	-814.7498		-814.7498		-814.7498	
Log-likelihood at convergence	-566.2787		-552.2533		-546.99	
McFadden R2	0.3049		0.32218		0.3281	
AIC	1184.6		1168.5		1163.1	

Notes: (Model 1) Fixed Parameter Ordered Probit Model; (Model 2) Random Parameter Ordered Probit Model; (Model 3) Random Parameter Ordered Probit - Heterogeneity-in-Means Model**; β** is parameter estimate; AIC is Akaike Information Criteria.

In the random parameter ordered probit model with segmented volatility indices (Table 6.3), a total of six variables are found to be normally distributed random parameters suggesting that their effects vary across crash events. These variables are coefficient of variation: longitudinal deceleration (2nd bin data), coefficient of variation: longitudinal acceleration (3rd bin data), coefficient of variation: lateral deceleration (3rd bin data), both hands on wheels, number of through lanes, and indicator variable for mist/light rain (Table 6.3). To conceptualize the heterogeneity in "direction of effects" of the random parameters, distributional statistics are provided in Table 6.4. Two of the six random parameters also exhibited significant heterogeneity in the means as well (see results of random parameter heterogeneity-in-means model in Table 6.3). For the coefficient of variation in longitudinal direction, unsafe and illegal action increased the mean parameter estimate making high order crash outcome more likely (Table 6.3). Contrarily, for coefficient of variation in lateral deceleration, crashes occurring in darkness but

on lighted roads decreased the mean of random parameter suggesting higher likelihood of low order crash outcome (Table 6.3).

A total of 23 variables are included in the specification presented in Table 6.3, out of which only 10 are statistically significant at 95% confidence level in the fixed-parameter model (Table 6.3). Significant improvements are observed for the random-parameters counterparts; 20 and 22 variables out of 23 are found statistically significant in the random parameter ordered probit and random-parameter ordered probit with heterogeneity-in-means. Regarding goodness of fit, the random parameter model with heterogeneity in means resulted in best fit[52] (see statistics in the lower panel of Table 6.3).

Finally, to help conceptualize the distribution effects of random-held parameters, key distributional statistics are provided in Table 6.4, whereas, Table 6.5 presents the marginal effects of best-fit random parameter heterogeneity-in-means models. It is important to note that for all the models presented in Table 6.2 and 6.3, the statistically significant heterogeneity-in-means underscores the importance of our model specification for the SHRP2 NDS data used. Interesting findings regarding the correlations between driving volatility (particularly regarding segmented volatility), speed, secondary tasks and durations, maneuver judgments, and crash severity outcomes are discussed next.

[52] Again, we tested for the possibility of heterogenous variances in addition to heterogeneous means for random parameters, but we faced convergence issues or if converged, the model exhibited poor fit. For instance, the log-likelihood at convergence of heterogeneity in means and variance model was -551.48 (degrees of freedom = 40) compared to the log-likelihood at convergence of -546.99 (degrees of freedom = 34) for best-fit random parameter model with heterogeneity in means (Table 6.3).

Table 6.4 Distribution Effects of the Random Parameters in Random Parameter Ordered Probit and Random Parameter Ordered Probit with Heterogeneity-in-the-Means.

Variables	Random Parameter Ordered Probit Model		Random Parameter Ordered Probit - Heterogeneity-in-Means Model	
	Below zero	***Above zero***	***Below zero***	***Above zero***
Model specification 1 (Table 2)				
Volatility based on entire 30-seconds driving data				
Coefficient of variation: longitudinal deceleration	1.02%	98.98%	8.61%	91.39%
Driver behavior				
Exceeded safe speed but not speed limit	39.63%	60.37%	43.71%	56.29%
Exceeded speed limit	33.34%	66.66%	35.65%	64.35%
Through lanes				
Number of through lanes	34.30%	65.70%	28.21%	71.79%
Roadway factors				
Divided Roadway	54.03%	45.97%	68.29%	31.71%
Locality				
Business/industrial	69.66%	30.34%	77.16%	22.84%
Model specification 2 (Table 3)				
Volatility based on second 10-seconds driving data				
Coefficient of variation: longitudinal deceleration	42.02%	59.98%	44.45%	55.55%
Volatility based on third 10-seconds driving data				
Coefficient of variation: longitudinal acceleration	15.02%	84.98%	20.49%	79.51%
Coefficient of variation: lateral deceleration	30.55%	69.45%	0.0005%	99.95%
Driver hand status				
Both hands on wheels	73.33%	26.67%	70.19%	29.09%
Through lanes				
Number of through lanes	37.99%	62.01%	39.33%	60.67%
Light and Weather				
Mist/Light rain	31.84%	68.16%	32.78%	67.22%

Table 6.5 Marginal Effects of the Random Parameters Heterogeneity-in-Means Models

Variable Name	Specification 1:Random Parameter Ordered Probit: Heterogeneity-in-Means Model				Specification 2:Random Parameter Ordered Probit: Heterogeneity-in-Means Model			
	1	*2*	*3*	*4*	*1*	*2*	*3*	*4*
Volatility based on entire 30-seconds driving data								
CV: longitudinal acceleration	-0.137	0.136	0.002	1.88E-05	---	---	---	---
CV: longitudinal deceleration	-0.342	0.338	0.004	4.70E-05	---	---	---	---
CV: lateral acceleration	-0.108	0.107	0.001	1.48E-05	---	---	---	---
CV: lateral deceleration	-0.086	0.085	0.001	1.18E-05	---	---	---	---
Volatility based on first 10-seconds driving data								
CV: longitudinal acceleration	---	---	---	---	-0.067	0.053	0.014	1.81E-06
CV: longitudinal deceleration	---	---	---	---	-0.172	0.136	0.033	4.65E-06
CV: lateral acceleration	---	---	---	---	-0.057	0.045	0.012	1.53E-06
CV: lateral deceleration	---	---	---	---	-0.058	0.046	0.012	1.58E-06
Volatility based on second 10-seconds driving data								
CV: longitudinal deceleration	---	---	---	---	-0.023	0.018	0.005	0.00E+00
CV: lateral acceleration	---	---	---	---	-0.038	0.030	0.008	1.02E-06
Volatility based on third 10-seconds driving data								
CV: longitudinal acceleration	---	---	---	---	-0.040	0.032	0.009	1.09E-05
CV: longitudinal deceleration	---	---	---	---	-0.155	0.122	0.033	4.18E-05
CV: lateral acceleration	---	---	---	---	0.112	-0.088	-0.024	-3.02E-06
CV: lateral deceleration	---	---	---	---	-0.067	0.053	0.014	-1.82E-06
Mean Speed (kph)	-0.0031	0.0031	0.0004	0	-0.002	0.002	0.000	0.00E+00

Notes: CV is coefficient of variation; KPH is kilometers per hour; (1) Low-risk tire strike; (2) Minor crash; (3) Police reportable; (4) Most severe; Marginal effects across rows for competing models may not sum up to zero due to rounding.

Table 6.5 Marginal Effects of the Random Parameters Heterogeneity-in-Means Models (Continued)

Variable Name	Specification 1:Random Parameter Ordered Probit: Heterogeneity-in-Means Model				Specification 2:Random Parameter Ordered Probit: Heterogeneity-in-Means Model			
	1	*2*	*3*	*4*	*1*	*2*	*3*	*4*
Secondary tasks & durations								
Texting on cell phone	-0.2754	0.2670	0.008	2.25E-04	-0.045	-0.014	0.059	5.27E-05
Duration in seconds of first secondary task	-0.0114	0.0113	0.0001	1.50E-06	-0.007	0.006	0.001	0.00E+00
Duration in seconds of second secondary task	-0.0273	0.0271	0.0003	3.76E-06	-0.008	0.007	0.002	0.00E+00
Driver hand status								
Both hands on wheels	0.0903	-0.0892	-0.001	-1.28E-05	0.069	-0.055	-0.014	-2.51E-06
None	---	---	---	---	-0.052	-0.175	0.227	1.40E-04
Maneuver judgement								
Maneuver is safe and legal	0.2021	-0.1985	-0.003	-6.02E-05	0.056	-0.033	-0.022	-6.58E-06
Maneuver is safe and illegal	0.1917	-0.1906	-0.001	-1.03E-05	0.092	-0.086	-0.007	0.00E+00
Driver behavior								
Exceeded safe speed but not speed limit	-0.042	0.041	0.0006	7.26E-06	---	---	---	---
Exceeded speed limit	-0.163	0.160	0.003	6.14E-05	---	---	---	---
Passengers & through lanes								
Number of rear seat passengers	-0.095	0.094	0.001	1.31E-05	---	---	---	---
Number of through lanes	-0.022	0.022	0.0003	2.99E-06	-0.020	0.016	0.004	0.00E+00
Roadway factors								
Intersection influence: Traffic Signal	-0.160	0.158	0.002	4.62E-05	-0.054	0.020	0.034	1.57E-05
Intersection influence: Uncontrolled	0.071	-0.070	-0.0007	-6.98E-06	---	---	---	---
Divided Roadway	0.180	-0.178	-0.002	-1.69E-05	---	---	---	---

Notes: (1) Low-risk tire strike; (2) Minor crash; (3) Police reportable; (4) Most severe; Marginal effects across rows for competing models may not sum up to zero due to rounding.

Table 6.5 Marginal Effects of the Random Parameters Heterogeneity-in-Means Models (Continued)

Variable Name	Specification 1:Random Parameter Ordered Probit: Heterogeneity-in-Means Model				Specification 2:Random Parameter Ordered Probit: Heterogeneity-in-Means Model			
	1	*2*	*3*	*4*	*1*	*2*	*3*	*4*
Other driver (Driver 2) on fault	-0.538	0.492	0.045	3.30E-04	---	---	---	---
Subject driver on fault	0.755	-0.571	-0.179	-4.31E-03	0.123	0.633	-0.74	-1.39E-02
Locality								
Business/industrial	0.189	-0.186	-0.002	-3.13E-05	---	---	---	---
Light and Weather								
Darkness, lighted	---	---	---	---	-0.08	-0.03	0.122	2.58E-04
Mist/Light rain	---	---	---	---	-0.05	-0.01	0.124	2.83E-04

Notes: (1) Low-risk tire strike; (2) Minor crash; (3) Police reportable; (4) Most severe; Marginal effects across rows for competing models may not sum up to zero due to rounding.

6.5 DISCUSSION

6.5.1 Safety Effects of Driving Volatility

The results and findings discussed here refer to the random-parameter models with heterogeneity-in-means given its relatively best fit. Overall, a statistically significant positive correlation is found between the four aggregate volatility measures and crash severity outcomes (Table 6.2). This suggests that greater driving volatility (both in longitudinal and lateral) 30-seconds prior to crash occurrence increases the likelihood of police reportable or severe crash events and decreases the likelihood of low-risk tire strike. See the marginal effects in Table 5 which measure the change in resulting probability of each ordinal outcome due to a unit change (or change from "0" to "1" for dummy variables) in the value of the specific independent variable (Quddus et al., 2002). Importantly, compared to the effect of volatility in longitudinal acceleration ($\beta = 0.391$), the effect of volatility in longitudinal deceleration on crash outcome is

significantly greater in magnitude ($\beta = 0.976$). For instance, a unit increase in volatility in longitudinal direction increases the probability of minor crash and police reportable crash by 0.1355 and 0.0015 units respectively. Importantly, a unit increase in volatility in longitudinal deceleration increases the probability of minor crash and police reportable crash by 0.3382 and 0.0039 units respectively (Table 6.5). However, the parameter estimates for coefficient of variation in longitudinal deceleration exhibited heterogeneity with positive effects for 91.39% of crashes and negative effects for 8.61% of crashes (Table 6.4). Also, as discussed in previous section, volatility in longitudinal deceleration also exhibited significant heterogeneity in the means as well, with mean of parameter estimates for volatility in longitudinal deceleration increasing when the subject driver is at-fault (see Table 6.3). Note that, mean speed 30-seconds prior to crash is also included in the specification which intuitively suggests that higher speeds are associated with high order crash outcomes (Table 6.2).

While the above findings regarding volatility and crash outcomes are interesting and new, the findings do not shed light on how volatility in time to collision is related to crash severity. This is important in the sense that if drivers' (intentional) volatility well in advance of a crash (20-30 seconds before the crash) is positively correlated with crash outcomes, control assists and warnings can be given to drivers in real-time to reduce the unsafe and erratic driving behavior and decrease the likelihood of severe crash outcomes. Having said this, the results presented in Table 6.3 offer important insights. The parameter estimates for all (except one) segmented volatility measures shown in Table 6.3 are positive and statistically significant.

The volatility measures calculated based on the first bin of 10-seconds driving data (Figure 6.1)

are found to be fixed parameters, and all positively associated with crash outcomes. This suggests that greater longitudinal and lateral volatility in driving decisions well in advance of a crash (likely to be intentional volatility) increase the likelihood of high order crash outcomes. A unit-increase in volatility in longitudinal acceleration increases the probability of a police-reportable crash by 0.0141 units, compared to a 0.0327-unit increase for a unit increase in volatility in longitudinal deceleration (see marginal effects in Table 6.5). Likewise, a one-unit increase volatility in lateral acceleration and lateral deceleration increases the probability of police-reportable crash by 1.19 and 1.23 percentage points respectively (Table 6.5).

The volatility measures calculated based on second bin of 10-seconds driving data are also positively correlated with crash outcomes. However, the parameter estimate for the coefficient of variation in longitudinal deceleration is normally distributed random parameter with significant heterogeneity (see Table 6.4). Two volatility measures based on the second bin of driving data were statistically insignificant and thus are excluded from the model specifications in Table 6.3. However, note that including these two insignificant variables have no significant effect on the parameter estimates of other volatility measures.

Finally, the volatility indices based on third 10-seconds driving data (i.e., immediately prior to the crash), and likely to be unintentional volatility, are also positively associated with crash outcomes (Table 6.3). In particular, two of the volatility measures (one for longitudinal acceleration and other for lateral deceleration) are found to be random parameters with significant variation in magnitudes of parameter estimates albeit lesser variation in the direction of effects (Table 6.4). Finally, the parameter estimate for volatility in the lateral direction is

negative and statistically significant. This may require further investigation in future studies.

The above volatility related findings have important implications for proactive safety. For instance, instantaneous driving decisions can be monitored in real-time and warnings and alerts can be issued to drivers in case driver's decisions in longitudinal and lateral directions exhibit greater volatility (especially well ahead of the crash). Given that instantaneous driving decisions during deceleration are more volatile and that the effect of volatility in deceleration on crash outcome is more severe, such alerts and warnings can potentially help in improving safety.

6.5.2 Safety Effects of Secondary Task Durations, Driver hand status and Legality of Maneuvers

The results also quantify the association between secondary tasks and crash severity outcomes. For brevity, we only discuss results of random-parameter ordered probit model with heterogeneity-in-means under specification 2 (Table 6.3). Results suggest that drivers texting on cell phones increases the likelihood of police-reportable crash and decreases likelihood of minor crash (Table 6.5). Note that this variable is statistically insignificant in the fixed-parameter counterpart (Table 6.3). Likewise, a one-second increase in durations of first and second secondary task increases the likelihood of a police-reportable crash by 0.149 and 0.176 percentage points (Table 6.5). Again, the variable related to the duration of the second secondary task was not statistically significant in the fixed-parameter counterpart (Table 6.3).

Regarding driver's hand status, results reveal that if both hands are on wheels, the likelihood of low-risk tire strike increases (Table 6.5). However, the parameter is normally distributed random parameter with positive and negative effects for 70.19% and 29.09% of the crash events (Table 6.4). Contrarily, if none of the driver's hand are on wheels, the likelihood of a police-reportable

crash increases by 0.2263 units (Table 6.5). Again, this variable is statistically insignificant in the fixed-parameter counterpart (Table 6.3). From an empirical perspective, these findings reveal the importance of incorporating heterogeneity in crash modeling. Finally, if a driver's maneuver is safe and legal, the likelihood of low-order injury outcomes intuitively increases.

6.5.3 Safety Effects of Other Factors

Several other factors such as the number of through lanes, signalized intersections, crash events in darkness but on lighted roads, and crashes in mist or light rain are positively associated with crash severity outcomes. However, the association between indicator variable for mist/light rain exhibited significant heterogeneity in the direction of effects across crash events; with positive parameter estimates for 67.22% of crashes and negative for the rest (Table 6.4). Another interesting finding relates to the fault-status of the driver. If the subject driver is at-fault, the likelihood of high order crash outcomes (for the subject driver) decreases. While the fault-status of the other driver (driver 2) is not statistically significant in specification 2 (Table 6.3), the results of specification 1 show that if the other driver is at-fault, the likelihood of receiving high order crash outcomes (for subject driver) increases (Table 6.2). Although this finding is in line with past research that shows that not-at-fault drivers tend to be more severely injured (Russo et al., 2014), this requires further investigation in future by simultaneously analyzing the crash outcomes of not-at-fault and at-fault driver in the context of the current study.

6.6 LIMITATIONS/FUTURE WORK

The present study is based on a sample of ~ 9800 events (baseline, near-crash, and crash events), out of which 671 were identified as crash events. However, the SHRP2 NDS Event Detail Table (EDT) currently has 36,816 records, out of which 1,469 are crash events

(https://insight.shrp2nds.us/data/index). The authors used a subset of EDT due to lack of access to the entire SHRP2 NDS database. With regard to future work, there are several pathways for extending the proposed framework. As more data become publicly available, the methodology presented in this study can be expanded. Another extension of the research can be to apply the proposed methodology to specific roadway types. Regarding the methodological framework, this study used ordinal framework given the ordinal nature of the response outcome. In future, it will be interesting to compare ordered and unordered discrete choice models for exploring associations between driving volatility and crash severity (Zhao and Khattak, 2015).

6.7 CONCLUSIONS

Driving volatility captures the extent of variations in driving, especially hard accelerations/braking and jerky maneuvers. It can be regarded as a measure of driving practice for characterizing instantaneous driving decisions, and importantly extreme driving behaviors. The main objective of this study was to investigate correlations between driving volatility and injury severity. To achieve this, a tight quasi-experimental study design is adopted to quantify real-world driving volatility immediately prior to the involvement in a crash, and how it relates to injury outcomes sustained by drivers. A unique Naturalistic Driving database of drivers involved in crash events is used. The raw microscopic driving data are complex and not informative to drivers. Thus, we propose a rigorous data analytic methodology to extract critical information embedded in real-world driving data. For all the crash events, large-scale microscopic instantaneous driving data immediately prior to involvement in crashes are analyzed, and volatility indices created using different driving performance measures. Driving volatility before involvement in the crash events may contain separate components, i.e.,

intentional vs. unintentional volatility. Thus, a total of 16 volatility indices are proposed, i.e., four aggregate volatility indices based on entire 30-seconds pre-crash data and 12 segmented volatility indices based on bin-wise data. For the empirical analysis, the volatility indices are then linked with individual crash events including data on crash severity, event-specific variables such as drivers' pre-crash maneuvers and behaviors, traffic flow factors, secondary tasks and durations, roadway factors, and fault status. Separate crash severity outcome models are presented using aggregated and bin-wise volatility measures.

Overall, statistically significant positive correlations are found between the four aggregate volatility measures and crash severity outcomes. This suggests that greater driving volatility (both in longitudinal and lateral direction) 30-seconds prior to crash occurrence increases the likelihood of police reportable or severe crash events, and decreases the likelihood of low-risk tire strike. Importantly, compared to the effect of volatility in longitudinal acceleration on crash outcomes, the effect of volatility in longitudinal deceleration is significantly greater in magnitude. Compared to the aggregate volatility measures, the results obtained from models with segmented volatility indices offer important insights. The parameter estimates for all (except one) segmented volatility measures are positive and statistically significant. In particular, an increase in driving volatility, both longitudinal and lateral, well in advance of a crash (likely to be intentional volatility) increase the likelihood of severe crash outcomes. Likewise, the longitudinal volatility indices immediately before the crash (i.e., 3rd bin of 10-seconds driving data) are also positively correlated with crash outcomes. Other interesting findings are discussed in detail. The above volatility related findings have important implications for proactive safety. For instance, instantaneous driving decisions can be monitored in real-time, and warnings and

alerts can be issued to drivers in case driver's decisions in longitudinal and lateral directions exhibit greater volatility. Given that instantaneous driving decisions during deceleration are more volatile, and that the effect of volatility in deceleration on the crash outcome is more severe, such alerts and warnings can potentially help in improving safety.

From an empirical perspective, the study contributes by presenting fixed- and random-parameter (with heterogeneity-in-means) discrete choice ordered models that account for both observed and unobserved heterogeneity. Unlike commonly-used random parameters models that typically assume the same mean for each random parameter, the models also account for possible (observed) heterogeneity in the means of the random parameters which vary as a function of several observed factors. To justify the use of different models, goodness-of-fit measures such as likelihood ratio test, AIC, and McFadden R^2 are used. After accounting for degrees of freedom, random-parameter ordered probit model outperformed its fixed parameter counterpart. Next, accounting for observed heterogeneity further resulted in a better fit and was reflected in the relatively best goodness-of-fit statistics of random parameter heterogeneity-in-mean model. From an explanatory power standpoint, several variables that were statistically insignificant in fixed parameter model became statistically significant in random parameter counterparts. A total of 23 variables is included in the final specification, out of which only 10 variables are statistically significant in the fixed-parameter model, whereas 22 variables are statistically significant in the random parameter ordered probit model with heterogeneity-in-means.

6.8 ACKNOWLEDGEMENT

The data for this study were provided through a collaborative effort between Virginia Tech Transportation Institute, the U.S. Federal Highway Administration (FHWA), and Oak Ridge National Laboratory (ORNL). The timely assistance and guidance of the ORNL team about data elements is highly appreciated. The authors would also like to recognize the contribution of Alexandra Boggs in proof-reading the manuscript. This paper is based upon work supported by the US National Science Foundation under grant No. 1538139. Additional support was provided by the US Department of Transportation through the Collaborative Sciences Center for Road Safety, a consortium led by The University of North Carolina at Chapel Hill in partnership with The University of Tennessee. Any opinions, findings, and conclusions or recommendations expressed in this paper are those of the authors and do not necessarily reflect the views of the sponsors.

CHAPTER 7 CONCLUSIONS AND IMPLICATIONS

This dissertation addressed the grand challenge of harnessing big data generated by connected vehicles and naturalistic driving systems to answer new questions using new statistical techniques. Driven by big data for science and engineering (S&E), we are at a cusp on a major transformation in transportation, where the future at the human-technology frontier needs to be researched. Among other factors, driving behavior is a critical and most unpredictable component of the surface transportation system, where it significantly contributes to as much as 90 percent of traffic crashes, significant energy use, and emissions. Understanding driver decisions is the key to implementing transportation improvement strategies. Also, the potential to improving safety and energy use through automation and connectivity of the transportation system is enormous. Rapid technological developments, ranging from vehicle-to-vehicle and vehicle-to-infrastructure communications, WI-FI, to continuous video and radar surveillance, have enabled collection of countless terabytes of spatiotemporal data about vehicle and human movement. Thus, in an attempt to prospect opportunities for engineering intelligent and proactive transportation systems, the dissertation focused on assembling and utilizing a new comprehensive multidimensional transportation database by combining connected vehicles data, naturalistic driving sensor and telematics data, and traditional transportation data.

Conceptually, the dissertation revolves around the key concept of "driving volatility" which describes the extent of variations in real-world microscopic driving decisions. The key idea was to understand (and where possible reduce) "driving volatility" in instantaneous driving decisions and increase driving and locational stability. The key motivation behind analyzing driving

volatility was to help predict what drivers will do in the short term, and which has significant implications for safety, mobility, and energy use.

Consequently, the dissertation developed a new concept of "driving volatility matrix" which takes a systems approach to operationalizing driving volatility at different levels. In particular, through an integrated research program, the focus was to conceptualize and model the extent of variations in real-world driving at several hierarchies of the real-world traffic ecosystem, i.e., 1) trip-based volatility, 2) location-based volatility, 3) event-based volatility, and 4) driver-based volatility, thus termed as driving volatility matrix. The concept of driving volatility matrix provides a systems framework for characterizing the health of three fundamental elements of a transportation system: health of driver, environment, and the vehicle.

To conceptualize volatility at a trip-level, a study was conducted to gain a fundamental understanding of instantaneous driving decisions, needed for hazard anticipation and notification systems, and distinguishing normal from anomalous driving. In particular, driving task was divided into distinct yet unobserved regimes. Thus, the research issue was to characterize and quantify these regimes in typical driving cycles and the associated volatility of each regime, explore when the regimes change and the key correlates associated with each regime. To answer these questions, emerging Basic Safety Message (BSM) data from the Safety Pilot Model Deployment in Ann Arbor, Michigan, were used to develop two- and three-regime Dynamic Markov switching models for several trips undertaken on various roadway types. The results indicated that acceleration and deceleration are two distinct regimes, and as compared to acceleration, drivers decelerate at higher rates, and braking is significantly more volatile than

acceleration. Owing to the important links between microscopic driving decisions and surrounding traffic states, differential correlations of the two regimes with instantaneous driving contexts were quantified. Furthermore, to reflect the reality and complexity of real-world transportation systems, a more generic three-regime model specification was formulated. The results revealed high-rate acceleration, high-rate deceleration, and cruise/constant as the three distinct regimes that characterize a typical driving cycle. Moreover, given in a high-rate regime, drivers' on-average tended to decelerate at a higher rate than their rate of acceleration. Importantly, compared to cruise/constant regime, drivers' instantaneous driving decisions were more volatile both in "high-rate" acceleration as well as "high-rate" deceleration regime. The study contributed to analyzing volatility in short-term driving decisions, and how changes in driving regimes can be mapped to a combination of local traffic states surrounding the vehicle. The new results obtained from this study have important implications. First, the study presented an appropriate analytical framework that can help in understanding instantaneous driving decisions and key correlates. Driving decisions primarily depend on surrounding traffic states. An in-depth analysis of such factors is important for understanding driver specific behavior and for developing customized driver based safety applications. For instance, researchers and practitioners can implement the proposed methodology to connected vehicle data generated by specific driver for several trips. For a specific driver, quantification of the associations between instantaneous driving decisions and driving contexts can help us understand driver-specific instantaneous volatility, and to develop hazard anticipation and notification systems if a driver is observed to deviate from his/her normal driving patterns. Furthermore, given a specific driver and keeping in view his/her historical instantaneous driving decisions with respect to local traffic

states, alerts and warnings can be provided well in advance to driver specifically if he/she is decelerating.

Continuing over the analysis of microscopic driving behaviors in connected vehicles environment, another two studies were conducted to extend the concept of "trip-based volatility" to specific locations, thus termed as "location-based volatility." As a proactive safety measure and a leading indicator of safety, location-based volatility (LBV) quantifies variability in instantaneous driving decisions at intersections. LBV represents the driving performance of connected vehicle drivers traveling through a specific intersection. By using big data generated by connected and automated vehicles, *the key goal was to identify roadway locations (such as intersections) where crashes have not yet happened but perhaps are waiting to happen.* Traditionally, evaluation of intersection safety has been largely reactive, based on historical crash frequency data. However, the emerging data from CAVs can complement historical data and help in proactively identify intersections which have high levels of variability in instantaneous driving behaviors prior to the occurrence of crashes. Based on data from Safety Pilot Model Deployment in Ann Arbor, Michigan, the second study developed a unique database that integrated intersection crash and inventory data with more than 65 million real-world Basic Safety Messages logged by 3,000 connected vehicles, providing a more complete picture of operations and safety performance of intersections. As such, by using coefficient of variation of acceleration/deceleration as a standardized measure of relative dispersion, LBVs are calculated for 116 intersections in Ann Arbor. To quantify relationships between intersection-specific volatilities and crash frequencies, rigorous heterogeneity-based count data models were estimated. While controlling for exposure related and other unobserved factors, the results

provide evidence of statistically significant (5% level) positive association between intersection-specific volatility and crash frequencies for signalized intersections.

Real-world driving decisions and performance is a complex task and as such it seems natural and imperative to explore other (vehicle kinematics based and statistical based) measures of capturing driving volatility in large-scale connected vehicles data. Along the lines of the new concept of location-based volatility, a third study was conducted to extend the data analytic framework for quantification of location-based volatility. From a conceptual stand-point, speed, acceleration/deceleration, and vehicular jerk based volatility measures were used. In particular, eight different volatility indices were introduced based on coefficient of variation, time-series volatility, dynamic speed varying thresholds, and mean absolute deviance based measures. The big data analytic methodology accounted for volatilities at trip level nested within location (intersection) level in a hierarchical fashion. To implement the methodology, more than 230 million real-world Basic Safety Messages by connected vehicles were analyzed for a total of 116 intersections, i.e., a total of 4832.2 hours of driving data were analyzed where an average of 28376.8 vehicle passings per intersection occurred. As a proof-of-concept, descriptive analysis was performed to spot differences between driving volatility at signalized and un-signalized intersections. Then, in-depth statistical analysis is conducted separately for all intersections (signalized and un-signalized) and signalized intersections only. Importantly, not all factors that may influence crash frequency can be observed in the data. If unobserved factors could be included in a model, then correlations between driving volatility and crash frequency can change, e.g., the relationship can become statistically insignificant. Given the important methodological concerns of unobserved heterogeneity and potential omitted variable bias, hierarchical fixed- and

random-parameter Poisson and Poisson log-normal models were developed. Full Bayesian estimation via Markov Chain Monte Carlo (MCMC) based Gibbs sampling is performed, providing more efficient results. For all intersections, after controlling for traffic exposure, geometrics, and unobserved factors, a one-percent increase in intersection-level volatility calculated through two standard deviations threshold for acceleration/deceleration, passing level volatility captured through coefficient of variation of speed, and mean absolute deviance of vehicular jerk results in a 1.25%, 0.25%, and 0.35% increase in crash frequencies respectively. However, the relationships between intersection-specific volatility and crash frequencies are different for signalized intersections. Several of the exogenous factors are found to be normally distributed random parameters, suggesting that the effects of such variables vary across different intersections. Overall, the new results from the two "location-based volatility" related studies have important real-world safety implications. For many intersections, it is found that observed crash frequency is lower but perhaps crashes are waiting to happen as instantaneous driving decisions are consistently more volatile at such intersections. For proactive intersection safety management, such information is crucial as it can highlight intersection locations where behaviors of drivers may differ, compared to their behaviors at other intersection locations. Thus, safety managers may consider proactive countermeasures at such locations, e.g., providing proactive alerts and warnings to drivers through connected vehicle roadside equipment (RSE).

The sequence of instantaneous driving decisions and its variations prior to involvement in safety critical events can be a leading indicator of safety. Thus, another study was conducted to extend the concept of driving volatility to specific normal and safety-critical events, thus named "event-based volatility." In particular, the research issue included characterization of volatility in

instantaneous driving decisions in longitudinal and lateral directions, and how it varies across drivers involved in normal driving, crash, and/or near-crash events. Using a unique real-world naturalistic driving database from the 2nd Strategic Highway Research Program (SHRP), a test set of 9,593 driving events featuring 2.2 million temporal samples of real-world driving were analyzed. By using information related to longitudinal and lateral accelerations and vehicular jerk, 24 different aggregate and segmented measures of driving volatility were proposed that captures variations in extreme instantaneous driving decisions. In doing so, careful attention was given to the issue of intentional vs. unintentional volatility. The volatility indices are then linked with safety critical events, crash propensity, and other event specific explanatory variables. Owing to the presence of unobserved heterogeneity and omitted variable bias, fixed- and random-parameter discrete choice models are developed that relate crash propensity to driving volatility and other factors. Importantly, statistically significant evidence was found that driver volatilities in near-crash and crash events are significantly greater than volatility in normal driving events. After controlling for traffic, roadway, and unobserved factors, the results suggest that greater intentional volatility increases the likelihood of both crash and near-crash events. Importantly, intentional volatility in longitudinal negative jerk (braking) has more negative consequences than intentional volatility in positive vehicular jerk. The study also found that compared to acceleration/deceleration, vehicular jerk can better characterize the volatility in microscopic instantaneous driving decisions prior to involvement in safety critical events. Finally, the magnitudes of correlations exhibit significant heterogeneity, and that accounting for the heterogeneous effects in the modeling framework can provide more reliable and accurate results. The study demonstrated the value of quasi-experimental study design and big data analytics for understanding extreme driving behaviors in safe vs. unsafe driving outcomes.

While the variations of microscopic driving decisions can influence crash risk (or crash propensity), it can also influence the injury outcomes given a crash. Thus, a fifth study was conducted for characterizing volatility in instantaneous driving decisions in longitudinal and lateral direction and to seek an understanding of how driving volatility relates to crash severity. As driving volatility prior to crash involvement can have different components, an in-depth analysis is conducted using the aggregate as well as segmented (based on time to collision) real-world driving data. To account for the issues of observed and unobserved heterogeneity, fixed and random parameter ordered models with heterogeneity in parameter means were estimated. The empirical results offered important insights regarding how driving volatility in time to collision may be related to crash severity outcomes. Overall, statistically significant positive correlations are found between the aggregate (as well as segmented) volatility measures and crash severity outcomes. The findings suggest that greater driving volatility (both in longitudinal and lateral direction) prior to crash occurrence increases the likelihood of police reportable or severe crash events. Importantly, compared to the effect of volatility in longitudinal acceleration on crash outcomes, the effect of volatility in longitudinal deceleration is significantly greater in magnitude. Methodologically, the random parameter models with heterogeneity-in-means significantly outperformed both the fixed parameter and random parameter counterparts; underscoring the importance of accounting for both observed and unobserved heterogeneity. The above event-based volatility related findings have important implications for proactive safety. For instance, instantaneous driving decisions can be monitored in real-time and warnings and alerts can be issued to drivers in case driver's decisions in longitudinal and lateral directions exhibit greater volatility (especially well ahead of the crash). Given that instantaneous driving

decisions during deceleration are more volatile and that the effect of volatility in deceleration on crash outcome is more severe, such alerts and warnings can potentially help in improving safety.

Overall, by studying driving volatility from different lenses, the dissertation contributed to the scientific analysis of real-world connected vehicles data, and to generate actionable knowledge relevant to the design of smart and intelligent transportation systems. Gaining a better understanding of microscopic driving decisions and the variations therein in real-world environments is fundamental to the design of personalized and intelligent driver feedback systems. By altering volatility in real-world microscopic driving decisions, vehicle kinematics, and roadway environment, the outcomes help improve transportation safety by proactively predicting crash occurrence and its severity given a crash.

7.1 IMPLICATIONS OF DRIVING VOLATILITY MATRIX FOR AUTOMATION IN A MIXED AND NON-MIXED TRAFFIC STATE

Note that the concept of "driving volatility matrix" presented in this dissertation is operationalized at a level 0 or level 1-2 automation. That is, keeping in view the existing transportation landscape, the driving volatility matrix provides full consideration to the fact that human driver is in control of the vehicle (level 0-2). Thus, a natural extension of the present work would be to explore the implications of driving volatility matrix for higher levels of automation. For instance, how will the driving volatility matrix evolve and how relevant it will be in a mixed traffic comprising connected and automated vehicles (CAVs) as well as conventional vehicles. As technology evolves, before getting to full automation, we will go

through a mixed traffic with conventional (human-driven) as well as automated vehicles. At a next level, the relevant question becomes how relevant driving volatility matrix will be in a completely non-mixed traffic of automated vehicles, including no conventional vehicles. To shed light on these questions, Figure 7.1 provides a general taxonomy of the relevance/value of driving volatility matrix as level of vehicle autonomy increases in a transportation network. Figure 7.1 also shows the expected relevance of driving volatility matrix in a mixed (combination of automated and conventional vehicles) as well as non-mixed (either automated vehicles only or conventional vehicles only) traffic system (Figure 7.1). In particular, moving across to the right in Figure 7.1 indicates the time horizon. For example, for a mixed traffic state, and at specific point in the time horizon (such as Level 2 automation), the mixed traffic state would include predominantly Level 2 automated vehicles as well as level 0 and 1 automation. In total, in a mixed traffic system, at any specific point in the time horizon, the predominant share of vehicles will be the corresponding level of automation and presence of small proportion of other vehicles corresponding to levels of automation below the reference level of automation.

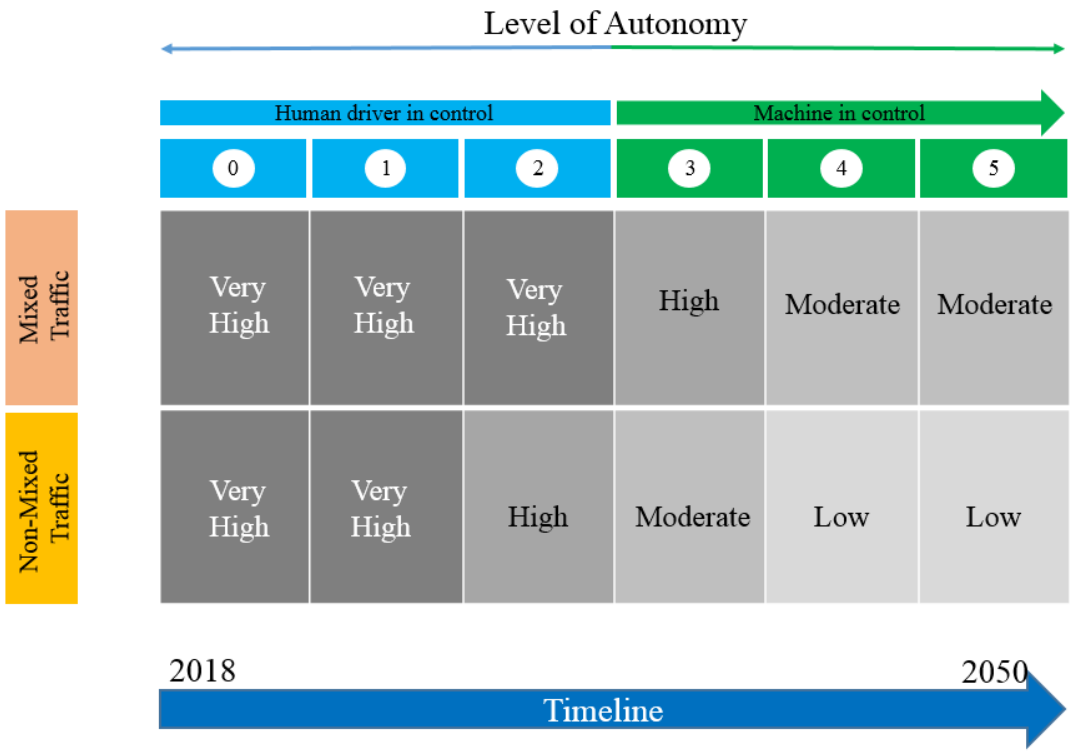

Figure 7.1 General taxonomy of relevance/value of driving volatility matrix as a function of level of vehicle autonomy in a transportation network
(Notes: Level 0 automation → no automation, Level 1 → driver assistance, Level 2 → partial automation, Level 3 → conditional automation, Level 4 → high automation, Level 5 → full automation. Mixed traffic indicates presence of both automated as well as conventional vehicles in traffic stream; Non-mixed traffic indicates presence of either automated vehicles only or conventional vehicles only in the traffic stream.)

Keeping in view the existing landscape of transportation systems, i.e., level 0 or level 1 automation (mixed traffic or non-mixed traffic), the concept of driving volatility matrix is of very high relevance as the human driver is in control of the vehicle operations (Figure 7.1). Moving to level 2 automation in a mixed traffic, the concept of driving volatility is still expected to be of "very high" value as the mixed traffic would also include vehicles with level 0 or level 1 automation (Figure 7.1). If the traffic system comprises of entirely level 2 automated vehicles (non-mixed traffic), the relevance of driving volatility would be high as driver is still in control in level 2 automation (Figure 7.1). Likewise, at levels of autonomy where the machine is in

control (i.e., level 3) in a mixed traffic state, driving volatility will still be of high relevance as the system would also comprise of vehicles where human is in control (see Figure 7.1)

As we move further in the time horizon where the level of vehicle autonomy increases in a mixed traffic state (such as level 4 and level 5 automation), the relevance of driver related elements in the volatility matrix will likely be reduced. However, specific elements of the driving volatility matrix will still be relevant (Figure 7.1). For example, in a mixed traffic comprising of Level 4 or 5 automated vehicles and conventional vehicles, the driving volatility will still be relevant for the conventional vehicles. Importantly, the volatility information of conventional vehicles can be shared with CAVs in order for CAVs to anticipate what a human-driven vehicle may do in short term, or for CAVs to behave in a more human manner. In this case, the volatility in surrounding traffic states (such as level of crowdedness, number of objects (presumably conventional vehicles) surrounding the CAV, and distances to the nearest objects) can be quantified in real-time and such information can be shared with the CAVs in which case the maneuvers and decisions by the highly automated vehicles will be well-informed in a highly volatile traffic environment. This is important because even if automated vehicles are doing everything they are supposed to do (presumably correct actions), the drivers of surrounding vehicles are still naturally error-prone humans, and errors of whom can lead to crashes involving automated vehicles. Keeping in view the greater uncertainty over the performance of a mixed CAV-conventional traffic system, the information generated by driving volatility matrix can be of significant value even at higher levels of automation in mixed traffic (Figure 7.1).

Finally, certain components of the driving volatility matrix will also be relevant to the CAVs in a non-mixed traffic, such as level 4 or level 5 automated vehicles running in a completely non-mixed traffic (such as fully dedicated lanes). For instance, while the CAV itself will be machine driven, the vehicle condition and/or state of environment (and the volatility therein) can majorly influence the operation of CAVs. Along these lines, there will still be a need to characterize volatility in environmental factors such as weather, rain, road terrain, and geometric features (to name a few), and all of which can affect the performance of CAVs. From a safety outcome perspective, another important concern would be how much volatility may exist in our forecasts of occurrence of unsafe outcomes, as a leading fully automated vehicle getting into a crash can affect the following vehicles as well. Finally, from an automated vehicle condition standpoint, characterization of variations and volatility in the probability of a sensor failure (as one example) can also be important and relevant. In conclusion, at highest level of automation in a non-mixed traffic state, and which would be the ultimate frontier of the current revolution of CAVs, the concept of driving volatility would still be of relevance primarily by helping us characterizing the volatility and variations in the environmental or external (to the automated vehicles) factors that can influence the performance of CAVs in significant ways.

LIST OF REFERENCES

Aarts, L. & Van Schagen, I. 2006. Driving speed and the risk of road crashes: A review. *Accident Analysis & Prevention,* 38**,** 215-224.

Abdel-Aty, M. 2003. Analysis of driver injury severity levels at multiple locations using ordered probit models. *Journal of Safety Research,* 34(5)**,** 597-603.

Abdel-Aty, M. & Haleem, K. 2011. Analyzing angle crashes at unsignalized intersections using machine learning techniques. *Accident Analysis & Prevention,* 43**,** 461-470.

Abdel-Aty, M. & Keller, J. 2005. Exploring the overall and specific crash severity levels at signalized intersections. *Accident Analysis & Prevention,* 37**,** 417-425.

Abe, G. & Richardson, J. 2006. Alarm timing, trust and driver expectation for forward collision warning systems. *Applied ergonomics,* 37**,** 577-586.

Åberg, L., Larsen, L., Glad, A. & Beilinsson, L. 1997. Observed vehicle speed and drivers' perceived speed of others. *Applied Psychology,* 46**,** 287-302.

Ahmed, A., Saeed, T. U., Murillo-Hoyos, J. & Labi, S. 2017. Pavement Repair Marginal Costs: Accounting for Heterogeneity Using Random-Parameters Regression. *Journal of Infrastructure Systems***,** 04017012.

Alarifi, S. A., Abdel-Aty, M. A., Lee, J. & Park, J. 2017. Crash modeling for intersections and segments along corridors: A Bayesian multilevel joint model with random parameters. *Analytic Methods in Accident Research,* 16**,** 48-59.

Anastasopoulos, P. C. & Mannering, F. L. 2009. A note on modeling vehicle accident frequencies with random-parameters count models. *Accident Analysis and Prevention,* 41(1)**,** 153-159.

Anastasopoulos, P. C., Mannering, F. L., Shankar, V. N. & Haddock, J. E. 2012. A study of factors affecting highway accident rates using the random-parameters tobit model. *Accident Analysis and Prevention,* 45**,** 628-633.

Banerjee, S., Carlin, B. P. & Gelfand, A. E. 2014. *Hierarchical modeling and analysis for spatial data*, Crc Press.

Bao, S. & Boyle, L. 2008. Driver performance at two-way stop-controlled intersections on divided highways. *Transportation Research Record: Journal of the Transportation Research Board***,** 26-32.

Barua, S., El-Basyouny, K. & Islam, M. T. 2014. A full Bayesian multivariate count data model of collision severity with spatial correlation. *Analytic Methods in Accident Research,* 3**,** 28-43.

Barua, S., El-Basyouny, K. & Islam, M. T. 2016. Multivariate random parameters collision count data models with spatial heterogeneity. *Analytic methods in accident research,* 9**,** 1-15.

Behnood, A. & Mannering, F. 2017a. Determinants of bicyclist injury severities in bicycle-vehicle crashes: A random parameters approach with heterogeneity in means and variances. *Analytic Methods in Accident Research,* 16**,** 35-47.

Behnood, A. & Mannering, F. 2017b. The effect of passengers on driver-injury severities in single-vehicle crashes: A random parameters heterogeneity-in-means approach. *Analytic methods in accident research,* 14**,** 41-53.

Behnood, A. & Mannering, F. L. 2015. The temporal stability of factors affecting driver-injury severities in single-vehicle crashes: some empirical evidence. *Analytic Methods in Accident Research,* 8**,** 7-32.

Bergenhem, C., Shladover, S., Coelingh, E., Englund, C. & Tsugawa, S. Overview of platooning systems. Proceedings of the 19th ITS World Congress, Oct 22-26, Vienna, Austria (2012), 2012.

Bhat, C. R. 2003. Simulation estimation of mixed discrete choice models using randomized and scrambled Halton sequences. *Transportation Research Part B: Methodological,* 37**,** 837-855.

Bhat, C. R., Astroza, S. & Lavieri, P. S. 2017. A new spatial and flexible multivariate random-coefficients model for the analysis of pedestrian injury counts by severity level. *Analytic Methods in Accident Research,* 16**,** 1-22.

Black, W. R. & Thomas, I. 1998. Accidents on Belgium's motorways: a network autocorrelation analysis. *Journal of Transport Geography,* 6**,** 23-31.

Bozdogan, H. 1987. Model selection and Akaike's information criterion (AIC): The general theory and its analytical extensions. *Psychometrika,* 52**,** 345-370.

Campbell, K. L. 2012. The SHRP 2 naturalistic driving study: Addressing driver performance and behavior in traffic safety. *TR News*.

Cheng, L., Henty, B. E., Stancil, D. D., Bai, F. & Mudalige, P. 2007. Mobile vehicle-to-vehicle narrow-band channel measurement and characterization of the 5.9 GHz dedicated short range communication (DSRC) frequency band. *IEEE Journal on Selected Areas in Communications,* 25**,** 1501-1516.

Chin, H. C. & Quddus, M. A. 2003. Applying the random effect negative binomial model to examine traffic accident occurrence at signalized intersections. *Accident Analysis & Prevention,* 35**,** 253-259.

Chou, C.-M., Li, C.-Y., Chien, W.-M. & Lan, K.-c. A feasibility study on vehicle-to-infrastructure communication: WiFi vs. WiMAX. 2009 Tenth International Conference on Mobile Data Management: Systems, Services and Middleware, 2009. IEEE, 397-398.

Choudhury, C. F. 2007. *Modeling driving decisions with latent plans (Doctoral dissertation, Massachusetts Institute of Technology).*

Choudhury, C. F., Ben-Akiva, M. & Abou-Zeid, M. 2010. Dynamic latent plan models. *Journal of Choice Modelling,* 3**,** 50-70.

Chrysler, S. T., Cooper, J. M. & Marshall, D. C. 2015. Cost of Warning of Unseen Threats: Unintended Consequences of Connected Vehicle Alerts. *Transportation Research Record: Journal of the Transportation Research Board***,** 79-85.

Dempster, A. P., Laird, N. M. & Rubin, D. B. 1977. Maximum likelihood from incomplete data via the EM algorithm. *Journal of the royal statistical society. Series B (methodological)***,** 1-38.

Doecke, S., Grant, A. & Anderson, R. W. 2015. The real-world safety potential of connected vehicle technology. *Traffic injury prevention,* 16**,** S31-S35.

Dong, C., Clarke, D. B., Nambisan, S. S. & Huang, B. 2016. Analyzing injury crashes using random-parameter bivariate regression models. *Transportmetrica A: Transport Science,* 12**,** 794-810.

Dong, C., Clarke, D. B., Yan, X., Khattak, A. & Huang, B. 2014. Multivariate random-parameters zero-inflated negative binomial regression model: An application to estimate crash frequencies at intersections. *Accident Analysis & Prevention,* 70**,** 320-329.

Drukker, D. M., Peng, H., Prucha, I. R. & Raciborski, R. 2013. Creating and managing spatial-weighting matrices with the spmat command. *Stata Journal,* 13**,** 242-286.

Du, L. & Dao, H. 2015. Information dissemination delay in vehicle-to-vehicle communication networks in a traffic stream. *Intelligent Transportation Systems, IEEE Transactions on,* 16**,** 66-80.

Duncan, C., Khattak, A. & Council, F. 1998. Applying the ordered probit model to injury severity in truck-passenger car rear-end collisions. *Transportation Research Record: Journal of the Transportation Research Board***,** 63-71.

El-Basyouny, K. & Sayed, T. 2009a. Accident prediction models with random corridor parameters. *Accident Analysis & Prevention,* 41**,** 1118-1123.

El-Basyouny, K. & Sayed, T. 2009b. Collision prediction models using multivariate Poisson-lognormal regression. *Accident Analysis & Prevention,* 41**,** 820-828.

El-Basyouny, K. & Sayed, T. 2009c. Urban arterial accident prediction models with spatial effects. *Transportation Research Record: Journal of the Transportation Research Board***,** 27-33.

El-Basyouny, K. & Sayed, T. 2011. A full Bayes multivariate intervention model with random parameters among matched pairs for before–after safety evaluation. *Accident Analysis & Prevention,* 43**,** 87-94.

Eluru, N., Bagheri, M., Miranda-Moreno, L. F. & Fu, L. 2012. A latent class modeling approach for identifying vehicle driver injury severity factors at highway-railway crossings. *Accident Analysis and Prevention,* 47**,** 119-127.

Fagnant, D. J. & Kockelman, K. 2015. Preparing a nation for autonomous vehicles: opportunities, barriers and policy recommendations. *Transportation Research Part A: Policy and Practice,* 77**,** 167-181.

Feng, F., Bao, S., Sayer, J. R., Flannagan, C., Manser, M. & Wunderlich, R. 2017. Can vehicle longitudinal jerk be used to identify aggressive drivers? An examination using naturalistic driving data. *Accident Analysis & Prevention,* 104**,** 125-136.

Figlewski, S. 1994. Forecasting volatility using historical data, New York University, Stern School of Business, Finance Department. *Working Paper Series, 1994.*

Fountas, G. & Anastasopoulos, P. C. 2017. A random thresholds random parameters hierarchical ordered probit analysis of highway accident injury-severities. *Analytic methods in accident research,* 15**,** 1-16.

Frühwirth-Schnatter, S. 2006. *Finite mixture and Markov switching models,* Springer Science & Business Media.

Genders, W. & Razavi, S. N. 2015. Impact of connected vehicle on work zone network safety through dynamic route guidance. *Journal of Computing in Civil Engineering,* 30**,** 04015020.

Ghiasi, A., Ma, J., Zhou, F. & Li, X. 2017. Speed Harmonization Algorithm Using Connected Autonomous Vehicles. *Transportation Research Board.*

GM. 2015. *General Motors: A Peek into GM's connected car future* [Online]. Available: http://fortune.com/2015/03/27/a-peek-into-gms-connected-car-future/.

Goldfeld, S. M. & Quandt, R. E. 1973. A Markov model for switching regressions. *Journal of econometrics,* 1**,** 3-15.

Golembiewski, G. & Chandler, B. 2011. Roadway Safety Information Analysis: A Manual for Local Rural Road Owners, U.S. Federal Highway Administration.

Goodall, N. J., Smith, B. L. & Park, B. B. 2014. Microscopic estimation of freeway vehicle positions from the behavior of connected vehicles. *Journal of Intelligent Transportation Systems*, 1-10.

Greene, W. H. 2003. *Econometric analysis*, Pearson Education India.

Guo, F., Wang, X. & Abdel-Aty, M. A. 2010. Modeling signalized intersection safety with corridor-level spatial correlations. *Accident Analysis & Prevention,* 42**,** 84-92.

Haglund, M. & Åberg, L. 2000. Speed choice in relation to speed limit and influences from other drivers. *Transportation Research Part F: Traffic Psychology and Behaviour,* 3**,** 39-51.

Hamilton, J. D. 1989. A new approach to the economic analysis of nonstationary time series and the business cycle. *Econometrica: Journal of the Econometric Society***,** 357-384.

Hamilton, J. D. 1993. Estimation, inference and forecasting of time series subject to changes in regime. *Handbook of statistics,* 11**,** 231-260.

Hamilton, J. D. 1994. *Time series analysis*, Princeton university press Princeton.

Hamilton, J. D. 2010. Regime switching models. *Macroeconometrics and Time Series Analysis*. Springer.

Hankey, J. M., Perez, M. A. & McClafferty, J. A. 2016. Description of the SHRP 2 naturalistic database and the crash, near-crash, and baseline data sets. Virginia Tech Transportation Institute. Available at: https://vtechworks.lib.vt.edu/handle/10919/70850. Accessed on: 09/27/2017. .

Hansen, B. E. 1992. The likelihood ratio test under nonstandard conditions: testing the Markov switching model of GNP. *Journal of applied Econometrics,* 7.

Hardy, M. R. 2001. A regime-switching model of long-term stock returns. *North American Actuarial Journal,* 5**,** 41-53.

Harvey, A. C. 1990. *Forecasting, structural time series models and the Kalman filter*, Cambridge university press.

Hazel, D. R. 2015. Safety at Intersections in Oregon–A Preliminary Update of Statewide Intersection Crash Rates.

Henclewood, D. 2014. Safety Pilot Model Deployment – One Day Sample Data Environment Data Handbook. *In:* RESEARCH AND TECHNOLOGY INNOVATION ADMINISTRATION. RESEARCH AND TECHNOLOGY INNOVATION ADMINISTRATION, U. D. O. T. (ed.). McLean, VA.

Hill, C. J. & Garrett, J. K. 2011. AASHTO connected vehicle infrastructure deployment analysis. Federal Highway Administration, USDOT, Washington, DC.

Hu, J., Park, B. B. & Lee, Y.-J. 2015. Coordinated transit signal priority supporting transit progression under Connected Vehicle Technology. *Transportation Research Part C: Emerging Technologies,* 55**,** 393-408.

Huber, P. J. 2005. *Robust statistics*, John Wiley & Sons.

Imprialou, M.-I. M., Quddus, M., Pitfield, D. E. & Lord, D. 2016. Re-visiting crash–speed relationships: A new perspective in crash modelling. *Accident Analysis & Prevention,* 86**,** 173-185.

Imprialou, M. & Quddus, M. 2017. Crash data quality for road safety research: current state and future directions. *Accident Analysis and Prevention*. https://doi.org/10.1016/j.aap.2017.02.022.

Ismail, K., Sayed, T. & Saunier, N. 2010. Automated analysis of pedestrian-vehicle: conflicts context for before-and-after studies. *Transportation Research Record: Journal of the Transportation Research Board***,** 52-64.

Ismail, K., Sayed, T., Saunier, N. & Lim, C. 2009. Automated analysis of pedestrian-vehicle conflicts using video data. *Transportation Research Record: Journal of the Transportation Research Board***,** 44-54.

Jovanis, P., Aguero-Valverde, J., Wu, K.-F. & Shankar, V. 2011. Analysis of naturalistic driving event data: Omitted-variable bias and multilevel modeling approaches. *Transportation Research Record: Journal of the Transportation Research Board***,** 49-57.

Kamalanathsharma, R. K. & Rakha, H. A. 2016. Leveraging connected vehicle technology and telematics to enhance vehicle fuel efficiency in the vicinity of signalized intersections. *Journal of Intelligent Transportation Systems,* 20**,** 33-44.

Kamrani, M., Abadi, S. M. H. E. & Golroudbary, S. R. 2014. Traffic simulation of two adjacent unsignalized T-junctions during rush hours using Arena software. *Simulation Modelling Practice and Theory,* 49**,** 167-179.

Kamrani, M., Arvin, R. & Khattak, A. J. 2018. Extracting Useful Information from Basic Safety Message Data: An Empirical Study of Driving Volatility Measures and Crash Frequency at Intersections. *Transportation Research Record: Journal of the Transportation Research Board*. 10.1177/0361198118773869.

Kamrani, M., Wali, B. & Khattak, A. J. 2017. Can Data Generated by Connected Vehicles Enhance Safety? Proactive Approach to Intersection Safety Management (forthcoming). *Transportation Research Record: Journal of the Transportation Research Board (2659)*. 10.3141/2659-09.

Karan, F. S. N. & Chakraborty, S. Detecting Behavioral Anomaly in Social Networks Using Symbolic Dynamic Filtering. theASME 2015 Dynamic Systems and Control Conference, 2015.

Karan, F. S. N. & Chakraborty, S. 2016. Dynamics of a Repulsive Voter Model. *IEEE Transactions on Computational Social Systems,* 3**,** 13-22.

Khattak, A., Nambisan, S. & Chakraborty, S. 2015. *Study of Driving Volatility in Connected and Cooperative Vehicle Systems. National Science Foundation (https://nsf.gov/awardsearch/showAward?AWD_ID=1538139)* [Online]. Available: http://tesp.engr.utk.edu/research21/projects.php.

Khattak, A. & Rocha, M. 2003. Are SUVs" supremely unsafe vehicles"?: Analysis of rollovers and injuries with sport utility vehicles. *Transportation Research Record: Journal of the Transportation Research Board***,** 167-177.

Khattak, A. & Targa, F. 2004. Injury severity and total harm in truck-involved work zone crashes. *Transportation Research Record: Journal of the Transportation Research Board***,** 106-116.

Khattak, A. J., Liu, J., Wali, B., Li, X. & Ng, M. 2016. Modeling Traffic Incident Duration Using Quantile Regression. *Transportation Research Record: Journal of the Transportation Research Board***,** 139-148.

Khattak, A. J. & Wali, B. 2017. Analysis of volatility in driving regimes extracted from basic safety messages transmitted between connected vehicles. *Transportation Research Part C: Emerging Technologies,* 84**,** 48-73.

Kianfar, J. & Edara, P. 2013. Placement of roadside equipment in connected vehicle environment for travel time estimation. *Transportation Research Record: Journal of the Transportation Research Board***,** 20-27.

Kim, C.-J. 1994. Dynamic linear models with Markov-switching. *Journal of Econometrics,* 60**,** 1-22.

Kim, C.-J. & Nelson, C. R. 1999. Has the US economy become more stable? A Bayesian approach based on a Markov-switching model of the business cycle. *Review of Economics and Statistics,* 81**,** 608-616.

Kim, C.-J., Piger, J. & Startz, R. 2008. Estimation of Markov regime-switching regression models with endogenous switching. *Journal of Econometrics,* 143**,** 263-273.

Kim, J.-K., Wang, Y. & Ulfarsson, G. F. 2007. Modeling the probability of freeway rear-end crash occurrence. *Journal of transportation engineering,* 133**,** 11-19.

Kim, S., Song, T.-J., Rouphail, N. M., Aghdashi, S., Amaro, A. & Gonçalves, G. 2016. Exploring the association of rear-end crash propensity and micro-scale driver behavior. *Safety science,* 89**,** 45-54.

Klauer, S. G., Dingus, T. A., Neale, V. L., Sudweeks, J. D. & Ramsey, D. J. 2006. The impact of driver inattention on near-crash/crash risk: An analysis using the 100-car naturalistic driving study data.

Klop, J. & Khattak, A. 1999. Factors influencing bicycle crash severity on two-lane, undivided roadways in North Carolina. *Transportation Research Record: Journal of the Transportation Research Board***,** 78-85.

Knight, D., Pearce, C. L., Smith, K. G., Olian, J. D., Sims, H. P., Smith, K. A. & Flood, P. 1999. Top management team diversity, group process, and strategic consensus. *Strategic Management Journal***,** 445-465.

Kockelman, K. M. & Kweon, Y.-J. 2002. Driver injury severity: an application of ordered probit models. *Accident Analysis and Prevention,* 34**,** 313-321.

Kodde, D. A. & Palm, F. C. 1986. Wald criteria for jointly testing equality and inequality restrictions. *Econometrica: journal of the Econometric Society***,** 1243-1248.

Koulakezian, A. & Leon-Garcia, A. CVI: Connected vehicle infrastructure for ITS. 2011 IEEE 22nd International Symposium on Personal, Indoor and Mobile Radio Communications, 2011. IEEE, 750-755.

Lee, J. D., Hoffman, J. D. & Hayes, E. Collision warning design to mitigate driver distraction. Proceedings of the SIGCHI Conference on Human factors in Computing Systems, 2004. ACM, 65-72.

Letter, C. & Elefteriadou, L. 2017. Efficient control of fully automated connected vehicles at freeway merge segments. *Transportation Research Part C: Emerging Technologies,* 80**,** 190-205.

Li, X., Khattak, A. J. & Wali, B. 2017. Role of Multiagency Response and On-Scene Times in Large-Scale Traffic Incidents. *Transportation Research Record: Journal of the Transportation Research Board***,** 39-48.

Liu, J. & Khattak, A. 2016a. Delivering Improved Alerts, Warnings, and Control Assistance Using Basic Safety Messages Transmited between Connected Vehicles. . *Transportation Research Part C: Emerging Technologies*.

Liu, J., Khattak, A. & Han, L. 2015a. How Much Information is Lost When Sampling Driving Behavior Data? . *Transportation Research Board Annual Meeting, National Academies.* Washington, D.C.

Liu, J., Khattak, A. & Wang, X. 2015b. The role of alternative fuel vehicles: Using behavioral and sensor data to model hierarchies in travel. *Transportation Research Part C: Emerging Technologies,* 55**,** 379-392.

Liu, J., Khattak, A. & Wang, X. 2017. A comparative study of driving performance in metropolitan regions using large-scale vehicle trajectory data: Implications for sustainable cities. *International Journal of Sustainable Transportation,* 11**,** 170-185.

Liu, J. & Khattak, A. J. 2016b. Delivering improved alerts, warnings, and control assistance using basic safety messages transmitted between connected vehicles. *Transportation Research Part C: Emerging Technologies,* 68**,** 83-100.

Liu, J., Wang, X. & Khattak, A. 2014. Generating Real-Time Driving Volatility Information. *2014 World Congress on Intelligent Transport Systems.* Detroit, MI.

Liu, J., Wang, X. & Khattak, A. 2016. Customizing driving cycles to support vehicle purchase and use decisions: Fuel economy estimation for alternative fuel vehicle users. *Transportation Research Part C: Emerging Technologies,* 67**,** 280-298.

Lord, D. & Mannering, F. 2010. The statistical analysis of crash-frequency data: a review and assessment of methodological alternatives. *Transportation Research Part A: Policy and Practice,* 44**,** 291-305.

Lu, N., Cheng, N., Zhang, N., Shen, X. & Mark, J. W. 2014. Connected vehicles: solutions and challenges. *Internet of Things Journal, IEEE,* 1**,** 289-299.

Ma, J., Kockelman, K. M. & Damien, P. 2008. A multivariate Poisson-lognormal regression model for prediction of crash counts by severity, using Bayesian methods. *Accident Analysis & Prevention,* 40**,** 964-975.

Malyshkina, N. V. & Mannering, F. L. 2009. Markov switching multinomial logit model: an application to accident-injury severities. *Accident Analysis and Prevention,* 41**,** 829-838.

Malyshkina, N. V., Mannering, F. L. & Tarko, A. P. 2009. Markov switching negative binomial models: an application to vehicle accident frequencies. *Accident Analysis and Prevention,* 41**,** 217-226.

Mannering, F. L. & Bhat, C. R. 2014. Analytic methods in accident research: methodological frontier and future directions. *Analytic Methods in Accident Research,* 1**,** 1-22.

Mannering, F. L., Shankar, V. & Bhat, C. R. 2016. Unobserved heterogeneity and the statistical analysis of highway accident data. *Analytic methods in accident research,* 11**,** 1-16.

McFadden, D. 1973. Conditional logit analysis of qualitative choice behavior.

Milton, J. C., Shankar, V. N. & Mannering, F. L. 2008. Highway accident severities and the mixed logit model: an exploratory empirical analysis. *Accident Analysis and Prevention,* 40**,** 260-266.

Mooradian, J., Ivan, J. N., Ravishanker, N. & Hu, S. 2013. Analysis of driver and passenger crash injury severity using partial proportional odds models. *Accident Analysis and Prevention,* 58**,** 53-58.

Moylan, E. & Skabardonis, A. Reliability-and median-based identification of toll locations in a connected vehicle context. Transportation Research Board 94th Annual Meeting, 2015.

Mustard, D. B. 2003. Reexamining criminal behavior: the importance of omitted variable bias. *Review of Economics and Statistics,* 85**,** 205-211.

Naik, B., Tung, L.-W., Zhao, S. & Khattak, A. J. 2016. Weather impacts on single-vehicle truck crash injury severity. *Journal of safety research,* 58**,** 57-65.

Naseri, H., Nahvi, A. & Karan, F. S. N. 2015. A new psychological methodology for modeling real-time car following maneuvers. *Travel behaviour and society,* 2**,** 124-130.

Nevarez, P., Abdel-Aty, M. A., Wang, X., Santos, P. & Joseph, B. Large-scale injury severity analysis for arterial roads: modeling scheme and contributing factors. Transportation Research Board 88th Annual Meeting, 2009 Washington DC.

NHTSA. 2000. *Resource Guide Describes Best Practices For Aggressive Driving Enforcement* [Online]. Washington, DC: National Highway Traffic Safety Administration, U.S. Department of Transportation. Available: http://www.nhtsa.gov/About+NHTSA/Traffic+Techs/current/Resource+Guide+Describes+Best+Practices+For+Aggressive+Driving+Enforcement [Accessed June 22nd 2016].

NHTSA 2016. National Highway Traffic Safety Administration, USA. Traffic Safety Facts Res. Note 2016; 2016: 1-9.

Noble, A. M., McLaughlin, S. B., Doerzaph, Z. R. & Dingus, T. A. 2014. Crowd-sourced Connected-vehicle Warning Algorithm using Naturalistic Driving Data.

Osman, O. A., Codjoe, J. & Ishak, S. 2015. Impact of Time-to-Collision Information on Driving Behavior in Connected Vehicle Environments Using A Driving Simulator Test Bed. *Journal of Traffic and Logistics Engineering Vol,* 3.

Osman, O. A. & Ishak, S. 2015. A network level connectivity robustness measure for connected vehicle environments. *Transportation Research Part C: Emerging Technologies,* 53**,** 48-58.

Paleti, R., Eluru, N. & Bhat, C. 2010. Examining the influence of aggressive driving behavior on driver injury severity in traffic crashes. *Accident Analysis & Prevention,* 42**,** 1839-1854.

Pelled, L. H., Eisenhardt, K. M. & Xin, K. R. 1999. Exploring the black box: An analysis of work group diversity, conflict and performance. *Administrative science quarterly,* 44**,** 1-28.

Persaud, B. & Nguyen, T. 1998. Disaggregate safety performance models for signalized intersections on Ontario provincial roads. *Transportation Research Record: Journal of the Transportation Research Board***,** 113-120.

Poch, M. & Mannering, F. 1996. Negative binomial analysis of intersection-accident frequencies. *Journal of Transportation Engineering,* 122**,** 105-113.

Qin, X., Ivan, J. N., Ravishanker, N. & Liu, J. 2005. Hierarchical Bayesian estimation of safety performance functions for two-lane highways using Markov chain Monte Carlo modeling. *Journal of Transportation Engineering,* 131**,** 345-351.

Quddus, M. 2013a. Exploring the relationship between average speed, speed variation, and accident rates using spatial statistical models and GIS. *Journal of Transportation Safety & Security,* 5**,** 27-45.

Quddus, M. 2013b. Exploring the relationship between average speed, speed variation, and accident rates using spatial statistical models and GIS. *Journal of Transportation Safety and Security,* 5**,** 27-45.

Quddus, M., Chin, H. & Wang, J. 2001. Motorcycle crash prediction model for signalised intersections. *WIT Transactions on The Built Environment,* 52.

Quddus, M. A. 2008. Modelling area-wide count outcomes with spatial correlation and heterogeneity: an analysis of London crash data. *Accident Analysis & Prevention,* 40**,** 1486-1497.

Quddus, M. A., Noland, R. B. & Chin, H. C. 2002. An analysis of motorcycle injury and vehicle damage severity using ordered probit models. *Journal of Safety Research,* 33**,** 445-462.

Quddus, M. A., Wang, C. & Ison, S. G. 2009. Road traffic congestion and crash severity: econometric analysis using ordered response models. *Journal of Transportation Engineering,* 136**,** 424-435.

Renski, H., Khattak, A. & Council, F. 1999. Effect of speed limit increases on crash injury severity: analysis of single-vehicle crashes on North Carolina interstate highways. *Transportation Research Record: Journal of the Transportation Research Board***,** 100-108.

Richards, D. & Cuerden, R. 2009. The relationship between speed and car driver injury severity. *Road Safety Web Publication, Department of Transport, London.*

Russo, B. J., Savolainen, P. T., Schneider, W. H. & Anastasopoulos, P. C. 2014. Comparison of factors affecting injury severity in angle collisions by fault status using a random parameters bivariate ordered probit model. *Analytic Methods in Accident Research,* 2**,** 21-29.

Saunier, N., Sayed, T. & Ismail, K. 2010. Large-scale automated analysis of vehicle interactions and collisions. *Transportation Research Record: Journal of the Transportation Research Board***,** 42-50.

Savolainen, P. T., Mannering, F. L., Lord, D. & Quddus, M. A. 2011. The statistical analysis of highway crash-injury severities: a review and assessment of methodological alternatives. *Accident Analysis & Prevention,* 43**,** 1666-1676.

Schneider, R. J., Ryznar, R. M. & Khattak, A. J. 2004. An accident waiting to happen: a spatial approach to proactive pedestrian planning. *Accident Analysis & Prevention,* 36**,** 193-211.

Sengupta, R., Rezaei, S., Shladover, S. E., Cody, D., Dickey, S. & Krishnan, H. 2007. Cooperative collision warning systems: Concept definition and experimental implementation. *Journal of Intelligent Transportation Systems,* 11**,** 143-155.

Seraneeprakarn, P., Huang, S., Shankar, V., Mannering, F., Venkataraman, N. & Milton, J. 2017. Occupant injury severities in hybrid-vehicle involved crashes: A random parameters approach with heterogeneity in means and variances. *Analytic Methods in Accident Research,* 15**,** 41-55.

Shah, S. A. A., Ahmad, N. & Ha, A. B. 2018. Pedestrians' exposure to road traffic crashes in urban environment: A case study of Peshawar, Pakistan. *Journal of The Pakistan Medical Association,* 68**,** 615-623.

Shaheed, M. S. & Gkritza, K. 2014. A latent class analysis of single-vehicle motorcycle crash severity outcomes. *Analytic Methods in Accident Research,* 2**,** 30-38.

Shin, J., Bhat, C. R., You, D., Garikapati, V. M. & Pendyala, R. M. 2015. Consumer preferences and willingness to pay for advanced vehicle technology options and fuel types. *Transportation Research Part C: Emerging Technologies,* 60**,** 511-524.

Shinar, D. 1998. Aggressive driving: the contribution of the drivers and the situation. *Transportation Research Part F: Traffic Psychology and Behaviour,* 1**,** 137-160.

Spiegelhalter, D., Thomas, A., Best, N. & Lunn, D. 2003. WinBUGS user manual. version.

Srinivasan, A. R., Karan, F. S. N. & Chakraborty, S. 2017. Pedestrian dynamics with explicit sharing of exit choice during egress through a long corridor. *Physica A: Statistical Mechanics and its Applications,* 468**,** 770-782.

Stata 2016. *Stata Reference Manual,* Stata Press.

Sugiura, A. & Dermawan, C. 2005. In traffic jam IVC-RVC system for ITS using Bluetooth. *IEEE Transactions on intelligent transportation systems,* 6**,** 302-313.

Tarko, A., Davis, G., Saunier, N., Sayed, T. & Washington, S. 2009. Surrogate measures of safety. *White paper, ANB20 (3) Subcommittee on Surrogate Measures of Safety*.

Tauchen, G. 1986. Finite state markov-chain approximations to univariate and vector autoregressions. *Economics letters,* 20**,** 177-181.

Tay, R. 2015. A random parameters probit model of urban and rural intersection crashes. *Accident Analysis and Prevention,* 84**,** 38-40.

Train, K. 2003. *Discrete choice methods with simulation*, Cambridge university press.

TRB 2013. The 2nd Strategic Highway Research Program Naturalistic Driving Study Dataset. Transportation Research Board of the National Academy of Sciences, 2013. Available from the SHRP 2 NDS InSight Data Dissemination web site: https://insight.shrp2nds.us.

Turnbull, K. F. Automated and Connected Vehicles: Summary of the 9th University Transportation Centers Spotlight Conference. Transportation Research Board Conference Proceedings on the Web, 2016.

US-DOT. 2016. *Intelligent Transportation Systems Joint Program Office, United States Department of Transportation* [Online]. Available: http://www.its.dot.gov/connected_vehicle/connected_vehicle_research.htm.

Venkataraman, N., Shankar, V., Ulfarsson, G. F. & Deptuch, D. 2014. A heterogeneity-in-means count model for evaluating the effects of interchange type on heterogeneous influences of interstate geometrics on crash frequencies. *Analytic Methods in Accident Research,* 2**,** 12-20.

Wali, B., Ahmed, A. & Ahmad, N. An ordered-probit analysis of enforcement of road speed limits. Proceedings of the Institution of Civil Engineers-Transport, 2017a. Thomas Telford Ltd, 1-10.

Wali, B., Ahmed, A., Iqbal, S. & Hussain, A. 2017b. Effectiveness of enforcement levels of speed limit and drink driving laws and associated factors–Exploratory empirical analysis using a bivariate ordered probit model. *Journal of Traffic and Transportation Engineering (English Edition)*, 4**,** 272-279.

Wali, B., Greene, D., Khattak, A. & Liu, J. 2018a. Analyzing within Garage Fuel Economy Gaps to Support Vehicle Purchasing Decisions - A Copula-Based Modeling & Forecasting Approach. *Transportation Research Part D: Transport and Environment,* 63**,** 186-208. https://doi.org/10.1016/j.trd.2018.04.023.

Wali, B., Khattak, A., David, G. & Liu, J. 2018b. Fuel Economy Gaps Within & Across Garages: A Bivariate Random Parameters Seemingly Unrelated Regression Approach (forthcoming). *International Journal of Sustainable Transportation*. 10.1080/15568318.2018.1466222.

Wali, B., Khattak, A., Waters, J., Chimba, D. & Li, X. 2018c. Development of Safety Performance Functions for Tennessee: Unobserved Heterogeneity & Functional Form Analysis (Accepted for publication). *Transportation Research Record: Journal of the Transportation Research Board* 10.1177/0361198118767409

Wali, B., Khattak, A. J., Bozdogan, H. & Kamrani, M. 2018d. How is Driving Volatility Related to Intersection Safety? A Bayesian Heterogeneity-Based Analysis of Instrumented Vehicles Data (Accepted for Publication). *Transportation Research Part C: Emerging Technologies*.

Wali, B., Khattak, A. J. & Karnowski, T. 2018e. How Driving Volatility in Time to Collision Relates to Crash Severity in a Naturalistic Driving Environment? *Presented at the Transportation Research Board 97th Annual Meeting, Washington DC, 2018.*

Wander, B. H. & D'Vari, R. 2003. The Limitations of Standard Deviation as a Measure of Bond Portfolio Risk. *The Journal of Wealth Management,* 6**,** 35-38.

Wang, X., Khattak, A. J., Liu, J., Masghati-Amoli, G. & Son, S. 2015. What is the level of volatility in instantaneous driving decisions? *Transportation Research Part C: Emerging Technologies,* 58**,** 413-427.

Washington, S. P., Karlaftis, M. G. & Mannering, F. 2010. *Statistical and econometric methods for transportation data analysis*, CRC press.

Weber, E. U., Shafir, S. & Blais, A.-R. 2004. Predicting risk sensitivity in humans and lower animals: risk as variance or coefficient of variation. *Psychological review,* 111**,** 430.

Weber, T. 2015. Mercedes Benz-The future of mobility at MBC: Emission-free, connected and autonomous. Available: https://www.daimler.com/dokumente/investoren/kapitalmarkttage/daimler-ir-mercedes-benzcarscapitalmarketdayprofdrthomasweber-20150611.pdf.

Weiss, H. B., Kaplan, S. & Prato, C. G. 2014. Analysis of factors associated with injury severity in crashes involving young New Zealand drivers. *Accident Analysis and Prevention,* 65**,** 142-155.

Wu, K.-F. & Jovanis, P. P. 2012. Crashes and crash-surrogate events: Exploratory modeling with naturalistic driving data. *Accident Analysis & Prevention,* 45**,** 507-516.

Xiong, Y. & Mannering, F. L. 2013. The heterogeneous effects of guardian supervision on adolescent driver-injury severities: A finite-mixture random-parameters approach. *Transportation Research Part B: Methodological,* 49**,** 39-54.

Xiong, Y., Tobias, J. L. & Mannering, F. L. 2014a. The analysis of vehicle crash injury-severity data: A Markov switching approach with road-segment heterogeneity. *Transportation research part B: methodological,* 67**,** 109-128.

Xiong, Y., Tobias, J. L. & Mannering, F. L. 2014b. The analysis of vehicle crash injury-severity data: A Markov switching approach with road-segment heterogeneity. *Transportation Research Part B: Methodological,* 67**,** 109-128.

Yang, Z., Kobayashi, T. & Katayama, T. 2000. Development of an intersection collision warning system using DGPS. SAE Technical Paper.

Yasmin, S., Eluru, N., Bhat, C. R. & Tay, R. 2014. A latent segmentation based generalized ordered logit model to examine factors influencing driver injury severity. *Analytic Methods in Accident Research,* 1**,** 23-38.

Ye, X., Pendyala, R. M., Washington, S. P., Konduri, K. & Oh, J. 2009. A simultaneous equations model of crash frequency by collision type for rural intersections. *Safety Science,* 47**,** 443-452.

Zajac, S. S. & Ivan, J. N. 2003. Factors influencing injury severity of motor vehicle–crossing pedestrian crashes in rural Connecticut. *Accident Analysis & Prevention,* 35**,** 369-379.

Zeng, Q., Wen, H., Huang, H. & Abdel-Aty, M. 2017. A Bayesian spatial random parameters Tobit model for analyzing crash rates on roadway segments. *Accident Analysis & Prevention,* 100**,** 37-43.

Zeng, X., Balke, K. N. & Songchitruksa, P. 2012. Potential Connected Vehicle Applications to Enhance Mobility, Safety, and Environmental Security. Southwest Region University Transportation Center, Texas Transportation Institute, Texas A & M University System.

Zhao, S. & Khattak, A. 2015. Motor vehicle drivers' injuries in train–motor vehicle crashes. *Accident Analysis and Prevention,* 74**,** 162-168.

Zhu, F. & Ukkusuri, S. V. 2015. A linear programming formulation for autonomous intersection control within a dynamic traffic assignment and connected vehicle environment. *Transportation Research Part C: Emerging Technologies,* 55**,** 363-378.

Zhu, S., Levinson, D. & Liu, H. 2009. Measuring winners and losers from the new I-35W Mississippi River Bridge. *Transportation***,** 1-14.

Zhu, X. & Srinivasan, S. 2011. A comprehensive analysis of factors influencing the injury severity of large-truck crashes. *Accident Analysis and Prevention,* 43**,** 49-57.

Zulkefli, M. A. M., Mukherjee, P., Sun, Z., Zheng, J., Liu, H. X. & Huang, P. 2017. Hardware-in-the-loop testbed for evaluating connected vehicle applications. *Transportation Research Part C: Emerging Technologies,* 78**,** 50-62.

Zulkefli, M. A. M., Zheng, J., Sun, Z. & Liu, H. X. 2014. Hybrid powertrain optimization with trajectory prediction based on inter-vehicle-communication and vehicle-infrastructure-integration. *Transportation Research Part C: Emerging Technologies,* 45**,** 41-63.

VITA

Mr. Behram Wali was born on January 19, 1992, and grew up in the city of Peshawar, the capital of Khyber Pakhtunkhwa Province in Pakistan. After high school, Mr. Wali attended University of Engineering & Technology, Peshawar, where he received his Bachelor's degree in Civil Engineering in 2013. In the same year, Mr. Wali was admitted in National University of Sciences & Technology, Pakistan, for his Master's program. He received his Master's degree in Transportation Engineering in 2015, and was the recipient of the "President of Pakistan Gold Medal Award for Outstanding Graduate Student." In the same year, Mr. Wali went to the United States of America and continued his studies at The University of Tennessee, Knoxville, pursuing his Ph.D. degree in Civil Engineering with a concentration in Transportation Engineering and his Master's degree in Statistics. Mr. Wali's research focuses on various types of innovations related to intelligent transportation systems, transportation safety, traffic operations, and sustainable transportation. In particular, he is highly excited about Big Data science and advanced statistical and econometric methods as it relates to intelligent transportation systems, connected and automated vehicles, and transportation safety, so almost all of his research is methodologically driven and application to engineering practice. To date, Mr. Wali has authored/co-authored 18 scientific articles in international peer-reviewed transportation journals.

During his Ph.D. study, Mr. Wali received several prestigious national and international awards, including the "Distinguished Scientific Papers-Americas" award by the ITS World Congress 2016 held in Melbourne, Australia, and 2017 TRB Outstanding Paper Award awarded by the TRB Safety Data, Analysis, and Evaluation Committee. Recently, his project proposal related to

Naturalistic Driving research was awarded and sponsored for further development by the highly competitive TRB's Strategic Highway Research Program Safety Data Bonanza. During his stay at University of Tennessee, Mr. Wali also received several scholarship awards including the Sixth and Seventh Annual Scholarship Awards for Outstanding Student Paper and Academic Qualifications by ITS-TN, and the 2016 and 2017 Tennessee Section ITE's (TSITE) Annual Student Paper Competition Awards. In addition, Mr. Wali received the 2016 and 2017 Traffic Bowl Competition Champion Awards, by the TSITE. Mr. Wali remained an active ITE student member and served as the Secretary of ITE Student Chapter at The University of Tennessee. In terms of campus service, Mr. Wali served as an Ambassador at Howard H. Baker Center for Public Policy, University of Tennessee, Senator & CEE representative at Graduate Student Senate, and Member Travel Award Committee, Graduate Student Senate, UTK.